DISSERTATION

Interference Management Techniques with Imperfect Channel State Information at the Transmitter

ausgefhrt zum Zwecke der Erlangung des akademischen Grades eines Doktors der technischen Wissenschaften

unter der Leitung von
Ao. Univ.-Prof. Dr. Gerald Matz
und Dr. Maxime Guillaud
Institute of Telecommunications

eingereicht an der Technischen Universitt Wien
Fakultt fr Elektrotechnik

von
Mohsen Rezaee Kheirabadi
Leo-Mathausergasse 69/2
1230, Wien

Wien, im Mai 2014 _____

Die Begutachtung dieser Arbeit erfolgte durch:

1. Ao. Univ.-Prof. Dipl.-Ing. Dr. Gerald Matz
   Institute of Telecommunications
   Technische Universität Wien

2. Prof. Constantinos Papadias
   Athens Information Technology

Abstract

Interference is the source of the most serious performance impairment in today's wireless communication networks. Recent research results have highlighted the importance of interference coordination in such networks. There are several schemes that effectively manage the interference assuming that the state of the channel is known at the transmitters. However, having access to perfect channel state information (CSI) at the transmitters is not a realistic assumption. The aim of this dissertation is to study and develop methods enabling interference coordination in a wireless network while having imperfect channel state information at the transmitters.

In the first part of this thesis, advanced channel state representations are employed in order to cope with the problem of interference when the transmit signals are designed based on imperfect CSI available at the transmitter. Efficient quantization of the CSI is investigated to reduce the requirement for information exchange over the network and in particular feedback to the transmitters. Different scenarios are considered where availability of CSI at the transmitter is crucial to achieve high throughput.

In the second part of this thesis, a particular type of CSI imperfection is considered where the available CSI at the transmitter is completely outdated with respect to the current state of the channel. A simple method is proposed to exploit the outdated CSI in a multiple-input multiple-output (MIMO) two-user Gaussian interference channel (IC). The proposed scheme is shown to achieve the optimal degrees of freedom (DoF) of this channel.

In the third part of this thesis, it is assumed that the transmitters have access to local CSI and the process of designing the transmit signal is distributed over the network. A message-passing framework is proposed to effectively model the information exchange over the network when the goal is to obtain an interference alignment (IA) solution in a distributed manner.

In the last part of this thesis, the uncertainty about the channels at the transmitters is modeled as an independent additive Gaussian error. This simplifies the performance analysis and allows for the optimization of the transmit signal to ensure robustness against channel uncertainty and obtain solutions that are adaptive to the channel condition. Two different approaches are proposed to minimize the impact of the residual interference caused by the channel uncertainty.

Kurzfassung

Interferenz ist die Quelle der meisten ernsthaften Effizienzeinbußen in heutigen drahtlosen Kommunikationsnetzen. Erst kürzlich veröffentlichte Ergebnisse haben die Wichtigkeit von Interferenz-Koordination in solchen Netzen gezeigt. Hierbei gibt es mehrere Methoden welche die Interferenz managen unter der Annahme, dass der Zustand des drahtlosen Kanals (CSI) beim Sender bekannt ist. Doch leider ist diese Annahme nicht realistisch in der Praxis. Daher ist das Ziel dieser Dissertation die Entwicklung und Analyse von Methoden für die Interferenz-Koordination in Drahtlosnetzen unter der Annahme dass der Sender nur über unvollständiges Wissen über den Kanalzustand verfügt.

Im ersten Teil dieser Arbeit werden fortgeschrittene Kanalzustandsmodelle herangezogen um das Interferenzproblem zu lösen wenn das Sendesignal aufgrund unvollständiger CSI generiert wird. Darüber hinaus werden effiziente Quantisierungsmethoden von der CSI untersucht um den benötigten Informationsaustausch im Netzwerk, insbesondere die Informationsrückführung zum Sender, zu reduzieren. Außerdem werden verschiedene Szenarien näher betrachtet, bei denen die Verfügbarkeit von CSI am Sender wichtig für das Erreichen von hohen Durchsätzen ist.

Im zweiten Teil wird eine spezielle Art der unvollständigen CSI näher betrachtet. Hierbei wird angenommen, dass das verfügbare CSI Wissen überholt im Bezug zum aktuellen Zustand ist. Eine einfache Methode wird vorgestellt, welche dennoch das veraltete Wissen in einem Multiple Input Multiple Output (MIMO) System mit zwei Benutzern und Gaußschen Kanal ausnutzt. Schlussendlich wird gezeigt, dass die vorgeschlagene Methode die optimalen Freiheitsgrade (DoF) des Kanals ausnützt.

Der dritte Teil befasst sich mit einem Szenario bei dem der Sender Zugriff auf lokales CSI hat und der Generierungsprozess des Sendesignals im Netzwerk verteilt wird. Hierfuer wird ein Message-Passing Algorithmus vorgestellt welcher das Interferenzausrichtungsproblem verteilt im Drahtlosnetzwerk effizient löst.

Zuletzt wird die Unsicherheit des Wissens über den Kanal als unabhängiger additiver Gaußscher Fehler modelliert. Dieser Ansatz vereinfacht die Leistungsanalyse und ermöglicht eine Optimierung des Sendesignals um eine Robustheit gegenüber Kanalunsicherheiten sicherzustellen und um Lösungen zu bekommen, welche adaptiv gegenüber des Kanalzustands ist. Schlussendlich werden zwei verschiedene Methoden welche den Einfluss der restlichen Interferenz verursacht durch die Kanalunsicherheit präsentiert.

Acknowledgments

I am very thankful to my supervisors Gerald Matz and Maxime Guillaud for their support and guidance over the last several years.

It is also my pleasure to express my thanks to Constantinos Papadias who kindly agreed to act as a referee.

I want to thank my colleagues at the institute, especially the people in my research group.

I am particularly grateful to Andreas Winkelbauer, Florian Xaver, Stefan Schwandter, and Valentin Schwarz for their collaboration and for helpful discussions.

Finally, I would like to thank my parents and my wife. Their patience and encouragement have been a great support.

Contents

Notation

$\mathrm{var}(\cdot)$	The variance of its argument
$\log$	Logarithm in base 2
$\mathcal{N}(r, \sigma^2)$	The real Gaussian distributions with mean r and variance σ^2
$\mathcal{CN}(r, \sigma^2)$	The complex circularly symmetric Gaussian distributions with mean r and variance σ^2
$\mathbf{a}(n)$	The nth element of $\mathbf{a}$
$\mathbf{A}(\mathrm{m}, \mathrm{n})$	The (m, n)th entry of $\mathbf{A}$
$\mathrm{E}_X\{\cdot\}$	Average of its argument
$(\cdot)^T$	Transpose of its argument
$(\cdot)^*$	Conjugate of its argument
$(\cdot)^H$	Hermitian transpose of its argument
$\mathrm{tr}(\cdot)$	Trace of its argument matrix
$\mathrm{span}(\cdot)$	Span of its argument matrix
$\mathrm{diag}(\cdot)$	Diagonal matrix with the elements of the argument as its diagonal elements
$\mathrm{Bdiag}(\cdot)$	Block diagonal matrix with the elements of the argument as its blocks
$\mathrm{rank}(\cdot)$	rank of its argument matrix
$\|\cdot\|$	Determinant/absolute value of its argument
$\|\cdot\|_F$	Frobenious norm of its argument matrix
$\mathbf{I}_N$	$\mathrm{N} \times \mathrm{N}$ Identity matrix
$\otimes$	Kronecker product
$\mathbf{A} \succeq \mathbf{B}$	**A-B** is positive semi-definite
$V_{n,p}$	the complex Stiefel manifold
$\mathcal{G}_{n,p}$	the complex Grassmann manifold
$\sim i$	the set $\{1, \ldots, i-1, i+1, \ldots K\}$ where K is the number of users
$\mathcal{N}(a)$	the set of neighbors of a node a in a graph
$\mathcal{C}(\cdot)$	the column space of its argument matrix
$\mathcal{R}(\cdot)$	the row space of its argument matrix
$\lambda_{\max}(\cdot)$	The largest eigenvalue of its argument matrix
$\nu_{\min}(\cdot)$	a truncated unitary matrix spanning the space associated with the d weakest eigenvalues of the argument matrix

1

Introduction

1.1 Importance of Interference Management

Wireless communication has developed significantly in the past several years alongside with the growth in the amount of information exchange as a result increasing demand for mobile connectivity, new wireless services, and smart phones. New wireless technologies facilitate the access to various services efficiently with minimal consumption of time and resources. The quality of information transfer in a wireless link is determined by several factors including the propagation conditions, interference levels and properties of the underlying frequency spectrum.

Interference management plays a crucial role in future wireless systems as the number of users sharing the same communication medium is growing rapidly. In fact, the amount of interference in the system scales with the number of users. This interference may cause a severe degradation in the system's performance. With the rapid increase in the usage of wireless systems, continuous development of wireless systems becomes inevitable to keep up with new expectations with minimum cost.

The general approaches to achieve higher system capacity can be categorized as improving the spectral efficiency or increasing the bandwidth. One can also reduce the physical distance of the interfering devices, e.g., in cellular systems, it amounts to deploying more base stations. However, the cost associated to each approach needs to be considered. Higher spectral efficiency at the physical layer necessitates the use of multiple antenna techniques or spectrally efficient transmission waveforms which increases the cost of the devices. Increasing the bandwidth also increases the cost of the device while facing the bandwidth scarcity problem. In cellular systems, increasing the density of base stations calls for decreasing the reuse factor which increases the interference among the reusing radio links. Therefore, more complex techniques are required for handling interference. Finally, in the design of future networks the tasks related to network deployment, optimization and interference management need to be adaptive. From the physical layer point of view, dynamic methods that facilitate avoiding, mitigating, and coordinating interference are crucial.

Shannon's work on the two-way channel in [1] was the start of the study of interaction between non-cooperative users sharing the same channel. The capacity of the two-user interference channel became a fundamental problem regarding interaction between interfering users. In this channel, two transmitters (TX) communicate independent information to their corresponding receivers (RX) in a shared channel. For more than 30 years, the characterization of the channel's capacity region has been an open problem. Meanwhile significant progress is achieved in the area and approximate characterizations are available now [2], [3]. For some special cases such as the strong and very strong interference channels and a class of deterministic interference channels the exact capacity region has been characterized [5, 6, 34]. The existence of different achievable schemes for those cases suggests that finding a universal achievable scheme for this problem is not likely.

By introduction of MIMO technology an interesting direction for expanding the capacity of wireless links was created. The devices could achieve rates beyond the capacity that was achievable by single-antenna systems. Similar to the limitation on transmit power and bandwidth, there are also many limitations that prevent the devices to arbitrarily increase the capacity by using an arbitrary number of antennas. For example, to achieve the potential gain of MIMO systems, the antennas need to be placed sufficiently far apart to avoid deficiency in the equivalent channels. Therefore devices with a size limitation cannot support more than a few antennas.

Despite the capacity improvement due to MIMO systems, with the increasing density of wireless devices, interference still remains the main problem and is more challenging in MIMO systems as it appears at multiple antennas. The relevant model for a network consisting of two or more interferers which are equipped with multiple antennas is the (K-user) MIMO IC. In this model the transmitters encode their own symbols without cooperating with each other and similarly the receivers decode their intended signal without any exchange of information with each other. Cooperation is defined as sharing any information about the transmitted symbols. Other types of coordination such as sharing the channel state information are allowed and in reality this type of information sharing requires little overhead compared to full cooperation. Similar to the single antenna systems where the symbols are assigned to different time/frequency sub channels, in the space domain, the symbols can also be allocated to different spatial directions. In other words, at any time/frequency sub channel, multiple symbols can be multiplexed in several spatial directions depending on the number of antennas. This task is usually performed by applying an appropriate precoder to the data symbols before sending the signal over the antennas. If the data symbols of each user are placed in a column vector, the precoder will be a matrix whose columns are the spatial directions corresponding to each symbol.

Any matrix with proper rank and dimensions that satisfies the power constraint can act as the precoding matrix. A very interesting problem is to find the best precoder matrices for transmitters that optimizes a performance metric such as the total communication rate achievable over of the network. The problem is challenging as it involves several precoding matrices that need to be optimized jointly. A precoding matrix at one transmitter also affects the performance of other users since it affects the amount of interference seen by other receivers. The fact that the optimization variables are continuous valued matrices also adds to the complexity of the problem.

Another aspect of precoder optimization is the fact that the optimization determines the precoders that need to be employed at the transmitter side. This requires that the necessary information for the optimization problem to be gathered at the transmitters. This amounts to feedback of channel state information from the receivers

to the transmitters. In other words, every transmitter needs to have access to the global information about the channels in order to compute its own precoder. With such limitations any method that can avoid or reduce the CSI feedback requirement will be of great interest. On the other hand, distributed schemes that rely on local information and are superior to classical approaches are desired. Since such an optimization problem is usually intractable and requires global CSI, any simplification that can lead to tractable sub problems exploiting local CSI would be another line of investigation. Interference alignment is a new method that provides a simple solution to the problem which is optimal at high SNR. This solution can be utilized and improved to reach better solutions at different SNR regimes.

In the past, interference management has been performed off-line. It has required exhaustive network planning effort and has been a centralized procedure by nature. This approach is a robust and reliable approach. On the other hand, it is not flexible and is not efficient in terms of spectrum usage and the overall cost of the network. In the future, interference management will become more dynamic, decentralized and autonomous. The aim is that future wireless systems achieve high capacity, and at the same time, the deployment, operation, and maintenance of the network would become cheaper and simpler.

1.2 Contributions

The focus of this dissertation is on multi-user transmission techniques that exploit CSI at the transmitter side. We consider different types of CSI imperfection at the transmitter and devise appropriate schemes to deal with interference. When quantized CSI is assumed to be available at the transmitter, a limited feedback scheme is proposed to reduce the feedback requirement for interference alignment. The proposed strategy is proven to be also effective in CSI sharing problem when the transmitters acquire their local CSI by reciprocity. Additionally, employing IA, distributed computation of the precoders is discussed using message passing arguments. For a two-user IC, a general scheme based on retrospective IA is proposed to achieve the DoF region using outdated CSIT. Furthermore, considering the effect of imperfect CSI as an additive noise, methods are proposed to increase the throughput in the K-user MIMO IC. The preliminary concepts are introduced in Chapter 2 and the main contributions of this dissertation are outlined in Chapters 3 to 6. The thesis is concluded in Chapter 7 following by an outlook for possible future continuation of this work. Detailed proofs and derivations are provided in the Appendices. In the following, a description of important contributions in each chapter is given.

Chapter 3

While CSI at the receiver is often assumed to be perfect, to exploit the CSI at the transmitter, the CSI is usually quantized and fed back to the transmitters. Concerning multi-user systems, the question of the scaling of the size of the codebook used for CSI feedback with increasing signal-to-noise ratio (SNR) has been explored in a number of recent works. Generally speaking, using imperfect CSI at the transmitter (CSIT) to compute the transmit precoders in a multi-user system causes interference at the receiver side. Since the power of this interference scales with the transmit power, it is necessary to compensate any increase in transmit power by decreasing the quantization error affecting the CSIT, if the interference at the receiver is to remain bounded. This has led several authors to study how the codebook size should scale with the SNR in order to preserve the degrees of freedom achievable with perfect CSI, for several feedback schemes. In the first part of this

chapter we analyze this problem for the K-user MIMO IC when the CSI is fed back from the receivers to the transmitters. This scenario arises in frequency division duplex (FDD) systems where feedback is necessary to provide the CSI to the transmitters.

A similar quantization problem arises in time division duplex (TDD) systems. For TDD systems, every base station can estimate its downlink channels from the uplink transmission phase thanks to reciprocity. In such systems, the interference channel is adopted very often in particular due to data sharing limitations of network MIMO. In the second part of this chapter we investigate the CSI sharing problem between the transmitters. Similar to the FDD case, we provide scaling laws to preserve the DoF that can be achieved with perfect CSI sharing.

In Chapter 3 we present a new CSI quantization scheme for IA over the K-user constant MIMO IC. The salient points of our contribution are:

- The proposed feedback scheme exploits the invariances in the IA equations to reduce the dimension of the quantization space, without requiring the heavy iterative processing of e.g. [7].
- We characterize the scaling (with SNR) of the codebook size under which the proposed feedback scheme achieves the same DoF as with perfect CSIT. This scaling is shown to be better (slower) than the scaling obtained using the schemes from [8] or [7] for all system dimensions where IA is feasible.
- At non-asymptotic SNR and for a fixed codebook size, the proposed scheme is shown by simulation to achieve better sum-rate performance than the methods from [8] or [7].
- As a by-product of our analysis, we introduce a statistical model that faithfully captures the properties of the quantization error of RVQ on the Grassmann manifold for large codebooks; we use it to generate rotations that closely approximate the true quantization error of RVQ. This tool enables numerical analysis of general Grassmannian RVQ schemes for large codebook sizes, without requiring the generation of the codebook nor the exhaustive search normally associated with the quantizer.
- A similar quantization scheme is proposed for CSI sharing in TDD systems which reduces the sharing requirement.
- For the CSI sharing problem, we characterize the scaling (with SNR) of the codebook size under which the proposed CSI sharing scheme achieves the same DoF as with perfect CSIT.
- Global optimization problems, i.e., sum rate maximization and mean square error minimization problems are considered and then decoupled into local optimization problems using the proposed IA filters.
- Methods are proposed to exploit the accuracy of the local CSI at individual transmitters and also incorporating the effect of direct channels.

Chapter 4

In this chapter, we focus on a scenario where the available CSI at the transmitter is outdated. This assumption is valid for many practical settings where the coherence time of the channel is too short compared to the time required for the arrival of feedback. We consider a two-user MIMO IC where each transmitter has access

to the channel matrices with a delay such that the instantaneous CSI becomes uncorrelated with the available CSI. Interestingly it has been shown that the existence of such outdated CSI at the transmitter can still increase the DoF of the network [9] compared to the case with no CSI. The DoF region with outdated CSI has been characterized for MIMO BC in [10] and MIMO IC in [11] where the achievable schemes are based on feedback and retransmission of the overheard interference at the receivers. We try to unify the achievable schemes and provide a compact representation for various configurations of antennas in MIMO IC. The contributions of this chapter can be summarized as follows :

- We introduce a model to apply retrospective interference alignment for MIMO IC with outdated CSIT.
- We propose a unified DoF-achieving scheme for the MIMO IC with outdated CSIT.
- The achievable DoF is verified analytically.
- We provide insights about extending our scheme to correlated channels.

Chapter 5

In this chapter, we introduce an iterative solution to the problem of interference alignment (IA) over MIMO channels based on a message-passing formulation. We propose a parameterization of the messages that enables the computation of IA precoders. Our scheme is particularly interesting in networks with a large number of users since centralized approaches are not feasible due to the increasing amount of information exchange and the growing computational complexity. The proposed formulation can also be applied to more general performance metrics and is not restricted to IA.

The contributions of this chapter are as follows:

- We introduce a min-sum algorithm capable of computing the IA precoders in a distributed manner, by associating a suitably chosen graph to the IA problem.
- We propose a parameterization of the messages that enables the use of this algorithm over continuous variable spaces – under this parameterization, suitable approximations of the messages can be computed in closed-form.
- We show that the iterative leakage minimization algorithm of Gomadam et al. [12] is a special case of our message-passing algorithm, obtained for a particular schedule.
- We evaluate numerically the performance of the proposed method, and compare it to the classical iterative leakage minimization.
- We discuss a distributed implementation.

Chapter 6

In this chapter, an additive Gaussian model is assumed for the uncertainty associated to each channel coefficient. For simplicity the uncertainty is assumed to be independent over different antennas. Two different criteria are considered in this chapter to analyze and optimize the performance in MIMO IC. We aim to maximize an expectation of the throughput while satisfying a set of constraints. In the first contribution, we focus

on discrete AMCP and aim to find the best transmission parameters to adapt the precoders determined by IA to the channel when the precoders are designed based on imperfect CSI. In this part, we assume a sum power constraint over the users and enforce a maximum BER constraint. In the second contribution, we maximize the expected throughput directly without restricting the precoders to be designed by IA. In this part, individual power constraints are assumed for the users. The contribution of each part can be summarized as follows:

Link adaptation through discrete AMCP:

- We analyze the statistics of the imperfect CSI for MIMO IC with IA.
- We design an adaptive transmission scheme based on the available imperfect CSI.
- In particular, we maximize a weighted sum of the average rates provided that a certain set of bit-error-rate and power constraints are satisfied by dynamically adapting coding, modulation and power settings.
- We provide simulations to show the accuracy of the approximations and the effectiveness of the proposed scheme.

Covariance matrix optimization:

- We propose a new method to determine precoding matrices that achieve local maxima of the expected sum rate in MIMO IC with imperfect CSIT. In particular, the expected sum rate of the K-user MIMO IC is approximated by a deterministic equivalent to which an iterative gradient scheme is applied to find local maxima of the approximated sum rate. The method is based on a random matrix analysis of the capacity of large dimensional Ricean channels.
- The method is shown to be superior to the conventional methods such as unknown error model or Gaussian error model (with known variance) via simulations.

2

Preliminaries

2.1 Wireless Communications

Wireless communications is one of the important areas in the communications field nowadays and it has been under investigation for more than 100 years. Development of new devices with higher computation capabilities and the growing interest for wireless data transfer in different applications have sparked a lot of research activities to deal with the long standing problems such as the optimal transmission strategy in different channels.

Increasing the reliability and efficiency of wireless systems is possible through different means. However these improvements are usually limited by two major problems: fading and interference. Fading which represents a variable channel strength, is resulted form superposition of signals coming from multiple paths with different channel conditions. The other problem which arises in multi-user communications is interference which is created when a receiver listening to its transmitter, also receives unwanted signals from other transmitters operating simultaneously on the same frequency band.

Improving the spectral efficiency and maintaining a reliable communication calls for careful design of wireless systems considering the effects of fading and interference. A common approach is to model their effects as simple impairments (e.g., to consider interference as additive noise). Such approaches usually lead to robust solutions while being sub-optimal. Recent developments suggest that one can exploit fading and interference to reduce their harmful effect. For example space-time codes exploit channel fading to improve the reliability [13] and interference is harnessed in methods such as interference alignment to improve the spectral efficiency [14].

A cellular network is an important example of a wireless network. A cellular network is a multi-user communication environment which exhibits interaction among nodes under fading and interference conditions. A cellular network is composed of a number of cells where each cell is identified by a base station (BS) and a set of mobile users with good communication coverage from the BS. The cells are usually modeled as hexagonal regions with the BS at the center of the cell. In reality the location of the BSs are irregular and the users are assigned to each BS according to the strength of their channel toward a BS. Therefore the cell boundaries will

also have irregular shapes. The BSs are connected to central units via wired networks. The information sent from different users to the BSs arrive at the central units and subsequently dispatched to their destinations via other BSs. As each BS communicates with several users, it should be capable of performing tasks such as multiplexing different signals destined for different users (in downlink) or separating the signals coming from different users (in uplink).

Other type of networks with some similarities to the downlink of cellular networks are the broadcasting systems such as TV and radio. However they operate on different frequency bands and have different data rates. Wireless local area network (LAN) is another type of networks designed to connect the devices in a local area with a high data rate. These networks have a central node which serves the other nodes of the network (similar to the role of a BS in cellular networks). On the other hand, a different type of local area networks is the ad hoc network in which all the nodes participate in network organization in a decentralized manner.

2.1.1 Channel Capacity

The communication rate can be increased by increasing the transmission bandwidth or increasing the transmission power. However bandwidth resources are scarce and the devices have limited transmission power. Therefore the task of efficient exploitation of such resources is of great interest for researchers. The notion of channel capacity was first introduced by Shannon. It is a measure of the maximum rate that can be communicated reliably over a channel [15, 16]. Considering a single-antenna fading channel with the following input output relationship

$$Y = \alpha X + W, \tag{2.1}$$

where X, Y and W are the transmitted signal, the received signal and noise respectively and α is the time-varying channel fade parameter, the capacity is

$$C = B \log(1 + \frac{\alpha P}{B N_0}). \tag{2.2}$$

In (2.2), B is a total bandwidth, N_0 is noise power spectral density, and P is transmit power. As the capacity depends on the channel fade, it will be a random variable. Therefore ergodic (or mean) capacity [16], is often adopted as a performance metric for the fading channel [17–19] which is the expectation of the capacity over different time instances. If the channel fade α can be modeled as a stationary and ergodic stochastic process over time, the ergodic capacity can be computed by taking the expectation of the capacity over the distribution of the channel fade.

2.1.2 Degrees of Freedom

In many channels including the interference channel, where exact characterization of the capacity is not available, approximate capacity characterizations are used to analyze the performance of the channel. In many cases the computation of approximate characterizations is tractable and they become exact in asymptotic cases. One of the useful metrics that is used as a proxy for capacity is the multiplexing gain or degrees of freedom (DoF). DoF is the pre-log factor in the capacity expression at high SNR regime, i.e.,

$$\mathrm{DoF} = \lim_{\mathrm{SNR}\to\infty} \frac{C(\mathrm{SNR})}{\log \mathrm{SNR}}. \tag{2.3}$$

The DoF is a measure of the number of independent parallel channels embedded in a network at high SNR that can be utilized to transmit information. For many channels with unknown capacity regions, DoF regions have been characterized and subsequently used as a measure of the performance which allows us to design the transmit signal that is optimal at high SNR.

2.2 Multiple Antenna Communications

From (2.2) it is clear that the capacity in a single antenna point to point link is limited by bandwidth and power resources. It has been shown that employing multiple antennas at the transceivers can lead to a capacity growth without requiring extra bandwidth or power [20], [21]. In MIMO systems the created paths between every pair of antennas are exploited to communicate with higher data rates or to increase the reliability. In general, MIMO systems can provide two types of advantages: diversity gain and spatial multiplexing gain [22]. Diversity is traditionally exploited to combat the fading and improve reliability in wireless systems. Sending multiple replicas of the information signal through independent fading links is the simplest example of diversity, where the probability that at least one or more of these links experiences a fade increases. Therefore, more reliable communication can be achieved by increasing the number of independent links. Assuming a MIMO point to point link with M transmit and N receive antennas, the maximum achievable diversity gain is equal to NM if the fading corresponding to different antenna pairs are independent. Space-time coding [13, 23, 24] is a coding/modulation scheme to maximize the diversity gain. From another point of view, fading can be beneficial by increasing the degrees of freedom [20, 25]. The use of multiple antennas at both sides creates multiple parallel data pipes within the same frequency band. By transmitting independent information through these spatial directions, the data rate can be increased. This process is called spatial multiplexing which increases the spectral efficiency in MIMO systems without extra power consumption and is therefore very attractive. In [20] and [21], it has been shown that at high SNR, the ergodic capacity for a MIMO channel with M transmit, N receive antennas, and independent and identically distributed (i.i.d.) Rayleigh fading between antenna pairs is given by

$$C = \min(M, N)\log(\mathrm{SNR}) + O(\mathrm{SNR}^{-1})(\mathrm{bps/Hz}), \tag{2.4}$$

which implies that the use of multiple antennas at both sides increases the capacity at high SNR linearly with $\min(M, N)$. It is a significant improvement over the single-antenna system. This linear capacity scaling of MIMO systems requires perfect channel knowledge at the receiver and a scattering environment such that the channel matrix has full rank. Clearly the DoF for this channel is $\min(M, N)$. In recent years, several schemes have been proposed to exploit the spatial multiplexing gain of MIMO systems (see, for example, [25]).

The channel state information is not required at the transmitter to achieve the DoF of a point to point MIMO system. However, it has been shown that in multi-user scenarios, the CSI needs to be exploited at the transmitter side in order to achieve the optimal DoF. This is due to the effect of inter-user interference which is an impairment when several users operate on a shared frequency band.

Spatial degrees of freedom have been characterized for several multiuser communication scenarios with multiple antenna nodes. The (M, N) point to point MIMO channel has $\min(M, N)$ degrees of freedom [20,21],

the (M_1, M_2, N) multiple access channel has $\min(M_1 + M_2, N)$ degrees of freedom [26], the (M, N_1, N_2) broadcast channel (BC) has $\min(M, N_1 + N_2)$ degrees of freedom [27–29], and the (M_1, M_2, N_1, N_2) interference channel has $\min(M_1 + M_2, N_1 + N_2, \max(M_1, N_2), \max(M_2, N_1))$ degrees of freedom [30], where M_i (or M when only one transmitter is present) and N_i (or N when only one receiver is present) indicate the number of antennas at the ith transmitter and receiver, respectively. For the K-user MIMO IC, the DoF region for the general antenna configuration setting is not clear. For symmetric antenna settings, under certain conditions, the total DoF is characterized in [45].

2.3 Interference in Wireless Networks

Interference plays an important role in wireless communication when multiple uncoordinated links share a common communication medium. In wireless systems, interference is usually treated in one of two ways:

- orthogonalize the communication links in time or frequency, so that they do not interfere with each other at all.
- allow the communication links to be active simultaneously, and treat each other's interference as an additive noise.

Clearly both approaches can be sub-optimal. The first approach loses the chance of transmission in both links, regardless of the strength and the shape of the potential interference. The second approach treats interference as pure noise while it can be a structured signal that can potentially be exploited or manipulated to mitigate its effect. A basic information theoretic model to study the general transmission scheme is the two-user Gaussian interference channel, where two point-to-point links with additive white Gaussian noise interfere with each other (Figure 2.1).

2.3.1 Interference Management

Interference created by non-intended transmitters is an inevitable phenomenon in wireless multi-user systems. Devices operating on a common frequency band, if not deployed in sufficiently distant geographical positions, will suffer from interference. Classical scheduling approaches such as multiplexing in time, frequency, etc, are known to provide robustness against interference while proven to be sub-optimal in terms of spectral efficiency. The rapid growth of demand for high rate data transfer along with increasing number of users calls for optimal resource management methods. Therefore the general task of interference management becomes more and more important in the design of future wireless systems.This also calls for adaptive design of the system as the interference management strategies depend on the network load.

First we discuss briefly two dominant types of interference in wireless networks:

Multiple Access Interference

Multi-user communication systems employing multiplexing methods are liable to multiple access interference (MAI). This MAI is due to non-orthogonality associated to multiplexing methods. A simple example is the use

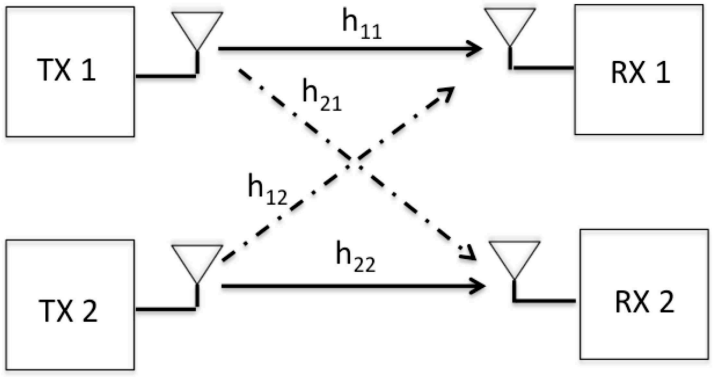

Figure 2.1. Interference Channel

of non-orthogonal spreading codes in code division multiple access (CDMA) systems. The systems that are designed to have orthogonal multiplexing in time or frequency are also subject to MAI due to synchronization errors or multi path effects.

In MIMO multi-user systems where information for different users is multiplexed in the spatial domain, the transmission parameters are designed based on the channel state information. In these systems MAI occurs when the parameters are designed based on inaccurate CSI. The transmission parameters can be optimized to minimize the impact of the resulting MAI. Several multi-user MIMO techniques are provided in [31].

Cochannel Interference

Cochannel interference (CCI), also known as inter-cell interference in the context of cellular networks, arises when users in different cells transmit/receive information simultaneously on the same frequency band. The impact of CCI on the performance of the system depends on the distance between the nodes operating on the same frequency band. In cellular systems the frequency band is divided into a set of orthogonal subbands. The number of cells which cannot use the same frequency subband in the network is called the frequency reuse factor. Figure 2.2 illustrates cellular frequency reuse with reuse factor equal to 3. High reuse factor places the interferers far away which reduces the CCI with the cost of increasing the bandwidth requirement.

The cellular deployments are often designed to tolerate a certain level of CCI for the users. However in extreme cases such as cell-edge users where the interferers are closer to the non-intended users, CCI significantly impacts the performance. Several resource management schemes can be employed to protect the cell-edge users. The recent trend is to develop networks with reuse factor of 1 [32, 33]. Such systems are generally interference-limited and it necessitates the use of powerful interference management schemes.

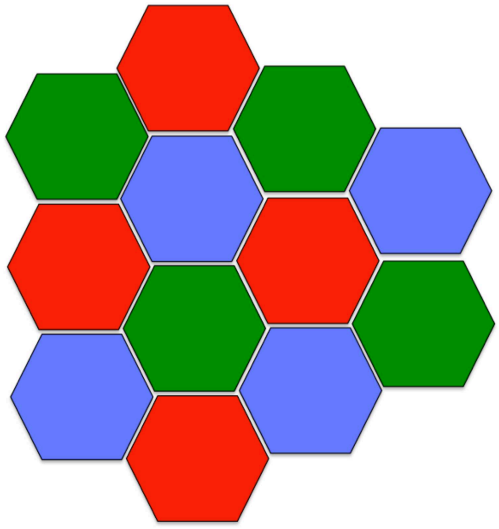

Figure 2.2. Cellular network with frequency reuse factor equal to 3.

Development of Interference Management

The processing capability of wireless devices has increased rapidly in recent years which facilitates implementation of complex interference management schemes. Also the possibility of installing multiple antennas at the BSs has opened the way of introducing multi-user MIMO transmission techniques. The use of multi-carrier systems such as OFDM based systems has resulted in a reliable and efficient communication in multi path environments.

Various advances such as MIMO, OFDM, and CDMA have contributed to the improvement of the communication systems by providing different advantages. With the rapid growth in computational power and reduced size of the devices, schemes that employ a combination of these methods are becoming more popular. Along with these approaches, scheduling and power allocation methods have been able to adapt the designed schemes to the dynamic nature of the networks.

The most recent development in interference management is the new technique of interference alignment [14]. In the interference alignment method, the transmit symbols are precoded over a number of dimensions (time, frequency, space, ...) constructing a subspace which is shaped to confine the resulting interference in a low dimensional subspace at each receiver. In spite of the great theoretical advances in this area since its introduction, practicality of the method is limited to certain conditions and further understanding of the practical implications is necessary. The extent of the applications of the method has made it a hot topic and a promising method which might be a part of interference management technologies in future wireless systems.

2.3.2 Gaussian Interference Channel

The Gaussian interference channel (GIC) is the information-theoretic model for a network consisting of two transmitter/receiver pairs operating over the same communication medium with additive Gaussian noise at the receivers. Cooperation is not allowed between the transmitters or receivers meaning that the nodes cannot share

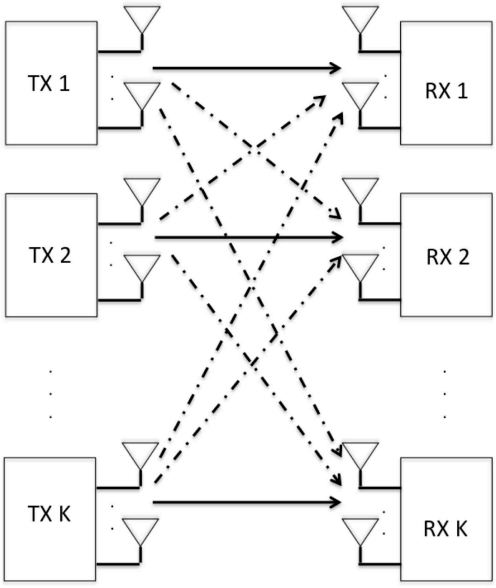

Figure 2.3. K-user MIMO IC

their transmitted or received information. The capacity region of the GIC is the set of rate pairs $(\mathrm{R}_1, \mathrm{R}_2)$ that are simultaneously achievable for the two communication links.

Characterization of the capacity region for the GIC has been an open problem for more than 30 years. A general solution to the problem is not known. However, several attempts have been made such as approximate characterizations or exact solutions in particular cases such as strong interference regime [2,34]. The scheme of Han and Kobayashi [2] provides the best achievable scheme wherein the information of each user is composed of a common and a private part. The common information is to be decoded at both receivers which then facilitates the decoding of the private part by removing the interference associated to the common part. There are three main outer bounds available for the capacity region of the GIC [35], [36], [3].

2.3.3 MIMO Gaussian Interference Channel

In MIMO GIC the nodes are equipped with multiple antennas. In this channel the capacity characterization is more complex than GIC. However the DoF region for this channel is characterized in [30]. When the transmitters have M_1 and M_2 antennas respectively and the the receivers have N_1 and N_2 antennas respectively, assuming that perfect CSI is available at all nodes, the total DoF of the channel is

$$\min(M_1 + M_2, N_2 + N_2, \max(M_1, N_2), \min(M_2, N_1)) \tag{2.5}$$

When more than two (multi-antenna) users share the same communication channel, the model is called

K-user MIMO GIC (Figure 2.3). In the K-user MIMO GIC the DoF region for symmetric antenna cases is characterized using interference alignment. An interesting result is that the total DoF increases with the number of users. However the achievable schemes usually depend on assumptions that are hardly satisfied in practice. In this dissertation, we usually focus on the K-user MIMO GIC. The input/output relationship in this channel reads

$$\mathbf{y}_i = \mathbf{H}_{ii}\mathbf{V}_i\mathbf{x}_i + \sum_{j=1, j\neq i}^{K} \mathbf{H}_{ij}\mathbf{V}_j\mathbf{x}_j + \mathbf{n}_i \tag{2.6}$$

in which $\mathbf{H}_{ij} \in \mathbb{C}^{N\times M}$ is the channel matrix between transmitter j and receiver i, $\mathbf{V}_j \in \mathbb{C}^{M\times d}$ and $\mathbf{x}_j \in \mathbb{C}^d$ are the precoding matrix and the data vector of transmitter j, respectively. Furthermore, $\mathbf{n}_i$ is the additive noise at receiver i whose entries are independent and distributed according to $\mathcal{CN}(0,1)$.

2.3.4 Interference Alignment

Moving from the two-user case to a larger number of users is challenging. Indeed, for K-user IC ($K > 2$), the Han-Kobayashi approach is not capable of managing the interference. Interference alignment is an effective method to deal with the K-user IC. Interference alignment was first introduced in [37] where it was shown to be capable of achieving the full DoF for certain classes of two-user X channels. Using this method, Cadambe and Jafar [14] showed that, a K-user Gaussian interference channel with varying channel gains can achieve a total DoF of $\frac{K}{2}$. Interference alignment provides a solution which forces the interference observed at each receiver to be confined in a low dimensional space. This is done by forcing the transmitters to create interference in overlapping subspaces.

The method is pictured in Figure 2.4 wherein a 3-user MIMO IC is considered and every node has 2 antennas while every transmitter wants to communicate one data symbol. Every transmitter uses a two dimensional vector to precode its data symbol. Without alignment (Figure 2.4, (b)), only two transmitters can be active since the received space is two dimensional and the receivers cannot distinguish between more than two independent vectors. When interference alignment is achieved (Figure 2.4, (a)), clearly all the three transmitters can send their messages since the two interfering vectors at each receiver are aligned in one dimension. This alignment is done by a careful choice of the transmit precoders altogether which necessitates the availability of global CSI at all the transmitters and additionally the knowledge of the subspace at the receiver.

In the case of spatial interference alignment which will be the focus of this dissertation, in a K-user MIMO IC with the channel matrix $\mathbf{H}_{ij} \in \mathbb{C}^{N\times M}$ between transmitter j and receiver i, a solution to the IA problem exists (see [38] and more recently [39, 40] for feasibility criteria – here we will assume that the dimensions are such that the problem is feasible almost surely (a.s.)) iff there exist full rank precoding matrices $\mathbf{V}_j$, $j = 1, \ldots, K$ and projection matrices $\mathbf{U}_i \in \mathbb{C}^{N\times d}$, $i = 1, \ldots, K$ such that

$$\mathbf{U}_i^{\mathrm{H}}\mathbf{H}_{ij}\mathbf{V}_j = \mathbf{0} \qquad \forall i, j \in \{1, \ldots, K\},\ j \neq i, \quad \text{and} \tag{2.7}$$

$$\operatorname{rank}\left(\mathbf{U}_i^{\mathrm{H}}\mathbf{H}_{ii}\mathbf{V}_i\right) = d. \tag{2.8}$$

With this we effectively align the interference at each receiver into a $N - d$ dimensional space, in order to achieve d interference-free dimensions per user. With the assumption that the channel matrices are generic

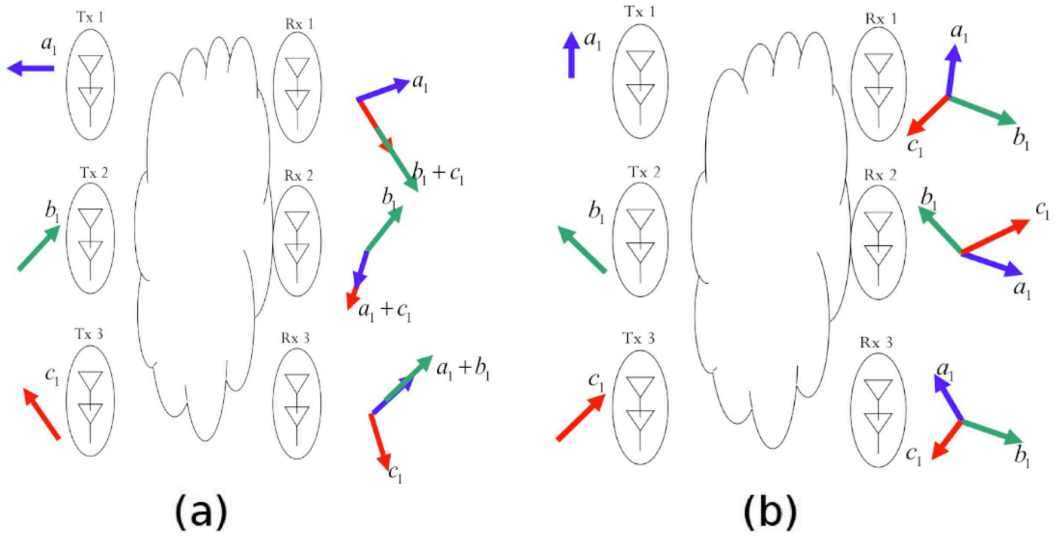

Figure 2.4. Illustration of transmit and receive vectors (a) with and (b) without interference alignment

(i.e., the channel entries are drawn independently according to a continuous distribution), the second condition is satisfied almost surely, hence we usually focus on the first condition. Clearly all the channel matrices (except the direct channels $\mathbf{H}_{ii}$, $i = 1 \dots K$) are required to design the precoders $\mathbf{V}_i$, $i = 1 \dots K$.

3

Interference Management with Quantized CSIT

Interference alignment is known to achieve the optimal DoF in the interference channel. This implies that at high SNR regime, IA improves the system throughput compared to the conventional orthogonal medium-sharing methods. However, implementation of IA in existing systems faces a lot of challenges. The necessity of CSI at the transmitters is one of the major issues which is not practical in many situations. Moreover, the accuracy of the CSIT should increase as the SNR increases in order to guarantee the DoF gains promised by IA [41]. While CSI at the receiver is often assumed to be perfect, to exploit the CSI at the transmitter, it is usually quantized and fed back to the transmitters.

In this chapter, quantization schemes are provided which reduce the amount of information exchange in the network. The proposed methods simplify the analysis of the performance degradation resulting from transmission based on imperfect CSI.

3.1 Background

For practical SNR values, the effect of imperfect CSI on the mutual information of the interference alignment scheme is analyzed in [42], [43], [44]. Tools from random matrix theory are employed in [44] in order to find an approximate expression for signal to interference plus noise ratio (SINR) of each stream when using IA with imperfect CSI. This expression helps to have an estimate of performance measures like sum rate and bit error rate (BER) for IA. In Chapter 6, a statistical analysis is conducted to approximate the sum rate under BER constraints for IA with imperfect CSI. The approximated sum rate is optimized considering adaptive modulation, coding and power while satisfying the BER constraint.

Concerning multi-user systems, the question of the scaling of the size of the codebook used for CSI feedback with increasing SNR has been explored in a number of recent works. Generally speaking, using imperfect CSIT to compute the transmit precoders in a multi-user system causes interference at the receiver side. Since the power of this interference scales with the transmit power, it is necessary to compensate any increase in transmit power by decreasing the quantization error affecting the CSIT, if the interference at the receiver is to remain bounded. This has led several authors to study how the codebook size should scale with the SNR in order to preserve the degrees of freedom achievable with perfect CSI, for several feedback schemes. The case of the broadcast channel was considered first; assuming zero-forcing precoding and single-antenna receivers, it has been determined in [8] that scaling the amount of feedback bits with $(M-1)\log P$ (where M is the number of antennas at the transmitter and P the transmit power) at each receiver is sufficient to achieve full DoF. For the K-user IC (Figure (3.1, a)), most results on CSI quantization focus on transmission schemes based on IA, since IA is instrumental in achieving the channel DoF [14,45]. Specifically, in that context, the CSI feedback problem is considered for L-tap frequency selective single-antenna links in [46], where it is shown that the channel DoF is achievable if the number of bits used to encode the CSI scales with $K(L-1)\log P$. This result was further extended to the $N \times M$ MIMO frequency-selective IC in [47], where $\min\{M,N\}^2 K(RL-1)\log P$ bits (with $R = \lfloor \frac{\max\{M,N\}}{\min\{M,N\}} \rfloor$) are shown to be required to achieve the perfect-CSI DoF. However, both [46] and [47] rely on the same analysis, which is not applicable to the flat-fading case[1].

In [7], the authors introduce two quantization schemes for the MIMO flat-fading K-user IC. The first one is based on quantization on the composite Grassmann manifold (inspired by [47]). The second method improves the quantization accuracy by introducing a virtual receive filter at each receiver which leaves the IA equations invariant; the quantization error can be reduced by optimizing this virtual filter, however the process is computationally complex and must be repeated for each codeword and each channel realization. No asymptotic (high SNR) analysis is provided in [7]; it is easy to figure out that the first considered method requires a scaling of $(K-1)(MN-1)\log P$ to achieve the channel DoF, however the scaling required for the second method to achieve full DoF is not clear.

In the first part of this chapter (Section 3.3) we present a new CSI quantization and feedback scheme for IA over the K-user constant MIMO IC. The proposed feedback scheme exploits the invariances in the IA equations

[1] It is noted in [46] that the result does not hold for low values of L, however the minimum L for which it holds can not be conclusively ascertained from the article. We note that in particular, for the flat-fading case ($L = 1$) of interest in this chapter, both [46] for the single-antenna case and [47] for the MIMO square case ($M = N$) yield a scaling independent of $\log P$, which is unrealistic.

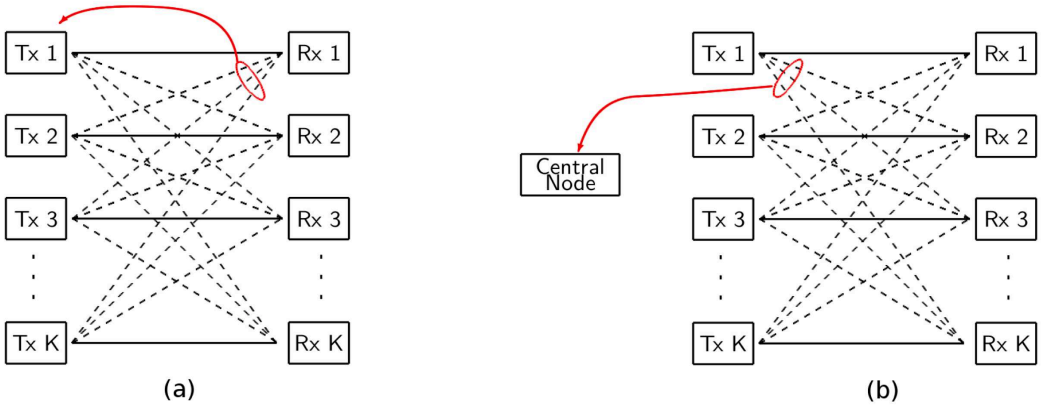

Figure 3.1. (a) CSI feedback over the air, (b) CSI sharing over the backhaul

to reduce the dimension of the quantization space.

Another scenario where quantization of CSI might be necessary happens when each transmitter has access to some local CSI and the transmitters share their local CSI using finite capacity links (Figure (3.1, b)). This scenario arises in TDD systems where the transmitters can acquire information about their downlink channels in the uplink phase by reciprocity. These type of systems are more desirable for implementation of IA. This is due to the fact that the transmission systems which are based on limited feedback from the RXs (such as FDD systems) become very inefficient since the potential gains only appear at high powers.

For TDD systems, network MIMO provides significant gains compared to transmission schemes based on the interference channel. However, the interference channel is adopted very often in particular due to data sharing limitations of network MIMO. These limitations are due to backhaul links which have finite capacity and also introduce delay. In interference channels, even though data is not exchanged between the transmitters, the global CSI needs to be shared in order to attain the degrees of freedom (DoF) of the channel. This highlights the necessity of reducing the amount of CSI exchange.

Considering CSI sharing (that is not perfect in reality), IA is not optimal and the rate saturates due to the leakage introduced by channel mismatch which increases as the transmit power of the interferers increase. Simple time-sharing outperforms IA at high SNR with limited CSI sharing. However middle-range SNR might be of practical interest for implementation of IA if CSI sharing is efficiently designed to be sufficiently accurate. Another limitation is that even with perfect CSI, at low SNR, this scheme is highly suboptimal since the precoders are designed only based on the interfering channels and the direct channels are ignored.

In the medium SNR range, methods based on performance metrics like sum-rate optimization or mean-

squared-error (MSE) minimization are more desirable since they exploit and balance the effect of both interfering channels and direct channels in a meaningful way [48–50]. In such methods the drawback is the requirement of all channel states (also the direct channels) at all the transmitters to compute an identical solution similar to a centralized processing. More liable to distributed implementation are the iterative schemes proposed in [51], [52]. These papers consider downlink precoder design where the transmitters can acquire information about their outgoing channels (denoted by local CSI) from the uplink transmission phase by reciprocity. However their proposed schemes still require some feedback from the receivers at each iteration. With this local CSI assumption, authors in [53] propose an algorithm which improves the sum-rate performance compared to IA in a single-stream setting. However their scheme also requires feedback from the receivers at every iteration.

In the second part of this chapter (Section 3.4), we focus on the scenario where the BSs have perfect but local CSI, and must share it to achieve IA. A CSIT sharing scheme is proposed which reduces the amount of information exchange required for interference alignment in such a system. The scaling (with the transmit power) of the number of bits to be transferred which is sufficient to preserve the multiplexing gain that can be achieved using perfect CSI is derived. In the second part, more general performance criteria like sum rate maximization and MSE minimization are considered. These problems are decoupled into distributed optimization problems using the proposed quantization scheme. The decoupled problems can be tackled at individual transmitters using only local CSI.

3.2 General Definitions

3.2.1 System Model

An interference channel is considered in which K base stations (BS) and K users (one user in each cell) are considered as transmitters and receivers, respectively. For the sake of simplicity of the exposition, we focus on the symmetric case, and assume that each BS has M antennas while each user is equipped with N antennas. These results trivially generalize to non-homogeneous antenna numbers and per-user DoF as long as IA is feasible for the chosen problem dimensions. Each BS employs a linear precoder $\mathbf{V}_j \in \mathbb{C}^{M\times d}$ to transmit d data streams $\mathbf{x}_j \in \mathbb{C}^d$ to its user. The input/output relationship is described by (2.6). Assuming $\mathrm{E}\left[\mathbf{x}_j\mathbf{x}_j^{\mathrm{H}}\right] = \mathbf{I}_d,\ \ j = 1,\ldots,K$, the covariance matrix of the signal transmitted by user j is given as $\mathbf{Q}_j = \mathbf{V}_j\mathbf{V}_j^{\mathrm{H}}$ in which the transmit power for user j is $\mathrm{tr}\left(\mathbf{Q}_j\right) = P_j$. We further assume that the elements of the data symbol are i.i.d. Gaussian random variables. The channels are modeled as

$$\mathbf{H}_{ij} = \sqrt{\gamma_{ij}}\tilde{\mathbf{H}}_{ij} \tag{3.1}$$

where $\tilde{\mathbf{H}}_{ij} \in \mathbb{C}^{N\times M}$ has i.i.d. elements from $\mathcal{CN}(0,1)$ and γ_{ij} denotes the slow-varying shadowing and path loss attenuation. The channels are assumed to be generic [54]; in particular, this includes channels with entries drawn independently from a continuous distribution.

For reference, let us first consider the case where the channel matrices $\mathbf{H}_{ij},\ \forall\ j \neq i$ themselves are known perfectly at the transmitter. The precoders $\mathbf{V}_i,\ i = 1\ldots K$ must be designed to align the interference at

each receiver into a $N-d$ dimensional space according to (2.7), (2.8) in order to achieve d interference-free dimensions per user.

At this point, some remarks are in order. As pointed out in [45], the difficulty in finding an IA solution typically lies in solving eq. (2.7), while (2.8) is fulfilled a.s. under the prevailing channel assumptions for any choice of full-column rank $\mathbf{U}_i$, $\mathbf{V}_j$ matrices. We also remark that despite the symmetry of eq. (2.7) with respect to transposition, only the precoders are required to be known at the transmitters; for a given set of precoders $\mathbf{V}_1,\ldots,\mathbf{V}_K$, the mere knowledge of the *existence* of full-column rank matrices $\mathbf{U}_1,\ldots,\mathbf{U}_K$ fulfilling (2.7) is sufficient to conclude that the precoders are interference-aligning. These considerations lead us to introduce the following definition:

Definition 1 (IA precoders)**.** *The full-column rank precoders $\mathbf{V}_1,\ldots,\mathbf{V}_K$ are interference-aligning for the considered MIMO IC iff there exist full-column rank matrices $\mathbf{U}_1,\ldots,\mathbf{U}_K$ fulfilling* (2.7).

3.2.2 Grassmann Manifold

In this chapter we exploit the symmetry and invariance properties of the underlying quantization variables in the proposed schemes to minimize the required information exchange between the users and to improve the efficiency of the quantization process. The considered quantization variables represent channel subspace information. Subspace information can be efficiently represented using the Grassmann manifold. The Grassmann manifold has been employed in several areas of wireless communications, including codebook design for limited feedback as well as interference alignment [47, 55, 56], space-time code design [57, 58] and many other applications. Therefore, here we briefly discuss the basics of the Grassmann manifold.

Definition of the Grassmann Manifold

The Grassmann manifold, also known as the Grassmannian, $\mathcal{G}_{\mathrm{m,n},\mathbb{K}}$ with $\mathrm{n}\leq\mathrm{m}$ is the set of all n-dimensional subspaces in the m-dimensional vector space $\mathbb{K}^{\mathrm{m}}$, for example with $\mathbb{K}=\mathbb{C}$. In this dissertation, the vector space $\mathbb{K}$ underlying the considered Grassmannian is the Euclidean space of complex numbers; for simplicity it is written as $\mathcal{G}_{\mathrm{m,n}}=\mathcal{G}_{\mathrm{m,n},\mathbb{C}}$. A point $X\in\mathcal{G}_{\mathrm{m,n}}$ on the Grassmann manifold can be represented by any matrix $\mathbf{X}\in\mathbb{C}^{\mathrm{m}\times\mathrm{n}}$ whose columns span the subspace defined by $\mathbf{X}$, i.e., $X=\mathrm{span}(\mathbf{X})$. To unify this representation, orthonormal bases (truncated unitary matrices) are employed throughput this thesis to identify points on the Grassmannian

$$X\in\mathcal{G}_{\mathrm{m,n}} \;\;\Rightarrow\;\; \mathbf{X}^{\mathrm{H}}\mathbf{X}=\mathbf{I}_{\mathrm{n}} \tag{3.2}$$

Distance Measures on the Grassmann Manifold

To determine the distance between points on the Grassmann manifold, several distance measures have been defined in the literature. In limited feedback MIMO wireless communications, three distance measures between two subspaces represented by truncated unitary matrices $\mathbf{X}$ and $\mathbf{Y}$ that are usually employed in the literature are the chordal distance, the projection two-norm and the Fubini-Study distance [55]. In this dissertation we use the chordal distance which is defined as

$$d_c(\mathbf{X},\mathbf{Y}) = \frac{1}{\sqrt{2}}\left|\left|\mathbf{X}\mathbf{X}^{\mathrm{H}} - \mathbf{Y}\mathbf{Y}^{\mathrm{H}}\right|\right|_{\mathrm{F}} \tag{3.3}$$

3.2.3 Feedback Dimension Analysis

In order to make comparisons to the proposed schemes, we consider the following CSI representations:

- **Full channel matrix (FCM):** for a given receiver i, the $K-1$ channel matrices $\mathbf{H}_{ij}$, $j \neq i$ appearing in (2.7) taken together have real dimension $N_{\mathrm{FCM}} = 2(K-1)MN$. In this case the exact channels are quantized to be used in IA equations.

- **Individually normalized channel matrices (INM):** in [7], it is proposed to independently vectorize and normalize the matrices representing the channels from each interferer. At each receiver i, this technique yields $K-1$ unit-norm vectors $\mathbf{z}_{ij} = \frac{\mathrm{vec}(\mathbf{H}_{ij})}{||\mathrm{vec}(\mathbf{H}_{ij})||_2}$, $j \neq i$, which are subsequently quantized jointly on the composite Grassmann manifold $\mathcal{G}_{MN,1}^{K-1}$. The real dimension of this manifold is $N_{\mathrm{INM}} = 2(K-1)(MN-1)$ [47]. TIhe fact that the strength of the channel matrices is irrelevant for computation of IA precoders is exploited in this method to eliminate unnecessary information from the channel matrices and quantize them more efficiently. Furthermore, using this method, the effect of the quantization error on the performance can be quantified using bounds on the Grassmann manifold.

- **Jointly normalized channel matrices (JNM)**[2]: noting that (3.4) can be rewritten as $\left(\mathbf{V}_{-i}^{\mathrm{H}} \otimes \mathbf{U}_i^{\mathrm{H}}\right)\mathrm{vec}(\mathbf{H}_i) = \mathbf{0}$, this approach consists in quantizing $\mathrm{vec}(\mathbf{H}_i)/||\mathrm{vec}(\mathbf{H}_i)||_2$ on $\mathcal{G}_{(K-1)MN,1}$. The real dimension of the fed back variable for this case is $N_{\mathrm{JNM}} = 2((K-1)MN-1)$. This approach is clearly a weaker version of the INM method as it eliminates the channel strength from the total concatenated channel and therefore is not efficient.

3.3 Quantized CSIT Feedback over the Air for FDD Systems

Let us consider the interference alignment problem of [45], and assume that the CSI is fed back from the receivers to the transmitters[3]. Specifically, assume that the ith receiver has perfect knowledge of the channel matrices $\mathbf{H}_{ij}$, $\forall\ j \neq i$ and feeds back the corresponding information to the transmitters so that every transmitter is capable of solving the alignment problem. In this section we consider perfect CSI feedback in order to highlight the intuition behind the dimensionality reduction associated with the proposed feedback scheme. We will further assume that $(K-1)M \geq N$, which represents the cases of interest where interference would occupy all dimensions of the receive subspace in the absence of alignment.

[2]This approach was proposed by an anonymous reviewer of one of our papers.

[3]The underlying assumption here is that all K transmitters can exchange CSI instantaneously and "for free." Alternatively, one can consider a central node (to which all the CSI would be forwarded) where the precoders are computed and subsequently distributed to the transmitters; this distinction is immaterial, and the results presented here apply to both cases. Variations on these assumptions are considered in [59].

3.3.1 Grassmannian Feedback Scheme for IA

Feedback Scheme for Perfect CSI

In order to introduce our proposed scheme, let us note that (2.7) can be rewritten from the point of view of receiver i in the form

$$\mathbf{U}_i^{\mathrm{H}}\mathbf{H}_i\mathbf{V}_{-i} = \mathbf{0} \quad \forall i \in \{1,\dots,K\}, \tag{3.4}$$

in which $\mathbf{V}_{-i} = \mathrm{Bdiag}(\mathbf{V}_1,\dots,\mathbf{V}_{i-1},\mathbf{V}_{i+1},\dots,\mathbf{V}_K) \in \mathbb{C}^{(K-1)M\times(K-1)d}$ is the block-diagonal concatenation of the precoders and $\mathbf{H}_i = [\mathbf{H}_{i\,1},\dots,\mathbf{H}_{i\,i-1},\mathbf{H}_{i\,i+1},\dots,\mathbf{H}_{i\,K}] \in \mathbb{C}^{N\times(K-1)M}$ is the concatenation of the channel matrices of all interfering links ending at receiver i, excluding the direct link. The proposed feedback scheme consists for each receiver i in feeding back only the row space of $\mathbf{H}_i$. Our first result consists in stating that this information is sufficient to perform IA:

Lemma 1. *In order for the IA computation unit to compute interference-aligning precoders $\mathbf{V}_1,\dots,\mathbf{V}_K$, it is sufficient that each receiver $i \in \{1,\dots,K\}$ feeds back a point on the Grassmann manifold $\mathcal{G}_{(K-1)M,N}$ representing the row space of $\mathbf{H}_i$.*

Proof. Let us consider perfect feedback of the row space of $\mathbf{H}_i$, $\forall i \in \{1,\dots,K\}$. Practically, since a linear subspace can be represented by any matrix whose columns span the same space, the Grassmannian feedback considered here can be considered to take the form of the availability at the IA computation unit of a matrix $\mathbf{F}_i$ of dimensions $(K-1)M \times N$ whose columns span the same subspace as the columns of $\mathbf{H}_i^{\mathrm{H}}$ (we assume that $\mathbf{H}_i^{\mathrm{H}}$ has full column rank, which is a.s. the case for generic channel coefficients). We now show that the IA transmit precoders computed by assuming $\mathbf{F}_i^{\mathrm{H}}$ as channel coefficients are interference-aligning for the true channel as well.

Let us consider an IA solution based on $\mathbf{F}_i^{\mathrm{H}}$, i.e. assume that there exist truncated unitary matrices $\tilde{\mathbf{U}}_i$ and $\tilde{\mathbf{V}}_i$ such that the following equation (similar to (3.4)),

$$\tilde{\mathbf{U}}_i^{\mathrm{H}}\mathbf{F}_i^{\mathrm{H}}\tilde{\mathbf{V}}_{-i} = \mathbf{0}, \tag{3.5}$$

is fulfilled for all $i \in \{1,\dots,K\}$. Note that since $\mathbf{H}_i$ and $\mathbf{F}_i^{\mathrm{H}}$ have the same dimensions, the feasibility (a.s.) of IA according to (3.4) and (3.5) is identical. Furthermore, since the columns of $\mathbf{H}_i^{\mathrm{H}}$ and $\mathbf{F}_i$ span the same N-dimensional subspace, there exists an invertible $N \times N$ matrix $\mathbf{C}_i$ such that $\mathbf{H}_i^{\mathrm{H}} = \mathbf{F}_i\mathbf{C}_i$. Clearly,

$$(3.5) \;\Leftrightarrow\; \tilde{\mathbf{U}}_i^{\mathrm{H}}\mathbf{C}_i^{-\mathrm{H}}\mathbf{C}_i^{\mathrm{H}}\mathbf{F}_i^{\mathrm{H}}\tilde{\mathbf{V}}_{-i} = \mathbf{0} \tag{3.6}$$

$$\Leftrightarrow\; \left(\mathbf{C}_i^{-1}\tilde{\mathbf{U}}_i\right)^{\mathrm{H}}\mathbf{H}_i\tilde{\mathbf{V}}_{-i} = \mathbf{0}. \tag{3.7}$$

Comparing to (2.7), eq. (3.7) shows that the rank-d matrices $\mathbf{C}_i^{-1}\tilde{\mathbf{U}}_i$, $i \in \{1,\dots,K\}$ cancel the interference at all receivers, i.e. the transmit precoders $\tilde{\mathbf{V}}_1,\dots\tilde{\mathbf{V}}_K$ forming the block-diagonal of $\tilde{\mathbf{V}}_{-i}$ are interference-aligning over the true channels. □

As already noted, the CSI feedback scheme considered here, is analogous to feeding back a point on the Grassmann manifold $\mathcal{G}_{(K-1)M,N}$ for each one of the K users. Using the fact that the real dimension of $\mathcal{G}_{n,d}$ is $2d(n-d)$ for any $d \leq n$ [60], the real dimension of the feedback outlined in Lemma 1 is $N_{\mathrm{G}} = 2N((K-$

$1)M - N)$. For comparison, let us consider the alternative CSI representations outlined in Section 3.2.3. It is straightforward to establish that $N_{\mathrm{INM}} \leq N_{\mathrm{JNM}} \leq N_{\mathrm{FCM}}$ for all meaningful cases ($K \geq 2$). In the particular case of a square system ($M = N$), we have the following result:

Lemma 2. *In a square system, if IA is feasible, then $N_{\mathrm{G}} < N_{\mathrm{INM}}$, i.e. the proposed scheme always requires strictly less real dimensions than FCM, INM or JNM.*

Proof. A necessary condition for IA to be feasible is [38]

$$d \leq \frac{M+N}{K+1}. \tag{3.8}$$

Together with the assumption that $M = N$ and using the fact that $d \geq 1$, (3.8) yields

$$K \leq \frac{2N}{d} - 1 < 2N. \tag{3.9}$$

Another necessary condition for IA feasibility is $N \geq 2d$, therefore $N > 1$ and consequently $2N < N^2 + 1$. Combining with (3.9), we obtain $K < N^2 + 1$, which is equivalent to $N_{\mathrm{G}} < N_{\mathrm{INM}}$. □

Note that the feedback scheme outlined here for the MIMO IC is in fact directly applicable to many other channel models where IA has been proposed, such as interfering multiple-access channels [61, 62], interfering broadcast channels [63, 64], as well as partially connected interference networks [65, 66].

3.3.2 Quantized CSI Feedback

In this section we introduce a transmission scheme where the alignment equations are solved based on the (error-free) feedback of a quantized version of the CSI, based on the Grassmannian representation from Section 3.3.1. For that scheme, we show how inter-user interference is related to the CSI codebook size, and characterize the required scaling of the codebook for interference to remain bounded at high SNR. For comparison, we also provide a similar analysis for the INM technique.

Grassmannian Quantized CSI

Let us assume that receiver i knows perfectly the state of its channels from all interfering transmitters, i.e. the coefficients of $\mathbf{H}_i$, and performs the economy-size QR decomposition $\mathbf{H}_i^{\mathrm{H}} = \mathbf{F}_i \mathbf{C}_i$, where $\mathbf{F}_i$ is a $(K-1)M \times N$ truncated unitary matrix, and $\mathbf{C}_i$ is $N \times N$ and a.s. invertible, under the prevailing channel assumptions. The use of the QR decomposition is a particular case of the decomposition used in the proof of Lemma 1: it ensures that $\mathbf{H}_i^{\mathrm{H}}$ and $\mathbf{F}_i$ have the same column space, and adds the requirement that the columns of $\mathbf{F}_i$ are orthonormal, which will simplify the subsequent analysis. According to the proposed scheme, receiver i quantizes the subspace spanned by the columns of $\mathbf{F}_i$ using B_{G} bits and feeds the index of the quantized codeword back to the unit in charge of computing the $\mathbf{V}_i$'s. We further assume that the receivers and the

computation unit share a predefined codebook[4] $\mathcal{S} = \{\mathbf{S}_1, \ldots, \mathbf{S}_{2^{B_\mathrm{G}}}\}$ which is composed of 2^{B_G} truncated unitary matrices of size $(K-1)M \times N$ and is designed via Grassmannian subspace packing [67]. The quantized codeword at receiver i is the point in $\mathcal{S}$ closest to $\mathbf{F}_i$, i.e.

$$\hat{\mathbf{F}}_i = \arg\min_{\mathbf{S}\in\mathcal{S}} \; d_c(\mathbf{S}, \mathbf{F}_i) \tag{3.10}$$

Let us consider the scheme where the interference alignment problem is solved at the IA computation unit based on the quantized CSI $\{\hat{\mathbf{F}}_i^{\mathrm{H}}\}_{i=1}^K$, yielding truncated unitary matrices $(\{\tilde{\mathbf{V}}_i\}_{i=1}^K, \{\tilde{\mathbf{U}}_i\}_{i=1}^K)$ fulfilling

$$\tilde{\mathbf{U}}_i^{\mathrm{H}} \hat{\mathbf{F}}_i^{\mathrm{H}} \tilde{\mathbf{V}}_{-i} = \mathbf{0}, \;\; \forall i \in \{1, \ldots, K\}. \tag{3.11}$$

At receiver i, inspired by the perfect feedback situation, we consider the receive filter $\mathbf{G}_i = \mathbf{C}_i^{-1} \mathbf{F}_i^{\mathrm{H}} \hat{\mathbf{F}}_i \tilde{\mathbf{U}}_i$ [5]. Also the transmitter i employs the precoder $\mathbf{V}_j = (\frac{P}{d})^{\frac{1}{2}} \tilde{\mathbf{V}}_j$. Let $\mathbf{y}_i'$ denote the received signal at receiver i after processing by $\mathbf{G}_i$:

$$\mathbf{y}_i' = \mathbf{G}_i^{\mathrm{H}} \mathbf{y}_i = \mathbf{G}_i^{\mathrm{H}} \mathbf{H}_{ii} \mathbf{V}_i \mathbf{x}_i + \mathbf{e}_i + \mathbf{G}_i^{\mathrm{H}} \mathbf{n}_i, \tag{3.12}$$

where the term

$$\mathbf{e}_i = \sum_{\substack{1 \le j \le K \\ j \neq i}} \mathbf{G}_i^{\mathrm{H}} \mathbf{H}_{ij} \mathbf{V}_j \mathbf{x}_j \tag{3.13}$$

is the interference leakage due to the imperfect CSI.

Generally speaking, the aim of our analysis is to provide sufficient conditions on the CSI quantization accuracy to ensure that $\mathcal{I}(\mathbf{x}_i; \mathbf{y}_i)$ grows with $d \log P$; $\mathbf{G}_i$ and $\mathbf{y}_i'$ are merely intermediate variables used to establish information-theoretic inequalities. In a practical system, we expect the equalizer $\mathbf{G}_i$ to be computed through classical channel estimation and equalization techniques – we omit these details here.

In the remainder of this section, we will focus on establishing bounds on the interference power $L_i = \mathrm{tr}\left(\mathrm{E}_{\mathbf{x}}(\mathbf{e}_i \mathbf{e}_i^{\mathrm{H}})\right)$; these results will be instrumental in proving our DoF result. We first establish in Lemma 3 and Corollary 1 the growth rate of the number of feedback bits with the SNR which guarantees that L_i remains bounded by a constant regardless of P when $P \to \infty$.

Lemma 3. *The interference leakage power (due to imperfect CSI) at receiver i can be bounded as*

$$L_i \le \frac{8P}{\left(c\, 2^{B_\mathrm{G}}\right)^{\frac{2}{N_\mathrm{G}}}} \left(1 + o\left(2^{-\frac{B_\mathrm{G}}{N_\mathrm{G}}}\right)\right) \tag{3.14}$$

[4] For notational simplicity we omit the dependency of $\mathcal{S}$ on i, however the proposed analysis generalizes trivially to cases where $\mathcal{S}$ and B_G are different across the receivers, as will be seen in Section 3.3.2.

[5] We note that if the quantization error is null, i.e. $d_c(\hat{\mathbf{F}}_i, \mathbf{F}_i) = 0$, then $\mathbf{F}_i^{\mathrm{H}} \hat{\mathbf{F}}_i$ is a unitary matrix corresponding to the uncertainty between the CSI encoder (at the receiver) and decoder (at the IA computation unit) in the matrix representation of the subspace being fed back.

where $N_{\mathrm{G}} = 2N((K-1)M-N)$ is the real dimension of $\mathcal{G}_{(K-1)M,N}$ introduced before, and c is the coefficient of the ball volume in the Grassmann manifold,

$$c \triangleq \frac{1}{\big(N((K-1)M-N)\big)!} \frac{\prod_{i=1}^{N}\big((K-1)M-i\big)!}{\prod_{i=1}^{N}\big(N-i\big)!}. \tag{3.15}$$

Proof. See appendix A.1. □

Corollary 1. *Quantizing CSI with*

$$B_{\mathrm{G}} = N((K-1)M-N)\log P \tag{3.16}$$

bits is sufficient to keep the interference leakage L_i bounded by a constant for arbitrarily large P.

Proof. From (3.14), since $o\left(2^{-\frac{B_{\mathrm{G}}}{N_{\mathrm{G}}}}\right) \to 0$ for large P, it is obvious that L_i is bounded by a constant if $2^{\frac{2B_{\mathrm{G}}}{N_{\mathrm{G}}}}$ scales at least linearly with P; in particular this holds for

$$B_{\mathrm{G}} = \frac{N_{\mathrm{G}}}{2}\log P = N((K-1)M-N)\log P. \tag{3.17}$$

□

Comparison to Naive Quantization

For comparison, let us now consider quantization for the INM method[6] chosen as a baseline in [7]. We recall that in that case, at receiver i the matrices representing the channels from the interferers are vectorized and normalized independently, yielding $K-1$ unit-norm vectors $\mathbf{z}_{ij} = \frac{\mathrm{vec}(\mathbf{H}_{ij})}{||\mathrm{vec}(\mathbf{H}_{ij})||_2}$, $j \neq i$. $\mathbf{Z}_i = [\mathbf{z}_{i1}, \ldots, \mathbf{z}_{i\,i-1}, \mathbf{z}_{i\,i+1}, \ldots, \mathbf{z}_{iK}] \in \mathcal{G}_{MN,1}^{K-1}$ is subsequently quantized according to

$$\hat{\mathbf{Z}}_i = \arg\min_{\mathbf{T}\in\mathcal{T}} \; D_c(\mathbf{T}, \mathbf{Z}_i), \tag{3.18}$$

where $D_c(\mathbf{T}, \mathbf{Z}_i) = \sqrt{\mathrm{tr}\left(\mathbf{I}_{\mathrm{K}-1} - \mathbf{T}^{\mathrm{H}}\mathbf{Z}_{\mathrm{i}}\right)}$ is the chordal distance defined for the composite Grassmann manifold. Let B_{INM} denote the number of feedback bits, i.e. $|\mathcal{T}| = 2^{B_{\mathrm{INM}}}$. At the transmitter side, the columns of $\hat{\mathbf{Z}}_i = [\hat{\mathbf{z}}_{i1}, \ldots, \hat{\mathbf{z}}_{i\,i-1}, \hat{\mathbf{z}}_{i\,i+1}, \ldots, \hat{\mathbf{z}}_{iK}]$ are used to reconstruct the quantized CSI: the channel matrices $\hat{\mathbf{H}}_{ij}$ used for the computation of the precoders are such that $\mathrm{vec}(\hat{\mathbf{H}}_{ij}) = \hat{\mathbf{z}}_{ij}$, $\forall i \neq j$. The interference alignment problem is then solved based on $\hat{\mathbf{H}}_{ij}$ to find $(\{\tilde{\mathbf{V}}_i\}_{i=1}^K, \{\tilde{\mathbf{U}}_i\}_{i=1}^K)$ fulfilling

$$\tilde{\mathbf{U}}_i^{\mathrm{H}}\hat{\mathbf{H}}_{ij}\tilde{\mathbf{V}}_j = \mathbf{0}, \;\; \forall i,j \in \{1,\ldots,K\}, \; j \neq i. \tag{3.19}$$

We now show that the leakage obtained by employing $\mathbf{V}_j = (\frac{P}{d})^{\frac{1}{2}}\tilde{\mathbf{V}}_j$ and $\tilde{\mathbf{U}}_i$, $\bar{L}_i = \frac{P}{d}||\tilde{\mathbf{U}}_i^{\mathrm{H}}\mathbf{H}_{ij}\mathbf{V}_j||_{\mathrm{F}}^2$ (using the true channel matrices) can remain bounded for arbitrarily large transmit power P under certain conditions. This is the object of Lemma 4, where we establish the scaling of B_{INM} with P required to achieve bounded interference leakage under this scheme.

[6] The authors of [7] attribute this method to [47]. Although quantization bounds for the composite Grassmann manifold are presented in [47], we note that the (frequency-selective) channel model in that paper is different from the flat-fading model considered here and in [7], and therefore the results are not immediately comparable.

Lemma 4. *Using the INM quantization scheme, quantizing* $\mathbf{Z}_i$ *with* $B_{\mathrm{INM}} = \frac{1}{2}N_{\mathrm{INM}}\log P = (K-1)(MN-1)\log P$ *bits is sufficient to keep* $\bar{L}_i$ *bounded for arbitrarily large* P*.*

Proof. See appendix A.2. □

Comparing the above result with the scaling obtained in Corollary 1 for the proposed scheme indicates that at high SNR, $B_{\mathrm{G}} < B_{\mathrm{INM}}$ (i.e. the proposed method outperforms INM) iff $N_{\mathrm{G}} < N_{\mathrm{INM}}$. As already analyzed in Lemma 2, this condition is fulfilled for many case of practical interest.

Rate-Loss due to CSI Quantization

In the previous section, we have used interference leakage as a proxy to evaluate how the quality of the available CSI influences alignment. Note however that having a bounded interference leakage is not sufficient in itself to ensure that the full DoF is achieved for asymptotically large P – in fact, the power of the signal of interest remaining after processing by the receive filter (eq. (3.12)) could remain bounded too, or its rank could be reduced. We now show that this is not the case, and that the proposed CSI quantization scheme achieves the same DoF as IA under the perfect CSI assumption, provided that the proper scaling of B_{G} with P is respected:

Theorem 1. *If IA with* d *DoF is feasible, the proposed CSI quantization scheme achieves* d *DoF for almost all channel realizations if* B_{G} *is scaled according to* (3.16).

Remark 1: Theorem 1 is not restricted to a particular distribution of the channel coefficients. The restriction to "almost all" channel realizations is due to the fact that under the assumptions of Section 3.2, there can exist a vanishing set of channel realizations for which (2.8) is not fulfilled; this is also the case when perfect CSI is considered [45], and is unrelated to the proposed quantization scheme.

Remark 2: The transmission scheme considered here is based on truncated unitary precoders $\tilde{\mathbf{V}}_j$, and therefore the transmitted signal is spatially white inside the d-dimensional subspace defined by the precoder. Clearly, this is suboptimal for finite values of the SNR, and spatial waterfilling in addition to IA would bring in performance improvement for $d > 1$. However, we remark that the performance gains of waterfilling vanish at asymptotically high SNR, provided that the channel is not rank deficient [68]. Therefore, the asymptotic analysis of this section holds regardless of whether spatial waterfilling is used in addition to IA or not.

Theorem 1 states that $\lim_{P\to\infty}\frac{R_i}{\log P} = d$ a.s.; in order to show this, we require a few intermediate results. Let us define the following values: $R_i \triangleq \mathcal{I}(\mathbf{x}_i;\mathbf{y}_i)$, $R_i' \triangleq \mathcal{I}(\mathbf{x}_i;\mathbf{y}_i')$ and $R_i'' \triangleq \log\left|\mathbf{G}_i^{\mathrm{H}}\mathbf{G}_i + \mathbf{Q}_{\mathrm{S}}^i\right|$ where $\mathbf{Q}_{\mathrm{S}}^i = \mathbf{G}_i^{\mathrm{H}}\mathbf{H}_{ii}\mathbf{V}_i\mathbf{V}_i^{\mathrm{H}}\mathbf{H}_{ii}^{\mathrm{H}}\mathbf{G}_i$ is the covariance of the signal of interest. From the data processing inequality and the definition of $\mathbf{y}_i'$, we have immediately that $R_i \geq R_i'$. In what follows, we will successively show that $R_i'' - R_i'$ remains bounded from above if B_{G} is scaled according to (3.16) (Lemma 5), and that $\lim_{P\to\infty}\frac{R_i''}{\log P} = d$ (Lemma 6). Let us start with the first result. Since all signal and noise terms are Gaussian circularly symmetric, we have

$$R_i' = \log\left|\mathbf{G}_i^{\mathrm{H}}\mathbf{G}_i + (\mathbf{Q}_{\mathrm{S}}^i + \mathbf{Q}_{\mathrm{I}}^i)\right| - \log\left|\mathbf{G}_i^{\mathrm{H}}\mathbf{G}_i + \mathbf{Q}_{\mathrm{I}}^i\right| \tag{3.20}$$

in which $\mathbf{Q}_{\mathrm{I}}^{i} = \mathbf{G}_i^{\mathrm{H}}\mathbf{H}_i\mathbf{V}_{-i}\mathbf{V}_{-i}^{\mathrm{H}}\mathbf{H}_i^{\mathrm{H}}\mathbf{G}_i$ is the covariance of the residual interference.

Lemma 5. *Under the quantization scheme of Section* 3.3.2*, the difference between R_i' and R_i'' can be bounded as*

$$R_i'' - R_i' \leq d \log\left(||\mathbf{C}_i^{-1}||_2^2 + \frac{8P}{(c\,2^{B_{\mathrm{G}}})^{\frac{2}{N_{\mathrm{G}}}}}\left(1 + o\left(2^{-\frac{B_{\mathrm{G}}}{N_{\mathrm{G}}}}\right)\right)\right). \tag{3.21}$$

Proof. See Appendix A.3. □

Lemma 6. *Under the proposed CSI quantization scheme, there exists a series of codebooks of increasing size following* (3.16) *for $P \to \infty$ s.t. $\lim_{P\to\infty} \frac{R_i''}{\log P} = d$ a.s.*

Proof. See Appendix A.4. □

We are now in the position to prove Theorem 1:

Proof. Substituting $P = 2^{\frac{2B_{\mathrm{G}}}{N_{\mathrm{G}}}}$ in the result of Lemma 5 yields

$$R_i' \geq R_i'' - d \log\left(||\mathbf{C}_i^{-1}||_2^2 + \frac{8}{c^{2/N_{\mathrm{G}}}}\left(1 + o\left(2^{-\frac{B_{\mathrm{G}}}{N_{\mathrm{G}}}}\right)\right)\right). \tag{3.22}$$

As $P \to \infty$ and with B_{G} following (3.16), the argument of the logarithm remains bounded by a constant, therefore

$$\lim_{P\to\infty} \frac{R_i'}{\log P} \geq \lim_{P\to\infty} \frac{R_i''}{\log P} = d \quad \text{a.s.} \tag{3.23}$$

using the result from Lemma 6. □

Average Rate-Loss under RVQ

Note that the results established so far hold for any codebook obtained by sphere-packing. Let us now briefly depart from this assumption, and consider RVQ instead. In that case, the previous results do not apply: the random choice of the codebook can lead to arbitrarily bad performance regardless of B_{G}, and bounding the performance loss uniformly over all codebooks is impossible. A more relevant performance metric for RVQ is the average sum rate over all possible codebooks. We have the following result:

Theorem 2. *Provided that the codebook $\mathcal{S}$ is generated from independent realizations of a random process uniformly distributed over $\mathcal{G}_{(K-1)M,N}$, the expectation over $\mathcal{S}$ of R_i is lower bounded as*

$$\mathrm{E}_{\mathcal{S}}(R_i) \geq R_i'' - d \log\left(||\mathbf{C}_i^{-1}||_2^2 + 2P\frac{\Gamma(\frac{2}{N_{\mathrm{G}}})}{\frac{N_{\mathrm{G}}}{2}(c\,2^{B_{\mathrm{G}}})^{\frac{2}{N_{\mathrm{G}}}}}\right), \tag{3.24}$$

where $\Gamma(\cdot)$ denotes the Gamma function.

Proof. See Appendix A.5. □

Per-User DoF for Asymmetric Feedback

An interesting consequence of the rate-loss analysis conducted previously can be observed when each receiver uses its own scaling of the CSI quantization codebook size with P. Formally, let B_{G}^{i} denote the number of bits used by receiver i to quantize $\mathbf{F}_i$.

Corollary 2. *If B_{G}^{i} scales with P such that*

$$\alpha_i \triangleq \lim_{P\to\infty} \frac{B_{\mathrm{G}}^{i}}{N_{\mathrm{G}}/2 \cdot \log P} \tag{3.25}$$

exists and is finite, then the DoF achievable by user i is

$$d_i^{\mathrm{q}} \geq d_i^{\mathrm{p}} \min\left(\alpha_i, 1\right), \tag{3.26}$$

where d_i^{p} is the achievable DoF of this user with perfect CSI.

Proof. The proof follows simply from (3.21) by taking the limit of the lower bound when $P \to \infty$. □

Practically, this means that the DoF achieved by a given user is independent of the quality of the feedback provided by the other users. This observation, obtained here for IA precoding, is consistent with the scaling obtained in [69] for centralized schemes using different precoding schemes such as zero-forcing.

3.3.3 Performance Investigation

This section presents simulations that numerically validate the results hitherto established. Note that constructing good Grassmannian packings for arbitrary dimensions is difficult [70]; therefore, in our simulations for relatively small codebook sizes (up to 2^{15}) we resort to random codebooks in place of sphere-packing codebooks. Note that the performance expected from RVQ codebooks constitutes a lower bound to the performance of sphere-packing codebooks; however as we shall see, in our simulations, RVQ codebooks attain the performance predicted for the sphere-packing codebooks.

For larger codebooks ($B_{\mathrm{G}} > 15$), even RVQ is not tractable due to the complexity of the exhaustive search through $\mathcal{S}$ in (3.10). Due to the lack of structured codebooks allowing a tractable implementation of the quantizer, the performance obtained for larger codebooks is extrapolated by using a perturbation method based on the analytical characterization of the distribution of the quantization error, the details of which being presented in Appendix A.6.

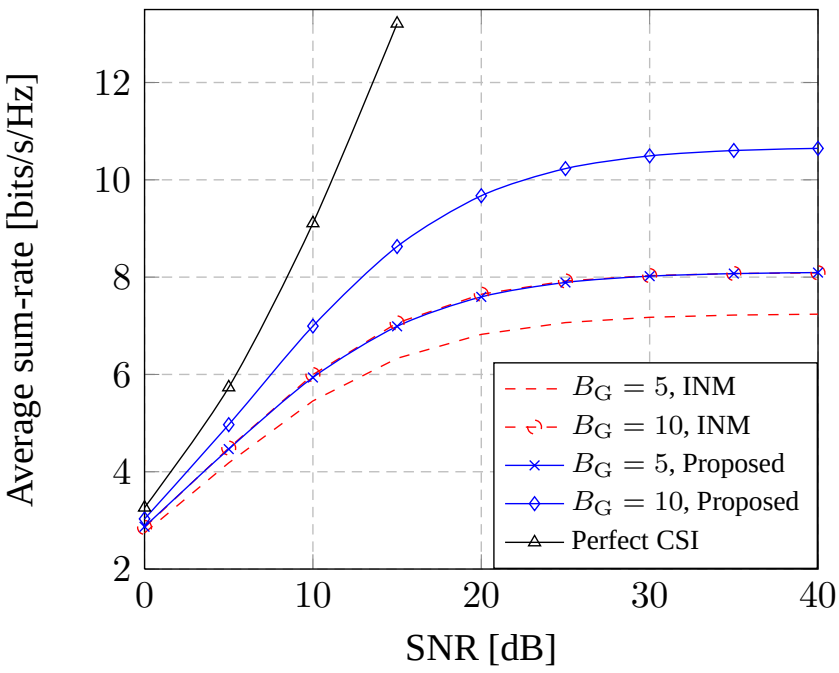

Figure 3.2. Average R_{sum} for various quantization methods, for the 3-user MIMO IC, $N = M = 2$.

Performance Results Using RVQ

In this section, we evaluate the performance of the quantization scheme of Section 3.3.2 with RVQ codebooks. The performance metric is the sum rate evaluated through Monte-Carlo simulations. The sum rate achievable over the MIMO IC using interference alignment precoders under the assumption that the input signals are Gaussian can be written as

$$R_{\mathrm{sum}} = \sum_{i=1}^{K} \log \left| \mathbf{I}_N + \frac{P}{d} \sum_{j=1}^{K} \mathbf{H}_{ij} \mathbf{V}_j \mathbf{V}_j^{\mathrm{H}} \mathbf{H}_{ij}^{\mathrm{H}} \right| - \sum_{i=1}^{K} \log \left| \mathbf{I}_N + \frac{P}{d} \sum_{j=1, j \neq i}^{K} \mathbf{H}_{ij} \mathbf{V}_j \mathbf{V}_j^{\mathrm{H}} \mathbf{H}_{ij}^{\mathrm{H}} \right|. \tag{3.27}$$

A 3-user IC with $M = N = 2$ antennas per node and $d = 1$ data stream for each transmitter is considered. Entries of the channel matrices are generated according to $\mathcal{CN}(0, 1)$ and the performance results are averaged over the channel realizations. The method proposed in Section 3.3.2 is compared to the INM quantization method from Section 3.2.3.

For the proposed method, the codebook entries are independent $(K-1)M \times N$ random truncated unitary matrices generated from the Haar distribution. For the INM method, random unit norm vectors are used in the codebook construction. Figure 3.2 shows the achievable sum rate versus transmit SNR for $B_{\mathrm{G}} = 5$ and 10 feedback bits when the precoders are designed based on the quantized feedback. Clearly the proposed scheme outperforms INM quantization for the same number of feedback bits. It can be also seen that for a fixed number of feedback bits, the sum-rate saturates at high SNR, while it grows unbounded (with the slope equal to the DoF) for the perfect CSI case.

The sum rate in (3.27) is achievable when optimum receivers (not including the projection filters $\mathbf{G}_i^{\mathrm{H}}$) are used at the receivers. Since the achievable scheme in Section 3.3.2 is using the projection filters $\mathbf{G}_i^{\mathrm{H}}$, we

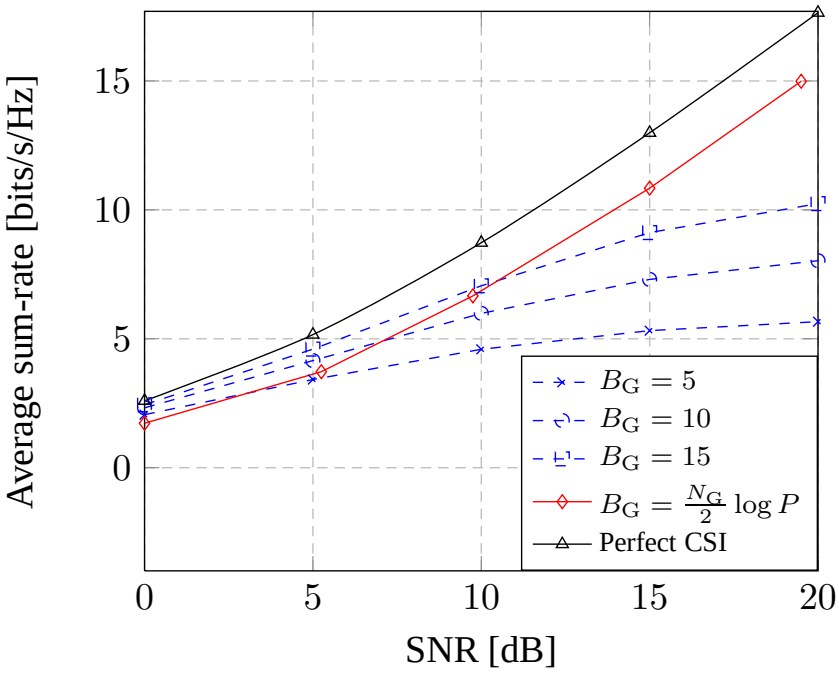

Figure 3.3. Sum-rate according to (3.28) of the proposed method for different number of bits, for the 3-user MIMO IC, $N = M = 2$.

evaluated the performance achieved by this scheme, defined as

$$R'_{\mathrm{sum}} = \sum_{i=1}^{K} \log \left| \mathbf{G}_i^{\mathrm{H}} \mathbf{G}_i + \frac{P}{d} \sum_{j=1}^{K} \mathbf{G}_i^{\mathrm{H}} \mathbf{H}_{ij} \mathbf{V}_j \mathbf{V}_j^{\mathrm{H}} \mathbf{H}_{ij}^{\mathrm{H}} \mathbf{G}_i \right| - \sum_{i=1}^{K} \log \left| \mathbf{G}_i^{\mathrm{H}} \mathbf{G}_i + \frac{P}{d} \sum_{j=1, j \neq i}^{K} \mathbf{G}_i^{\mathrm{H}} \mathbf{H}_{ij} \mathbf{V}_j \mathbf{V}_j^{\mathrm{H}} \mathbf{H}_{ij}^{\mathrm{H}} \mathbf{G}_i \right|. \tag{3.28}$$

Results are provided in Figure 3.3. The slope of the curves at high SNR gives an indication of the achieved DoF. It is clear from Figure 3.3 that the slope of the sum-rate curve with quantized feedback matches that of perfect CSI when the number of feedback bits is scaled according to (3.16) (here we have used $B_{\mathrm{G}} = [0,\ 7,\ 13,\ 20,\ 26]$ bits and the corresponding powers $P = 2^{\frac{2B_{\mathrm{G}}}{N_{\mathrm{G}}}}$). Conversely, when the codebook size is fixed, the performance always saturates at high SNR, with the achieved performance depending on the codebook size. Simulations were performed only up to $20\,\mathrm{dB}$ SNR due to the complexity associated to the growth of the codebook size with P.

Perturbations on the Grassmann Manifold

In order to validate the DoF results of Section 3.3.2, an evaluation of the achieved sum-rate at high SNR is required. In order to deal with exponentially large codebooks, we propose to replace the quantization process with a perturbation which approximates the quantization error. In other words, we propose to replace $\hat{\mathbf{F}}_i$ by a matrix that can be computed directly by an appropriate perturbation of $\mathbf{F}_i$. This approach provides a good approximation of the achievable performance, while sparing the complexity associated with the codebook generation and the quantization in RVQ. The perturbation method appears in Appendix A.6.

Simulations were performed in order to validate experimentally the perturbation method proposed above.

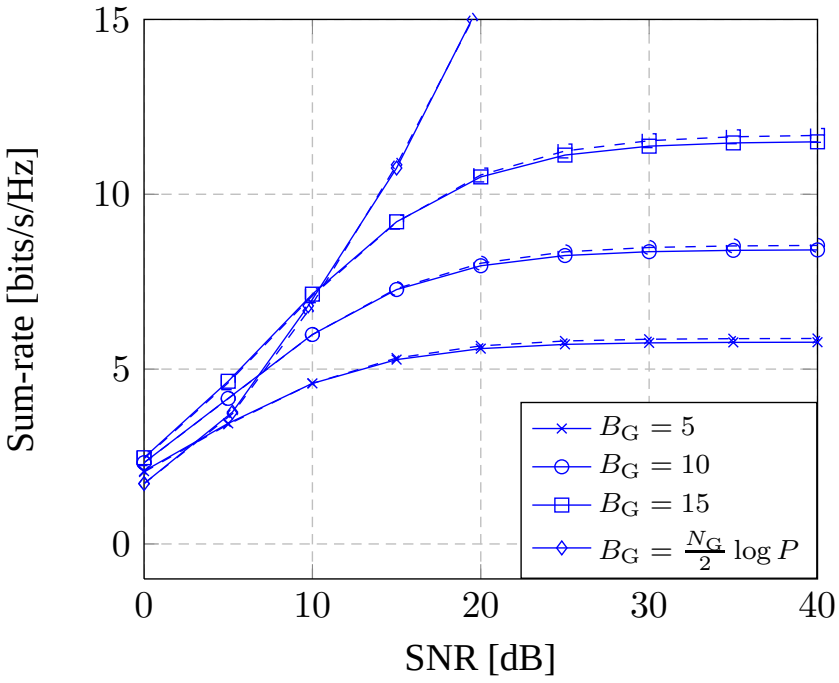

Figure 3.4. Comparison of the perturbation scheme from Appendix A.6 (solid) to the real quantizer (3.10) (dashed), for the 3-user MIMO IC, $N = M = 2$.

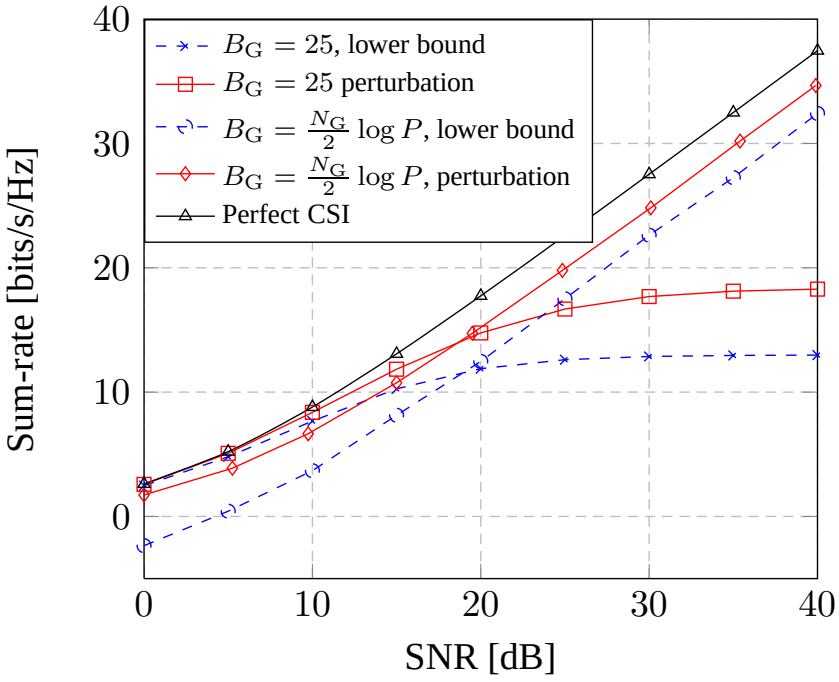

Figure 3.5. Sum rate performance using the perturbation method compared to perfect CSI and the lower bound derived in (3.24), for the 3-user MIMO IC, $N = M = 2$.

The sum-rate performance achieved by IA for the CSI obtained from the perturbation method is plotted against the performance obtained for the actual quantization scheme in Figure 3.4. It is clear that the proposed perturbation method accurately approximates the Grassmannian quantization process, even for small codebooks.

Validation of the DoF Results

We now use the perturbation technique introduced in the previous section to analyze the CSI feedback scheme from Section 3.3.2 in the high SNR regime. Figure 3.5 depicts the sum rate performance using the perturbation method compared to perfect CSI and to the lower bound derived in (3.24). The slope of the sum rate at high SNR regime obtained for the quantizer with $B_{\mathrm{G}} = \frac{N_{\mathrm{G}}}{2} \log P$ bits is identical to that of perfect CSI, as is the case for the lower bound derived in (3.24).

3.4 Quantized CSIT Sharing over the Backhaul for TDD Systems

In this section we assume equal transmit power for all BSs, i.e., $P_j = P,\ \forall j$. Let us consider TDD transmission. Specifically, we assume that the jth BS estimates the channel matrices $\mathbf{H}_{ij},\ i = 1, \ldots, K,\ i \neq j$ (denoted by *local CSI*) from the uplink phase, via reciprocity. We first assume that local CSI is known perfectly at BS j. However, global CSI (excluding the direct channels $\mathbf{H}_{ii}$) is required in order to design IA precoders. In this section we consider CSI exchange in the network, and work under the assumption that perfect local CSI is conveyed from each BS to a processing node which computes all precoders and provides them to the BSs (Figure 3.1, (b)).

3.4.1 Efficient CSI Sharing for IA with Grassmannian Representation

Here we assume a feasible IA setting [45], i.e. there exist precoding matrices $\mathbf{V}_j,\ j = 1, ..., K$ and projection matrices $\mathbf{U}_i \in \mathbb{C}^{N \times d},\ i = 1, ..., K$ that satisfy (2.7) and (2.8). Condition (2.7) can be rewritten as

$$\mathbf{U}_{-j}^{\mathrm{H}} \mathbf{H}_j \mathbf{V}_j = \mathbf{0} \quad \forall j \in \{1, ..., K\}, \tag{3.29}$$

in which $\mathbf{U}_{-j} = \mathrm{Bdiag}(\mathbf{U}_1, \ldots, \mathbf{U}_{j-1}, \mathbf{U}_{j+1}, \ldots, \mathbf{U}_K)$ and $\mathbf{H}_j = [\mathbf{H}_{1,j}^{\mathrm{H}}, ..., \mathbf{H}_{j-1,j}^{\mathrm{H}}, \mathbf{H}_{j+1,j}^{\mathrm{H}}, ..., \mathbf{H}_{K,j}^{\mathrm{H}}]^{\mathrm{H}}$ is a $(K-1)N \times M$ matrix.

We will further assume that $(K-1)N > M$, which represents the cases where transmitter-side zero-forcing is not sufficient to eliminate all interference, and therefore IA is required. The following lemma highlights the intuition behind our CSI sharing scheme.

Lemma 7. *In order to design IA precoders, it is sufficient that each BS j sends a point on the Grassmann manifold $\mathcal{G}_{(K-1)N,M}$ representing the column space of $\mathbf{H}_j$ to the IA processing node.*

Proof. Let $\mathbf{F}_j$ denote a $(K-1)N \times M$ matrix containing an orthonormal basis of the column space of $\mathbf{H}_j$, i.e. $\mathbf{H}_j = \mathbf{F}_j \mathbf{C}_j$ for some $M \times M$ matrix $\mathbf{C}_j$ (invertible almost surely for generic channels). According to our assumption that only the column space of $\mathbf{H}_i$ is known at the central unit, we can assume that the central unit

has only access to a rotated version of $\mathbf{F}_j$, i.e., $\mathbf{F}_j\mathbf{O}_j$ for some unknown $M \times M$ unitary matrix $\mathbf{O}_j$. We now show that alignment can be achieved based on the knowledge of $\mathbf{F}_j\mathbf{O}_j$ rather than of $\mathbf{H}_j$. Let us assume that the processing node designs a set $(\{\tilde{\mathbf{U}}_j\}_{j=1}^K, \{\tilde{\mathbf{V}}_j\}_{j=1}^K)$ of IA transmit precoders and receive projection filters for the channels $\{\mathbf{F}_j\mathbf{O}_j\}_{j=1}^K$ using (3.29). Then, $\forall j$

$$\tilde{\mathbf{U}}_{-j}^{\mathrm{H}}(\mathbf{F}_j\mathbf{O}_j)\tilde{\mathbf{V}}_j = \mathbf{0} \;\Rightarrow\; \tilde{\mathbf{U}}_{-j}^{\mathrm{H}}\mathbf{F}_j\mathbf{C}_j\mathbf{C}_j^{-1}\mathbf{O}_j\tilde{\mathbf{V}}_j = \mathbf{0} \tag{3.30}$$

$$\Rightarrow\; \tilde{\mathbf{U}}_{-j}^{\mathrm{H}}\mathbf{H}_j\mathbf{C}_j^{-1}\mathbf{O}_j\tilde{\mathbf{V}}_j = \mathbf{0}. \tag{3.31}$$

This indicates that IA is achieved over the actual channel by using $\mathbf{C}_j^{-1}\mathbf{O}_j\tilde{\mathbf{V}}_j$ as precoder and $\tilde{\mathbf{U}}_j$ as the projection filter at user j. Assuming that $\tilde{\mathbf{V}}_j$ is transmitted from the processing node back to BS j, and that $\mathbf{O}_j$ is known at BS j since the reconstruction codebook of the processing node is known, the BS is in a position to compute the precoder $\mathbf{C}_j^{-1}\mathbf{O}_j\tilde{\mathbf{V}}_j$. □

Note that the feedback of $\tilde{\mathbf{V}}_j$ from the processing node to BS j also takes the form of a point on $\mathcal{G}_{M,d}$, and will be analyzed in further detail in the sequel.

Analogy to the CSI Feedback Problem

Clearly the Grassmannian representation outlined in Section 3.4.1 is very similar to the analysis conducted for the FDD systems in Section 3.3.1. For FDD systems the quantization variable is the subspace corresponding to the concatenation of the incoming channels toward a given receiver while in the TDD systems the outgoing channels from a given transmitter are concatenated. Different topologies arise in the TDD case as we have a CSI sharing scheme rather than a feedback scheme. For example one of the transmitters can play the role of the central node. In the designed transmission scheme for quantized feedback in FDD case, the IA precoders are modified while in the TDD case the IA projection filters need to be transformed. As will be seen later, unlike the FDD systems, this modification of the receive filters in the TDD case changes the covariance of the noise which has to be taken into consideration.

3.4.2 Quantized CSI Sharing over Finite-Capacity Links

In this section, using the Grassmannian representation outlined in the previous section, we explore several scenarios where CSI is quantized and exchanged between the nodes over finite capacity links. Three different scenarios regarding the CSIT sharing problem can be considered:

I. The IA processing node is a separate central node that computes and distributes the IA precoders to the K BSs,

II. One BS also acts as the IA processing node,

III. Each BS receives all the required CSI and independently computes the IA precoders.

In scenario I (Fig. 3.6(a)), the CSI (in the form of $\mathbf{F}_j$) is quantized, yielding $\hat{\mathbf{F}}_j$, and sent to the central node. The central node computes the precoders and provides BS j with a quantized version $\hat{\mathbf{V}}_j$ of $\tilde{\mathbf{V}}_j$. Here we assume that each BS uses N_b bits to quantize $\mathbf{F}_j$ and the central node uses N_c bits to quantize $\tilde{\mathbf{V}}_j$. Therefore, the total number of bits exchanged over the network for scenario I is equal to $K(N_b + N_c)$. Scenario II can be

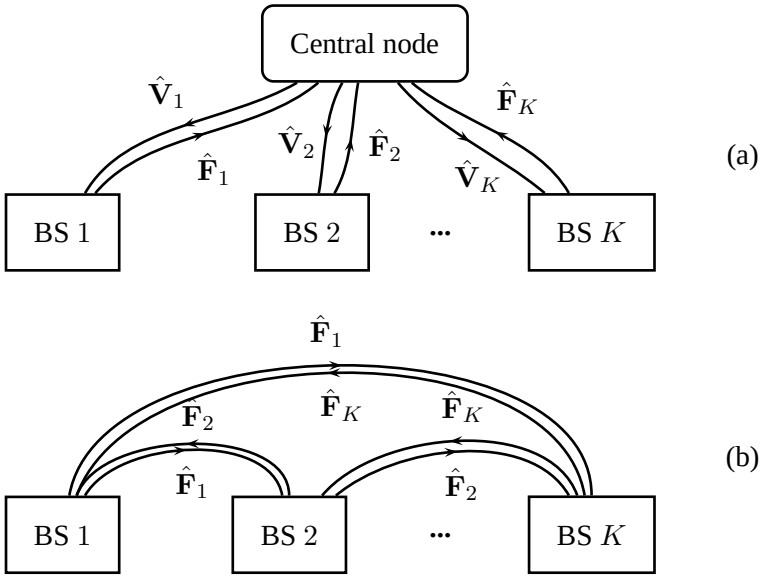

Figure 3.6. CSIT sharing, (a) with and (b) without central node.

considered as a special case of scenario I where one (bi-directional) BS-central node link is saved; the number of bits to be transferred in the network is $(K-1)(N_b+N_c)$. In scenario III (Fig. 3.6(b)), the IA solution is computed independently at each BS, requiring global CSI at each of them. Therefore each BS needs to quantize and send its local CSI to all other $K-1$ BSs. The precoders are subsequently computed at the BSs and no further information exchange is required. In this scenario, a total of $K(K-1)N_b$ bits must be exchanged to distribute the CSI. For simplicity of the exposition, we focus on scenario I and characterize the scaling of N_b and N_c with P, noting that a generalization of the analysis to scenarios II and III is straightforward.

Precoder Design with Efficient Information Exchange

Let us first consider the feedback from a BS to the central node. BS j performs the QR decomposition $\mathbf{H}_j = \mathbf{F}_j\mathbf{C}_j$ and quantizes the subspace spanned by the columns of $\mathbf{F}_j$ using N_b bits and sends the index of the quantized codeword to the central node. We further assume that the BSs and the central node share a predefined codebook $\mathcal{S} = \{\mathbf{S}_1, ..., \mathbf{S}_{2^{N_b}}\}$ which is composed of 2^{N_b} truncated unitary matrices of size $(K-1)N \times M$ and is designed using Grassmannian subspace packing. For simplicity, let us assume that all K codebooks have the same size and the powers of the transmitted signals and receiver noise are symmetric across the network. The quantized codeword is the closest point in $\mathcal{S}$ w.r.t. the chordal distance, i.e.,

$$\hat{\mathbf{F}}_j = \arg\min_{\mathbf{S}\in\mathcal{S}} \; d_c(\mathbf{S}, \mathbf{F}_j). \tag{3.32}$$

The interference alignment problem is then solved at the central node based on $\{\hat{\mathbf{F}}_j\}_{j=1}^K$ to find truncated unitary matrices $(\{\tilde{\mathbf{U}}_j\}_{j=1}^K, \{\tilde{\mathbf{V}}_j\}_{j=1}^K)$ fulfilling

$$\tilde{\mathbf{U}}_{-j}^{\mathrm{H}}\hat{\mathbf{F}}_j\tilde{\mathbf{V}}_j = \mathbf{0}, \;\; \forall j \in \{1, ..., K\}. \tag{3.33}$$

We now consider the feedback of $\tilde{\mathbf{V}}_j$ from the central node to BS j. Using another codebook $\mathcal{T} = \{\mathbf{T}_1, ..., \mathbf{T}_{2^{N_c}}\}$ of truncated unitary matrices representing points in $\mathcal{G}_{M,d}$, the central node quantizes the alignment precoder $\tilde{\mathbf{V}}_j$ for each BS on $\mathcal{G}_{M,d}$ according to

$$\hat{\mathbf{V}}_j = \arg\min_{\mathbf{T}\in\mathcal{T}} \; d_c(\mathbf{T}, \tilde{\mathbf{V}}_j), \tag{3.34}$$

and sends the corresponding index to BS j. At BS j, by analogy to the perfect CSI case (Lemma 7), we define the total precoder as

$$\mathbf{V}_j = \left(\frac{P}{q_j}\right)^{1/2} \mathbf{C}_j^{-1}\mathbf{F}_j^{\mathrm{H}}\hat{\mathbf{F}}_j\hat{\mathbf{V}}_j, \tag{3.35}$$

in which $q_j = \mathrm{tr}(\mathbf{C}_j^{-1}\mathbf{F}_j^{\mathrm{H}}\hat{\mathbf{F}}_j\hat{\mathbf{V}}_j\hat{\mathbf{V}}_j^{\mathrm{H}}\hat{\mathbf{F}}_j^{\mathrm{H}}\mathbf{F}_j\mathbf{C}_j^{-\mathrm{H}})$ is introduced to satisfy the power constraint. q_j is nonzero with probability 1 and is upperbounded by a constant regardless of P as shown below

$$\begin{aligned} q_j &= ||\mathbf{C}_j^{-1}\mathbf{F}_j^{\mathrm{H}}\hat{\mathbf{F}}_j\hat{\mathbf{V}}_j||_{\mathrm{F}}^2 && (3.36)\\ &\le ||\mathbf{C}_j^{-1}||_{\mathrm{F}}^2||\mathbf{F}_j^{\mathrm{H}}||_{\mathrm{F}}^2||\hat{\mathbf{F}}_j||_{\mathrm{F}}^2||\hat{\mathbf{V}}_j||_{\mathrm{F}}^2 && (3.37)\\ &\le ||\mathbf{C}_j||_{\mathrm{F}}^2. && (3.38)\end{aligned}$$

Using the precoders $\mathbf{V}_j$ and after applying the receive filter $\tilde{\mathbf{U}}_i$ to (6.43), the interference leakage (due to the quantizations (3.32) and (3.34)) at user i is defined as

$$\mathbf{e}_i = \sum_{\substack{1\le j\le K\\ j\neq i}} \tilde{\mathbf{U}}_i^{\mathrm{H}}\mathbf{H}_{ij}\mathbf{V}_j\mathbf{x}_j. \tag{3.39}$$

We denote the leakage power at user i by L_i

$$L_i = \mathrm{tr}(\mathrm{E}(\mathbf{e}_i\mathbf{e}_i^{\mathrm{H}})) = \mathrm{tr}(\mathbf{Q}_I^i), \tag{3.40}$$

where

$$\mathbf{Q}_I^i = \sum_{j=1, j\neq i}^{K} \tilde{\mathbf{U}}_i^{\mathrm{H}}\mathbf{H}_{ij}\mathbf{V}_j\mathbf{V}_j^{\mathrm{H}}\mathbf{H}_{ij}^{\mathrm{H}}\tilde{\mathbf{U}}_i. \tag{3.41}$$

We now consider the sum over all users of the leakage powers:

$$\begin{aligned} L &= \sum_{i=1}^{K} \mathrm{tr}\Big(\sum_{j=1, j\neq i}^{K} \tilde{\mathbf{U}}_i^{\mathrm{H}}\mathbf{H}_{ij}\mathbf{V}_j\mathbf{V}_j^{\mathrm{H}}\mathbf{H}_{ij}^{\mathrm{H}}\tilde{\mathbf{U}}_i\Big)\\ &= \sum_{j=1}^{K} ||\tilde{\mathbf{U}}_{-j}^{\mathrm{H}}\mathbf{H}_j\mathbf{V}_j||_{\mathrm{F}}^2. \end{aligned} \tag{3.42}$$

Substituting $\mathbf{V}_j = (\frac{P}{q_j})^{1/2}\mathbf{C}_j^{-1}\mathbf{F}_j^{\mathrm{H}}\hat{\mathbf{F}}_j\hat{\mathbf{V}}_j$ and $\mathbf{H}_j = \mathbf{F}_j\mathbf{C}_j$ gives

$$||\tilde{\mathbf{U}}_{-j}^{\mathrm{H}}\mathbf{H}_j\mathbf{V}_j||_{\mathrm{F}}^2 = \frac{P}{q_j}||\tilde{\mathbf{U}}_{-j}^{\mathrm{H}}\mathbf{F}_j\mathbf{F}_j^{\mathrm{H}}\hat{\mathbf{F}}_j\hat{\mathbf{V}}_j||_{\mathrm{F}}^2. \tag{3.43}$$

From (3.33) we have $\tilde{\mathbf{U}}_{-j}^{\mathrm{H}}\hat{\mathbf{F}}_j\tilde{\mathbf{V}}_j\tilde{\mathbf{V}}_j^{\mathrm{H}}\hat{\mathbf{V}}_j = \mathbf{0}$, therefore by some manipulations, from (3.42), (3.43) we get

$$L = \sum_{j=1}^{K}\frac{P}{q_j}||\mathbf{X}_j^b + \mathbf{X}_j^c||_{\mathrm{F}}^2 \le \sum_{j=1}^{K}\frac{P}{q_j}(||\mathbf{X}_j^b||_{\mathrm{F}} + ||\mathbf{X}_j^c||_{\mathrm{F}})^2 \tag{3.44}$$

where

$$\begin{aligned}\mathbf{X}_j^b &= \tilde{\mathbf{U}}_{-j}^{\mathrm{H}}(\mathbf{F}_j\mathbf{F}_j^{\mathrm{H}} - \hat{\mathbf{F}}_j\hat{\mathbf{F}}_j^{\mathrm{H}})\hat{\mathbf{F}}_j\hat{\mathbf{V}}_j \quad \text{and} \\ \mathbf{X}_j^c &= \tilde{\mathbf{U}}_{-j}^{\mathrm{H}}\hat{\mathbf{F}}_j(\hat{\mathbf{V}}_j\hat{\mathbf{V}}_j^{\mathrm{H}} - \tilde{\mathbf{V}}_j\tilde{\mathbf{V}}_j^{\mathrm{H}})\hat{\mathbf{V}}_j\,.\end{aligned} \tag{3.45}$$

Using the fact that all the matrices involved in $\mathbf{X}_j^b$ and $\mathbf{X}_j^c$ are truncated unitary, it can be shown that

$$||\mathbf{X}_j^b||_{\mathrm{F}} \leq \sqrt{2d}\, d_c(\mathbf{F}_j, \hat{\mathbf{F}}_j), \tag{3.46}$$

$$||\mathbf{X}_j^c||_{\mathrm{F}} \leq \sqrt{2d}\, d_c(\tilde{\mathbf{V}}_j, \hat{\mathbf{V}}_j). \tag{3.47}$$

Using bounds on the quantization error for codebooks designed by sphere packing, it can be shown [71] that L in (3.44) is upper bounded by a constant c_0 independent of P when

$$N_b = \frac{G_b}{2}\log P \quad \text{and} \quad N_c = \frac{G_c}{2}\log P, \tag{3.48}$$

in which $G_b = 2M((K-1)N - M)$ and $G_c = 2d(M-d)$ are the real dimension of $\mathcal{G}_{(K-1)N,M}$ and $\mathcal{G}_{M,d}$ respectively. Under the conditions (3.48), it is clear that the leakage power at every receiver would be bounded by a constant since $L_i \leq L$.

Analysis of the Achievable Rate and DoF

In order to establish the DoF achievable using the proposed CSI quantization scheme, we provide a lower bound for the achievable rate. First consider the following lemma:

Lemma 8. *For N_b and N_c according to* (3.48) *we have,*

$$\lim_{P\to\infty} \frac{\log\left|\mathbf{I}_d + \mathbf{Q}_{\mathrm{S}}^i\right|}{\log P} = d, \tag{3.49}$$

with $\mathbf{Q}_{\mathrm{S}}^i = \tilde{\mathbf{U}}_i^{\mathrm{H}}\mathbf{H}_{ii}\mathbf{V}_i\mathbf{V}_i^{\mathrm{H}}\mathbf{H}_{ii}^{\mathrm{H}}\tilde{\mathbf{U}}_i$, almost surely.

Proof. We have

$$\mathbf{Q}_{\mathrm{S}}^i = \frac{P}{q_i}\mathbf{W}_{\mathrm{S}}^i \tag{3.50}$$

in which $\mathbf{W}_{\mathrm{S}}^i = \tilde{\mathbf{U}}_i^{\mathrm{H}}\mathbf{H}_{ii}\mathbf{C}_i^{-1}\mathbf{F}_i^{\mathrm{H}}\hat{\mathbf{F}}_i\hat{\mathbf{V}}_i\hat{\mathbf{V}}_i^{\mathrm{H}}\hat{\mathbf{F}}_i^{\mathrm{H}}\mathbf{F}_i\mathbf{C}_i^{-\mathrm{H}}\mathbf{H}_{ii}^{\mathrm{H}}\tilde{\mathbf{U}}_i$. Note that the limit in (3.49) involves codebooks of increasing size since N_b and N_c increase with P. $\mathbf{W}_{\mathrm{S}}^i$ does not necessarily admit a limit when $P \to \infty$ due to the fact that $\tilde{\mathbf{U}}_i$ and $\hat{\mathbf{V}}_i$ are functions of the codebooks. We tackle this problem by resorting to an argument based on the compactness of the solution space, and show that there exists a series of codebooks of increasing size for which $\mathbf{W}_{\mathrm{S}}^i$ admits a limit and is full rank a.s. The full proof is similar to the proof of Lemma 6 in Section 3.3.2 and is omitted here. □

We are now in the position of proving that the proposed method achieves the full IA DoF:

Theorem 3. *The proposed quantization scheme, with N_b and N_c according to* (3.48)*, achieves the same DoF as IA under perfect CSI.*

Proof. Recall that (3.48) ensures that L_i is upper bounded by a nonzero constant c_0. Therefore, $\lambda_{\max}\left(\mathbf{Q}_I^i\right) \leq \mathrm{tr}\left(\mathbf{Q}_I^i\right) = L_i \leq c_0$, which yields

$$\log\left|\mathbf{I}_d + \mathbf{Q}_{\mathrm{I}}^i\right| \leq d\log\left(1+\lambda_{\max}\left(\mathbf{Q}_I^i\right)\right) \leq d\log(1+c_0). \tag{3.51}$$

Hence, the achievable rate using the designed precoders and receive filters denoted by R_q^i for user i can be lower-bounded as follows,

$$\begin{aligned} R_q^i &= \log\left|\mathbf{I}_d + \mathbf{Q}_{\mathrm{S}}^i + \mathbf{Q}_{\mathrm{I}}^i\right| - \log\left|\mathbf{I}_d + \mathbf{Q}_{\mathrm{I}}^i\right| && (3.52)\\ &\geq \log\left|\mathbf{I}_d + \mathbf{Q}_{\mathrm{S}}^i\right| - \log\left|\mathbf{I}_d + \mathbf{Q}_{\mathrm{I}}^i\right| && (3.53)\\ &\geq \log\left|\mathbf{I}_d + \mathbf{Q}_{\mathrm{S}}^i\right| - d\log(1+c_0), && (3.54)\end{aligned}$$

where (3.53) follows from the fact that $\mathbf{Q}_{\mathrm{I}}^i$ is positive semi-definite and the second inequality follows from (3.51). Combining (3.54) with Lemma 8 brings us to the conclusion that

$$\lim_{P\to\infty}\frac{R_q^i}{\log P} \geq d, \tag{3.55}$$

i.e. the same DoF as in the case of perfect CSI is achieved. □

Performance Evaluation

In this section, the performance of the proposed scheme is evaluated through numerical simulations. The performance metric is the sum-rate evaluated through Monte-Carlo simulations using the precoders designed with the quantization scheme.

A three-user IC is considered where each BS is equipped with $M = 5$ antennas while every receiver has $N = 3$ antennas and $d = 2$ data streams for each user is considered. Entries of the channel matrices are generated according to $\mathcal{CN}(0,1)$ and the performance results are averaged over the channel realizations. In Fig. 3.7, the quantized CSI sharing method of Section 3.4.2 (denoted by "Proposed") is compared (for scenario I) to the naive method where the interfering channel matrices from the BSs are independently vectorized, normalized and quantized using N_b bits based on the idea of composite Grassmann manifold [47] and finally the indices of the quantized vectors are sent to the central node (denoted by Normalized Channel Composite Grassmann Quantization, NC-CGQ). At the central node, for the proposed method, the precoders are quantized on $\mathcal{G}_{M,d}$ while for the NC-CGQ method, each precoder is vectorized, normalized and quantized on $\mathcal{G}_{Md,1}$ using N_c bits, and sent to the corresponding BS. Figure 3.7 shows the achievable sum-rate versus transmit SNR (P) for $(N_b, N_c) = (5,6)$ and $(N_b, N_c) = (10,12)$ bits. A random codebook is used with codebook entries chosen as independent truncated unitary matrices generated from the Haar distribution. For the independent quantization method, random unit norm vectors are used in the codebook construction. Clearly the proposed scheme outperforms the independent quantization method for the same number of bits.

The use of random codebooks for large values of N_b and N_c is not tractable, due to the exponential requirements in terms of storage and of computation of (3.32) and (3.34). In order to benchmark the sum-rate

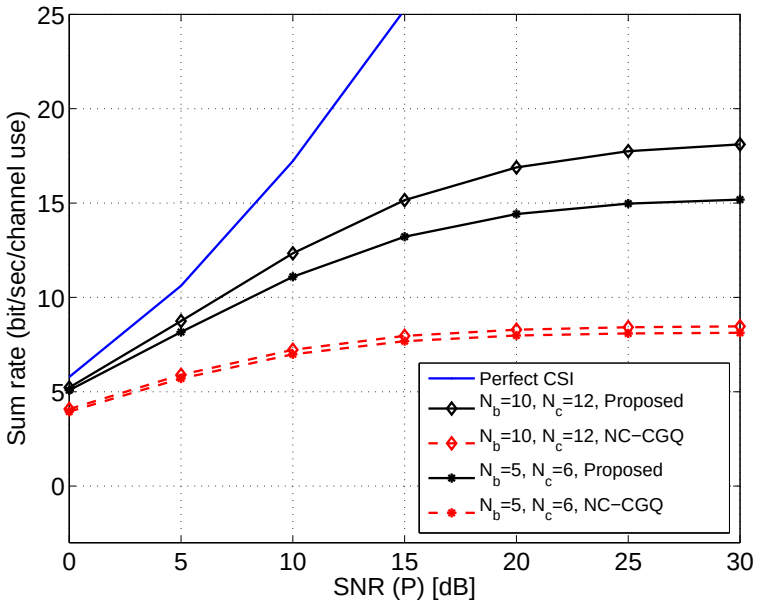

Figure 3.7. Sum-rate comparison of quantization methods, for the 3-user MIMO IC, $M = 5$, $N = 3$, $d = 2$, based on optimal decoding of $\mathbf{y}_i$.

achievable under the proposed scheme for the high power region (large N_b and N_c) we replace the quantization process with the perturbation scheme from Appendix A.6. As will be seen, this approach provides a good approximation of the effect of quantization on the considered system.

This replacement of the quantization error is performed at BSs as well as the central node. The sum-rate performance $\sum_{i=1}^{K} R_q^i$ obtained using the perturbation method is plotted against SNR for various codebook sizes in Fig. 3.8. For the considered antenna configuration, according to (3.48), the scaling that is sufficient to achieve the perfect DoF is $N_b = 5 \log P$ and $N_c = 6 \log P$. In the simulations, the codebook sizes are chosen as $N_b = 5A$ and $N_c = 6A$ for integer values of A, and the corresponding SNR is computed according to $P = 2^A$. The results are also compared to perfect CSIT sharing. It is clear that this perturbation method effectively approximates the quantization process when the desired performance metric is the sum-rate, allowing us to rely on the curves resulting from this method to confirm the DoF result of Theorem 3.

3.5 Distributed Precoding

In this section we discuss possible methods to design precoders distributedly at the transmitters. By reciprocity of the channels, the jth BS estimates the channel matrices $\mathbf{H}_{ij},\ i = 1, ..., K\ ,\ i \neq j$ from the uplink phase. Here, we again assume that $\mathbf{H}_{ij},\ i = 1, ..., K\ ,\ i \neq j$ are known perfectly at BS j. We assume that each BS shares a quantized version of its channels with other BSs via finite capacity links. Therefore all the quantized CSI is available at all BSs (assuming error-free links). We consider the following objective for any given

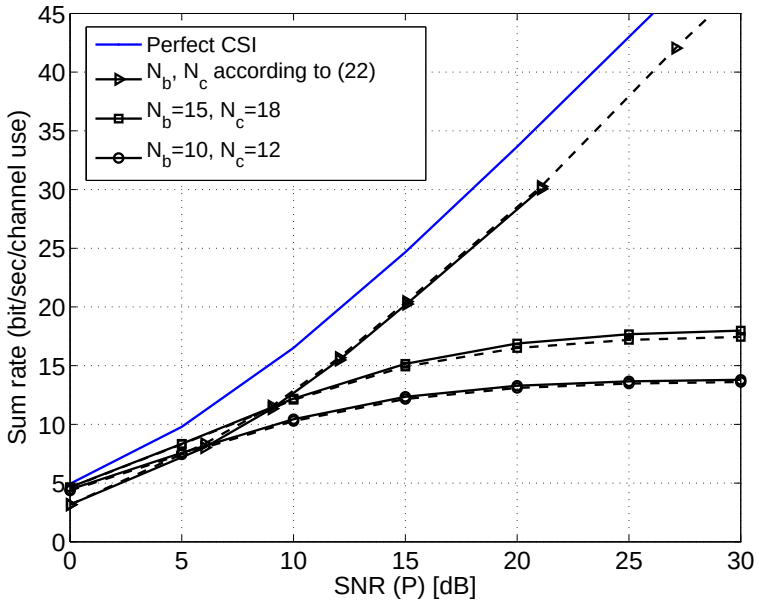

Figure 3.8. Sum rate comparison between perturbation method (dashed) and quantization (solid), for the 3-user MIMO IC, $M = 5$, $N = 3$ and $d = 2$, based on (3.52).

channel realization:

$$\max_{\{\mathbf{V}_i\}_{i=1}^{K},\, \mathrm{tr}(\mathbf{V}_i\mathbf{V}_i^{\mathrm{H}})=P_i} \sum_{i=1}^{K} \mathcal{I}^i, \tag{3.56}$$

in which $\mathcal{I}^i$ is a performance measure corresponding to link i (for example the achievable rate of link i).

3.5.1 Assumptions and Methods for Distributed Precoding

For measures such as rate or MSE, (3.56) is a non-convex problem and the known solutions are sub-optimal and mostly based on iterative algorithms. Moreover, to have a distributed implementation, (3.56) has to be solved independently at each transmitter which necessitates global CSI (or other types of global information) which has to be identical at all the nodes. Since most of the (close to optimal) solutions are based on iterative algorithms, slightly different CSI at different nodes might result in different convergence trajectories, yielding a totally different set of precoders. Even in special cases where closed form solutions exist (like doing IA in 3-user IC), designing the precoders based on different CSI quality would result in a poor performance [72]. In a practical scenario where CSI is quantized and exchanged between the BSs (as the scheme presented in Section 3.3.2), one viable option is that all the BSs design the precoders based on the common knowledge of the whole quantized channels. Under this assumption, the BSs should not use their own accurate CSI because the others only have a quantized version of that CSI. Based on the common CSI, every BS will be able to compute its precoder based on a previously agreed method, assuming that the quantized CSI is the true CSI. Different performance metrics can be employed similar to the perfect CSI scenario. Most of the known methods require all the channel matrices between any pair of nodes (for example iterative sum-rate maximization or MSE minimization algorithms). On the other hand, interference alignment does not require the direct channel

matrices. Even though IA has poor performance at low SNR, it needs less CSI exchange between the BSs which allows for a more accurate quantization given a backhaul link with a certain capacity. Moreover, we have shown in Section 3.3.2 that one can further reduce CSI sharing requirements when using IA. This prompts us to use IA as a starting point and look for further improvements by taking advantage of the accurate local CSI at each BS in a second step.

Assuming that precoders are designed based on the shared knowledge at the BSs, the main issue is that if one BS modifies its own precoder to improve its performance by using its local CSI, the others do not have access to the new precoder of that BS and therefore cannot perform their own optimization. One option is to have a fixed interference space at each receiver [73] and to constrain the transmitters to create interference only in those spaces. However, this reduces the DoF that can be achieved over the network. Here we use the IA projection filters (designed by using quantized CSI) to fix the interference space at the receivers. After fixing the receive interference space we can look for improving the performance using the local accurate CSI. For example if we employ a rate maximization after fixing the interference spaces, we can ensure the achievability of DoF that could be achieved by the quantized CSI and additionally have an improvement in the sum-rate. Note that our scheme relies only on the CSI that is exchanged among the transmitters and there is no interaction between the TX side and the RX side. (Clearly such iterative information exchange between the TX side and the RX side can improve the performance). Again, we assume that BS j will quantize $\mathbf{F}_j$ over the Grassmann manifold and send the quantized version of $\mathbf{F}_j$ (denoted by $\hat{\mathbf{F}}_j$) to the other BSs as shown in Fig. 3.6(b). We start by solving IA for the quantized CSI $\hat{\mathbf{F}}_j$ (assuming a feasible IA setting), i.e., finding truncated unitary precoding matrices $\mathbf{V}_j^{\mathrm{IA}}$, $j = 1, ..., K$ and projection matrices $\mathbf{U}_i^{\mathrm{IA}} \in \mathbb{C}^{N \times d}$, $i = 1, ..., K$ such that

$$\mathbf{V}_j^{\mathrm{IA}} \in \mathrm{span}(\mathbf{C}_j^{-1}\mathbf{F}_j^{\mathrm{H}}\hat{\mathbf{F}}_j\tilde{\mathbf{V}}_j), \tag{3.57}$$

$$\mathbf{U}_i^{\mathrm{IA}} \in \mathrm{span}(\tilde{\mathbf{U}}_i), \tag{3.58}$$

where $\tilde{\mathbf{U}}_i$ and $\tilde{\mathbf{V}}_j$ are computed from (3.33).

Fixing the receive filters decouples the problem (3.56). Afterward, it remains to design precoders locally assuming fixed receive filters $\mathbf{U}_i^{\mathrm{IA}}$ for the users, using the locally available CSI. We now present two possible solutions:

3.5.2 MSE Minimization

Let us first consider the following MMSE problem

$$\min_{\{\mathbf{V}_i\}_{i=1}^K, \mathrm{tr}(\mathbf{V}_i\mathbf{V}_i^{\mathrm{H}})=P_i} \sum_{i=1}^{K} \mathrm{E}(||\mu_i\mathbf{A}_i\mathbf{x}_i - \mathbf{U}_i^{\mathrm{IA}\,\mathrm{H}}\mathbf{y}_i||_{\mathrm{F}}^2) \tag{3.59}$$

where $\mathbf{A}_i = \mathbf{U}_i^{\mathrm{IA}\,\mathrm{H}}\mathbf{H}_{ii}\mathbf{V}_i^{\mathrm{IA}}$ and μ_i is a constant. The considered metric is based on approaching (in the mean-square error sense) $\mu_i\mathbf{A}_i\mathbf{x}_i$, which is a scaled version of the signal of interest obtained when using the IA precoders and projection filters computed from the estimated CSI. By taking the Lagrangian of the objective function in (3.59), it can be shown that the set of precoders that optimize (3.59) have the form $\mathbf{V}_j = \mu_j\mathbf{V}_j^{\star}$ with

$$\mathbf{V}_j^{\star} = (\sum_{i=1}^{K} \bar{\mathbf{H}}_{ij}^{\mathrm{H}}\bar{\mathbf{H}}_{ij} + \omega_j\mathbf{I}_M)^{-1}\bar{\mathbf{H}}_{jj}^{\mathrm{H}}\mathbf{A}_j \tag{3.60}$$

where $\bar{\mathbf{H}}_{ij} = \mathbf{U}_i^{\mathrm{IA}\,\mathrm{H}}\mathbf{H}_{ij}, \forall i,j$ are the equivalent channel matrices after projection with the IA receive filters. ω_j is the Lagrangian multiplier associated with the power constraint $\mathrm{tr}(\mathbf{V}_j\mathbf{V}_j^{\mathrm{H}}) = P_j$. The optimal values for $\omega_j, \mu_j, \forall j$ do not have a closed form solution for individual power constraints. Moreover, finding the optimal values requires global CSI. Here we pick those values heuristically as follows

$$\omega_j = \frac{1}{P_j}, \quad \mu_j = \sqrt{\frac{P_j}{\mathrm{tr}(\mathbf{V}_j^{\star}\mathbf{V}_j^{\star\mathrm{H}})}}, \ \forall j. \tag{3.61}$$

Note that with this particular choice of μ_j, the power constraints are satisfied. At low SNR, the identity matrix in (3.60) is dominant which results in an egoistic transmission. At high SNR, the interference created for other receivers becomes significant and the altruistic precoding (which is obtained as $\omega_j \to 0$) becomes preferable. Note however that this scheme is not expected to be optimal at low SNR since only d modes are used while at low SNR the optimal transmission scheme uses all available modes.

To summarize, we solve IA at all BSs based on the quantized CSI available globally and afterwards, every BS fixes the receive filters with the receive filters computed by IA and finds its MSE minimizing precoder $\mathbf{V}_j = \mu_j\mathbf{V}_j^{\star}$ according to (3.60), (3.61), approximately solving (3.59).

3.5.3 Approximate Sum-Rate Maximization

Defining $\mathbf{Q}_I^{ij} \triangleq \bar{\mathbf{H}}_{ij}\mathbf{Q}_j\bar{\mathbf{H}}_{ij}^{\mathrm{H}}$, we have

$$\mathbf{Q}_S^i = \bar{\mathbf{H}}_{ii}\mathbf{Q}_i\bar{\mathbf{H}}_{ii}^{\mathrm{H}} \tag{3.62}$$

$$\mathbf{Q}_I^i = \sum_{j=1, j\neq i}^{K} \mathbf{Q}_I^{ij} \tag{3.63}$$

which are the covariance matrices of the desired signal and interference after projecting by the IA receive filter respectively.

After projection with the IA receive filters, the sum-rate can be written as

$$\bar{R}_{\mathrm{sum}} = \sum_{i=1}^{K} \left[\log\left|\mathbf{I}_d + \mathbf{Q}_S^i + \mathbf{Q}_I^i\right| - \log\left|\mathbf{I}_d + \mathbf{Q}_I^i\right| \right]. \tag{3.64}$$

We consider the following objective function

$$\begin{aligned} &\max_{\mathbf{Q}_1,\ldots,\mathbf{Q}_K} \bar{R}_{\mathrm{sum}} \\ &\text{s.t.} \qquad \mathrm{tr}(\mathbf{Q}_j) = P_j \quad \forall\ j = 1, ..., K. \end{aligned} \tag{3.65}$$

The first term in (6.45) can be approximated as

$$\log\left|\mathbf{I}_d + \mathbf{Q}_S^j + \mathbf{Q}_I^j\right| \approx \log\left|\mathbf{I}_d + \mathbf{Q}_S^j\right| \tag{3.66}$$

where the approximation comes from the fact that by interference alignment (even though it is imperfect since based on quantized CSI), the interference power inside the desired signal space is reduced significantly, i.e., $\mathbf{Q}_I^i$ is negligible compared to $\mathbf{Q}_S^i$. Therefore

$$\bar{R}_{\mathrm{sum}} \approx \sum_{i=1}^{K} \left[\log\left|\mathbf{I}_d + \mathbf{Q}_S^i\right| - \log\left|\mathbf{I}_d + \mathbf{Q}_I^i\right| \right] = \tilde{R}_{\mathrm{sum}}. \tag{3.67}$$

Using the concavity of the $\log$ function, Jensen's inequality gives

$$\log\left|\mathbf{I}_d + \mathbf{Q}_I^i\right| \geq \frac{1}{K-1}\sum_{j=1,j\neq i}^{K} \log\left|\mathbf{I}_d + (K-1)\mathbf{Q}_I^{ij}\right|. \tag{3.68}$$

Therefore we get

$$\tilde{R}_{\text{sum}} \leq \sum_{j=1}^{K} \tilde{R}_j, \tag{3.69}$$

where

$$\tilde{R}_j = \log\left|\mathbf{I}_d + \mathbf{Q}_S^j\right| - \sum_{i=1,i\neq j}^{K} \frac{\log\left|\mathbf{I}_d + (K-1)\mathbf{Q}_I^{ij}\right|}{K-1}. \tag{3.70}$$

Clearly each $\tilde{R}_j$ is only a function of $\mathbf{Q}_j$ and the outgoing channels from BS j. Therefore the optimization problem in (3.65) can be approximately decoupled into the following K distributed optimization problems :

$$\begin{aligned} &\max_{\mathbf{Q}_j} \tilde{R}_j \qquad \forall\ j = 1, ..., K \\ &\text{s.t.} \quad \text{tr}(\mathbf{Q}_j) = P_j. \end{aligned} \tag{3.71}$$

Clearly we are optimizing an approximate upper bound of the sum rate which is suboptimal. Here, we propose to use a gradient ascent method to determine a local maximum of $\tilde{R}_j$ as summarized in Algorithm 1. The gradient ascent algorithm consists in starting from an arbitrary initial unnormalized precoder $\dot{\mathbf{V}}_j = \dot{\mathbf{V}}_j^{(0)}$, calculating the gradient matrix and moving in the gradient direction with some step size, which gives a new precoder $\dot{\mathbf{V}}^1$. The algorithm unfolds similarly as in the initial step until convergence.

Algorithm 1 Iterative optimization at BS j

Find the IA solution $\{\mathbf{U}_i^{\text{IA}}, \mathbf{V}_i^{\text{IA}}\}_{i=1}^K$, based on $\{\hat{\mathbf{F}}_j\}_{j=1}^K$.
Calculate the equivalent channels, $\bar{\mathbf{H}}_{ij} = {\mathbf{U}_i^{\text{IA}}}^{\text{H}}\mathbf{H}_{ij}, \forall i$.
Initialization: $m = 0$ and $\dot{\mathbf{V}}_j^{(0)}$ arbitrary.
Repeat

- Evaluate the gradient w.r.t. $\dot{\mathbf{V}}_j$, $\nabla_j \tilde{R}_j$
- Let $\dot{\mathbf{V}}_j^{(m+1)} = \dot{\mathbf{V}}_j^{(m)} + \beta\nabla_j \tilde{R}_j$ (for some step-size β)
- $m \leftarrow m + 1$

until convergence.

We now derive the expression of the gradient w.r.t. the precoders. Having $\mathbf{Q}_j = \mathbf{V}_j\mathbf{V}_j^{\text{H}}$ such that $\mathbf{V}_j = \sqrt{\frac{P_j}{\text{tr}(\dot{\mathbf{V}}_j\dot{\mathbf{V}}_j^{\text{H}})}}\dot{\mathbf{V}}_j$, the optimization finds $\dot{\mathbf{V}}_j$ such that the corresponding $\mathbf{V}_j$ maximizes the objective function at BS j and therefore the transmit power constraint is always satisfied. The gradient of $\tilde{R}_j$ w.r.t. $\dot{\mathbf{V}}_j$ is calculated as

$$\nabla_j \tilde{R}_j = \eta_j(\mathbf{\Omega}_j - \alpha_j\mathbf{I}_M)\dot{\mathbf{V}}_j \tag{3.72}$$

where $\alpha_j = \frac{\mathrm{tr}(\mathbf{\Omega}_\mathrm{j}\dot{\mathbf{V}}_\mathrm{j}\dot{\mathbf{V}}_\mathrm{j}^\mathrm{H})}{\mathrm{tr}(\dot{\mathbf{V}}_\mathrm{j}\dot{\mathbf{V}}_\mathrm{j}^\mathrm{H})}$, $\eta_j = \frac{P_j}{\mathrm{tr}(\dot{\mathbf{V}}_\mathrm{j}\dot{\mathbf{V}}_\mathrm{j}^\mathrm{H})}$ and

$$\mathbf{\Omega}_j = \bar{\mathbf{H}}_{jj}^\mathrm{H}(\mathbf{I}_d + \mathbf{Q}_S^j)^{-1}\bar{\mathbf{H}}_{jj} - \sum_{i=1,i\neq j}^{K} \bar{\mathbf{H}}_{ij}^\mathrm{H}(\mathbf{I}_d + (K-1)\mathbf{Q}_I^{ij})^{-1}\bar{\mathbf{H}}_{ij}. \tag{3.73}$$

Considering single stream IA, instead of running Algorithm 1, one can obtain a closed-form solution to $\nabla_j \tilde{R}_j = 0$ as follows:

$$\begin{aligned}&\bar{\mathbf{H}}_{jj}^\mathrm{H}(\mathbf{I}_d + \mathbf{Q}_S^j)^{-1}\bar{\mathbf{H}}_{jj}\dot{\mathbf{V}}_j \\ &= \left(\alpha_j \mathbf{I}_M + \sum_{i=1,i\neq j}^{K} \bar{\mathbf{H}}_{ij}^\mathrm{H}(\mathbf{I}_d + (K-1)\mathbf{Q}_I^{ij})^{-1}\bar{\mathbf{H}}_{ij}\right)\dot{\mathbf{V}}_j\end{aligned} \tag{3.74}$$

therefore

$$\begin{aligned}\dot{\mathbf{V}}_j = &\left(\alpha_j \mathbf{I}_M + \sum_{i=1,i\neq j}^{K} \bar{\mathbf{H}}_{ij}^\mathrm{H}(\mathbf{I}_d + (K-1)\mathbf{Q}_I^{ij})^{-1}\bar{\mathbf{H}}_{ij}\right)^{-1} \\ &\cdot \bar{\mathbf{H}}_{jj}^\mathrm{H}(\mathbf{I}_d + \mathbf{Q}_S^j)^{-1}\bar{\mathbf{H}}_{jj}\dot{\mathbf{V}}_j.\end{aligned} \tag{3.75}$$

For that case the algorithm consists in initializing the precoder $\dot{\mathbf{V}}_j$ (which is a vector in this case), updating $\mathbf{Q}_S^j, \mathbf{Q}_I^{ij}$ and iteratively finding new precoders according to (3.75).

3.5.4 Performance Comparison

In this section, the performance of the proposed distributed schemes is evaluated through numerical simulations. The performance metric is again the sum rate evaluated through Monte-Carlo simulations using the precoders designed in Sections 3.5.2 and 3.5.3.

A three-user IC is considered. Entries of the channel matrices are generated according to $\mathcal{CN}(0, \gamma_{ij})$ (where γ_{ij} is the path-loss coefficient for the channel between BS j and user i) and the performance results are averaged over the channel realizations. In all simulations, the direct links are assumed to have no path-loss, i.e., $\gamma_{ii} = 1,\ \forall i$. Our proposed methods ("Approx-MSR and Min-MSE") are compared to the following schemes:

- IAQ: IA with quantized CSI according to Section 3.4.2. This scheme requires quantized CSI of the interfering links to be available at the transmitters (or the central node).
- IAP: IA with perfect CSI. This scheme is a hypothetic case which is presented to see how the other schemes perform relative to the scenario that alignment is done based on the true CSI.
- EW: The eigen water filling method. In this method the BSs maximize their rate selfishly using only the knowledge of their direct channel and treating interference as noise. Assuming that the interference is white, the power of interference at the receiver is calculated and added to the noise power to find the equivalent noise power. Then the BSs perform water filling over the eigen modes of their direct channels with the equivalent noise power. Clearly in this scheme the transmitters need to know their direct channels as well as the path loss values for the interfering links.

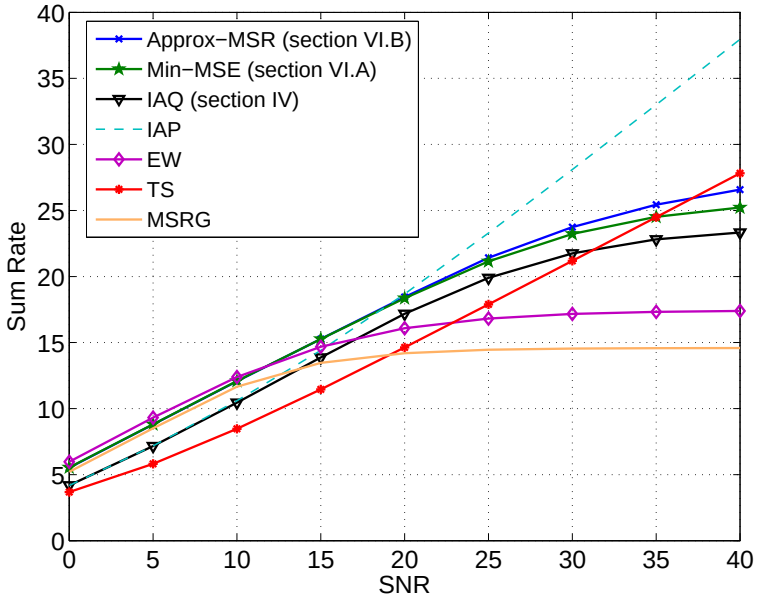

Figure 3.9. Comparison of sum-rate for $K = 3, M = N = 2, d = 1, N_b = 12$ and $\gamma_{ij} = -10\text{dB}$ for $i \neq j$

- TS: Time sharing method. In this case, the transmission time is divided among the links and at a given time instant, only one transmitter is active and the total power is allocated to the active transmitter. The transmission strategy for the active link is water filling over the eigen modes of the direct channel. Clearly in this case, only the direct channel information is required at each transmitter.

- MSRG: Maximum sum rate algorithm using Gradient method [48] with quantized CSI. In this method, the channel matrices (including the direct channels) are vectorized, normalized and quantized using random unit norm vectors. The quantized vectors are then fed back to the transmitters and an optimization problem is solved based on this quantized information at every transmitter. The optimization problem determines a local maximum for the problem of sum rate maximization using the quantized channels. The power constraint associated to the precoders is absorbed into the cost function and a Gradient ascent algorithm is used over the equivalent cost function to find the locally optimum precoders. In this method, all the channel matrices need to be quantized and fed back to the transmitters.

Figures 3.9, 3.10, 3.11 show the achievable sum rate versus transmit SNR when each BS is allowed to share N_b bits with the other BSs for different antenna configurations and different number of bits. For the quantization phase in the proposed scheme (and also in IAQ), instead of the optimal subspace packing codebook, a random codebook is used where the codebook entries are independent random truncated unitary matrices generated from the Haar distribution. In this method, in order to simplify the quantization, we assume that the norm of the vectors are known at all the BSs perfectly.

Clearly the Approx-MSR and Min-MSE schemes outperforms the other methods for the same number of bits in a wide range of practical SNRs.

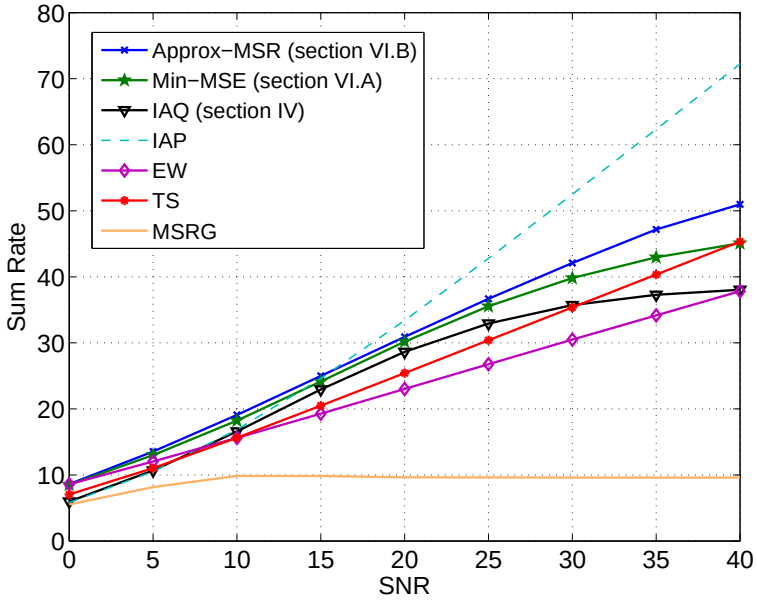

Figure 3.10. Comparison of sum-rate for $K = 3, M = 5, N = 3, d = 2, N_b = 12$ and $\gamma_{ij} = -3\text{dB}$ for $i \neq j$

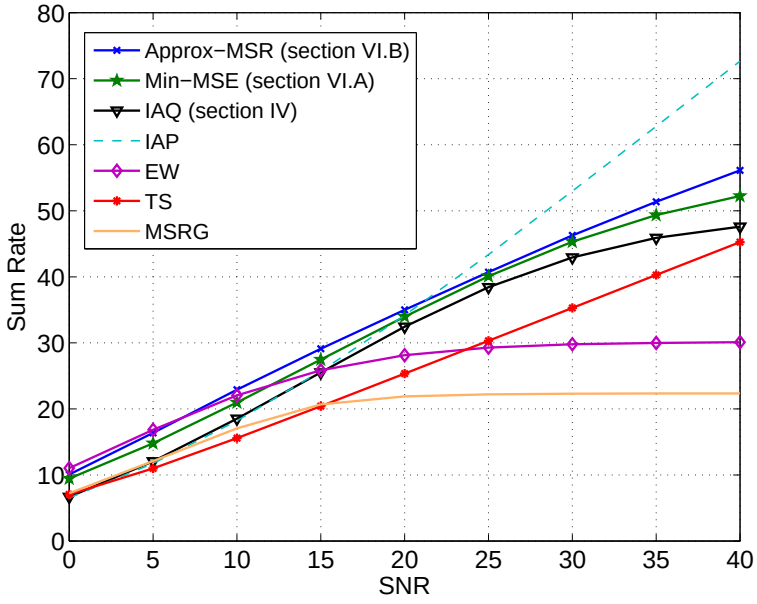

Figure 3.11. Comparison of sum-rate for $K = 3, M = 5, N = 3, d = 2, N_b = 9$ and $\gamma_{ij} = -10\text{dB}$ for $i \neq j$

4

Interference Management with Outdated CSIT

CSIT may be neither perfect, due to the limited capacity of the feedback link, nor instantaneous, due to the delays involved in the channel estimation and feedback. The first problem of having imperfect CSIT is considered in Chapter 1 and Chapter 6. The second problem of having only delayed CSIT, a setting that is highly relevant in mobile environments with short channel coherence times, is discussed in this chapter. The delayed CSI is known to bring improvement in terms of DoF compared to having no CSI in BC and IC. We consider the two-user MIMO IC where the transmitters are provided with delayed CSI. The DoF region for this channel is characterized in [11]. We aim to devise an intuitive achievable scheme which is relatively simple compared to [11] and has a unified structure for different antenna configurations. Furthermore, our simple scheme allows for extensions to more general settings (like correlated channels) through slight modifications which can be justified intuitively.

4.1 Background and State of the Art

The study of DoF with delayed CSIT was initiated by the work of Maddah-Ali and Tse [9]. They proved that over the multiple-input single-output (MISO) BC with i.i.d fast fading, delayed (i.e., outdated) CSIT can lead to a DoF gain compared to the case with no CSIT. The DoF gains are realized via an interference alignment scheme. That scheme is based on the idea that the interference seen at each of the receivers at the previous time slots (which is a linear combination of the data symbols intended for the other users), can be reconstructed by the transmitter at the current time instant using delayed CSIT, and subsequently forwarded to the receivers. The receivers can exploit this interference to decode their own signal. As an example consider a two-user broadcast channel in which the transmitter has two antennas and each user has one antenna. It has been shown that with delayed CSI this channel has 4/3 DoF [9]. Using three time slots two symbols can be transmitted to each user. In the first time slot, two symbols x_1, y_1 of the first user are transmitted and in the second time slot the symbols x_2, y_2 intended for the second user are transmitted. In these two time slots every user i will have a linear combination of its own symbols $L_i(x_i, y_i)$ and also a linear combination of the interfering symbols $L_i(x_j, y_j)$. In the third time slot, the transmitter sends a linear combination of the interference terms observed at the two users, i.e., $L_2(x_1, y_1)$ and $L_1(x_2, y_2)$ (which are assumed to be available at the transmitter by delayed CSI assumption). Clearly the first user can subtract $L_1(x_2, y_2)$ from the received signal in the third time slot and the remaining part provides another linear combination of its own signal. Similar argument holds for the second user. Therefore every user will have two linear combinations of its own symbols which is enough to decode the information.

This interference alignment scheme achieves DoF gains and is sum-DoF optimal for the class of MISO BCs, wherein the transmitter has at least K antennas where K is the number of users. This work was then extended to the case of the MIMO BC in [10] and also for the K-user case an outer bound to the DoF region was derived.

Moving from BC to interference channel and X channel, the authors of [74] have shown that using ideas similar to that of [9], higher DoF can be achieved compared to the no CSIT case. The results of [74] were improved in [75, 76]. The DoF region of the two-user MIMO IC was fully characterized in [11] for different possible antenna configurations. Their proposed achievable scheme is based on transmitting on a stream per antenna basis which makes the scheme complicated and difficult to implement. In this chapter, we propose a unified DoF-achievable scheme for the two user MIMO IC with outdated CSIT based on linear matrix precoding which covers all possible antenna configurations and avoids the many case distinctions required by other methods.

4.2 Perfect Outdated CSIT

Consider a MIMO interference channel. We assume that all terminals are equipped with multiple antennas. The channel between transmitter j and receiver i at time slot t is $\mathbf{H}_{ij}^{(t)} \in \mathbb{C}^{\mathrm{N_i} \times \mathrm{M_j}}$ for $i, j = 1, 2$. The received signal at time instant t at receiver $i \neq j$ reads

$$\mathbf{y}_i^{(t)} = \mathbf{H}_{ii}^{(t)}\mathbf{V}_i^{(t)}\mathbf{x}_i + \mathbf{H}_{ij}^{(t)}\mathbf{V}_j^{(t)}\mathbf{x}_j + \mathbf{n}_i^{(t)}, \text{ for } t = 1, \cdots, T \tag{4.1}$$

where $\mathbf{x}_j$ is the symbol of transmitter j which has to be transmitted over T time slots and $\mathbf{V}_j^{(t)}$ is the precoder of transmitter j at time slot t. $\mathbf{n}_i^{(t)}$ is the additive Gaussian noise vector at time slot t at receiver i whose entries have zero mean and unit variance.

The CSI is provided to the TXs by delay and is completely outdated. The transmitters wish to convey their symbols to their respective receivers exploiting the outdated CSI. DoF-achievable schemes are presented in [11] for different configuration of antennas.

4.2.1 The DoF Region of the Two-User MIMO IC with Outdated CSIT

For $i \in \{1, 2\}$ and $j \in \{1, 2\}$ with $j \neq i$, the following inequality is called condition i:

$$M_i > N_1 + N_2 - M_j > N_i > N_j > M_j > N_j \frac{N_j - M_j}{N_i - M_j}. \tag{4.2}$$

Clearly, the two conditions are symmetric in user indices. The two conditions cannot hold simultaneously, and Condition i cannot hold if $N_j \geq N_i$.

The DoF region is characterized in [11] and the region is different for any particular configuration of antennas. Depending on the configuration, a set of the following bounds will determine the DoF region:

$$L_{o1} : 0 \leq d_1 \leq \min(M_1, N_1), \quad L_{o2} : 0 \leq d_2 \leq \min(M_2, N_2) \tag{4.3}$$

$$L_1 : \frac{d_1}{\min(N_1 + N_2, M_1)} + \frac{d_2}{\min(N_2, M_1)} \leq \frac{\min(N_2, M_1 + M_2)}{\min(N_2, M_1)} \tag{4.4}$$

$$L_2 : \frac{d_1}{\min(N_1, M_2)} + \frac{d_2}{\min(N_1 + N_2, M_2)} \leq \frac{\min(N_1, M_1 + M_2)}{\min(N_1, M_2)} \tag{4.5}$$

$$L_3 : d_1 + d_2 \leq \min(M_1 + M_2, N_1 + N_2, \max(M_1, N_2), \max(M_2, N_1)) \tag{4.6}$$

$$\text{if condition 1 holds} : L_4 : d_1 + d_2 \frac{N_1 + 2N_2 - M_2}{N_2} \leq N_1 + N_2 \tag{4.7}$$

$$\text{if condition 2 holds} : L_5 : d_2 + d_1 \frac{N_2 + 2N_1 - M_1}{N_1} \leq N_1 + N_2. \tag{4.8}$$

For the case of instantaneous CSIT, the DoF region is described by L_{o1}, L_{o2}, and L_3 [30].

4.2.2 General Achievable Scheme for Different Antenna Configurations

We try to provide a general achievable scheme which encompasses all possible antenna configurations. The scheme is composed of two phases (successive in time) where each phase is composed of T time slots. The channel outputs (concatenated over T time slots) can be written as

$$\mathbf{y}_1 = \mathbf{H}_{11}\mathbf{V}_1\mathbf{x}_1 + \mathbf{H}_{12}\mathbf{V}_2\mathbf{x}_2 + \mathbf{n}_1 \tag{4.9}$$

$$\mathbf{y}_2 = \mathbf{H}_{21}\mathbf{V}_1\mathbf{x}_1 + \mathbf{H}_{22}\mathbf{V}_2\mathbf{x}_2 + \mathbf{n}_2 \tag{4.10}$$

where $\mathbf{H}_{ij} = \mathrm{Bdiag}(\mathbf{H}_{ij}^{(1)}, ..., \mathbf{H}_{ij}^{(T)})$ and $\mathbf{V}_j = \begin{bmatrix} \mathbf{V}_j^{(1)} \\ \cdots \\ \mathbf{V}_j^{(T)} \end{bmatrix}$. Also we have $\mathbf{y}_i = \begin{bmatrix} \mathbf{y}_i^{(1)} \\ \cdots \\ \mathbf{y}_i^{(T)} \end{bmatrix}$ and $\mathbf{n}_i = \begin{bmatrix} \mathbf{n}_i^{(1)} \\ \cdots \\ \mathbf{n}_i^{(T)} \end{bmatrix}$.

The proposed scheme is based on transmitting with random precoders in the first phase and transmiting with a designed precoder in the second phase. We assume that the duration of phase 1 for TX i is $T - q_j$ with $j \neq i \in \{1, 2\}$. Therefore TX i uses the last q_j time slots to facilitate the decoding at both RXs using a properly designed precoder in this phase and exploiting the CSIT corresponding to phase 1. We define $d_1^* = Td_1$ and $d_2^* = Td_2$.

Let us now consider the received signal space (signal and interference) at each RX:

RX1:

$$\mathbf{R_1} = [\mathbf{H}_{11}\mathbf{V}_1 \ \mathbf{H}_{12}\mathbf{V}_2] = \begin{bmatrix} \mathbf{H}_{11}^{(1)}\mathbf{V}_1^{(1)} & \mathbf{H}_{12}^{(1)}\mathbf{V}_2^{(1)} \\ \mathbf{H}_{11}^{(2)}\mathbf{V}_1^{(2)} & \mathbf{H}_{12}^{(2)}\mathbf{V}_2^{(2)} \\ \cdots & \cdots \\ \mathbf{H}_{11}^{(\mathrm{T})}\mathbf{V}_1^{(\mathrm{T})} & \mathbf{H}_{12}^{(\mathrm{T})}\mathbf{V}_2^{(\mathrm{T})} \end{bmatrix} = \begin{bmatrix} \mathbf{H}_{11}^{\mathrm{ph1}}\mathbf{V}_1^{\mathrm{ph1}} & \mathbf{H}_{12}^{\mathrm{ph1}}\mathbf{V}_2^{\mathrm{ph1}} \\ \mathbf{H}_{11}^{\mathrm{ph2}}\mathbf{V}_1^{\mathrm{ph2}} & \mathbf{H}_{12}^{\mathrm{ph2}}\mathbf{V}_2^{\mathrm{ph2}} \end{bmatrix} \tag{4.11}$$

RX2:

$$\mathbf{R_2} = [\mathbf{H}_{22}\mathbf{V}_2 \ \mathbf{H}_{21}\mathbf{V}_1] = \begin{bmatrix} \mathbf{H}_{22}^{(1)}\mathbf{V}_2^{(1)} & \mathbf{H}_{21}^{(1)}\mathbf{V}_1^{(1)} \\ \mathbf{H}_{22}^{(2)}\mathbf{V}_2^{(2)} & \mathbf{H}_{21}^{(2)}\mathbf{V}_1^{(2)} \\ \cdots & \cdots \\ \mathbf{H}_{22}^{(\mathrm{T})}\mathbf{V}_2^{(\mathrm{T})} & \mathbf{H}_{21}^{(\mathrm{T})}\mathbf{V}_1^{(\mathrm{T})} \end{bmatrix} = \begin{bmatrix} \mathbf{H}_{22}^{\mathrm{ph1}}\mathbf{V}_2^{\mathrm{ph1}} & \mathbf{H}_{21}^{\mathrm{ph1}}\mathbf{V}_1^{\mathrm{ph1}} \\ \mathbf{H}_{22}^{\mathrm{ph2}}\mathbf{V}_2^{\mathrm{ph2}} & \mathbf{H}_{21}^{\mathrm{ph2}}\mathbf{V}_1^{\mathrm{ph2}} \end{bmatrix} \tag{4.12}$$

where $\mathbf{H}_{ij}^{\mathrm{ph1}} = \mathrm{Bdiag}(\mathbf{H}_{ij}^{(1)}, ..., \mathbf{H}_{ij}^{(T-q_i)})$ and $\mathbf{H}_{ij}^{\mathrm{ph2}} = \mathrm{Bdiag}(\mathbf{H}_{ij}^{(T-q_i+1)}, ..., \mathbf{H}_{ij}^{(T)})$. Also we have $\mathbf{V}_j^{\mathrm{ph1}} = \begin{bmatrix} \mathbf{V}_j^{(1)} \\ \cdots \\ \mathbf{V}_j^{(T-q_i)} \end{bmatrix}$ and $\mathbf{V}_j^{\mathrm{ph2}} = \begin{bmatrix} \mathbf{V}_j^{(T-q_i+1)} \\ \cdots \\ \mathbf{V}_j^{(T)} \end{bmatrix}$.

Here we present our simple achievable scheme which is based on retrospective interference alignment.

Proposition 1. *The following scheme (almost surely) achieves all the corner points (d_1, d_2) of the DoF region for all antenna configurations for which delayed CSIT is beneficial compared to no CSIT.*
Suppose that $i, j \in \{1, 2\}$ and $j \neq i$. The precoder of TX j is designed as follows :

- *if $d_1 + d_2 \leq N_i$ then a precoder $\mathbf{V}_j \in \mathbb{C}^{TM_j \times d_j^*}$ is randomly generated (i.i.d. Gaussian entries) and fixed during the whole transmission.*
- *if $d_1 + d_2 > N_i$, choosing $q_i = \frac{d_i^*}{N_i}$, then $\mathbf{V}_j = \begin{bmatrix} \mathbf{V}_j^{\mathrm{ph1}} \\ \mathbf{V}_j^{\mathrm{ph2}} \end{bmatrix}$ in which $\mathbf{V}_j^{\mathrm{ph1}} \in \mathbb{C}^{(T-q_i)M_j \times d_j^*}$ is chosen randomly (i.i.d. Gaussian entries) and fixed. Also we have $\mathbf{V}_j^{\mathrm{ph2}} = \mathbf{V}_{j,1}^{\mathrm{ph2}}\mathbf{V}_{j,2}^{\mathrm{ph2}}$ where $\mathbf{V}_{j,1}^{\mathrm{ph2}} \in \mathbb{C}^{q_i M_j \times l_{ij}}$ is again generated randomly (i.i.d. Gaussian entries) and $\mathbf{V}_{j,2}^{\mathrm{ph2}} \in \mathbb{C}^{l_{ij} \times d_j^*}$ has full row rank of $l_{ij} = min(q_i M_j, (T - q_i)N_i)$ and is chosen such that $\mathbf{V}_{j,2}^{\mathrm{ph2}} \in \mathcal{R}(\mathbf{H}_{ij}^{\mathrm{ph1}}\mathbf{V}_j^{\mathrm{ph1}})$ where $\mathcal{R}(\cdot)$ is the row space of its argument matrix.*

	Name in [11]	Condition
G_2	A.I.3	$M_1, M_2 \geq N_1 > N_2$
G_1	A.II.2	$M_1 > N_1 > M_2 \geq N_2$
	B.I	$N_1 \geq M_1 > N_2 > M_2$
	B.II.1	$M_1 > N_1 > N_2 > M_2$ and $M_2 \leq m$
	B.II.2	$M_1 > N_1 > N_2 > M_2$ and $M_2 > m$ and $M_1 = M'_1$
	B.III.1	$M_1 > M'_1 > N_1 > N_2 > M_2 > m$ and $M_1 \geq N_1 + N_2 - m$
	B.III.2	$M_1 > M'_1 > N_1 > N_2 > M_2 > m$ and $M_1 < N_1 + N_2 - m$

Table 4.1. Antenna configurations with larger DoF for delayed CSIT compared to no CSIT. $m = N_2\frac{M'_1-N_1}{M'_1-N_2}$ and $M'_1 = \min(M_1, N_1 + N_2 - M_2)$ with the assumption of $N_1 \geq N_2$.

In the rest of this chapter we prove the achievability of our scheme.

Without loss of generality assume that $N_1 \geq N_2$. According to [11] we have listed the configurations for which delayed CSIT DoF region is strictly larger than the no CSIT case in Table 4.1.

Remark 1. *For the case A.I.3 we have $d_1 + d_2 > N_1$ and for all other cases we have $N_2 < d_1 + d_2 \leq N_1$. This can be easily shown from the achievable points and the antenna relations for each case.*

Interference alignment is needed when the rank of the received space is smaller than the total number of streams. The consequence of Remark 1 is that in order to achieve the DoF region for case A.I.3 we need to align interference at both receivers while for the other cases it is sufficient to align interference only at one RX (RX 2 in our setting). Therefore we divide all the cases into the following two groups and prove the achievability for each group separately:

- Group G_1: This group includes the cases A.II.2, B.I, B.II.1, B.II.2, B.III.1,B.III.2 (which satisfy $N_2 < d_1 + d_2 \leq N_1$)
- Group G_2: This group includes only the case A.I.3 (which satisfies $d_1 + d_2 > N_1$).

Transmission Scheme for Group G_1

Theorem 4. *The precoders defined in Proposition 1 achieve all the corner points (d_1, d_2) of the DoF region for group G_1.*

Proof. To see the dimensions, we use the following notations for the TX/RX spaces defined earlier.

$$\mathbf{V}_1 = \begin{bmatrix} \left[\mathbf{V}_1^{\text{ph1}}\right]_{(T-q)M_1 \times d_1^*} \\ \left[\mathbf{V}_1^{\text{ph2}}\right]_{qM_1 \times d_1^*} \end{bmatrix} \qquad \mathbf{R_1} = \begin{bmatrix} \bar{\mathbf{S}}^{11}_{(T-q)N_1 \times d_1^*} & \bar{\mathbf{I}}^{12}_{(T-q)N_1 \times d_2^*} \\ \tilde{\mathbf{S}}^{11}_{qN_1 \times d_1^*} & \tilde{\mathbf{I}}^{12}_{qN_1 \times d_2^*} \end{bmatrix} \tag{4.13}$$

$$\mathbf{V}_2 = \begin{bmatrix} \left[\mathbf{V}_2^{\text{ph1}}\right]_{(T-q)M_2 \times d_2^*} \\ \left[\mathbf{V}_2^{\text{ph2}}\right]_{qM_2 \times d_2^*} \end{bmatrix} \qquad \mathbf{R_2} = \begin{bmatrix} \bar{\mathbf{I}}^{21}_{(T-q)N_2 \times d_1^*} \\ \mathbf{S}^{22}_{TN_2 \times d_2^*} \\ \tilde{\mathbf{I}}^{21}_{qN_2 \times d_1^*} \end{bmatrix} \tag{4.14}$$

where the precoders are chosen according to Proposition 1 and we have $\bar{\mathbf{S}}^{11} = \mathbf{H}_{11}^{\mathrm{ph1}}\mathbf{V}_1^{\mathrm{ph1}}$, $\tilde{\mathbf{S}}^{11} = \mathbf{H}_{11}^{\mathrm{ph2}}\mathbf{V}_1^{\mathrm{ph2}}$, $\bar{\mathbf{I}}^{12} = \mathbf{H}_{12}^{\mathrm{ph1}}\mathbf{V}_2^{\mathrm{ph1}}$, $\tilde{\mathbf{I}}^{12} = \mathbf{H}_{12}^{\mathrm{ph2}}\mathbf{V}_2^{\mathrm{ph2}}$ and $\mathbf{S}^{22} = \mathbf{H}_{22}\mathbf{V}_2$, $\bar{\mathbf{I}}^{21} = \mathbf{H}_{21}^{\mathrm{ph1}}\mathbf{V}_1^{\mathrm{ph1}}$, $\tilde{\mathbf{I}}^{21} = \mathbf{H}_{21}^{\mathrm{ph2}}\mathbf{V}_1^{\mathrm{ph2}}$. Since we align interference only at RX 2, we set $q = q_2 = \frac{d_2^*}{N_2}$. Clearly the precoder of TX 2 is generated randomly over the whole T time slots. However we have also split the precoder of TX 2 in two phases (with the same q) for simplicity of analysis.

Theorem 5. *The following set of conditions hold for group G_1:*

C.I *:* $d_i \leq \min(M_i, N_i),\ i = 1, 2$ and $N_2 < d_1 + d_2 \leq N_1$

C.II *:* $T(\mathrm{d_1 + d_2}) \leq (\mathrm{T - q})\mathrm{N_1} + \mathrm{qM_2} + \min(\mathrm{qN_1}, \mathrm{qM_1}, (\mathrm{T - q})\mathrm{N_2})$

C.III *:* $Td_1 \leq (T - q)M_1$

Proof. See Appendix B.1. □

Lemma 9. *If* C.I *holds then the scheme in Proposition 1 gives* $\mathrm{rank}(\mathbf{R_2}) = TN_2$ *for group* G_1.

Proof. We have $\mathbf{V}_{1,2}^{\mathrm{ph2}} \in \mathcal{R}(\mathbf{H}_{21}^{\mathrm{ph1}}\mathbf{V}_1^{\mathrm{ph1}}) = \mathcal{R}(\bar{\mathbf{I}}^{21})$. This gives $\mathbf{V}_1^{\mathrm{ph2}} \in \mathcal{R}(\bar{\mathbf{I}}^{21})$. Since $\tilde{\mathbf{I}}^{21} = \mathbf{H}_{21}^{\mathrm{ph2}}\mathbf{V}_1^{\mathrm{ph2}}$ therefore $\tilde{\mathbf{I}}^{21} \in \mathcal{R}(\bar{\mathbf{I}}^{21})$ which means that the interference of phase 2 is aligned in the space spanned by interference in phase 1. Since in group G_1 we have $d_1 + d_2 > N_2$ and $N_2 < M_1$ therefore we have

$$\mathrm{rank}(\bar{\mathbf{I}}^{21}) = \min((T - q)M_1, (T - q)N_2, d_1^*) = (T - q)N_2. \tag{4.15}$$

which means that $\bar{\mathbf{I}}^{21}$ has full row rank of $(T - q)N_2$. Since $l_{21} = \min(qM_1, (T - q)N_2)$, therefore $\mathbf{V}_{1,2}^{\mathrm{ph2}}$ has the maximum possible rank (l_{21}) that ensures the alignment condition, i.e., $\mathbf{V}_1^{\mathrm{ph2}} \in \mathcal{R}(\bar{\mathbf{I}}^{21})$. Further, the role of $\mathbf{V}_{1,1}^{\mathrm{ph2}}$ is to maximize the rank of the product of the channel with precoder of phase 2. This is crucial for decoding the desired signal.

From alignment we have $\mathrm{rank}\left(\begin{bmatrix}\bar{\mathbf{I}}^{21}\\ \\ \tilde{\mathbf{I}}^{21}\end{bmatrix}\right) = (T - q)N_2$. Also we have $\mathrm{rank}(\mathbf{S}^{22}) = \min(TM_2, TN_2, d_2^*) = d_2^*$, therefore

$$\mathrm{rank}(\mathbf{R_2}) = \mathrm{rank}\left(\begin{bmatrix}\bar{\mathbf{I}}^{21}\\ \\ \tilde{\mathbf{I}}^{21}\end{bmatrix}\right) + \mathrm{rank}(\mathbf{S}^{22}) = (T - q)N_2 + d_2^* = TN_2. \tag{4.16}$$

This is due to the fact that $\mathbf{S}^{22}$ is full rank and every column of $\mathbf{S}^{22}$ involves random entries which are generated independent of the columns of interference. Therefore the signal can be decoded at RX 2. □

Lemma 10. *If* C.III *holds, there is no overlap between the span of* $\bar{\mathbf{S}}^{11}$ *and* $\tilde{\mathbf{S}}^{11}$.

Proof. Note that if C.III holds then $\mathbf{V}_1^{\text{ph1}}$ will be full column rank and this means that $\mathcal{R}(\bar{\mathbf{S}}^{11})$ does not depend on $\mathbf{V}_1^{\text{ph1}}$ (it might depend on $\mathbf{H}_{11}^{\text{ph1}}$) and $\mathcal{R}(\bar{\mathbf{I}}^{21})$ depends on $\mathbf{H}_{21}^{\text{ph1}}$ (since $(T-q)N_2 \leq d_1^*$). We have $\mathcal{R}(\tilde{\mathbf{S}}^{11}) \in \mathcal{R}(\mathbf{V}_1^{\text{ph2}}) \in \mathcal{R}(\bar{\mathbf{I}}^{21})$ therefore the row spaces corresponding to $\bar{\mathbf{S}}^{11}$ and $\tilde{\mathbf{S}}^{11}$ are independent. □

Lemma 11. *If* C.I, C.II, C.III *are satisfied then the scheme in Proposition 1 gives* $\text{rank}(\mathbf{R_1}) \geq d_1^* + d_2^*$ *for group* G_1.

Proof. Since C.III holds, from Lemma 10 we have independence between $\bar{\mathbf{S}}^{11}$ and $\tilde{\mathbf{S}}^{11}$. Also we know that $\bar{\mathbf{I}}^{12}$ and $\tilde{\mathbf{I}}^{12}$ are independent. Therefore we can conclude that

$$\text{rank}(\mathbf{R_1}) = \text{rank}(\left[\bar{\mathbf{S}}^{11}\ \bar{\mathbf{I}}^{12}\right]) + \text{rank}(\begin{bmatrix}\tilde{\mathbf{S}}^{11}\ \tilde{\mathbf{I}}^{12}\end{bmatrix}). \tag{4.17}$$

It is easy to show that

$$\text{rank}(\left[\bar{\mathbf{S}}^{11}\ \bar{\mathbf{I}}^{12}\right]) = (T-q)N_1 \tag{4.18}$$

$$\text{rank}(\tilde{\mathbf{S}}^{11}) = \min(qN_1, qM_1, (T-q)N_2) \tag{4.19}$$

$$\text{rank}(\tilde{\mathbf{I}}^{12}) = qM_2 \tag{4.20}$$

$$\text{rank}(\begin{bmatrix}\tilde{\mathbf{S}}^{11}\ \tilde{\mathbf{I}}^{12}\end{bmatrix}) = \min(qN_1, \text{rank}(\tilde{\mathbf{I}}^{12}) + \text{rank}(\tilde{\mathbf{S}}^{11})). \tag{4.21}$$

Using the facts that $d_1 + d_2 \leq N_1$, if $\text{rank}(\begin{bmatrix}\tilde{\mathbf{S}}^{11}\ \tilde{\mathbf{I}}^{12}\end{bmatrix}) = qN_1$ we have

$$\begin{aligned} T(d_1+d_2) &\leq (T-q)N_1 + qN_1 \\ &= \text{rank}(\left[\bar{\mathbf{S}}^{11}\ \bar{\mathbf{I}}^{12}\right]) + \text{rank}(\begin{bmatrix}\tilde{\mathbf{S}}^{11}\ \tilde{\mathbf{I}}^{12}\end{bmatrix}) \\ &= \text{rank}(\mathbf{R_1}). \end{aligned}$$

If $\text{rank}(\begin{bmatrix}\tilde{\mathbf{S}}^{11}\ \tilde{\mathbf{I}}^{12}\end{bmatrix}) = \text{rank}(\tilde{\mathbf{I}}^{12}) + \text{rank}(\tilde{\mathbf{S}}^{11})$, from C.II we get

$$\begin{aligned} T(d_1+d_2) &\leq \text{rank}(\left[\bar{\mathbf{S}}^{11}\ \bar{\mathbf{I}}^{12}\right]) + \text{rank}(\tilde{\mathbf{I}}^{12}) + \text{rank}(\tilde{\mathbf{S}}^{11}) \\ &= \text{rank}(\left[\bar{\mathbf{S}}^{11}\ \bar{\mathbf{I}}^{12}\right]) + \text{rank}(\begin{bmatrix}\tilde{\mathbf{S}}^{11}\ \tilde{\mathbf{I}}^{12}\end{bmatrix}) \\ &= \text{rank}(\mathbf{R_1}). \end{aligned}$$

□

Based on Lemma 11 and Lemma 9 and Theorem 5, we have

$$\text{rank}(\mathbf{R_2}) = TN_2 \tag{4.22}$$

$$\text{rank}(\mathbf{R_1}) \geq d_1^* + d_2^*. \tag{4.23}$$

Since interference at RX2 is aligned in $(T-q)N_2$ dimensions and interference at RX1 is in a d_2^* dimensional space, the desired signal of both users can be decoded. Therefore the proof of Theorem 4 is complete.

□

Transmission Scheme for Group G_2

Theorem 6. *The precoders designed in Proposition 1 achieve all the corner points (d_1, d_2) of the DoF region for group G_2.*

Proof. In the case A.I.3 we have $M_1, M_2 > N_1 > N_2$ and the corner point of the region is $d_1 = \frac{N_1 M'_1(M'_2-N_2)}{N_1(M'_2-N_2)+M'_2(M'_1-N_1)}$ and $d_2 = \frac{N_2 M'_2(M'_1-N_1)}{N_1(M'_2-N_2)+M'_2(M'_1-N_1)}$ in which $M'_i = \min(M_i, N_1+N_2)$. If we choose the number of time slots equal to the denominator we will have $T = N_1(M'_2 - N_2) + M'_2(M'_1 - N_1)$ which gives $d_1^* = N_1 M'_1(M'_2 - N_2)$ and $d_2^* = N_2 M'_2(M'_1 - N_1)$.

Theorem 7. *The following conditions hold for group G_2:*

$\bar{\text{C}}$.I *:* $d_i \leq \min(M_i, N_i),\ i = 1, 2$ and $d_1 + d_2 > N_1$

$\bar{\text{C}}$.III *:* $Td_j \leq (T - q_i)M_j,\ i, j = 1, 2,\ i \neq j$.

Proof. See Appendix B.2. □

We know that the corner point of the outer bound is $d_1 = \frac{N_1 M'_1(M'_2-N_2)}{N_1(M'_2-N_2)+M'_2(M'_1-N_1)}$ and $d_2 = \frac{N_2 M'_2(M'_1-N_1)}{N_1(M'_2-N_2)+M'_2(M'_1-N_1)}$. Here we choose $q_1 = \frac{d_1^*}{N_1} = M'_1(M'_2 - N_2)$ and $q_2 = \frac{d_2^*}{N_2} = M'_2(M'_1 - N_1)$. With this choice we aim to align the interference at both RXs where we align the interference from phase 2 in the space of interference in phase 1 such that at RX i, the whole interference lies in a space of dimension $(T - q_i)N_i = TN_i - d_i^*$ which leaves d_i^* dimensions for the desired signal.

Here we show that the scheme presented in Proposition 1 achieves the desired DoF. The TX/RX spaces are shown below.

$$\mathbf{V}_1 = \begin{bmatrix} \begin{bmatrix}\mathbf{V}_1^{\text{ph1}}\end{bmatrix}_{(T-q_2)M_1 \times d_1^*} \\ \begin{bmatrix}\mathbf{V}_1^{\text{ph2}}\end{bmatrix}_{q_2 M_1 \times d_1^*} \end{bmatrix} \qquad \mathbf{R_1} = \begin{bmatrix} \bar{\mathbf{S}}^{11}_{(T-q_2)N_1 \times d_1^*} & \bar{\mathbf{I}}^{12}_{(T-q_1)N_1 \times d_2^*} \\ \tilde{\mathbf{S}}^{11}_{q_2 N_1 \times d_1^*} & \tilde{\mathbf{I}}^{12}_{q_1 N_1 \times d_2^*} \end{bmatrix} \tag{4.24}$$

$$\mathbf{V}_2 = \begin{bmatrix} \begin{bmatrix}\mathbf{V}_2^{\text{ph1}}\end{bmatrix}_{(T-q_1)M_2 \times d_2^*} \\ \begin{bmatrix}\mathbf{V}_2^{\text{ph2}}\end{bmatrix}_{q_1 M_2 \times d_2^*} \end{bmatrix} \qquad \mathbf{R_2} = \begin{bmatrix} \bar{\mathbf{S}}^{22}_{(T-q_1)N_2 \times d_2^*} & \bar{\mathbf{I}}^{21}_{(T-q_2)N_2 \times d_1^*} \\ \tilde{\mathbf{S}}^{22}_{q_1 N_2 \times d_2^*} & \tilde{\mathbf{I}}^{21}_{q_2 N_2 \times d_1^*} \end{bmatrix} \tag{4.25}$$

where we have $\bar{\mathbf{S}}^{11} = \mathbf{H}_{11}^{\text{ph1}}\mathbf{V}_1^{\text{ph1}}$, $\tilde{\mathbf{S}}^{11} = \mathbf{H}_{11}^{\text{ph2}}\mathbf{V}_1^{\text{ph2}}$, $\bar{\mathbf{I}}^{12} = \mathbf{H}_{12}^{\text{ph1}}\mathbf{V}_2^{\text{ph1}}$, $\tilde{\mathbf{I}}^{12} = \mathbf{H}_{12}^{\text{ph2}}\mathbf{V}_2^{\text{ph2}}$ and $\bar{\mathbf{S}}^{22} = \mathbf{H}_{22}^{\text{ph1}}\mathbf{V}_2^{\text{ph1}}$, $\tilde{\mathbf{S}}^{22} = \mathbf{H}_{22}^{\text{ph2}}\mathbf{V}_2^{\text{ph2}}$, $\bar{\mathbf{I}}^{21} = \mathbf{H}_{21}^{\text{ph1}}\mathbf{V}_1^{\text{ph1}}$, $\tilde{\mathbf{I}}^{21} = \mathbf{H}_{21}^{\text{ph2}}\mathbf{V}_1^{\text{ph2}}$.

Similar to the previous section we have $\tilde{\mathbf{I}}^{21} \in \mathcal{R}(\bar{\mathbf{I}}^{21})$ and additionally $\tilde{\mathbf{I}}^{12} \in \mathcal{R}(\bar{\mathbf{I}}^{12})$. Note that $\bar{\mathbf{I}}^{12}$ and $\bar{\mathbf{I}}^{21}$ are full rank which indicates that the designed precoders $\mathbf{V}_{1,2}^{\text{ph2}}$ and $\mathbf{V}_{2,2}^{\text{ph2}}$ have the maximum possible rank that ensures the alignment condition. Also similar to the previous case we have used a random precoder in order to make sure that the ranks of the received signals at the RXs are maximized which facilitates the decoding of the desired streams.

In phase 2, TX 1 needs to have access to $\bar{\mathbf{I}}^{21}$ and TX 2 needs to have access to $\bar{\mathbf{I}}^{12}$. This means that although the phases are not synchronized (q_1 and q_2 might be different), the TXs can have access to the necessary information after transmitting in their corresponding first phase.

Lemma 12. *If conditions* $\bar{\text{C}}$.I *and* $\bar{\text{C}}$.III *hold, the scheme in Proposition 1 ensures that the received spaces* $\mathbf{R_1}$ *and* $\mathbf{R_2}$ *are full rank for group* G_2.

Proof. We know that $TN_1 < d_1^* + d_2^* = q_1N_1 + q_2N_2 < (q_1+q_2)N_1$ which gives $q_1 + q_2 > T$. Assume that $i, j \in \{1, 2\}$ and $i \neq j$. Using this fact and based on the condition $\bar{\text{C}}$.I, the relations between the number of antennas and the condition on the rank of the precoders, we get:

$$\text{rank}(\bar{\mathbf{S}}^{ii}) = (T - q_j)N_i, \quad \text{rank}(\bar{\mathbf{I}}^{ij}) = (T - q_i)N_i \tag{4.26}$$

$$\text{rank}(\tilde{\mathbf{S}}^{ii}) = \min(q_jN_i, (T - q_j)N_j), \quad \text{rank}(\tilde{\mathbf{I}}^{ij}) = \min(q_iN_i, (T - q_i)N_i) \tag{4.27}$$

Consider RX i. From alignment condition we get $\text{rank}\left(\begin{bmatrix}\bar{\mathbf{I}}^{ij}\\ \\ \tilde{\mathbf{I}}^{ij}\end{bmatrix}\right) = (T - q_i)N_i$. Therefore using the same argument as in the previous section we have

$$\text{rank}(\mathbf{R_i}) = \text{rank}\left(\begin{bmatrix}\bar{\mathbf{I}}^{ij}\\ \\ \tilde{\mathbf{I}}^{ij}\end{bmatrix}\right) + \text{rank}\left(\begin{bmatrix}\bar{\mathbf{S}}^{ii}\\ \\ \tilde{\mathbf{S}}^{ii}\end{bmatrix}\right) = (T - q_i)N_i + \text{rank}\left(\begin{bmatrix}\bar{\mathbf{S}}^{ii}\\ \\ \tilde{\mathbf{S}}^{ii}\end{bmatrix}\right).$$

From $\bar{\text{C}}$.III we have independence between $\bar{\mathbf{S}}^{ii}$ and $\tilde{\mathbf{S}}^{ii}$ which gives $\text{rank}\left(\begin{bmatrix}\bar{\mathbf{S}}^{ii}\\ \\ \tilde{\mathbf{S}}^{ii}\end{bmatrix}\right) = \text{rank}(\bar{\mathbf{S}}^{ii}) + \text{rank}(\tilde{\mathbf{S}}^{ii})$.

Therefore we get

$$\text{rank}(\mathbf{R_i}) = (T - q_i)N_i + \text{rank}(\bar{\mathbf{S}}^{ii}) + \text{rank}(\tilde{\mathbf{S}}^{ii}). \tag{4.28}$$

Substituting for T, q_i, q_j, we have $(T - q_j)M'_i = q_iN_i$ and since $M'_i \leq N_i + N_j$, we have $(T - q_j)N_i + (T - q_j)N_j \geq (T - q_j)M'_i = q_iN_i$. Also we have $(T - q_j)N_i + q_jN_i = TN_i \geq q_iN_i$. Therefore

$$\begin{aligned}&(T - q_j)N_i + \min(q_jN_i, (T - q_j)N_j) \geq q_iN_i\\ &\Rightarrow \text{rank}(\bar{\mathbf{S}}^{ii}) + \text{rank}(\tilde{\mathbf{S}}^{ii}) \geq q_iN_i\\ &\Rightarrow \text{rank}(\mathbf{R_i}) \geq TN_i.\end{aligned}$$

□

Similarly, from Lemma 12 and Theorem 7, it can be inferred that the signal at both receivers can be decoded, hence the proof of Theorem 6 is complete.

□

5

Distributed Interference Alignment

Despite its deceptively simple mathematical formulation, IA has no general closed-form solution (although the solution exists for certain dimensions, see e.g. [77]). In large networks, or when the network topology cannot be assumed to be known, distributed implementations are desirable due to the increasing amount of information exchange requirement along with the growing computational complexity. An iterative distributed implementation relying on over-the-air estimation of interference covariance was proposed in [12].

Message-passing algorithms, and in particular the sum-product algorithm [78], have been used to solve decoding problems in communications. In a nutshell, they provide an efficient way to compute functions involving a large number of variables when the function in question can be decomposed (factorized) into terms that involve only a subset of the variables. Such algorithms are known to distribute the complexity associated to the increasing size of the network over the individual nodes of the network. In this chapter we aim to model the procedure of finding the alignment precoders as a message passing problem. It turns out that our message passing solution includes the well known minimum leakage algorithm [12] as a special case.

5.1 State of the Art

MP solutions can be formulated for a variety of problems requiring computations on a commutative semiring, i.e. they are not restricted to the computation of probability distributions [79]. In fact, depending on the choice of the semiring (and the associated binary operations, such as sum, product or minimum), MP solutions are available for Bayesian inference (yielding the belief-propagation approach of ML decoding [80]) as well as optimization problems (e.g. the min-sum algorithm [81]).

A major motivation for considering MP is that the resulting algorithms are well suited for distributed implementation. This is because for most practical applications, each factor in the function only depends on *local* data (in our application, channel state information). MP has already been considered for beamformer optimization in [82], where the sum-product algorithm is applied to a function broadly related to the sum-rate. In [83], the min-sum algorithm is applied to the sum-rate function. The proposed algorithm is restricted to discrete precoders.

In this work, we introduce a message-passing technique which optimizes the leakage function associated with interference alignment. We deal with continuous variables, i.e. we let the precoders and receive filter matrices take any value in the Stiefel manifold, in contrast to the results of [82, 83] where the precoders are chosen from a finite set. This is motivated by the fact that the number of IA solutions is in general finite [84] – therefore, solving the leakage minimization problem on a discrete subset of the Stiefel manifold will in general not yield an exact IA solution, while solving it on the (continuous) Stiefel manifold will do.

5.2 Factor Graphs

Factor graphs are a family of graphical models which have been very useful in signal processing and communications. Factor graphs subsume many other graphical models in signal processing, probability theory and coding, including Markov random fields [85–87], Bayesian networks [88, 89] and Tanner graphs [90, 91]. A factor graph is a representation for a function of several variables that can be decomposed into a product/sum of factors each involving a subset of variables. For instance the function

$$f(x_1, x_2, x_3, x_4) = f_1(x_1, x_2, x_4) + f_2(x_3, x_4) \tag{5.1}$$

is defined for variables $x_1, ..., x_4$ and has factors f_1, f_2. In the associated factor graph (Figure 5.1), every variable is depicted by a circle while every function is represented by a square. An edge between a function node f_i and a variable node x_j indicates that f_i is a function of x_j. For example the function f_1 is a function of x_1, x_2, x_4 and therefore the variable nodes x_1, x_2, x_4 are connected to the function node f_1.

A particular assignment of a value to each of the variables is referred to as a configuration of the variables. The configuration space is the set of all possible configurations which is the domain of the function f. We are interested to find the configuration which minimizes the value of f.

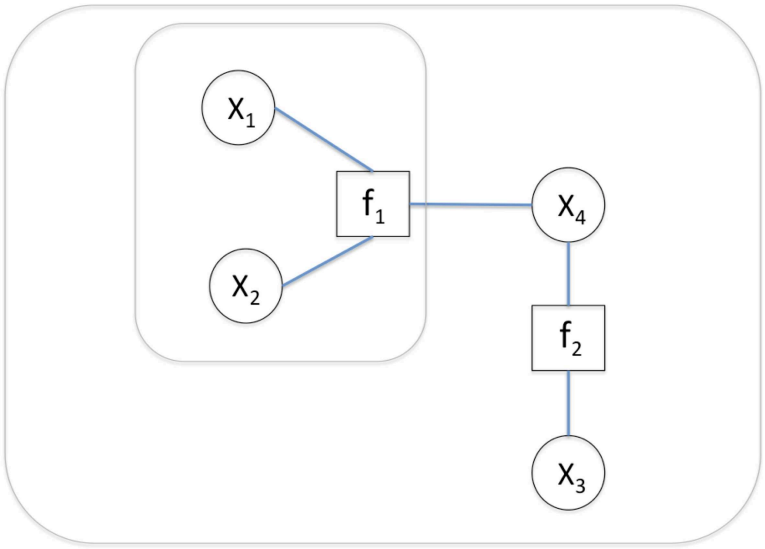

Figure 5.1. Factor Graph associated to the function f

We consider marginal functions $g_i(x_i)$ associated with every function $f(x_1, ..., x_n)$. For each feasible a, the value of $g_i(a)$ is obtained by taking the minimum value of $f(x_1, ..., x_n)$ over all configurations of the variables that have $x_i = a$. This definition of marginal function is a particular choice which is desirable for our problem and in general marginal functions can be defined in different ways. Instead of indicating the variables being minimized over, we indicate those variables not involved in the minimization. For example, if f_1 is a function of three variables x_1, x_2, x_3, then the summary for x_2 is denoted by

$$\min_{\sim x_2} f_1(x_1, x_2, x_3) = \min_{x_1} \min_{x_3} f_1(x_1, x_2, x_3) \tag{5.2}$$

In this notation we have

$$g_i(x_i) = \min_{\sim x_i} f(x_1, ..., x_n) \tag{5.3}$$

i.e., the ith marginal function associated with $f(x_1, ..., x_n)$ is the summary for x_i of f. When the marginals are available, a local optimization of the marginal function over the corresponding variable leads to a solution for this variable which is a globally optimal solution (when the graph is a tree), i.e.,

$$\min_{x_i} g_i(x_i) = \min_{x_i} \min_{\sim x_i} f(x_1, ..., x_n) = \min_{x_1,...,x_n} f(x_1, ..., x_n). \tag{5.4}$$

In our example the computation complexity of (5.3) can be reduced by exploiting the distributive law:

$$\min_{\sim x_3} f(x_1, ..., x_4) = \min_{x_4} \left[f_2(x_3, x_4) + \min_{x_1,x_2} f_1(x_1, x_2, x_4) \right]. \tag{5.5}$$

Comparing the above expression to the factor graph, we observe that each minimization corresponds to replacing each box with a new quantity which is a function of the summary variable. This quantity is referred to as a message. After replacing the small box in Figure 5.1 with its corresponding message ($m_{f_1 \to x_4}(x_4)$), the marginal can be rewritten as

$$\min_{\sim x_3} f(x_1, ..., x_4) = \min_{x_4} \left[f_2(x_3, x_4) + m_{f_1 \to x_4}(x_4) \right] \tag{5.6}$$

Similarly the replacement for the large box will be a minimization of the function $f_2(x_3, x_4) + m_{f_1 \to x_4}(x_4)$ over x_4. The example describes the message updates procedure where we start from the leave nodes of the factor graph and messages are passed along the edges. The updated messages are propagated to other nodes of the factor graph.

As a generalization of the above example, the following message update rules can be derived for the message initiating from a variable node to a function node and vice versa.

The general form of the variable-to-function updates in the considered message-passing algorithm can be computed as [81]

$$m_{a \to b}(x_a) = \sum_{i \in \mathcal{N}(a) \setminus b} m_{i \to a}(x_a), \tag{5.7}$$

where a is the variable node (and x_a the corresponding variable), b represents the function node, and $\mathcal{N}(a)$ denotes the set of neighbors of a.

Updates from function node b to a variable node $a \in \mathcal{N}(b)$ take the general form

$$m_{b \to a}(x_a) = \min_{X_b \setminus x_a} \left[C_b(X_b) + \sum_{j \in \mathcal{N}(b) \setminus a} m_{j \to b}(x_j) \right] \tag{5.8}$$

where C_b is the function associated to node b and X_b is the set of all variables which are arguments of C_b.

5.2.1 Min-Sum Algorithm

The marginal functions can be derived in parallel to avoid further calculations of intermediate messages. The specific algorithm that performs this calculations is called min-sum algorithm [81]. The algorithm starts at the leaves of the graph (assuming that the graph is a tree). The initial messages originating from leaves that are variable nodes is set to 0 and the leaves that are function nodes send the function value to their neighbors. The message update rules are applied as soon as the necessary information is available at the edges to compute the outgoing messages. The updated messages are then propagated to the neighbors. The marginal function $g_k(x_k)$ of a variable nodes x_k is obtained as sum of all incoming messages

$$g_k(x_k) = \sum_{l \in \mathcal{N}(k)} m_{l \to k}(x_k). \tag{5.9}$$

In case that the underlying factor graph has cycles, the min-sum algorithm can be still applied. However, the obtained marginals from this algorithm do not represent the true marginals. Consider an example obtained by slightly modifying the function,

$$f(x_1, ..., x_4) = f_1(x_1, x_2, x_4) + f_2(x_3, x_4) + f_3(x_2, x_3). \tag{5.10}$$

Running min-sum algorithm for this graph results in infinite propagation of messages in a round. There is no guarantee that the algorithm converges and if it does, there is no theoretical result to show the optimality of the convergence point. In many practical applications the sum-product algorithm which is another message passing algorithm is seen to provide good performance. For example LDPC codes and turbo codes are represented by graphs that have many cycles and application of the sum-product algorithm on these graphs has shown surprisingly good results.

5.3 Distributed Design of the Alignment Precoders

5.3.1 Modeling Interference Alignment as a Message Passing Problem

Consider the IA equations (2.7) for the K-user interference channel. Our aim is to solve for the $\mathbf{U}_i$ and $\mathbf{V}_j$, given the channel matrices. Here we focus on the cases where the dimensions are such that IA is feasible for almost all channels with coefficients drawn from continuous distributions [92].

We reformulate the above IA conditions using the interference leakage metric:

$$(2.7) \quad \overset{(a)}{\Leftrightarrow} \quad \sum_{i=1}^{K} \sum_{j \neq i} \mathrm{tr}\left(\mathbf{U}_i^H \mathbf{H}_{ij} \mathbf{V}_j \mathbf{V}_j^H \mathbf{H}_{ij}^H \mathbf{U}_i\right) = 0 \tag{5.11}$$

$$\overset{(b)}{\Leftrightarrow} \quad \sum_{i=1}^{K} \underbrace{\sum_{j \neq i} \mathrm{tr}\left(\mathbf{U}_i^H \mathbf{H}_{ij} \mathbf{V}_j \mathbf{V}_j^H \mathbf{H}_{ij}^H \mathbf{U}_i\right)}_{f_i(\mathbf{U}_i, \mathbf{V}_{\sim i})} + \sum_{j=1}^{K} \underbrace{\sum_{i \neq j} \mathrm{tr}\left(\mathbf{V}_j^H \mathbf{H}_{ij}^H \mathbf{U}_i \mathbf{U}_i^H \mathbf{H}_{ij} \mathbf{V}_j\right)}_{g_j(\mathbf{V}_j, \mathbf{U}_{\sim j})} = 0. \tag{5.12}$$

In the above, (a) follows from the fact that $\mathbf{X} = \mathbf{0} \Leftrightarrow \mathrm{tr}\left(\mathbf{X}\mathbf{X}^H\right) = 0$ and the sum is zero iff all the (non-negative) summands are zero; and (b) holds because $\sum_{i=1}^{K} f_i(\mathbf{U}_i, \mathbf{V}_{\sim i}) = \sum_{j=1}^{K} g_j(\mathbf{V}_j, \mathbf{U}_{\sim j})$. Using the notations introduced above, where f_i and g_j are non-negative real functions, we note that (2.7) admits the same solution set as the optimization problem

$$\min_{\substack{\mathbf{U}_1, \ldots, \mathbf{U}_K \in V_{N,d}, \\ \mathbf{V}_1, \ldots, \mathbf{V}_K \in V_{M,d}}} \sum_{i=1}^{K} f_i(\mathbf{U}_i, \mathbf{V}_{\sim i}) + \sum_{j=1}^{K} g_j(\mathbf{V}_j, \mathbf{U}_{\sim j}). \tag{5.13}$$

We propose to solve (5.13) via message passing, specifically using the min-sum algorithm. In order to do that, we construct a graph with $2K$ variable nodes $\mathbf{U}_i$, $i = 1 \ldots K$ and $\mathbf{V}_j$, $j = 1 \ldots K$, and $2K$ function nodes f_i, $i = 1 \ldots K$ and g_j, $j = 1 \ldots K$. A connection in the graph represents dependency of a function on the corresponding variable. An example of such a graph obtained for a 3-user network is shown in Fig. 5.2.

Note that according to the above graph construction, f_i depends on $\mathbf{U}_i$ and on all $\mathbf{V}_j$, $j \neq i$; this assumption is valid for fully connected networks ($\mathbf{H}_{ij} \neq \mathbf{0}\ \forall (i,j)$). For partially connected networks (see [93, 94]), the connectivity of the graph should be adjusted accordingly, i.e. if $\mathbf{H}_{ij} = \mathbf{0}$, the edges between f_i and $\mathbf{V}_j$, as well as between g_j and $\mathbf{U}_i$ should be removed.

Variable-to-Function Messages

For the considered problem, considering for instance the messages originating from $\mathbf{U}_i$ (and the set of its neighbors $\mathcal{N}(\mathbf{U}_i) = \{f_i, g_{\sim i}\}$), we must particularize (5.7) and distinguish between messages going to f_i and those going to one of the $g_j, j \neq i$:

$$m_{\mathbf{U}_i \to f_i}(\mathbf{U}_i) = \sum_{j \neq i} m_{g_j \to \mathbf{U}_i}(\mathbf{U}_i) \tag{5.14}$$

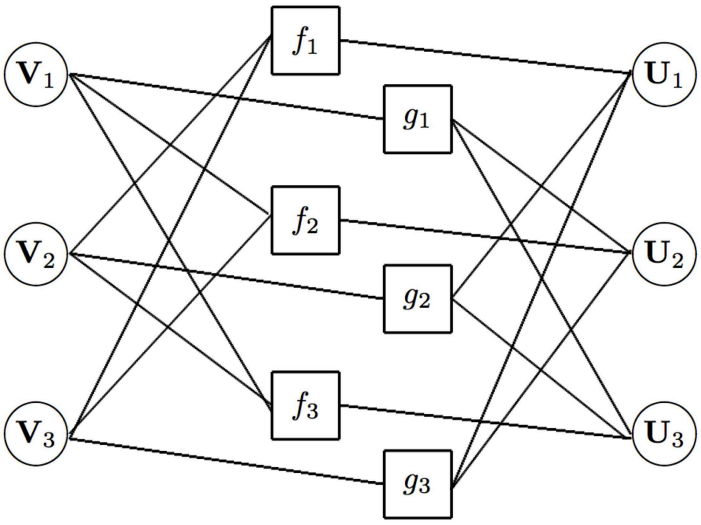

Figure 5.2. Graph obtained for IA over the 3-user, fully connected interference channel.

while

$$m_{\mathbf{U}_i \to g_j}(\mathbf{U}_i) = m_{f_i \to \mathbf{U}_i}(\mathbf{U}_i) + \sum_{k \neq i,j} m_{g_k \to \mathbf{U}_i}(\mathbf{U}_i) \tag{5.15}$$

(note that, by a slight abuse of notation, we use the same name for the nodes in the graph and the matrices or functions they represent). By symmetry, we have

$$m_{\mathbf{V}_j \to g_j}(\mathbf{V}_j) = \sum_{i \neq j} m_{f_i \to \mathbf{V}_j}(\mathbf{V}_j) \tag{5.16}$$

and

$$m_{\mathbf{V}_j \to f_i}(\mathbf{V}_j) = m_{g_j \to \mathbf{V}_j}(\mathbf{V}_j) + \sum_{k \neq i,j} m_{f_k \to \mathbf{V}_j}(\mathbf{V}_j). \tag{5.17}$$

Function-to-Variable Messages

Here again, considering a function node f_i and its set of neighbors $\mathcal{N}(f_i) = \{\mathbf{U}_i, \mathbf{V}_{\sim i}\}$, we particularize (5.8) depending on whether the message is going to $\mathbf{U}_i$ or to one of the $\mathbf{V}_j, j \neq i$:

$$m_{f_i \to \mathbf{U}_i}(\mathbf{U}_i) = \min_{\mathbf{V}_{\sim i}} \Big[f_i(\mathbf{U}_i, \mathbf{V}_{\sim i}) + \sum_{j \neq i} m_{\mathbf{V}_j \to f_i}(\mathbf{V}_j) \Big] \tag{5.18}$$

$$m_{f_i \to \mathbf{V}_j}(\mathbf{V}_j) = \min_{\mathbf{U}_i, \mathbf{V}_{\sim i,j}} \Big[f_i(\mathbf{U}_i, \mathbf{V}_{\sim i}) + m_{\mathbf{U}_i \to f_i}(\mathbf{U}_i) + \sum_{k \neq i,j} m_{\mathbf{V}_k \to f_i}(\mathbf{V}_k) \Big]. \tag{5.19}$$

Note that the optimization domain is implicitly understood to be $V_{N,d}$ (for the $\mathbf{U}_i$ variables) or $V_{M,d}$ (for the $\mathbf{V}_j$). Again, by symmetry, we have

$$m_{g_j \to \mathbf{V}_j}(\mathbf{V}_j) = \min_{\mathbf{U}_{\sim j}} \Big[g_j(\mathbf{V}_j, \mathbf{U}_{\sim j}) + \sum_{i \neq j} m_{\mathbf{U}_i \to g_j}(\mathbf{U}_i) \Big] \tag{5.20}$$

$$m_{g_j \to \mathbf{U}_i}(\mathbf{U}_i) = \min_{\mathbf{V}_j, \mathbf{U}_{\sim i,j}} \Big[g_j(\mathbf{V}_j, \mathbf{U}_{\sim j}) + m_{\mathbf{V}_j \to g_j}(\mathbf{V}_j) + \sum_{k \neq i,j} m_{\mathbf{U}_k \to g_j}(\mathbf{U}_k) \Big]. \tag{5.21}$$

Convergence

When considering tree-like graphs, propagating messages from the leaves to the root ensures that an exact solution is found with a finite number of message exchanges. Clearly, this is not the case here, since the considered graphs have loops – in that case, the messages are initialized with random values, and message-passing is executed until convergence. In that case, the schedule (the order in which messages are propagated in the graph) can be arbitrary. Although convergence is not always provable (see [95] for some convergence results applying to the min-sum algorithm), this will not constitute a problem here, as the proposed algorithm has been observed to converge reliably, as will be seen in Section 5.4.

After convergence, the variables of interest are computed from the local beliefs at each variable node, according to

$$\mathbf{U}_i^* = \arg\min_{\mathbf{U}_i} \sum_{a \in \mathcal{N}(\mathbf{U}_i)} m_{a \to \mathbf{U}_i}(\mathbf{U}_i), \tag{5.22}$$

$$\mathbf{V}_j^* = \arg\min_{\mathbf{V}_j} \sum_{a \in \mathcal{N}(\mathbf{V}_j)} m_{a \to \mathbf{V}_j}(\mathbf{V}_j). \tag{5.23}$$

Note that the messages considered here are in fact functions: in (5.18) for example, the message consists in the value of $m_{f_i \to \mathbf{U}_i}$ evaluated at all possible $\mathbf{U}_i$. If $\mathbf{U}_i$ takes on a finite number of values, it can be practical to compute the message by solving the minimization problem in the right-hand side for each possible value of $\mathbf{U}_i$. However, this method is clearly impractical for continuous variables. In the sequel, we turn our attention to the continuous case.

5.3.2 Continuous Variable Case

In order to have a compact (and computationally manageable) representation of continuous functions, we introduce a parameterization of our messages. Let us assume that every message $m_{a \to b}(\mathbf{X})$, where $\mathbf{X}$ is a truncated unitary matrix, takes the form

$$m_{a \to b}(\mathbf{X}) = \mathrm{tr}\left(\mathbf{X}^H \mathbf{Q}_{a \to b} \mathbf{X}\right) \tag{5.24}$$

for some positive semidefinite matrix $\mathbf{Q}_{a \to b}$. Clearly, under this assumption, the message $m_{a \to b}$ is equivalently represented by the corresponding matrix $\mathbf{Q}_{a \to b}$. Using this parameterization, and resorting to approximations where necessary, we now show that the message computations from Section 5.3.1 admit closed-form expressions of the form (5.24).

Starting with (5.14), we notice that it can be transformed as

$$m_{\mathbf{U}_i \to f_i}(\mathbf{U}_i) = \sum_{j \neq i} \mathrm{tr}\left(\mathbf{U}_i^H \mathbf{Q}_{g_j \to \mathbf{U}_i} \mathbf{U}_i\right) = \mathrm{tr}\left(\mathbf{U}_i^H \left[\sum_{j \neq i} \mathbf{Q}_{g_j \to \mathbf{U}_i}\right] \mathbf{U}_i\right). \tag{5.25}$$

Identifying this expression with (5.24) shows that

$$\mathbf{Q}_{\mathbf{U}_i \to f_i} = \sum_{j \neq i} \mathbf{Q}_{g_j \to \mathbf{U}_i}. \tag{5.26}$$

Using a similar reasoning, (5.15)–(5.17) yield trivially

$$\mathbf{Q}_{\mathbf{U}_i \to g_j} = \mathbf{Q}_{f_i \to \mathbf{U}_i} + \sum_{k \neq i,j} \mathbf{Q}_{g_k \to \mathbf{U}_i}, \tag{5.27}$$

$$\mathbf{Q}_{\mathbf{V}_j \to g_j} = \sum_{i \neq j} \mathbf{Q}_{f_i \to \mathbf{V}_j} \tag{5.28}$$

$$\mathbf{Q}_{\mathbf{V}_j \to f_i} = \mathbf{Q}_{g_j \to \mathbf{V}_j} + \sum_{k \neq i,j} \mathbf{Q}_{f_k \to \mathbf{V}_j}. \tag{5.29}$$

The case of the the function-to-variable messages is more interesting, since we now seek the closed-form expressions of the solutions to the minimization problems (5.18)–(5.21). Let us first turn our attention to (5.18), and notice that

$$\begin{aligned} &f_i(\mathbf{U}_i, \mathbf{V}_{\sim i}) + \sum_{j \neq i} m_{\mathbf{V}_j \to f_i}(\mathbf{V}_j) \\ &= \sum_{j \neq i} \left[\mathrm{tr}\left(\mathbf{U}_i^H \mathbf{H}_{ij} \mathbf{V}_j \mathbf{V}_j^H \mathbf{H}_{ij}^H \mathbf{U}_i \right) + \mathrm{tr}\left(\mathbf{V}_j^H \mathbf{Q}_{\mathbf{V}_j \to f_i} \mathbf{V}_j \right) \right]. \end{aligned} \tag{5.30}$$

Note that each term in the above sum depends only on a single $\mathbf{V}_j$. This indicates that the minimization over $\mathbf{V}_{\sim i}$ in (5.18) is separable, and therefore

$$\begin{aligned} m_{f_i \to \mathbf{U}_i}(\mathbf{U}_i) &= \sum_{j \neq i} \min_{\mathbf{V}_j} \left[\mathrm{tr}\left(\mathbf{U}_i^H \mathbf{H}_{ij} \mathbf{V}_j \mathbf{V}_j^H \mathbf{H}_{ij}^H \mathbf{U}_i \right) + \mathrm{tr}\left(\mathbf{V}_j^H \mathbf{Q}_{\mathbf{V}_j \to f_i} \mathbf{V}_j \right) \right] \\ &= \sum_{j \neq i} \min_{\mathbf{V}_j} \mathrm{tr}\left(\mathbf{V}_j^H \left[\mathbf{H}_{ij}^H \mathbf{U}_i \mathbf{U}_i^H \mathbf{H}_{ij} + \mathbf{Q}_{\mathbf{V}_j \to f_i} \right] \mathbf{V}_j \right). \end{aligned} \tag{5.31}$$

Here, we resort to our first approximation, and assume that

$$\arg\min \mathrm{tr}\left(\mathbf{V}_j^H \left[\mathbf{H}_{ij}^H \mathbf{U}_i \mathbf{U}_i^H \mathbf{H}_{ij} + \mathbf{Q}_{\mathbf{V}_j \to f_i} \right] \mathbf{V}_j \right) \approx \arg\min \mathrm{tr}\left(\mathbf{V}_j^H \mathbf{Q}_{\mathbf{V}_j \to f_i} \mathbf{V}_j \right). \tag{5.32}$$

Note that this approximation becomes exact if $\mathbf{V}_j^H \mathbf{H}_{ij}^H \mathbf{U}_i = \mathbf{0}$, i.e. in particular at convergence, when (2.7) is fulfilled. Letting $\mathbf{V}_j^0 = \nu_{\min}\left(\mathbf{Q}_{\mathbf{V}_j \to f_i} \right)$ for all $j \neq i$, we have

$$\begin{aligned} m_{f_i \to \mathbf{U}_i}(\mathbf{U}_i) &= \sum_{j \neq i} \mathrm{tr}\left(\mathbf{U}_i^H \mathbf{H}_{ij} \mathbf{V}_j^0 \mathbf{V}_j^{0H} \mathbf{H}_{ij}^H \mathbf{U}_i \right) + \mathrm{tr}\left(\mathbf{V}_j^{0H} \mathbf{Q}_{\mathbf{V}_j \to f_i} \mathbf{V}_j^0 \right) \\ &= \mathrm{tr}\left(\mathbf{U}_i^H \left[\sum_{j \neq i} \mathbf{H}_{ij} \mathbf{V}_j^0 \mathbf{V}_j^{0H} \mathbf{H}_{ij}^H + \mathrm{I} \frac{1}{d} \mathrm{tr}\left(\mathbf{V}_j^{0H} \mathbf{Q}_{\mathbf{V}_j \to f_i} \mathbf{V}_j^0 \right) \right] \mathbf{U}_i \right). \end{aligned} \tag{5.33}$$

This yields the final message computation rule

$$\mathbf{Q}_{f_i \to \mathbf{U}_i} = \sum_{j \neq i} \mathbf{H}_{ij} \mathbf{V}_j^0 \mathbf{V}_j^{0H} \mathbf{H}_{ij}^H + \mathrm{I} \frac{1}{d} \mathrm{tr}\left(\mathbf{V}_j^{0H} \mathbf{Q}_{\mathbf{V}_j \to f_i} \mathbf{V}_j^0 \right). \tag{5.34}$$

The case of (5.19) follows a similar derivation:

$$\begin{aligned} m_{f_i \to \mathbf{V}_j}(\mathbf{V}_j) = \min_{\mathbf{U}_i, \mathbf{V}_{\sim i,j}} \Bigg[&\mathrm{tr}\left(\mathbf{U}_i^H \left[\sum_{k \neq i} \mathbf{H}_{ik} \mathbf{V}_k \mathbf{V}_k^H \mathbf{H}_{ik}^H \right] \mathbf{U}_i \right) \\ &+ \mathrm{tr}\left(\mathbf{U}_i^H \mathbf{Q}_{\mathbf{U}_i \to f_i} \mathbf{U}_i \right) + \sum_{k \neq i,j} \mathrm{tr}\left(\mathbf{V}_k^H \mathbf{Q}_{\mathbf{V}_k \to f_i} \mathbf{V}_k \right) \Bigg] \end{aligned} \tag{5.35}$$

$$= \min_{\mathbf{U}_i, \mathbf{V}_{\sim i,j}} \Bigg[\mathrm{tr}\left(\mathbf{U}_i^H \mathbf{H}_{ij} \mathbf{V}_j \mathbf{V}_j^H \mathbf{H}_{ij}^H \mathbf{U}_i\right) + \mathrm{tr}\Bigg(\mathbf{U}_i^H \underbrace{\left[\mathbf{Q}_{\mathbf{U}_i \to f_i} + \frac{1}{2} \sum_{k \neq i,j} \mathbf{H}_{ik} \mathbf{V}_k \mathbf{V}_k^H \mathbf{H}_{ik}^H \right]}_{\mathbf{R}} \mathbf{U}_i \Bigg) \tag{5.36}$$

$$+ \sum_{k \neq i,j} \mathrm{tr}\Bigg(\mathbf{V}_k^H \underbrace{\left[\mathbf{Q}_{\mathbf{V}_k \to f_i} + \frac{1}{2} \mathbf{H}_{ik}^H \mathbf{U}_i \mathbf{U}_i^H \mathbf{H}_{ik} \right]}_{\mathbf{S}_k} \mathbf{V}_k \Bigg) \Bigg].$$

Again, we choose to approximate the minimization above by assuming that

$$\arg \min_{\mathbf{U}_i, \mathbf{V}_{\sim i,j}} \Big[\mathrm{tr}\left(\mathbf{U}_i^H \mathbf{H}_{ij} \mathbf{V}_j \mathbf{V}_j^H \mathbf{H}_{ij}^H \mathbf{U}_i\right) + \mathrm{tr}\left(\mathbf{U}_i^H \mathbf{R} \mathbf{U}_i\right) + \sum_{k \neq i,j} \mathrm{tr}\left(\mathbf{V}_k^H \mathbf{S}_k \mathbf{V}_k\right) \Big] \tag{5.37}$$

$$\approx \arg \min_{\mathbf{U}_i, \mathbf{V}_{\sim i,j}} \Big[\mathrm{tr}\left(\mathbf{U}_i^H \mathbf{R} \mathbf{U}_i\right) + \sum_{k \neq i,j} \mathrm{tr}\left(\mathbf{V}_k^H \mathbf{S}_k \mathbf{V}_k\right) \Big]. \tag{5.38}$$

Note however that $\mathbf{R}$ depends on $\mathbf{V}_{\sim i,j}$ and $\mathbf{S}_k$ is a function of $\mathbf{U}_i$, so the resulting minimization problem is not separable. We resort to alternating minimization of $\mathrm{tr}\left(\mathbf{U}_i^H \mathbf{R} \mathbf{U}_i\right)$ and the $\mathrm{tr}\left(\mathbf{V}_k^H \mathbf{S}_k \mathbf{V}_k\right)$; starting from an arbitrary $\mathbf{U}_i^{(0)} \in V_{N,d}$, we apply the following update rules at iteration n:

$$\mathbf{V}_k^{(n+1)} = \nu_{\min}\Big(\mathbf{Q}_{\mathbf{V}_k \to f_i} + \frac{1}{2} \mathbf{H}_{ik}^H \mathbf{U}_i^{(n)} \mathbf{U}_i^{(n)^H} \mathbf{H}_{ik} \Big), \forall k \neq i,j \tag{5.39}$$

$$\mathbf{U}_i^{(n+1)} = \nu_{\min}\Big(\mathbf{Q}_{\mathbf{U}_i \to f_i} + \frac{1}{2} \sum_{k \neq i,j} \mathbf{H}_{ik} \mathbf{V}_k^{(n+1)} \mathbf{V}_k^{(n+1)^H} \mathbf{H}_{ik}^H \Big). \tag{5.40}$$

Clearly, when $n \to \infty$, the objective function $\mathrm{tr}\left(\mathbf{U}_i^H \mathbf{R} \mathbf{U}_i\right) + \sum_{k \neq i,j} \mathrm{tr}\left(\mathbf{V}_k^H \mathbf{S}_k \mathbf{V}_k\right)$ converges (it is non-negative and non-increasing at each iteration). We cannot provide any proof of optimality for this approach; nonetheless, experimental results obtained via this technique have been satisfactory. Letting $\mathbf{U}_i^*, \mathbf{V}_k^*$ denote the convergence points of the iterations of (5.39)–(5.40), we finally obtain

$$m_{f_i \to \mathbf{V}_j}(\mathbf{V}_j) = \mathrm{tr}\left(\mathbf{V}_j^H \mathbf{H}_{ij}^H \mathbf{U}_i^* \mathbf{U}_i^{*H} \mathbf{H}_{ij} \mathbf{V}_j\right) + \sum_{k \neq i,j} \mathrm{tr}\left(\mathbf{U}_i^{*H} \mathbf{H}_{ik} \mathbf{V}_k^* \mathbf{V}_k^{*H} \mathbf{H}_{ik}^H \mathbf{U}_i^*\right)$$
$$+ \mathrm{tr}\left(\mathbf{U}_i^{*H} \mathbf{Q}_{\mathbf{U}_i \to f_i} \mathbf{U}_i^*\right) + \sum_{k \neq i,j} \mathrm{tr}\left(\mathbf{V}_k^{*H} \mathbf{Q}_{\mathbf{V}_k \to f_i} \mathbf{V}_k^*\right), \tag{5.41}$$

which corresponds to the following rule:

$$\mathbf{Q}_{f_i \to \mathbf{V}_j} = \mathbf{H}_{ij}^H \mathbf{U}_i^* \mathbf{U}_i^{*H} \mathbf{H}_{ij} + \mathrm{I} \frac{1}{d} \Bigg[\sum_{k \neq i,j} \mathrm{tr}\Big(\mathbf{U}_i^{*H} \mathbf{H}_{ik} \mathbf{V}_k^* \mathbf{V}_k^{*H} \mathbf{H}_{ik}^H \mathbf{U}_i^*\Big)$$
$$+ \mathrm{tr}\left(\mathbf{U}_i^{*H} \mathbf{Q}_{\mathbf{U}_i \to f_i} \mathbf{U}_i^*\right) + \sum_{k \neq i,j} \mathrm{tr}\Big(\mathbf{V}_k^{*H} \mathbf{Q}_{\mathbf{V}_k \to f_i} \mathbf{V}_k^*\Big) \Bigg]. \tag{5.42}$$

Note that the terms proportional to the identity matrix that appear in $\mathbf{Q}_{f_i \to \mathbf{U}_i}$ or $\mathbf{Q}_{f_i \to \mathbf{V}_j}$ above only add a constant (independent of the considered variable) to the objective function. As such, these terms can be omitted from the message-passing implementation. The matrices corresponding to the messages in (5.20) and (5.21) are obtained in a similar manner.

We summarize below the message computation rules using the parametric form, which form the proposed message-passing IA (MPIA) algorithm:

$$\mathbf{Q}_{\mathbf{U}_i \to f_i} = \sum_{j \neq i} \mathbf{Q}_{g_j \to \mathbf{U}_i} \tag{5.43}$$

$$\mathbf{Q}_{\mathbf{U}_i \to g_j} = \mathbf{Q}_{f_i \to \mathbf{U}_i} + \sum_{k \neq i,j} \mathbf{Q}_{g_k \to \mathbf{U}_i} \tag{5.44}$$

$$\mathbf{Q}_{\mathbf{V}_j \to g_j} = \sum_{i \neq j} \mathbf{Q}_{f_i \to \mathbf{V}_j} \tag{5.45}$$

$$\mathbf{Q}_{\mathbf{V}_j \to f_i} = \mathbf{Q}_{g_j \to \mathbf{V}_j} + \sum_{k \neq i,j} \mathbf{Q}_{f_k \to \mathbf{V}_j} \tag{5.46}$$

$$\mathbf{Q}_{f_i \to \mathbf{U}_i} = \sum_{j \neq i} \mathbf{H}_{ij} \mathbf{V}_j^0 {\mathbf{V}_j^0}^H \mathbf{H}_{ij}^H,$$

$$\text{where} \quad \mathbf{V}_j^0 = \nu_{\min}\left(\mathbf{Q}_{\mathbf{V}_j \to f_i}\right) \ \forall j \neq i \tag{5.47}$$

$$\mathbf{Q}_{f_i \to \mathbf{V}_j} = \mathbf{H}_{ij}^H \mathbf{U}_i^* {\mathbf{U}_i^*}^H \mathbf{H}_{ij} \tag{5.48}$$

$$\mathbf{Q}_{g_j \to \mathbf{V}_j} = \sum_{i \neq j} \mathbf{H}_{ij}^H \mathbf{U}_i^0 {\mathbf{U}_i^0}^H \mathbf{H}_{ij},$$

$$\text{where} \quad \mathbf{U}_i^0 = \nu_{\min}\left(\mathbf{Q}_{\mathbf{U}_i \to g_j}\right) \ \forall i \neq j \tag{5.49}$$

$$\mathbf{Q}_{g_j \to \mathbf{U}_i} = \mathbf{H}_{ij} \mathbf{V}_j^* {\mathbf{V}_j^*}^H \mathbf{H}_{ij}^H. \tag{5.50}$$

In (5.48), $\mathbf{U}_i^*$ is computed by iterating (5.39)–(5.40), while in (5.50), $\mathbf{V}_j^*$ is obtained by iterating

$$\mathbf{U}_k^{(n+1)} = \nu_{\min}\Big(\mathbf{Q}_{\mathbf{U}_k \to g_j} + \frac{1}{2}\mathbf{H}_{kj}\mathbf{V}_j^{(n)}{\mathbf{V}_j^{(n)}}^H \mathbf{H}_{kj}^H\Big), \ \forall k \neq i,j \tag{5.51}$$

$$\mathbf{V}_j^{(n+1)} = \nu_{\min}\Big(\mathbf{Q}_{\mathbf{V}_j \to g_j} + \frac{1}{2}\sum_{k \neq i,j} \mathbf{H}_{kj}^H \mathbf{U}_k^{(n+1)} {\mathbf{U}_k^{(n+1)}}^H \mathbf{H}_{kj}\Big) \tag{5.52}$$

after initialization with an arbitrary $\mathbf{V}_j^{(0)}$.

5.3.3 Link with the Iterative Leakage Minimization Algorithm

We now point out some ties between the MPIA algorithm for the continuous case described in Section 5.3.2 and the iterative leakage minimization (ILM) algorithm [12, Algorithm 1]; for simplicity, in this section, we will consider only centralized implementations of both MPIA and ILM. It can be shown that ILM is a particular case of MPIA, obtained for a certain schedule. To see this, assume that all messages in the MPIA are initialized with zero matrices, and propagate the messages according to the following schedule: $m_{g_j \to \mathbf{V}_j} \ \forall j$, $m_{\mathbf{V}_j \to f_i} \ \forall i \neq j$, $m_{f_i \to \mathbf{U}_i} \ \forall i$, and $m_{\mathbf{U}_i \to g_j} \ \forall j \neq i$. The other messages are never updated, and therefore $\mathbf{Q}_{\mathbf{U}_i \to f_i}$, $\mathbf{Q}_{\mathbf{V}_j \to g_j}$, $\mathbf{Q}_{f_i \to \mathbf{V}_j}$ and $\mathbf{Q}_{g_j \to \mathbf{U}_i}$ remain at their initial value $\mathbf{0}$ throughout the algorithm.

In order to see the correspondence, consider the first computation of (5.49). Since $\mathbf{Q}_{\mathbf{U}_i \to g_j} = \mathbf{0}$, the $\nu_{\min}$ operator returns random, isotropically distributed matrices $\mathbf{U}_i^0$, and therefore $\mathbf{Q}_{g_j \to \mathbf{V}_j}$ is random. (5.46) yields $\mathbf{Q}_{\mathbf{V}_j \to f_i} = \mathbf{Q}_{g_j \to \mathbf{V}_j} \forall i$ since all other terms in the sum are zero. Next, considering (5.47), the $\mathbf{V}_j^0$ computed as $\nu_{\min}\left(\mathbf{Q}_{\mathbf{V}_j \to f_i}\right)$ correspond to the random initialization of the transmit precoders $\mathbf{V}^{[j]}$ in [12, Algorithm 1]. From this point on, it is easy to prove by induction that the two algorithms perform the same computations since (using the notations $\mathbf{V}^{[j]}$ and $\mathbf{U}^{[i]}$ respectively for the precoders and receive filters from [12]):

$$(m_{f_i \to \mathbf{U}_i}) \quad \begin{cases} \mathbf{V}_j^0 = \nu_{\min}\left(\sum_{i \neq j} \mathbf{H}_{ij}^H \mathbf{U}^{[i]} {\mathbf{U}^{[i]}}^H \mathbf{H}_{ij}\right) = \mathbf{V}^{[j]} \\ \mathbf{Q}_{f_i \to \mathbf{U}_i} = \sum_{j \neq i} \mathbf{H}_{ij} \mathbf{V}^{[j]} {\mathbf{V}^{[j]}}^H \mathbf{H}_{ij}^H \end{cases} \tag{5.53}$$

$$(m_{\mathbf{U}_i \to g_j}) \quad \mathbf{Q}_{\mathbf{U}_i \to g_j} = \mathbf{Q}_{f_i \to \mathbf{U}_i} \tag{5.54}$$

$$(m_{g_j \to \mathbf{V}_j}) \quad \begin{cases} \mathbf{U}_i^0 = \nu_{\min}\left(\sum_{j \neq i} \mathbf{H}_{ij} \mathbf{V}^{[j]} {\mathbf{V}^{[j]}}^H \mathbf{H}_{ij}^H\right) = \mathbf{U}^{[i]} \\ \mathbf{Q}_{g_j \to \mathbf{V}_j} = \sum_{i \neq j} \mathbf{H}_{ij}^H \mathbf{U}^{[i]} {\mathbf{U}^{[i]}}^H \mathbf{H}_{ij} \end{cases} \tag{5.55}$$

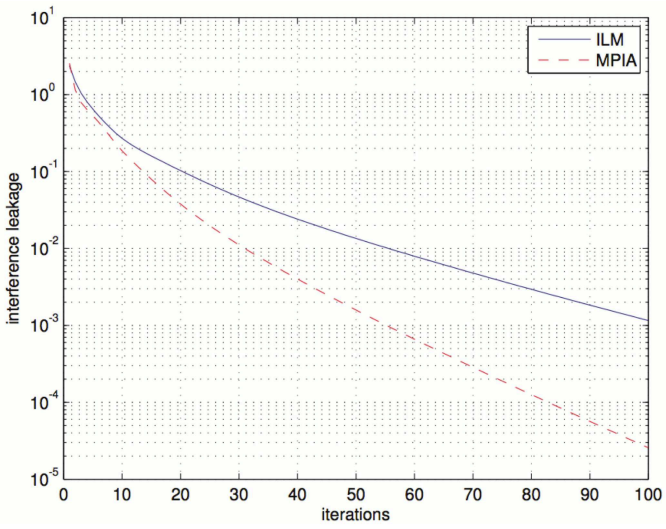

Figure 5.3. Convergence trajectory (leakage vs. iterations) of ILM and MPIA for one random channel realization

$$(m_{\mathbf{V}_j \to f_i}) \quad \mathbf{Q}_{\mathbf{V}_j \to f_i} = \mathbf{Q}_{g_j \to \mathbf{V}_j}. \tag{5.56}$$

5.4 Performance Investigation

In this section, the proposed algorithm is validated using numerical simulations, and compared to the ILM algorithm from [12]. All simulations presented here are for a 3-user IC, with 4×4 MIMO channels and $d = 2$ streams per user. A regular schedule was used for the MPIA algorithm, whereby the messages are propagated in the following order: $m_{g_j \to \mathbf{V}_j}$, $m_{f_i \to \mathbf{V}_j}$, $m_{\mathbf{V}_j \to f_i}$, $m_{\mathbf{V}_j \to g_j}$, $m_{f_i \to \mathbf{U}_i}$, $m_{g_j \to \mathbf{U}_i}$, $m_{\mathbf{U}_i \to g_j}$, $m_{\mathbf{U}_i \to f_i}$ (this sequence constituting one iteration). For the ILM algorithm, one iteration consists in $m_{g_j \to \mathbf{V}_j}$, $m_{\mathbf{V}_j \to f_i}$, $m_{f_i \to \mathbf{U}_i}$, and $m_{\mathbf{U}_i \to g_j}$, as outlined in Section 5.3.3.

We first compare the MPIA algorithm to the ILM in terms of convergence speed. Fig. 5.3 depicts the interference leakage – the objective function from (5.13) – versus the number of iterations for both algorithms for a random channel realization (the same channel values were used for both algorithms). Observe that MPIA converges faster than ILM to zero leakage (i.e. the exact solution). Note that although the curves in Fig. 5.3 are related to one particular channel realization, this behavior is observed consistently for other channel values.

In order to evaluate the respective accuracy of MPIA and ILM over a distribution of channels, we compare in Fig. 5.4 the statistics of the leakage achieved after 100 iterations of each algorithm, for channels with coefficients drawn i.i.d. from a complex circularly symmetric Gaussian distribution. The curves depict the empirical distribution of the leakage obtained by running both algorithms over 2000 channel realizations. These results show that, for a fixed number of iterations, MPIA achieves a lower leakage than ILM, the bulk of the leakage

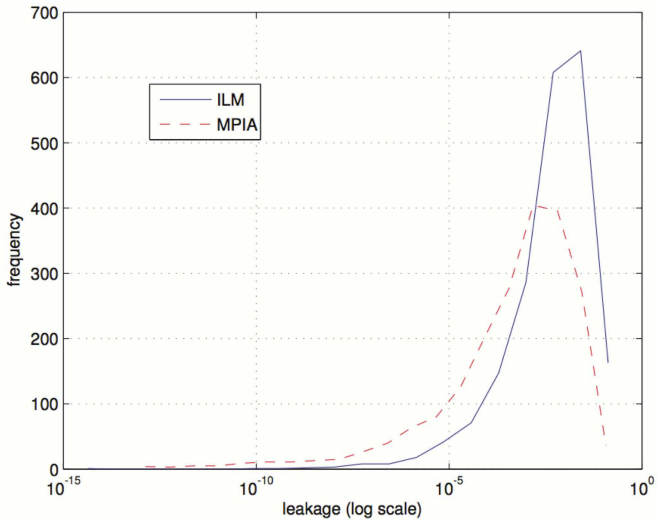

Figure 5.4. Empirical leakage distributions over 2000 Gaussian i.i.d. channels realizations, after 100 iterations of MPIA and ILM.

distribution being further left (towards lower values) for MPIA compared to ILM. The mean (computed in log-scale) leakage is $4 \cdot 10^{-3}$ for ILM, and $3.8 \cdot 10^{-4}$ for MPIA.

Arguably, the faster convergence of MPIA should be mitigated by the fact that the complexity per iteration in ILM and in MPIA are not comparable. However, we argue in the next section that computational complexity is not the most relevant metric in the case of a distributed implementation.

5.5 Distributed Implementation

A distributed implementation of the proposed algorithm can be obtained by distributing the computations associated with the nodes in the graph (Fig. 5.2) among the physical devices in the network. Clearly, this mapping will influence the amount of data exchanged between the devices (e.g. in wireless systems, exchanging data between devices is costly in terms of energy and bandwidth; on the other hand, it is reasonable to assume that messages exchanged on the graph between nodes on the same device do not incur any communication costs. In such systems, we expect communication costs to outweigh computational complexity).

An obvious mapping of the graph to the devices which preserves the symmetry between transmitters and receivers is obtained by associating $\mathbf{U}_i$ and f_i to receiver i, while g_j and $\mathbf{V}_j$ are associated to transmitter j. In that case, only $m_{f_i \to \mathbf{V}_j}$, $m_{\mathbf{V}_j \to f_i}$, $m_{g_j \to \mathbf{U}_i}$ and $m_{\mathbf{U}_i \to g_j}$ need to be transmitted over the air, while the computation and exchange of $m_{g_j \to \mathbf{V}_j}$, $m_{\mathbf{V}_j \to g_j}$, $m_{f_i \to \mathbf{U}_i}$ and $m_{\mathbf{U}_i \to f_i}$ is confined to a single device.

There is no guarantee however that this mapping is optimal in any sense. In fact, a meaningful evaluation of a distributed implementation should involve an analysis of the amount of data required to faithfully

represent the messages (e.g. by considering the quantization of matrix $\mathbf{Q}_{a\to b}$ in (5.24)) and of the costs of communication between devices in the network (in some cases this would include considering out-of-band communications over e.g. a backhaul network, and potential optimizations enabled by the broadcast nature of the wireless medium). This analysis however is not carried out in this dissertation. We envision this as a future research direction.

6

Robust Interference Management with Gaussian CSI Uncertainty

Imperfect CSI at the transmitter is a degraded version of the actual CSI due to several effects. The main sources of degradation are delay, Doppler frequency, quantization and measurement noise. Due to the variety of the imperfection sources and the randomness associated to each factor, a Gaussian additive error model with proper parameters is usually adopted. The Gaussian additive uncertainty provides an accurate while simple approximation to the actual degradation and more importantly, it simplifies the analysis of the performance of the system. In this chapter we focus on such a model for uncertainty to evaluate and optimize the performance of the MIMO IC. Two different approaches are employed in this chapter. In the first contribution, the transmit spaces are determined by IA and subsequently optimized by link adaptation (to adjust the transmission rate and power) while the precoders remain in the original space. In the second contribution, a general throughput optimization problem is considered without restricting the precoders.

6.1 Background and State of the Art

In the first part of this contribution we focus on multi-user systems where the spatial precoding at the transmitters is based on IA. If the CSI is not accurate, the performance gains disappear quickly and simple time-sharing methods can be superior [42]. In practice, the accuracy of the CSI is limited by quantization, feedback latency and Doppler effects.

While many researchers have investigated IA assuming perfect CSIT, there exist a few papers in which the effect of imperfect CSIT on the performance of IA is explored [42, 44, 49, 96–98]. A closed-form expression for the SINR of every stream in IA is derived in [44] using random matrix theory tools. The expression is then utilized to find an approximation of the performance measures such as sum rate and bit-error-rate (BER) for IA. The error performance of IA with one stream per user is analyzed in [98] and adaptive schemes are proposed to improve the performance. The scaling of the feedback with SNR in order to preserve the DoF which is achievable with perfect CSIT is analyzed for single-antenna systems in [41, 47] while we explored this problem for multi-antenna systems in Chapter 3. Those are important results as they provide insight about design considerations and practical issues. However, an improved IA-based scheme that accounts for the imperfect CSIT is still missing. Reducing the CSIT requirement of IA was investigated in Chapter 3 and the results indicate that a significant reduction is very unlikely to happen in general (specially for the symmetric antenna settings). This suggests that we need to contain the effect of residual interference caused by imperfect CSIT and investigate methods that can deal with this residual interference properly. Link adaptation methods can be very helpful to deal with residual interference and exploiting the knowledge about the direct channels.

Link adaptation improves the goodput (amount of data successfully decoded per unit of time) of a wireless link by adjustment of the rate and/or power at the TX based on the estimated CSI fed back from the receiver [99]. Extensive research has been done on link adaptation for point-to-point links. Discrete rate link adaptation for practical systems was introduced in [99] by using adaptive modulation (AM) and was extended to adaptive modulation and coding (AMC) in [100]. In AMC systems, a number of transmission modes are set up based on different pairs of modulation and channel coding schemes. In [101–105], for a wireless system with adaptive modulation, transmission rate is chosen such that an average bit error rate constraint is satisfied for the link.

We consider the general additive uncertainty model for the CSI imperfection. As the accuracy of the CSI at the transmitter side is crucial for interference alignment, we explore the situation where the precoders are designed based on imperfect CSI. We consider a MIMO IC where the transmit and receive spaces are determined by IA. Assuming perfect CSIT, IA decomposes the interference channel into a set of parallel point-to-point channels. Modeling the effect of imperfect CSIT as an additive noise enables the use of link adaptation methods used in point-to-point channels. Considering practical modulation schemes, we investigate the problem of maximizing a weighted sum of the average rates while having a sum-power constraint across the users and ensuring that the BER for every stream in the network remains below a certain threshold. This is performed by using adaptive modulation, coding and power (AMCP) for every stream in the network. Performing this optimization exactly is not tractable. Therefore, we use approximations where the accuracy of the approximated functions is validated via simulations.

In the second part of this contribution we focus on optimization of the expected sum rate without restricting

the precoders to satisfy alignment constraints. The sum rate expression used in this chapter is used under the assumption of Gaussian signaling. Optimizing the performance for every realization of the channel would be the ultimate goal. However, this is an exhaustive task. For example, maximizing the rate in a single-user MIMO system requires the channel matrix to be available at the transmitter perfectly and without delay. Therefore, optimizing the statistics of the desired metrics have become popular since they only depend on the statistics of the channel which is not likely to change for a certain period of time and this results in a huge reduction in overhead and of the computational burden. For some simple problems, closed form expressions are derived for the statistical parameters. However, it is difficult to find closed form expressions for many other problems. One can think about the optimization of the parameters derived from Monte-Carlo simulations which is also computationally inefficient.

Another approach is to approximate the statistics of the desired metric. There are methods which approximate the average mutual information and most of them assume that the number of antennas goes to infinity in order to find simplified approximations. For example in single user transmissions, this problem is explored for separately-correlated Rayleigh and uncorrelated Rician MISO channels in [106] and extended to MIMO in [107] and [108].

Another method to approximate the average mutual information is presented in [109] and developed in [110], which provides a deterministic equivalent of the expected rate. This method also assumes that the number of antennas is large. However, it has been shown that it works very well even with a few antennas.

We investigate the optimization of the deterministic equivalent expression for maximizing the expected sum rate over the K-user MIMO IC. In particular, the expected sum rate is approximated by a deterministic equivalent and optimization is performed on the approximated expression. Simulation results exhibit the effectiveness of such an approach.

6.1.1 Link Adaptation

In the context of link adaptation, transmission rate and power of the TX is adjusted depending on the instantaneous channel condition. There are two different approaches for link adaptation in the literature, namely continuous and discrete link adaptation. In the first case, capacity achieving codes with vanishing error probability are employed and it is assumed that the rate can be adjusted continuously according to the channel condition. In this case if we denote the equivalent channel gain, the average power of noise (and interference) and the transmission power by h_{eq}, δ_{eq} and p respectively, then the spectral efficiency of the link is equal to

$$\log_2(1 + ps_{eq}) \quad (\text{bit/Sec/Hz}) \tag{6.1}$$

where $s_{eq} = \frac{|h_{eq}|^2}{\delta_{eq}}$ is the equivalent SINR of the link.

Continuous link adaptation is not a practical method, even though it is suitable for performance analysis. In practical systems, a small error probability is allowed and the transmission rate is chosen from a set of discrete rates. In the context of discrete link adaptation, adaptive coding is used along with adaptive modulation which improves the performance significantly. In this method, $M + 1$ transmission modes are considered where every mode m corresponds to a pair of modulation and coding configuration associated to a transmission rate denoted

by R_m. The rates for different modes are sorted as $0 = R_0 < R_1 < ... < R_M$. Mode 0 represents the case where no information is transmitted. In mode m the BER is approximated by the following expression [111]:

$$p_e(ps_{eq}, R_m) = A_m \exp(-A'_m ps_{eq}), \;\; s_{eq} \geq 0 \tag{6.2}$$

where A_m and A'_m are constants that are determined by the transmission mode. This model is based on approximating the BER curve which is realized using Monte Carlo simulation over a large range of SNR. The process is repeated for every mode m which yields the parameters A_m and A'_m via curve fitting. In the transmission mode m, the minimum required SINR to ensure a maximum BER of B_0 is denoted by $g_{B_0}(m)$, i.e.,

$$ps_{eq} \geq g_{B_0}(m) \Rightarrow p_e(ps_{eq}, m) \leq B_0 \tag{6.3}$$

where

$$g_{B_0}(m) \triangleq \frac{-1}{A'_m} \ln(\frac{B_0}{A_m}), \;\; B_0 \leq \min(1/2, A'_m). \tag{6.4}$$

In this section we will use adaptive power, modulation and coding to exploit the statistical properties of the interference created by channel imperfections.

6.1.2 Interference Alignment Solution

Assuming that perfect global CSI is available at every TX, the precoders $\mathbf{V}_i$, $i = 1 \dots K$ should be designed to align the interference at each receiver into a $N_r - d$ dimensional space, in order to achieve d interference-free dimensions per user. A solution to the IA problem exists iff there exist full rank precoding matrices $\mathbf{V}_j \in \mathbb{C}^{N_t \times d}$, $j = 1, ..., K$ and projection matrices $\mathbf{U}_i \in \mathbb{C}^{N_r \times d}$, $i = 1, ..., K$ such that (2.7) and (2.8) are satisfied.

We focus on (2.7) since (2.8) is satisfied almost surely when the channel entries are drawn independently from a continuous distribution.

It is clear that any truncated unitary matrix that has the same column space as $\mathbf{V}_i$ also fulfills (2.7) and the same argument holds for the RX filters. This means that we can assume without loss of generality that the equivalent direct channels, i.e., $\mathbf{U}_i^{\mathrm{H}} \mathbf{H}_{ii} \mathbf{V}_i$ for $i = 1, ..., K$ are diagonal.

When the CSIT is not perfect at the TXs, the IA filters designed based on imperfect CSIT are denoted by truncated unitary matrices $\hat{\mathbf{V}}_i$ and $\hat{\mathbf{U}}_i$ where

$$\hat{\mathbf{U}}_i^{\mathrm{H}} \hat{\mathbf{H}}_{ij} \hat{\mathbf{V}}_j = \mathbf{0} \qquad \forall i, j \in \{1, ..., K\}, \;\; j \neq i, \tag{6.5}$$

where the estimated channels are denoted by $\hat{\mathbf{H}}_{ij}$. Similar to the perfect CSI scenario, we assume that the filters are such that the direct equivalent channels which we denote by $\hat{\mathbf{G}}_{ii}$,

$$\hat{\mathbf{G}}_{ii} \triangleq \hat{\mathbf{U}}_i^{\mathrm{H}} \hat{\mathbf{H}}_{ii} \hat{\mathbf{V}}_i \text{ for } i = 1, ..., K, \tag{6.6}$$

are diagonal. Using the filters designed according to imperfect CSI, the received signal after projection by the RX filters can be written as

$$\mathbf{r}_i = \hat{\mathbf{U}}_i^{\mathrm{H}} \mathbf{y}_i = \mathbf{G}_{ii} \mathbf{x}_i + \sum_{\substack{1 \leq j \leq K \\ j \neq i}} \mathbf{G}_{ij} \mathbf{x}_j + \hat{\mathbf{U}}_i^{\mathrm{H}} \mathbf{n}_i \tag{6.7}$$

where $\mathbf{G}_{ii} = \hat{\mathbf{U}}_i^{\mathrm{H}} \mathbf{H}_{ii} \hat{\mathbf{V}}_i$ and $\mathbf{G}_{ij} = \hat{\mathbf{U}}_i^{\mathrm{H}} \mathbf{H}_{ij} \hat{\mathbf{V}}_j$.

Clearly the second term is due to the interference leakage from other users which is caused by designing the filters based on imperfect CSI. Also the equivalent channel $\mathbf{G}_{ii}$ for each user is not diagonal anymore which introduces inter-stream interference. To simplify the notation, we denote the qth diagonal elements of $\mathbf{G}_{ii}$ and $\hat{\mathbf{G}}_{ii}$ by G_i^q and $\hat{G}_i^q$ respectively, for $q = 1, ..., d$.

6.2 Link Adaptation for IA in Presence of Channel Uncertainty

As mentioned in the previous section, when the CSI is perfectly known at the TXs, IA and link adaptation methods are very effective. If the CSI is not perfect, direct use of imperfect CSI instead of the true CSI in these methods will be sub-optimal and introduces performance degradation. Based on our assumptions, since the available CSI at each TX is a degraded version of the true CSI, the IA and link adaptation methods should be revisited taking the effect of residual interference into account.

In this section a new scheme is presented where AMCP is performed using imperfect CSIT to improve the performance of IA. The objective function is a weighted sum of average rates of the users where the weights are allocated depending on the importance and requirement of different links. The problem is investigated given a maximum average sum-power constraint and a maximum average BER constraint.

According to Section 6.3, every TX has d data streams. For stream q of user i, we denote the average power of interference and noise which affects this stream by δ_i^q. Furthermore, the instantaneous true SINR and the estimate of the instantaneous SINR (which is available at the transmitters) are denoted respectively by γ_i^q and $\hat{\gamma}_i^q$, where

$$\gamma_i^q = \frac{|G_i^q|^2}{\delta_i^q}, \qquad \hat{\gamma}_i^q = \frac{|\hat{G}_i^q|^2}{\delta_i^q}. \tag{6.8}$$

Note that the SINR values do not include the transmit power and only represent a measure of the quality of the channel for a given stream. The instantaneous rate and power for stream q of user i are denoted by $k_i^q = \Phi_i^q(\hat{\gamma}_i^q)$ and $p_i^q = \Psi_i^q(\hat{\gamma}_i^q)$ respectively, for $1 \le i \le K$ and $1 \le q \le d$. Based on the available CSIT at the TXs ($\hat{\mathbf{H}}_{ij},\ \forall i, j$), the TXs choose the precoders $\hat{\mathbf{V}}_j$ according to (6.5), while the rate and power are determined by the mappings $\Phi_i^q(\cdot)$ and $\Psi_i^q(\cdot)$ which should be designed such that the average sum-power is at most P_0 and the BER at each RX is less or equal to B_0, while a weighted sum of the average rates is maximized. The weights for different users are denoted by ω_i, $i = 1, ..., K$. With these definitions, the overall optimization problem can be formulated as

$$\begin{aligned}
&\max_{\Phi_i^q(\cdot), \Psi_i^q(\cdot), \forall i,q} \sum_{i=1}^{K} \omega_i \sum_{q=1}^{d} \mathrm{E}_{\hat{\gamma}_i^q}\{\Phi_i^q(\hat{\gamma}_i^q)\} \\
&\text{s.t.} \\
&\sum_{i=1}^{K} \sum_{q=1}^{d} \mathrm{E}_{\hat{\gamma}_i^q}\{\Psi_i^q(\hat{\gamma}_i^q)\} \le P_0 \qquad (C1) \\
&\mathrm{E}_{\hat{\gamma}_i^q, \gamma_i^q}\{p_e(\Psi_i^q(\hat{\gamma}_i^q)\gamma_i^q, \Phi_i^q(\hat{\gamma}_i^q))\} \le B_0,\ \forall i, q. \quad (C2)
\end{aligned} \tag{6.9}$$

Solving the exact optimization problem in (6.9) is intractable especially since the optimization is performed using imperfect information about the channels. We divide the optimization into the following three steps:

- In the first step (Section 6.2.2), we analyze the effect of imperfect CSI on the IA solution. In this case every stream will be affected by interference from all other streams;
  - The average interference power for every stream is characterized in terms of the average transmit powers.
  - This leads to an estimation of the SINR for every stream.
  - Finally, the statistical properties of the true SINR conditioned on the estimated SINR are derived.
- In the second step (Section 6.2.3), we consider a point-to-point single antenna system. Using the statistical description of the SINR values derived in the first step:
  - A discrete link adaptation method is designed with the assumption of having imperfect CSI.
  - The average rate of this system is approximated by a closed form expression as a function of the average transmit power, the average BER and the average SINR of the link.
- In the third step (Section 6.2.4), considering the closed form expression derived for a point-to-point system:
  - We find the optimum values for the average powers of all the streams in the original problem. This is performed by solving an optimization problem which involves the closed form expressions for all streams.
  - Using the resulting average powers, by solving Kd parallel problems similar to the point-to-point system in the second step and using the statistics of the current SINR, one can find the optimum instantaneous rate and power for every stream.

In the following we describe each step in more detail.

6.2.1 Specific Model of Channel Uncertainty

We assume that the entries of the true channels $\mathbf{H}_{ij}$ and the channel estimates available at the TX side $\hat{\mathbf{H}}_{ij}$ are $\mathcal{CN}(0, \Delta_{ij})$. The channel uncertainty is modeled as follows

$$\mathbf{H}_{ij} = \rho_0 \hat{\mathbf{H}}_{ij} + \sqrt{1-\rho_0^2}\mathbf{E}_{ij}, \tag{6.10}$$

where we have assumed that the entries of the perturbation matrix $\mathbf{E}_{ij}$ have the same distribution as the true channel. With this model the parameter ρ_0 represents the correlation between the true channel elements and the estimated ones. Denoting the real and imaginary parts of $\mathbf{H}_{ij}$ by $\mathbf{X}_{ij}$ and $\mathbf{Y}_{ij}$ respectively and that of $\hat{\mathbf{H}}_{ij}$ by $\hat{\mathbf{X}}_{ij}$ and $\hat{\mathbf{Y}}_{ij}$ respectively, due to the circular symmetry we have $\forall m, n$

$$\mathrm{E}\{\mathbf{X}_{ij}(m,n)\hat{\mathbf{X}}_{ij}(m,n)\} = \mathrm{E}\{\mathbf{Y}_{ij}(m,n)\hat{\mathbf{Y}}_{ij}(m,n)\} = \frac{1}{2}\Delta_{ij}\rho_0 \tag{6.11}$$

$$\mathrm{E}\{\mathbf{X}_{ij}(m,n)\hat{\mathbf{Y}}_{ij}(m,n)\} = \mathrm{E}\{\mathbf{Y}_{ij}(m,n)\hat{\mathbf{X}}_{ij}(m,n)\} = 0 \tag{6.12}$$

$$\mathrm{E}\{\mathbf{X}_{ij}(m,n)\mathbf{Y}_{ij}(m,n)\} = \mathrm{E}\{\hat{\mathbf{X}}_{ij}(m,n)\hat{\mathbf{Y}}_{ij}(m,n)\} = 0. \tag{6.13}$$

Using the above expressions and considering the fact that the variables are Gaussian, the probability density function of $\mathbf{X}_{ij}(m,n)$ given $\hat{\mathbf{X}}_{ij}(m,n)$ can be written as

$$f_{\mathbf{X}_{ij}(m,n)|\hat{\mathbf{X}}_{ij}(m,n)}(x_1,x_2) = \frac{1}{\sqrt{(1-\rho_0^2)\pi\Delta_{ij}}}\exp\left\{-\frac{1}{(1-\rho_0^2)\Delta_{ij}}(x_1-\rho_0 x_2)^2\right\}. \tag{6.14}$$

The pdf of $\mathbf{Y}_{ij}(m,n)$ given $\hat{\mathbf{Y}}_{ij}(m,n)$ can be written similarly. From (6.14) we have

$$\mathrm{E}\{\mathbf{X}_{ij}(m,n)|\hat{\mathbf{X}}_{ij}(m,n)\} = \rho_0\hat{\mathbf{X}}_{ij}(m,n) \tag{6.15}$$

$$\mathrm{E}\{\mathbf{X}_{ij}^2(m,n)|\hat{\mathbf{X}}_{ij}(m,n)\} = (1-\rho_0)^2\frac{\Delta_{ij}}{2} + \rho_0^2\hat{\mathbf{X}}_{ij}^2(m,n). \tag{6.16}$$

Therefore we get $\forall m,n$

$$\mathrm{E}\{\mathbf{H}_{ij}(m,n)|\hat{\mathbf{H}}_{ij}(m,n)\} = \rho_0\hat{\mathbf{H}}_{ij}(m,n) \tag{6.17}$$

$$\mathrm{E}\{|\mathbf{H}_{ij}(m,n)|^2|\hat{\mathbf{H}}_{ij}(m,n)\} = (1-\rho_0)^2\Delta_{ij} + \rho_0^2|\hat{\mathbf{H}}_{ij}(m,n)|^2. \tag{6.18}$$

6.2.2 Effect of Imperfect CSI on IA

Here we investigate the properties of the residual interference affecting the decoding of every stream when the precoders are designed using IA. For simplicity we define $\hat{\mathbf{v}}_{i,q}$ and $\hat{\mathbf{u}}_{i,q}$ as the qth column of $\hat{\mathbf{V}}_i$ and $\hat{\mathbf{U}}_i$ respectively. Therefore from (6.7) we have

$$\mathbf{r}_i(q) = G_i^q\mathbf{x}_i(q) + I_{i,q} + I'_{i,q} + \mathbf{n}'^q_i \tag{6.19}$$

where $G_i^q = \hat{\mathbf{u}}_{i,q}^{\mathrm{H}}\mathbf{H}_{ii}\hat{\mathbf{v}}_{i,q}$ is the qth diagonal element of $\mathbf{G}_{ii}$, $I_{i,q} = \sum_{\substack{1\le l\le d\\ l\neq q}}\hat{\mathbf{u}}_{i,q}^{\mathrm{H}}\mathbf{H}_{ii}\hat{\mathbf{v}}_{i,l}\mathbf{x}_i(l)$ is the interference from other streams of the same user, $I'_{i,q} = \sum_{\substack{1\le j\le K\\ j\neq i}}\hat{\mathbf{u}}_{i,q}^{\mathrm{H}}\mathbf{H}_{ij}\hat{\mathbf{V}}_j\mathbf{x}_j$ is the interference from other users and $\mathbf{n}'^q_i = \hat{\mathbf{u}}_{i,q}^{\mathrm{H}}\mathbf{n}_i$ is the equivalent noise for this stream. If the channels are perfectly known ($\hat{\mathbf{H}}_{ij} = \mathbf{H}_{ij},\ \forall i,j$), then the terms $I_{i,q}$ and $I'_{i,q}$ will be zero due to the alignment equations. In the following, we derive the statistical properties of G_i^q (given the information about $\hat{G}_i^q$) which can be used to derive the statistics of the true SINR. Then we derive the power of each interference term depending on the level of imperfectness of the channels controlled by ρ_0.

Statistics of G_i^q

It can be shown that $|G_{\mathrm{i}}^{\mathrm{q}}|^2$ and $|\hat{G}_{\mathrm{i}}^{\mathrm{q}}|^2$ are approximately distributed as exponential random variables (this holds exactly in the single-stream case) [112]. Henceforth we work under the assumption that $|G_{\mathrm{i}}^{\mathrm{q}}|^2$ and $|\hat{G}_{\mathrm{i}}^{\mathrm{q}}|^2$ are exponentially distributed with parameter $\frac{1}{\Delta_{\mathrm{ii}}}$. Note that the value of $\hat{G}_{\mathrm{i}}^{\mathrm{q}}$ is the estimation of the direct channel gain at the transmitter and this value is used to have an instantaneous estimate of the SINR.

Calculating the Power of Interference Plus Noise

In this part we calculate the power of interference plus noise for every stream at each RX. Clearly, assuming $\hat{\mathbf{U}}_i, \hat{\mathbf{V}}_i, \hat{\mathbf{H}}_{ij}\ \forall i,j$ are given, $I_{i,q}$ is a sum of $d-1$ random variables and $I'_{i,q}$ is a sum of $K-1$ random variables. It can be shown that every two distinct factors of $I_{i,q}$, $I'_{i,q}$ and $\mathbf{n}'^q_i$ are independent. This gives

$$\begin{aligned}\delta_i^q &= \mathrm{E}\{|I_{i,q} + I'_{i,q} + \mathbf{n}'^q_i|^2\} \\ &= \mathrm{E}\{|I_{i,q}|^2\} + \mathrm{E}\{|I'_{i,q}|^2\} + \mathrm{E}\{|\mathbf{n}'^q_i|^2\}.\end{aligned} \tag{6.20}$$

The power of the interference terms can be calculated as follows (see Appendix C.1):

$$\mathrm{E}\{|I_{i,q}|^2\} = \Delta_{ii}(1-\rho_0^2) \sum_{\substack{1\le l\le d \\ l\neq q}} \bar{P}_i(l), \tag{6.21}$$

$$\mathrm{E}\{|I'_{i,q}|^2\} = (1-\rho_0^2) \sum_{\substack{1\le j\le K \\ j\neq i}} \Delta_{ij} \sum_{1\le l\le d} \bar{P}_i(l). \tag{6.22}$$

Also it is clear that the noise variance will not change after projection by the receive filters.

Statistics of γ_i^q Conditioned on $\hat{\gamma}_i^q$

In the considered link adaptation method, transmission rate and power are designed based on the SINR of the link. Since only $\hat{\gamma}_i^q$ is available at the TX, in order to do link adaptation, we need to find the relationship between γ_i^q and $\hat{\gamma}_i^q$ or, more precisely, the statistics of γ_i^q given $\hat{\gamma}_i^q$ should be determined. We know that both $|G_i^q|^2$ and $|\hat{G}_i^q|^2$ and therefore γ_i^q and $\hat{\gamma}_i^q$ are approximately exponential random variables. Two correlated exponential random variables can be described by the following pdf

$$f_{\gamma_i^q|\hat{\gamma}_i^q}(x_1|x_2) = \frac{1}{\Gamma_i^q(1-\rho)} \exp\left\{\frac{-\rho}{1-\rho}\frac{x_2}{\hat{\Gamma}_i^q}\right\} I_0\left\{\frac{2\sqrt{\rho}}{1-\rho}\sqrt{\frac{x_2}{\Gamma_i^q\hat{\Gamma}_i^q}}\sqrt{x_1}\right\} \exp\left\{\frac{-x_1}{\Gamma_i^q(1-\rho)}\right\} \tag{6.23}$$

where $\Gamma_i^q \triangleq \mathrm{E}\{\gamma_i^q\}$ and $\hat{\Gamma}_i^q \triangleq \mathrm{E}\{\hat{\gamma}_i^q\}$, ρ is the correlation coefficient and

$$\Gamma_i^q = \hat{\Gamma}_i^q = \frac{\Delta_{ii}}{\sigma^2 + \mathrm{E}\{|I_{i,q}|^2\} + \mathrm{E}\{|I'_{i,q}|^2\}}. \tag{6.24}$$

and it is shown in Appendix C.2 that in our problem $\rho = \rho_0^2$.

6.2.3 Transmission in a Point-to-Point Link Using Imperfect CSIT

In Section 6.2.2, it was shown that using IA in the K-user MIMO IC, there will be Kd parallel channels to transmit the streams and the statistics of the SINR for each stream was derived based on the imperfect estimates of the channels. It is clear that the SINR values are functions of the average powers of all other streams. Also it is clear that the effect of the power of the interferers increases as the channels become less accurate (which is captured by ρ_0). This section is composed of two parts: First, for a point-to-point link, the AMC mappings $\Phi(\cdot)$ and $\Psi(\cdot)$ for achieving the maximum average rate are optimized. The design is based on imperfect CSI and subject to a maximum average power constraint along with a maximum average BER constraint (the average

is over the channel uncertainty). In the second part, the maximum average rate is approximated as a closed-form function of the average power and the SINR of the link using curve-fitting. Clearly the coefficients in the approximated expression are functions of the maximum average BER. This closed-form approximation simplifies the optimization problem in (6.9) which is finally solved as described in Section 6.2.4.

Transmission in a Point-to-Point Link with Average Power and BER Constraints

Denoting the true SINR and the estimated SINR by γ and $\hat{\gamma}$ respectively and Γ and $\hat{\Gamma}$ their respective expectations, the conditional distribution $f_{\gamma|\hat{\gamma}}$ is according to (6.23). The goal is to design the transmission scheme using adaptive power and rate $p = \Psi(\hat{\gamma})$ and $k = \Phi(\hat{\gamma})$ which are functions of the estimated SINR. The design parameters are the functions $\Psi(\cdot)$ and $\Phi(\cdot)$ such that the average rate is maximized while the average power and average BER constraints are satisfied as formulated in the following optimization problem

$$\begin{aligned} &\max_{\Phi(\cdot),\Psi(\cdot)} \mathrm{E}\{\Phi(\hat{\gamma})\} \\ &\text{s.t.} \\ &\mathrm{E}\{\Psi(\hat{\gamma})\} \leq P^{\max} \qquad (C'1) \\ &\mathrm{E}_{\gamma,\hat{\gamma}}\{p_e(\Psi(\hat{\gamma})\gamma, \Phi(\hat{\gamma}))\} \leq B_0. \quad (C'2) \end{aligned} \tag{6.25}$$

Condition $(C'2)$ is complicated and instead we enforce the same condition for any instance of the estimated SINR $\hat{\gamma}$, i.e., we require $\mathrm{E}_{\gamma}\{p_e(p\gamma, k)|\hat{\gamma}\} \leq B_0, \ \forall \hat{\gamma}$. By satisfying this condition, $(C'2)$ is always satisfied.

Lemma 13. *Defining $A_0 = \max(A_1, \cdots, A_M)$, the following condition is sufficient to satisfy the BER condition $(C'2)$:*

$$\frac{g_{B_0}(m)}{Q_1\hat{\gamma} + Q_2} \leq \Psi(\hat{\gamma}) \tag{6.26}$$

where $Q_1 = \rho_0^2 \frac{\Gamma}{\hat{\Gamma}}$ and $Q_2 = (1-\rho_0^2)\Gamma \ln(\frac{B_0}{A_0})$.

Proof. See Appendix C.3. □

Considering the limitation on the transmit power (condition $C'1$), (6.26) is satisfied with equality, i.e., $\Psi(\hat{\gamma}) = \frac{g_{B_0}(m)}{Q_1\hat{\gamma}+Q_2}$. Clearly when $\rho_0 \to 1$ (more accurate channels), (6.26) becomes similar to (6.3) which was derived for perfect channels.

Similar to [100], where link adaptation is performed using perfect SINR estimates, we divide the range of $\hat{\gamma}$ using thresholds t_m, $0 \leq m \leq M$ (and $t_{M+1} = +\infty$), such that when $\hat{\gamma} \in [t_m, t_{m+1})$ then the transmission rate is chosen to be R_m. Therefore the optimization problem (6.25) can be turned into the following problem,

$$\begin{aligned} &\max_{\{t_m\}_{m=0}^{M}} \sum_{m=0}^{M} R_m \int_{t_m}^{t_{m+1}} f_{\hat{\gamma}}(\hat{\gamma}) d\hat{\gamma} \\ &\text{s.t.} \quad \sum_{i=0}^{M} g_{B_0}(i) \int_{t_i}^{t_{i+1}} \frac{f_{\hat{\gamma}}(\hat{\gamma})}{Q_1\hat{\gamma} + Q_2} d\hat{\gamma} \leq P^{\max}. \end{aligned} \tag{6.27}$$

Note that we have implicitly included the BER constraint. In order to find the optimal thresholds, we write the Lagrangian of the objective function as follows

$$\mathcal{L} = \sum_{m=0}^{M} R_m \int_{t_m}^{t_{m+1}} f_{\hat{\gamma}}(\hat{\gamma}) d\hat{\gamma} - \lambda \sum_{i=0}^{M} g_{B_0}(i) \int_{t_i}^{t_{i+1}} \frac{f_{\hat{\gamma}}(\hat{\gamma})}{Q_1\hat{\gamma} + Q_2} d\hat{\gamma}. \tag{6.28}$$

For every t_m we have $\frac{\partial^2 \mathcal{L}}{\partial t_m^2} = \lambda \frac{Q_1(g_{B_0}(m) - g_{B_0}(m-1))}{(Q_1\hat{\gamma}+Q_2)^2} \geq 0$ therefore, $\frac{\partial \mathcal{L}}{\partial t_m} = 0$ gives the minimum of the Lagrangian. Therefore the optimal thresholds are given by

$$t_m = \frac{\lambda \frac{(g_{B_0}(m) - g_{B_0}(m-1))}{R_m - R_{m-1}} - Q_2}{Q_1}, \quad 0 \leq m \leq M. \tag{6.29}$$

The Lagrange multiplier λ is computed such that the power constraint is satisfied with equality. We find the solution for λ using a simple bi-section method knowing that the left-hand side of the power constraint is a monotonic function of λ. For small values of λ, the thresholds are small and the SINR will be larger than all the thresholds which means that the maximum rate is chosen (which requires high power). As λ increases, the thresholds start to increase which gradually causes the lower rates to be assigned and thereby a decrease in the transmission power. Finally, all the thresholds go to infinity which indicates that zero rate (therefore zero power) will be chosen. This implies that a solution for λ can be obtained by using a bi-section root finding method.

At this point, the functions $\Phi(\cdot)$ and $\Psi(\cdot)$ can be explicitly written as

$$\Phi(\hat{\gamma}) = R_m, \;\; \hat{\gamma} \in [t_m, t_{m+1}) \tag{6.30}$$

$$\Psi(\hat{\gamma}) = \frac{g_{B_0}(m)}{Q_1\hat{\gamma} + Q_2}. \tag{6.31}$$

Closed-form approximation for the average rate in a point-to-point link

Inspired by the Gaussian channel, we approximate the average rate achievable in the link by $\mathrm{E}\{k\} = L\log(1 + L'\Gamma P^{\max})$ where L and L' are functions of the transmission modes m, maximum error probability B_0 and the CSI uncertainty parameter ρ_0. We have used a curve-fitting method to find the values for L and L'. We verified the accuracy of this approximation compared to the actual average rate via extensive simulations for different values of B_0. Figure 6.1 shows the comparison between the approximated expression and the true value of the rate for $B_0 = 10^{-5}$, $P^{\max} = 1$ and different values of ρ.

6.2.4 Optimization of the Weighted Sum of the Approximate Average Rates

Using the approximated closed-form expression for the average rate we equivalently look at the following problem

$$\max_{\bar{P}_i(q),\, 1\leq i\leq K,\; 1\leq q\leq d} \sum_{i=1}^{K} \omega_i \sum_{q=1}^{d} \bar{K}_i(q)$$

$$\text{s.t.} \tag{6.32}$$

$$\sum_{i=1}^{K}\sum_{q=1}^{d} \bar{P}_i(q) \leq P_0$$

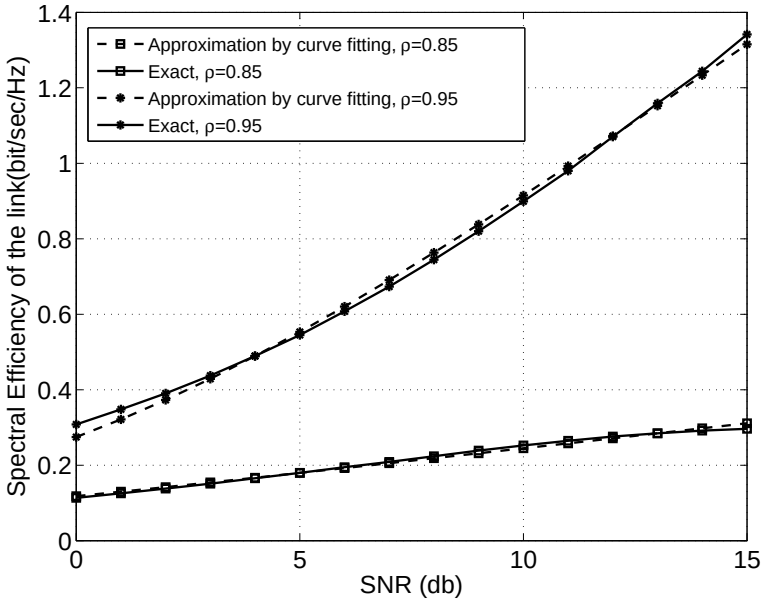

Figure 6.1. Comparison of the approximated expression with the true value of the rate for $B_0 = 10^{-5}$, $P^{\max} = 1$.

where $\bar{K}_i(q) = L\log(1 + L'\Gamma_i^q \bar{P}_i(q)) \approx \mathrm{E}\{k_i^q\}$. Note that Γ_i^q is also a function of the average powers. The above problem is a non-convex constrained optimization problem. We resort to numerical optimization methods to find a (locally) optimum solution. The optimization problem is solved using the active-set method [113]. This method determines which constraints influence the final result and watches them while searching for the solution. It performs a line search by updating the Hessian matrix of the Lagrangian. This technique reduces the complexity of the search. We used the standard MATLAB implementation to compute the average powers to be assigned to different streams of different users. After finding the average powers, the instantaneous rates and powers can be chosen independently for each stream similar to the point-to-point scenario discussed in Section 6.2.3.

The overall procedure summarizing the above steps is presented in Algorithm 2.

6.2.5 Performance Investigation

Orthogonal Transmission in the K-User MIMO IC Using AMCP

Due to the imperfectness of the CSI and sub-optimality of IA, it is natural to ask whether we are better off performing IA rather than simply using an orthogonal resource-sharing transmission scheme. In orthogonal transmission we assume that the channel resources (time/bandwidth) are divided equally among different users in the network. In order to have a fair comparison with the proposed scheme, we consider a similar problem where we look for maximizing a weighted sum of the average rates of the users while having a total transmission power constraint P_0 and a maximum average BER of B_0. Here we have K point-to-point MIMO links where for each link $d' = \min(N_t, N_r)$ parallel streams are transmitted. Therefore the optimization problem can be

Algorithm 2 Link adaptation for IA

- Find the IA filters $\hat{\mathbf{V}}_i$ and $\hat{\mathbf{U}}_i$ that fulfill (6.5) and diagonalize the direct channels (using the estimated CSI $\hat{\mathbf{H}}_{ij},\ \forall i,j$)
- Derive the closed-form approximation for the average rate in a point-to-point link using the parameters L and L' which are calculated based on $B_0, P^{\max}, \rho_0$
- Compute the optimal average powers associated to every stream of each user $\bar{P}_i(q),\ \forall i,q$ from (6.32)
- Compute the thresholds for every stream according to (6.29) using the average power associated to that stream (computed in the previous step).
- Calculate the instantaneous rate and power for every stream according to (6.30) and (6.31) using the estimated SINR of that stream $\hat{\gamma}_i^q$
- Transmit using the modulation and coding pair associated to the rate which is allocated to each stream

formulated as

$$\begin{aligned}&\max_{\Phi'^q_i(\cdot),\Psi'^q_i(\cdot)} \sum_{i=1}^{K}\omega_i\sum_{q=1}^{d'}\mathrm{E}\{\Phi'^q_i(\hat{\gamma'}^q_i)\}\\ &\text{s.t.}\\ &\sum_{i=1}^{K}\sum_{q=1}^{d'}\mathrm{E}\{\Psi'^q_i(\hat{\gamma'}^q_i)\}\le P_0\\ &\mathrm{E}\{p_e(\Psi'^q_i(\hat{\gamma'}^q_i)\gamma'^q_i,\Phi'^q_i(\hat{\gamma'}^q_i))\}\le B_0,\ \forall i,q\end{aligned} \tag{6.33}$$

where the instantaneous rate and power for stream q of user i are denoted by $k'^q_i=\Phi'^q_i(\hat{\gamma'}^q_i)$ and $p'^q_i=\Psi'^q_i(\hat{\gamma'}^q_i)$ respectively, for $1\le i\le K$ and $1\le q\le d'$. We use the truncated unitary precoders and receive filters that diagonalize the estimated channel matrices, i.e.,

$$\hat{\mathbf{U}}'^{\mathrm{H}}_i\hat{\mathbf{H}}_{ii}\hat{\mathbf{V}}'_i=\hat{\mathbf{G}}'_{ii}=\mathrm{diag}(\hat{G}'^1_i,...,\hat{G}'^{d'}_i)\ \text{for}\ i=1,...,K. \tag{6.34}$$

However, due to imperfect CSI, the equivalent channel

$$\mathbf{G}'_{ii}=\hat{\mathbf{U}}'^{\mathrm{H}}_i\mathbf{H}_{ii}\hat{\mathbf{V}}'_i \tag{6.35}$$

will not be exactly diagonal which indicates the presence of self-interference from the other streams. Writing the received signal after projecting with the designed receive filters we get

$$\mathbf{r}'_i(q)=G'^q_i\mathbf{x}_i'(q)+I''_{i,q}+\mathbf{n}''^q_i, \tag{6.36}$$

where $G'^q_i=\hat{\mathbf{u}}'^{\mathrm{H}}_{i,q}\mathbf{H}_{ii}\hat{\mathbf{v}}'_{i,q}$ is the qth diagonal element of $\mathbf{G}'_{ii}$, $I''_{i,q}=\sum_{\substack{1\le l\le d'\\ l\ne q}}\hat{\mathbf{u}}'^{\mathrm{H}}_{i,q}\mathbf{H}_{ii}\hat{\mathbf{v}}'_{i,l}\mathbf{x}_i'(l)$ is the interference from other streams of the same user and $\mathbf{n}''^q_i=\hat{\mathbf{u}}'^{\mathrm{H}}_{i,q}\mathbf{n}_i$ is the equivalent noise for this stream. Similar to

the previous section, it can be shown that both $|G_i'^q|^2$ and $|\hat{G}_i'^q|^2$ are exponential random variables with average and variance equal to Δ_{ii}. Also the power of the interference and noise can be calculated as

$$\mathrm{E}\{|I''_{i,q} + \mathbf{n}''^q_i|^2\} = \Delta_{ii}(1-\rho_0^2) \sum_{\substack{1\le l\le d' \\ l\neq q}} \bar{P}'_i(l) + \sigma^2. \tag{6.37}$$

Also denoting the true SINR by $\gamma'^q_i = \frac{|G'^q_i|^2}{\mathrm{E}\{|I''_{i,q}+\mathbf{n}''^q_i|^2\}}$ and the estimated SINR by $\hat{\gamma}'^q_i = \frac{|\hat{G}'^q_i|^2}{\mathrm{E}\{|I''_{i,q}+\mathbf{n}''^q_i|^2\}}$, we will have the following average SINR values,

$$\hat{\Gamma}'^q_i = \Gamma'^q_i = \mathrm{E}\{\gamma'^q_i\} = \frac{\Delta_{ii}}{\Delta_{ii}(1-\rho_0^2)\sum_{\substack{1\le l\le d' \\ l\neq q}} \bar{P}'_i(l) + \sigma^2}. \tag{6.38}$$

Therefore, the original optimization problem can be replaced with the following problem,

$$\begin{aligned} &\max_{\bar{P}'_i(q),\, 1\le i\le K,\, 1\le q\le d'} \sum_{j=1}^{K} \omega_j \sum_{q=1}^{d'} \bar{K}'_i(q) \\ &\text{s.t.} \\ &\sum_{j=1}^{K}\sum_{q=1}^{d'} \bar{P}'_i(q) \le P_0 \end{aligned} \tag{6.39}$$

where $\bar{K}'_i(q) = L'_1 \log(1 + L'_2 \Gamma'^q_i \bar{P}'_i(q))$ is the approximated closed-form expression for the average rate $\mathrm{E}\{k'^q_i\}$. Again this problem is a constrained optimization problem that we solve using the active-set method. After finding the optimal average powers, the instantaneous rates and powers can be chosen similar to the point-to-point scenario.

Simulation Results

To evaluate the performance of the proposed scheme, we use the AMC modes defined in the IEEE 802.11-a standard [105]. In this setting there are 8 different modes each of which is associated to a particular modulation and coding pair. These modes provide the set of rates $\{0, .5, .75, 1, 1.5, 2, 3, 4\}$. The parameters of the BER estimation according to (6.2) are extracted from [111]. We assume that the TXs and the RXs are placed such that the distance between TX j and RX i equals $\sqrt{\alpha^2 + (i-j)^2\beta^2}$ and the variance of the channel entries equals $\mathrm{E}\{|\mathbf{H}_{ij}|^2\} = \Delta_{ij} = \frac{\Psi_0}{(\alpha^2+(i-j)^2\beta^2)^{1.5}}$ where Ψ_0, α and β are constants. α is the distance between a pair of TX and RX. We assume that the TXs and the RXs are equipped with the same number of antennas and that the weights for different users are equal ($\omega_j = 1,\ \forall j$). Also the noise variance is 0.1 and $B_0 = 10^{-5}$.

In Figure 6.2, the sum rate of the system is plotted for different number of users comparing the proposed scheme (interfering transmission which is labeled by "IA" in the figures) with the orthogonal transmission (which also uses AMC). The number of antennas increases with the number of users according to $N_t = N_r = \lceil \frac{K+1}{2} \rceil$. The parameters are set as $\beta = 2$, $P_0 = 2$ and $\rho = 0.95$. As shown in this figure, the sum rate increases when the number of users grows. This of course presumes that the amount of feedback also increases due to the increase in the number of antennas. For a fixed feedback budget, the performance could be degraded by increasing the number of users. Clearly the proposed scheme outperforms the orthogonal scheme as it provides higher sum-rate.

In Figure 6.3, assuming $K = 3$, $N_t = N_r = 4$ and $d = 2$, $P_0 = 1$ and $\beta = 2$, the sum rate (for both interfering and orthogonal transmission) is plotted for different values of ρ and α (the distance between every TX and its RX). Clearly, by decreasing ρ, the CSI becomes less accurate and it degrades the overall performance. It is evident that for small ρ, the orthogonal scheme is superior.

Figure 6.4 shows the sum rate comparison for a fixed value of $\alpha = 3$ and different values for β and ρ. The other parameters are the same as in Figure 6.3. Clearly the adaptive IA scheme outperforms orthogonal transmission. Note that the performance of the orthogonal scheme is independent of β as the gain of the interfering links does not affect the performance of orthogonal transmission.

Figure 6.5 shows the performance comparison when the variable parameter is α (which affects the SNR). Here we have considered $K = 5$, $N_t = N_r = 3$ and $d = 1$, $P_0 = 2$ and $\rho = 0.95$. The curves are plotted for two different values of β. From both figures 6.3, 6.5, it is clear that for smaller values of α, the improvement of the proposed scheme compared to the orthogonal scheme is greater. Also it can be seen that higher values of β increases the performance gain of the proposed scheme (as it corresponds to lower interference power).

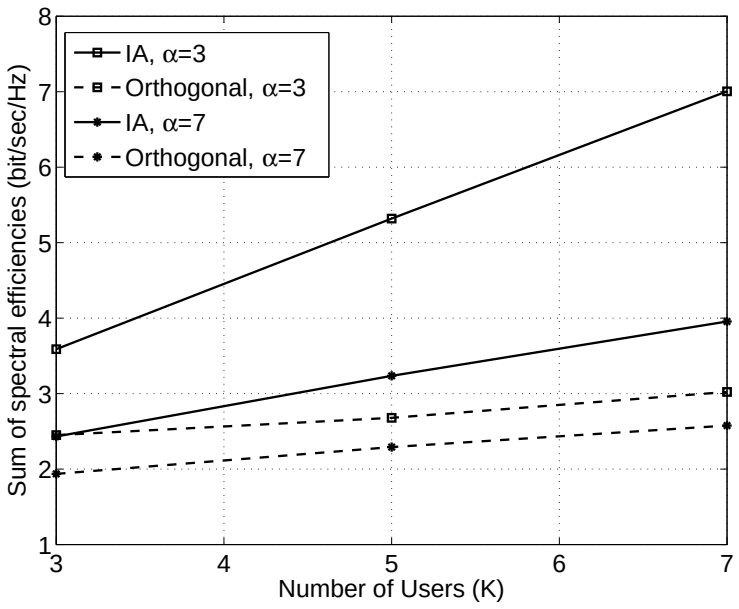

Figure 6.2. Sum rate comparison for different number of users. $N_t = N_r = \lceil \frac{K+1}{2} \rceil$, $d = 1$, $\beta = 2$, $\rho = 0.95$, $P_0 = 2$.

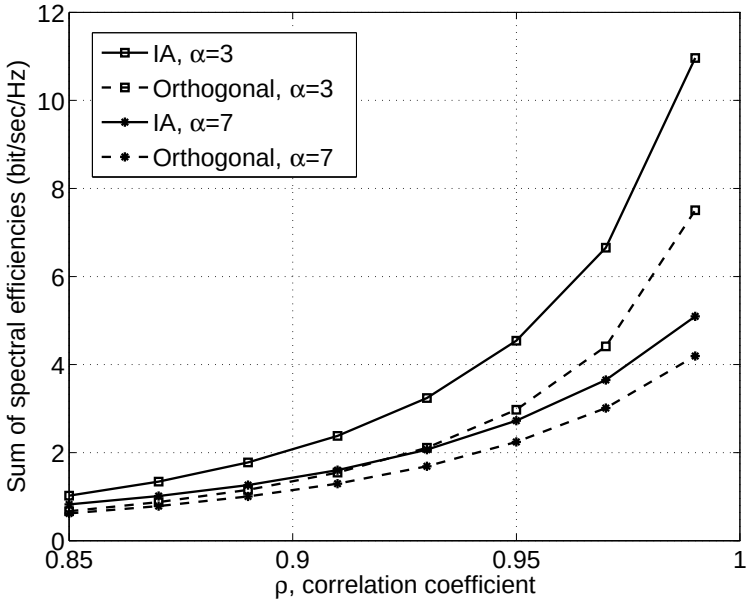

Figure 6.3. Rate comparison for different values of correlation coefficient and α. $K = 3$, $N_t = N_r = 4$, $d = 2$, $\beta = 2$, $P_0 = 1$.

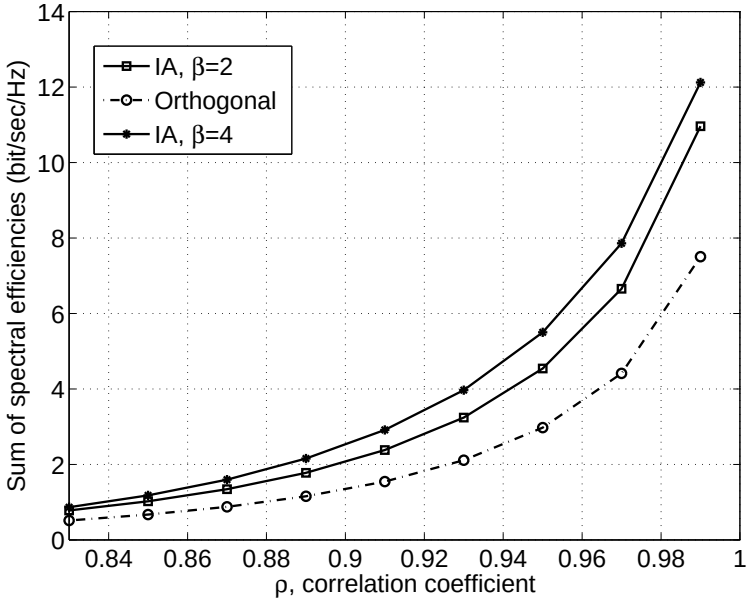

Figure 6.4. Rate comparison for different values of correlation coefficient and β. $K = 3$, $N_t = N_r = 4$, $d = 2$, $\alpha = 3$, $P_0 = 1$.

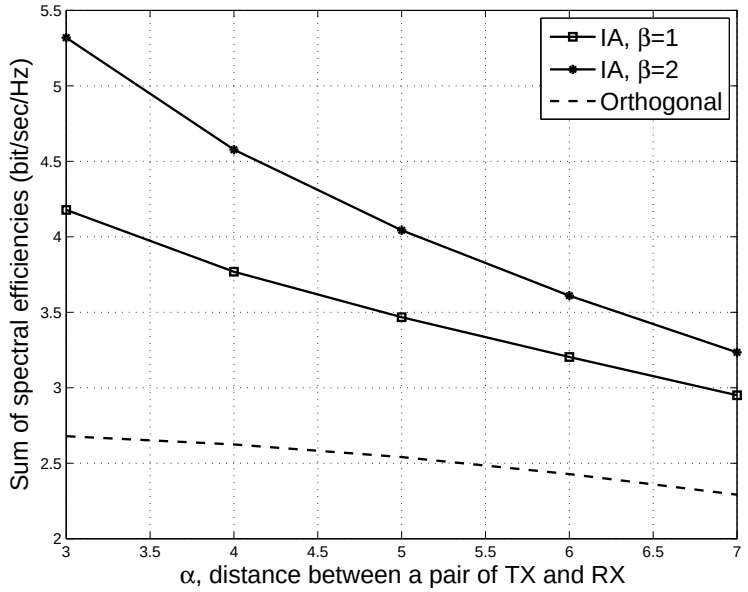

Figure 6.5. Sum rate comparison for different values of distance α. $K = 5$, $N_t = N_r = 3$, $d = 1$, $\rho = 0.95$, $P_0 = 2$.

6.3 Throughput Maximization Using Tools from Random Matrix Theory

Consider the following expression

$$\mathcal{V} = \log \left| \mathbf{I}_M + \frac{1}{\sigma^2} \mathbf{H}\mathbf{Q}\mathbf{H}^{\mathrm{H}} \right| \tag{6.40}$$

where $\mathbf{Q} \in \mathbb{C}^{N \times N}$ is a positive semi-definite matrix, $\mathbf{H} \in \mathbb{C}^{M \times N}$ is random and $\sigma^2 > 0$. The following theorems provide useful information about the mean of $\mathcal{V}$ in different situations.
We start with the following Lemma

Lemma 14. *Let $\bar{\mathbf{H}} \in \mathbb{C}^{M \times N}$ and positive semi-definite matrices $\mathbf{Q}, \tilde{\mathbf{C}} \in \mathbb{C}^{N \times N}$ be deterministic matrices and $\sigma^2 > 0$. Define $\mathbf{G}(\delta) = \left(\mathbf{I}_N + \delta \mathbf{Q}^{\frac{1}{2}} \tilde{\mathbf{C}} \mathbf{Q}^{\frac{1}{2}} \right)^{-1}$ and*

$$g(\mathbf{Q}, \delta, \tilde{\delta}) = \frac{1}{N} \mathrm{tr} \left(\sigma^2 (1 + \tilde{\delta}) \mathbf{I}_M + \bar{\mathbf{H}} \mathbf{Q}^{\frac{1}{2}} \mathbf{G}(\delta) \mathbf{Q}^{\frac{1}{2}} \bar{\mathbf{H}}^{\mathrm{H}} \right)^{-1},$$

$$\tilde{g}(\mathbf{Q}, \delta, \tilde{\delta}) = \frac{1}{N} \mathrm{tr} \left(\mathbf{Q}^{\frac{1}{2}} \tilde{\mathbf{C}} \mathbf{Q}^{\frac{1}{2}} \left(\sigma^2 (\mathbf{G}(\delta))^{-1} + \frac{\mathbf{Q}^{\frac{1}{2}} \bar{\mathbf{H}}^{\mathrm{H}} \bar{\mathbf{H}} \mathbf{Q}^{\frac{1}{2}}}{1 + \tilde{\delta}} \right)^{-1} \right),$$

then the system of equations

$$\begin{cases} \delta &= g(\mathbf{Q}, \delta, \tilde{\delta}), \\ \tilde{\delta} &= \tilde{g}(\mathbf{Q}, \delta, \tilde{\delta}), \end{cases} \tag{6.41}$$

has a unique solution $(\delta^\star, \tilde{\delta}^\star) \in (0, \infty)^2$. Moreover, $\delta^\star$ and $\tilde{\delta}^\star$ can be numerically computed via Algorithm 3.

Proof. A sketch of the proof is given in Appendix C.5. □

Algorithm 3 Fixed point solution

Initialization: $m = 0$ and $\delta^{(0)}, \tilde{\delta}^{(0)} > 0$

Repeat

- $\delta^{(m+1)} = g(\delta^{(m)}, \tilde{\delta}^{(m)})$
- $\tilde{\delta}^{(m+1)} = \tilde{g}(\delta^{(m)}, \tilde{\delta}^{(m)})$
- $m \leftarrow m + 1$

until convergence.

Output: $(\delta^\star, \tilde{\delta}^\star) = (\delta^{(m)}, \tilde{\delta}^{(m)})$.

Theorem 8. *Let* $\mathbf{H} = \bar{\mathbf{H}} + \mathbf{E}$*, in which* $\bar{\mathbf{H}} \in \mathbb{C}^{M\times N}$ *is deterministic with bounded spectral norm, and* $\mathbf{E} = \frac{1}{\sqrt{N}}\mathbf{W}\tilde{\mathbf{C}}^{\frac{1}{2}}$ *with* $\mathbf{W} \in \mathbb{C}^{M\times N}$ *having i.i.d. elements from* $\mathcal{CN}(0,1)$ *and* $\tilde{\mathbf{C}}$ *diagonal nonnegative with bounded spectral norm. Let also* $\mathbf{Q} \in \mathbb{C}^{N\times N}$ *be deterministic Hermitian nonnegative with bounded spectral norm. Then, as* $M, N \to \infty$ *with* $M/N \to c > 0$*,*

$$R - \bar{R} \to 0$$

where $R = \mathrm{E}\left[\log\left|\mathbf{I}_M + \frac{1}{\sigma^2}\mathbf{H}\mathbf{Q}\mathbf{H}^{\mathrm{H}}\right|\right]$*,*

$$\bar{R} = \log\left|(1+\tilde{\delta})\mathbf{I}_M + \frac{1}{\sigma^2}\bar{\mathbf{H}}\mathbf{Q}^{\frac{1}{2}}\mathbf{G}(\delta)\mathbf{Q}^{\frac{1}{2}}\bar{\mathbf{H}}^{\mathrm{H}}\right| - \log|\mathbf{G}(\delta)| - N\sigma^2\delta\tilde{\delta},$$

and δ *and* $\tilde{\delta}$ *are the unique positive solution of* (6.41)*.*

Proof. The proof follows directly from [110, Theorem 2], where only functional uniqueness of δ, $\tilde{\delta}$ (seen as functions of σ^2) was obtained. Lemma 14 completes [110] by adding point-wise uniqueness of δ, $\tilde{\delta}$ for each $\sigma^2 > 0$. □

The expression given by $\bar{R}$ is called the deterministic equivalent of R because it does not involve an expectation. An interesting property of $\bar{R}$ is that its partial derivative with respect to δ and $\tilde{\delta}$ vanishes at $(\delta^\star, \tilde{\delta}^\star)$,

$$\left.\frac{\partial\bar{R}}{\partial\delta}\right|_{(\delta^\star,\tilde{\delta}^\star)} = \left.\frac{\partial\bar{R}}{\partial\tilde{\delta}}\right|_{(\delta^\star,\tilde{\delta}^\star)} = 0. \tag{6.42}$$

6.3.1 Approximating the Expected Sum Rate

Consider an interference channel in which K transmitters communicate with their respective receivers in a shared medium. Transmitter j and receiver i are equipped with N_j and M_i antennas, respectively. Data symbols are spatially precoded at the transmitters. The number of data streams sent by transmitter i equals d^i. The vector at receiver i reads

$$\mathbf{y}_i = \mathbf{H}_{ii}\sqrt{\lambda_i}\mathbf{V}_i\mathbf{x}_i + \sum_{\substack{1\le j\le K\\ j\neq i}} \mathbf{H}_{ij}\sqrt{\lambda_j}\mathbf{V}_j\mathbf{x}_j + \mathbf{n}_i \tag{6.43}$$

in which $\mathbf{H}_{ij} \in \mathbb{C}^{M_i \times N_j}$ is the channel matrix between transmitter j and receiver i, $\mathbf{V}_j \in \mathbb{C}^{N_j \times d^j}$ and $\mathbf{x}_j \in \mathbb{C}^{d^j}$ are the precoding matrix and the data vector of transmitter j, respectively. Furthermore, $\mathbf{n}_i \sim \mathcal{CN}(0, \sigma^2 \mathbf{I}_{M_i})$ is the additive noise at receiver i. Assuming $\mathrm{E}\left[\mathbf{x}_i \mathbf{x}_i^{\mathrm{H}}\right] = \mathbf{I}_{d^i},\ i = 1, \ldots, K$, the covariance matrix of the signal transmitted by user j is given by $\mathbf{Q}_j = \lambda_j \mathbf{V}_j \mathbf{V}_j^{\mathrm{H}}$ in which $\lambda_j = \frac{P_j}{\mathrm{tr}\left(\mathbf{V}_j \mathbf{V}_j^{\mathrm{H}}\right)}$. The transmit power for user j is $\mathrm{tr}\left(\mathbf{Q}_j\right) = P_j$.

In order to simplify the analysis for imperfect CSIT, we consider the following uncertainty model for the channel matrices which is equivalent to (6.10) with proper normalization.

$$\mathbf{H}_{ij} = \bar{\mathbf{H}}_{ij} + \mathbf{E}_{ij},$$

in which $\mathbf{E}_{ij}$ is the estimation error, whose entries are modeled as independent and identically distributed (i.i.d.) Gaussian random variables with zero mean and variance σ_{ij}^2. Both $\bar{\mathbf{H}}_{ij}$ and σ_{ij}^2 are provided to a central node through feedback. We define the feedback quality for $\mathbf{H}_{ij}$ as

$$\eta_{ij} = \frac{\mathrm{tr}(\bar{\mathbf{H}}_{ij} \bar{\mathbf{H}}_{ij}^{\mathrm{H}})}{\mathrm{tr}(\mathrm{E}\left[\mathbf{E}_{ij} \mathbf{E}_{ij}^{\mathrm{H}}\right])}. \tag{6.44}$$

The objective function is the achievable expected sum rate of the MIMO IC under the assumption that the input signals are circularly symmetric Gaussian. Considering the received signal in (6.43), this reads

$$R_{\mathrm{sum}} \quad = \quad \mathrm{E}\left[\sum_{i=1}^{K} \log\left|\mathbf{I}_{M_i} + \frac{1}{\sigma^2}\sum_{j=1}^{K} \mathbf{H}_{ij}\mathbf{Q}_j\mathbf{H}_{ij}^{\mathrm{H}}\right| - \sum_{i=1}^{K} \log\left|\mathbf{I}_{M_i} + \frac{1}{\sigma^2}\sum_{j=1, j\neq i}^{K} \mathbf{H}_{ij}\mathbf{Q}_j\mathbf{H}_{ij}^{\mathrm{H}}\right|\right] \tag{6.45}$$

where the expectation is w.r.t. $\mathbf{E}_{ij}$, $1 \leq i, j \leq K$. $\mathbf{E}_{ij} = \sigma_{ij}\mathbf{W}_{ij}$ and $\mathbf{W}_{ij}$ with i.i.d. $\mathcal{CN}(0,1)$ entries. Therefore, it is sufficient to optimize jointly the covariance matrices $\mathbf{Q}_1, \ldots, \mathbf{Q}_K$. Here we aim to reformulate our problem in a way such that the theorems defined earlier can be used to approximate our objective function.

Defining $N = \sum_{j=1}^{K} N_j$, (6.45) can be rewritten as

$$R_{\mathrm{sum}} = \mathrm{E}\left[\sum_{i=1}^{K} \log\left|\mathbf{I}_{M_i} + \frac{1}{\bar{\sigma}^2}\mathbf{H}_i\mathbf{Q}\mathbf{H}_i^{\mathrm{H}}\right| - \sum_{i=1}^{K} \log\left|\mathbf{I}_{M_i} + \frac{1}{\bar{\sigma}^2}\mathbf{H}_i\mathbf{Q}_{-i}\mathbf{H}_i^{\mathrm{H}}\right|\right], \tag{6.46}$$

where $\bar{\sigma}^2 = \frac{\sigma^2}{N}$, the equivalent channels of size $M_i \times N$ are defined as $\mathbf{H}_i = \frac{1}{\sqrt{N}}\left[\mathbf{H}_{i1}, ..., \mathbf{H}_{iK}\right]$ for $i = 1, ..., K$, $\mathbf{Q} = \mathrm{Bdiag}\left(\mathbf{Q}_1, ..., \mathbf{Q}_K\right)$ and $\mathbf{Q}_{-i}$ is equal to $\mathbf{Q}$ except that the ith block is replaced by the $N_i \times N_i$ zero matrix. Therefore

$$\mathbf{H}_i = \bar{\mathbf{H}}_i + \mathbf{E}_i, \tag{6.47}$$

with $\bar{\mathbf{H}}_i = \frac{1}{\sqrt{N}}\left[\bar{\mathbf{H}}_{i1}, ..., \bar{\mathbf{H}}_{iK}\right]$, $\mathbf{E}_i = \frac{1}{\sqrt{N}}\mathbf{W}_i\tilde{\mathbf{C}}_i^{\frac{1}{2}}$, $\mathbf{W}_i = [\mathbf{W}_{i1}, ..., \mathbf{W}_{iK}]$ and $\tilde{\mathbf{C}}_i = \mathrm{Bdiag}\left(\sigma_{i1}^2\mathbf{I}_{N_1}, ..., \sigma_{iK}^2\mathbf{I}_{N_K}\right)$. With these definitions, $\mathbf{W}_i$ has $\mathcal{CN}(0,1)$ elements and $\tilde{\mathbf{C}}_i$ is diagonal nonnegative. Therefore we are within the conditions of application of Theorem 8.

Defining R_i^+ and R_i^- as

$$R_i^+ = \mathrm{E}\left[\log\left|\mathbf{I}_{M_i} + \frac{1}{\bar{\sigma}^2}\mathbf{H}_i\mathbf{Q}\mathbf{H}_i^{\mathrm{H}}\right|\right],$$
$$R_i^- = \mathrm{E}\left[\log\left|\mathbf{I}_{M_i} + \frac{1}{\bar{\sigma}^2}\mathbf{H}_i\mathbf{Q}_{-i}\mathbf{H}_i^{\mathrm{H}}\right|\right],$$

where the expectation is over $\mathbf{E}_i$, the expected sum rate is

$$R_{\text{sum}} = \sum_{i=1}^{K} \left(R_i^+ - R_i^- \right).$$

Using Theorem 8, we approximate R_i^+ and R_i^- by deterministic equivalents. In particular, we have

$$R_i^+ - \bar{R}_i^+ \Big|_{(\delta_i^{+\star}, \tilde{\delta}_i^{+\star})} \to 0$$

as $N_j, M_j \to \infty$ with $N_j/M_j \to c_j > 0$ for all j, where

$$\begin{aligned} \bar{R}_i^+ &= f_i(\mathbf{Q}, \delta_i^+, \tilde{\delta}_i^+) \\ &= \log \left| (1+\tilde{\delta}_i^+)\mathbf{I}_{M_i} + \frac{1}{\bar{\sigma}^2} \bar{\mathbf{H}}_i \mathbf{Q}^{\frac{1}{2}} \mathbf{G}_i(\delta_i^+) \mathbf{Q}^{\frac{1}{2}} \bar{\mathbf{H}}_i^{\mathrm{H}} \right| - \log \left| \mathbf{G}_i(\delta_i^+) \right| - N\bar{\sigma}^2 \delta_i^+ \tilde{\delta}_i^+ \end{aligned} \tag{6.48}$$

in which $\mathbf{G}_i(x) = (\mathbf{I}_N + x\mathbf{Q}^{\frac{1}{2}} \tilde{\mathbf{C}}_i \mathbf{Q}^{\frac{1}{2}})^{-1}$, and $\delta_i^{+\star}$ and $\tilde{\delta}_i^{+\star}$ are the unique positive solutions to

$$\left\{ \begin{array}{rcl} \delta_i^+ &=& g_i(\mathbf{Q}, \delta_i^+, \tilde{\delta}_i^+), \\ \tilde{\delta}_i^+ &=& \tilde{g}_i(\mathbf{Q}, \delta_i^+, \tilde{\delta}_i^+), \end{array} \right. \tag{6.49}$$

where

$$g_i(\mathbf{Q}, \delta_i^+, \tilde{\delta}_i^+) = \frac{1}{N} \mathrm{tr} \left(\bar{\sigma}^2 (1+\tilde{\delta}_i^+) \mathbf{I}_{M_i} + \bar{\mathbf{H}}_i \mathbf{Q}^{\frac{1}{2}} \mathbf{G}_i(\delta_i^+) \mathbf{Q}^{\frac{1}{2}} \bar{\mathbf{H}}_i^{\mathrm{H}} \right)^{-1}, \tag{6.50}$$

$$\tilde{g}_i(\mathbf{Q}, \delta_i^+, \tilde{\delta}_i^+) = \frac{1}{N} \mathrm{tr} \left(\mathbf{Q}^{\frac{1}{2}} \tilde{\mathbf{C}}_i \mathbf{Q}^{\frac{1}{2}} \left(\bar{\sigma}^2 (\mathbf{G}_i(\delta_i^+))^{-1} + \frac{\mathbf{Q}^{\frac{1}{2}} \bar{\mathbf{H}}_i^{\mathrm{H}} \bar{\mathbf{H}}_i \mathbf{Q}^{\frac{1}{2}}}{1+\tilde{\delta}_i^+} \right)^{-1} \right). \tag{6.51}$$

Similarly we define $\bar{R}_i^- = f_i(\mathbf{Q}_{-i}, \delta_i^-, \tilde{\delta}_i^-)$ and $(\delta_i^{-\star}, \tilde{\delta}_i^{-\star})$ the unique nonnegative solution to

$$\left\{ \begin{array}{rcl} \delta_i^- &=& g_i(\mathbf{Q}_{-i}, \delta_i^-, \tilde{\delta}_i^-), \\ \tilde{\delta}_i^- &=& \tilde{g}_i(\mathbf{Q}_{-i}, \delta_i^-, \tilde{\delta}_i^-). \end{array} \right. \tag{6.52}$$

Defining $\bar{R}_{\text{sum}} = \sum_{i=1}^{K} \left(\bar{R}_i^+ \Big|_{(\delta_i^{+\star}, \tilde{\delta}_i^{+\star})} - \bar{R}_i^- \Big|_{(\delta_i^{-\star}, \tilde{\delta}_i^{-\star})} \right)$, with K finite, we have from Theorem 8 that, for all $\mathbf{Q}_i$ with bounded spectral norm,

$$\sup_{\substack{\mathbf{Q}, \\ \|\mathbf{Q}\| \text{ bounded}}} R_{\text{sum}}(\mathbf{Q}) \quad - \quad \sup_{\substack{\mathbf{Q}, \\ \|\mathbf{Q}\| \text{ bounded}}} \bar{R}_{\text{sum}}(\mathbf{Q}) \to 0, \tag{6.53}$$

as N_i, M_i grow large with $M_i/N_i \to c_i > 0$. Thus, optimizing R_{sum} over $\mathbf{Q}$, for any family of bounded precoders, is equivalent, in the asymptotic regime, to optimizing $\bar{R}_{\text{sum}}$ over $\mathbf{Q}$.

6.3.2 Optimizing the Approximation of the Expected Sum Rate

$\bar{R}_{\text{sum}}$ does not involve expectations. Hence we propose to use a gradient ascent method to determine a local maximum as summarized in Algorithm 4. At each step of the gradient algorithm, $\delta_i^{+\star}, \delta_i^{-\star}, \tilde{\delta}_i^{+\star}, \tilde{\delta}_i^{-\star}$ are evaluated using Algorithm 3, allowing an evaluation of the gradient from which a new set of precoders is derived.

Algorithm 4 Iterative optimization

Initialization: $m = 0$ and $\mathbf{Q}^{(0)}$ arbitrary.

Repeat

- Compute $\delta_i^{+\star}, \delta_i^{-\star}, \tilde{\delta}_i^{+\star}, \tilde{\delta}_i^{-\star}, i = 1, ..., K$, using Algorithm 3
- Evaluate the gradient $\nabla \bar{R}_{\text{sum}}$ w.r.t. $\mathbf{V} = [\mathbf{V}_1, ..., \mathbf{V}_K]^{\text{T}}$
- Let $\mathbf{V} = \mathbf{V} + \beta \nabla \bar{R}_{\text{sum}}$ (for some step-size β)
- Let $\mathbf{Q}^{(m+1)} = \text{Bdiag}\left(P_1 \frac{\mathbf{V}_1 \mathbf{V}_1^{\text{H}}}{\text{tr}(\mathbf{V}_1 \mathbf{V}_1^{\text{H}})}, ..., P_K \frac{\mathbf{V}_K \mathbf{V}_K^{\text{H}}}{\text{tr}(\mathbf{V}_K \mathbf{V}_K^{\text{H}})} \right)$
- $m \leftarrow m + 1$

until convergence.

The remainder of this section is dedicated to deriving explicit expressions for the gradients required in Algorithm 4.

We know from (6.42) that the partial derivative of $\bar{R}_i^+$ w.r.t. $\delta_i^+, \tilde{\delta}_i^+$ for $i = 1, ..., K$ is zero at $(\delta_i^{+\star}, \tilde{\delta}_i^{+\star})$ (the same applies to $\bar{R}_i^-$ w.r.t. $\delta_i^-, \tilde{\delta}_i^-$ at $(\delta_i^{-\star}, \tilde{\delta}_i^{-\star})$). This fact simplifies the calculation of the gradient when using the differentiation chain rule.

In order to differentiate $\bar{R}_{\text{sum}}$, we rewrite $\bar{R}_i^+$ as

$$\bar{R}_i^+ = \log \left| (1 + \tilde{\delta}_i^+) \mathbf{I}_{M_i} + \frac{1}{\bar{\sigma}^2} \sum_{j=1}^{K} \bar{\mathbf{H}}_{ij} \mathbf{Q}_j^{\frac{1}{2}} \mathbf{Z}_{ij}(\delta_i^+) \mathbf{Q}_j^{\frac{1}{2}} \bar{\mathbf{H}}_{ij}^{\text{H}} \right| - \sum_{j=1}^{K} \log \left| \mathbf{Z}_{ij}(\delta_i^+) \right| - N \bar{\sigma}^2 \delta_i^+ \tilde{\delta}_i^+ \tag{6.54}$$

in which $\mathbf{Z}_{ij}(x) = (\mathbf{I}_{N_j} + x \sigma_{ij}^2 \mathbf{Q}_j)^{-1}$, and

$$\delta_i^+ = \frac{1}{N} \text{tr} \left(\bar{\sigma}^2 (1 + \tilde{\delta}_i^+) \mathbf{I}_{M_i} + \sum_{j=1}^{K} \bar{\mathbf{H}}_{ij} \mathbf{Q}_j^{\frac{1}{2}} \mathbf{Z}_{ij}(\delta_i^+) \mathbf{Q}_j^{\frac{1}{2}} \bar{\mathbf{H}}_{ij}^{\text{H}} \right)^{-1}.$$

It is shown in Appendix C.4 that the gradient with respect to $\mathbf{V}_n$ is given by

$$\nabla_n \bar{R}_i^+ = \mathbf{\Omega}_{in}^+ \mathbf{V}_n - \frac{\text{tr}\left(\mathbf{\Omega}_{in}^+ \mathbf{V}_n \mathbf{V}_n^{\text{H}} \right)}{\text{tr}\left(\mathbf{V}_n \mathbf{V}_n^{\text{H}} \right)} \mathbf{V}_n, \tag{6.55}$$

where

$$\mathbf{\Omega}_{in}^+ = \mathbf{Z}_{in}(\delta_i^+) \left(\frac{1}{\bar{\sigma}^2} \bar{\mathbf{H}}_{in}^{\text{H}} (\mathbf{F}_i(\delta_i^+))^{-1} \bar{\mathbf{H}}_{in} \mathbf{Z}_{in}(\delta_i^+) + \delta_i^+ \sigma_{in}^2 \mathbf{I}_{N_n} \right). \tag{6.56}$$

The same procedure holds for $\bar{R}_i^-$ with $\mathbf{Q}_{-i}$ instead of $\mathbf{Q}$, and therefore we have $\nabla_n \bar{R}_{\text{sum}} = \sum_{i=1}^{K} (\nabla_n \bar{R}_i^+ - \nabla_n \bar{R}_i^-)$. Defining $\mathbf{V} = \left[\mathbf{V}_1, ..., \mathbf{V}_K \right]^{\text{T}}$, the gradient with respect to $\mathbf{V}$ is $\nabla \bar{R}_{\text{sum}} = \left[\nabla_1 \bar{R}_{\text{sum}}, ..., \nabla_K \bar{R}_{\text{sum}} \right]$.

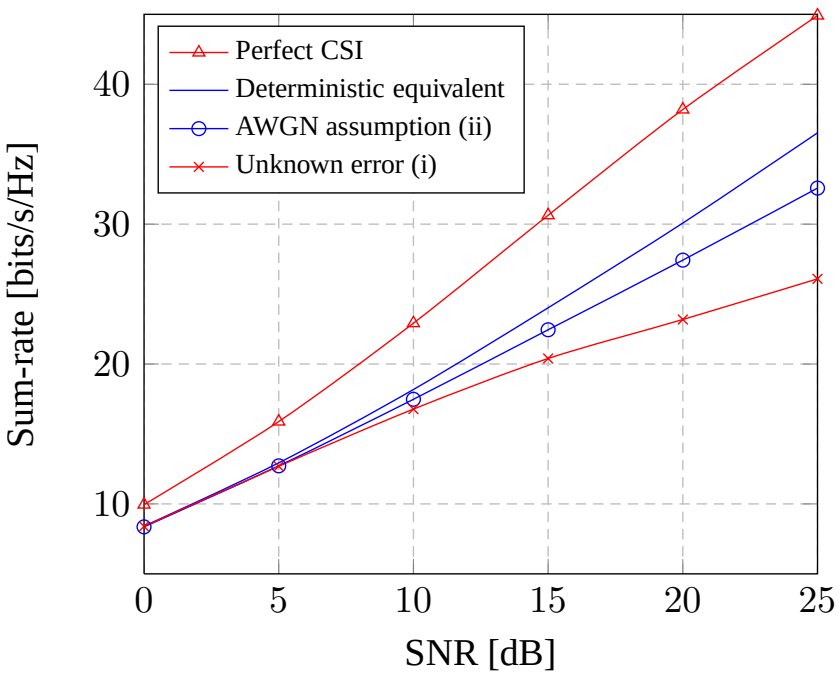

Figure 6.6. Performance comparison of precoder optimization methods, for 3-user MIMO IC, $N_j = 4$, $M_i = 4$, $\eta_{ij} = 3$.

6.3.3 Performance Investigation

In this section, the performance of the proposed scheme is evaluated through numerical simulations. The performance metric is the expected sum rate (6.45) evaluated through Monte-Carlo simulations employing the covariance matrices designed with Algorithm 4. The whole process is repeated and averaged over realizations of $\bar{\mathbf{H}}_{ij}$, with entries $\mathcal{CN}(0,1)$.

Figure 6.6 shows the expected sum rate versus transmit SNR for a three-user IC with four antennas per node and two data streams for each transmitter, using different precoder optimization schemes. We assume $\sigma_{ij} = 0.5$ and $\eta_{ij} = 3$ for $i,j = 1,...,K$. We compare the performance of the precoders provided by Algorithm 4 to two alternative approaches: (i) precoders are designed to maximize the sum rate under the assumption that $\bar{\mathbf{H}}_{ij}$ is the true channel (i.e. the transmitter assumes $\sigma_{ij}^2 = 0$), (ii) the signal resulting from the channel estimation error is modeled as an additive white Gaussian noise term. In that case, the last two terms in

$$\mathbf{y}_i = \bar{\mathbf{H}}_{ii}\sqrt{\lambda_i}\mathbf{V}_i\mathbf{x}_i + \sum_{j=1,j\neq i}^{K} \bar{\mathbf{H}}_{ij}\sqrt{\lambda_j}\mathbf{V}_j\mathbf{x}_j + \mathbf{n}_i$$
$$+ \mathbf{E}_{ii}\sqrt{\lambda_i}\mathbf{V}_i\mathbf{x}_i + \sum_{j=1,j\neq i}^{K} \mathbf{E}_{ij}\sqrt{\lambda_j}\mathbf{V}_j\mathbf{x}_j$$

are considered as noise and therefore the covariance matrix of the equivalent noise vector is $\sigma_i^2\mathbf{I}_{M_i}$ with $\sigma_i^2 = M_i \sum_{j=1}^{K} P_j N_j \sigma_{ij}^2 + \sigma^2$. In this case the precoders are designed as in (i) except for the different noise variance. We also provide as a reference the performance of precoders optimized with perfect CSI.

The results clearly show that our deterministic equivalent approach is superior to (i) and (ii). This suggests that, even though the system dimensions are small in this example, and therefore we operate far from the asymptotic regime $N_i, M_j \to \infty$, the approximation through deterministic equivalents outperforms the classical simplifying assumptions (i) and (ii).

7

Conclusions and Outlook

Finally, we summarize the important contributions and provide some insights for future development and extension of our results. In this thesis, we devised efficient quantization schemes to reduce the CSI feedback overhead in a K-user MIMO IC. We analyzed the system performance when quantized CSI is used to design the transmit signals.

We next considered a scenario where the CSI available at the transmitters is outdated and does not provide any information about the current state of the channel. A retrospective alignment scheme was proposed to achieve the DoF region of the two-user MIMO IC with outdated CSI.

In the third part of this thesis, we focused on distributed calculation of the transmit precoders over the network. A distributed approach to the interference alignment problem was proposed using a message-passing formulation.

Finally, the problem of sum rate maximization was considered assuming a Gaussian additive channel uncertainty model. Two different methods were proposed to approximately maximize the sum rate in a K-user MIMO IC.

7.1 Conclusions

In the following we draw conclusions based on the results presented in the previous chapters.

Quantized CSI

- A new CSI feedback scheme for interference alignment on the K-user MIMO interference channel was proposed consisting in a parsimonious representation based on the Grassmann manifold.
- We characterized the scaling of the number of feedback bits with the SNR required in order to preserve the multiplexing gain achievable using perfect CSI. This scaling is shown to be better (slower) than the scaling obtained using the schemes from [8] or [7] for all system dimensions where IA is feasible.
- Simulations results confirm that our scheme provides a better sum rate performance compared to quantization of the normalized channel matrices for the same number of feedback bits. Furthermore, at non-asymptotic SNR and for a fixed codebook size, the proposed scheme is shown by simulation to achieve better sum-rate performance than the methods from [8] or [7].
- We introduced a model for the chordal distance of the quantization error which facilitates the numerical performance analysis of schemes requiring intractably large codebooks; it can be used to generate rotations that closely approximate the true quantization error of RVQ. This tool enables numerical analysis of general Grassmannian RVQ schemes for large codebook sizes, without requiring the generation of the codebook nor the exhaustive search normally associated with the quantizer.
- In downlink interference alignment for TDD cellular systems a CSI sharing scenario was considered and efficient sharing of CSIT among interfering BSs was proposed similar to the feedback method.
- The growth rate of the bits to be transferred with respect to the transmit power was characterized in order to preserve the total multiplexing gain. This scaling is shown to be better (slower) than the scaling obtained by naively sharing the channel matrices.
- Furthermore, methods were proposed to improve the performance by exploiting the accurate local CSI available at each transmitter. Global optimization problems are considered and then decoupled into local optimization problems using the proposed IA filters. The methods start from an IA solution and improve the precoders exploiting the accurate local CSI available at each transmitter(which also includes the direct channel at each transmitter). The proposed methods are shown to be superior to classical interference management techniques via simulations.

Outdated CSI

- We modeled the problem of transmission in a MIMO IC with outdated CSIT as a retrospective alignment scheme. The model is a MIMO generalization of the scheme proposed in [74] wherein the procedure of feeding back and forwarding the overheard interference as in [9] is done in a systematic way.

- We propose a unified and simple DoF-achievable scheme for the MIMO IC with outdated CSIT which encompasses every configuration of antennas and does not require the complicated transmission scheme of [11]. Our proposed scheme provides a matrix representation for the precoders to be employed when CSIT is outdated.
- The achievable DoF of the MIMO IC with outdated CSIT is verified analytically.
- The proposed scheme is very flexible and insights are provided to extend the method for more interesting scenarios like having time correlated channels.

Distributed Interference Alignment

- We have introduced an iterative solution to the problem of interference alignment over MIMO channels based on message passing applied to a suitable graph. A parameterization of the messages that enables the use of this algorithm over continuous variable spaces was introduced, and closed-form approximations of the messages were derived.
- We have shown that the iterative leakage minimization algorithm of Gomadam et al. [12] is a particular case of our message-passing algorithm obtained for a particular schedule.
- The proposed algorithm was shown to outperform ILM in terms of convergence speed.
- As the associated nodes of the graph correspond to TXs/RXs in the network, we discussed different allocation of the nodes of the graph to the transceivers and also the distributed implementation of the proposed technique.

Robust Interference Management

Link Adaptation for Interference Alignment

- Interference alignment based on imperfect CSI was investigated. As the accuracy of CSI at the transmitter side is crucial for interference alignment, we analyzed the statistics of the imperfect CSI in order to handle the resulting interference.
- We considered a MIMO interference channel where the transmit and receive spaces are determined by IA. Considering practical modulation schemes, we looked at maximizing a weighted sum of the average rates provided that a certain set of bit-error-rate and power constraints are satisfied by choosing appropriate modulation coding and powers.
- Since the problem is quite general and intractable, we resorted to some approximations and provided simulations to show the accuracy of the approximations in the regimes of practical interest.
- An adaptive rate and power allocation scheme is devised to enhance the performance of interference alignment.

Optimization of the Expected Sum Rate

- Optimization of a deterministic equivalent of the expected sum rate for the K-user IC was explored. Our approach is shown to be beneficial when the original problem is complicated to analyze and therefore an approximated problem is liable for investigation.
- The analysis is based on tools from random matrix theory applicable to matrices of large dimensions (representing the channel matrices). The results are proved to be very accurate even for small dimensions.
- The expected sum rate maximization problem was tackled using a gradient ascent method employing the properties of the derivative of the deterministic equivalent.
- The method is shown to be superior to the conventional methods via simulations.

7.2 Outlook

Here we present some directions for future research:

Quantized CSI

- We have used Grassmannian representation to quantize the channel matrices in order to perform interference alignment. There exist other objective functions that are invariant under unitary transformation of the precoders, hence the quantization scheme might generalize to more interesting objective functions.
- One of the interesting directions to extend the current work is to show whether the scaling of the bits derived here is the optimal scaling or not. In other words, one could show whether it is possible to achieve full DoF with IA with a slower scaling of the feedback bits.
- Since the scheme is based on quantization on the Grassmann manifold which requires large code books at high SNR, structured codebooks for Grassmann manifold are desirable. Approximate but structured solutions for the codebook design problem will be of great interest.

Outdated CSI

- Clearly the extension of the proposed scheme to the case of time correlated channels is very interesting and promising. The scheme is very flexible and extensions can be applied in a simple and intuitive manner.
- The current study is solely for the two user IC, while the scheme can be generalized to different channels like K-user IC or the X channel. As the set of different configuration of antennas gets larger by increasing the number of users, having a general scheme for every possible antenna configuration in the K-user IC is desirable.

Distributed Interference Alignment

- One possible direction of future research on this problem is to consider a reciprocal channel where the messages are sent over the air from both sides (TXs/RXs). In this scenario every TX/RX has access to its local CSI and this information has to be exploited for computation of messages at every node. This can lead to a systematic approach for the well known leakage minimization algorithm.
- The objective function considered in this chapter is quite arbitrary. Clearly minimizing the leakage is not optimal at low and medium SNR. Many different objectives (with different factor graphs) can be defined and analyzed in terms of convergence and performance (e.g., achievable sum rate).

Robust Interference Management

- The results of the link adaptation scheme can be improved by making another degree of adaptation, i.e., having adaptive CSI quantization. The channels can be quantized with an accuracy associated to the channel quality. This would improve the performance by avoiding bad quality channels to undergo interference alignment.
- The analysis of the deterministic equivalent deals with the expectation of sum rate while a generalization can include higher order statistics. For example outage capacity can be analyzed by considering the deterministic equivalent of the variance of rate. More objective functions can be tackled in this way.

A

A.1 Proof of Lemma 3

The power of the interference leakage at receiver i reads

$$\begin{aligned} L_i &= \mathrm{tr}\left(\sum_{j=1,j\neq i}^{K} \mathbf{G}_i^{\mathrm{H}}\mathbf{H}_{ij}\mathbf{V}_j\mathbf{V}_j^{\mathrm{H}}\mathbf{H}_{ij}^{\mathrm{H}}\mathbf{G}_i\right) \\ &= \mathrm{tr}\left(\mathbf{G}_i^{\mathrm{H}}\mathbf{H}_i\mathbf{V}_{-i}\mathbf{V}_{-i}^{\mathrm{H}}\mathbf{H}_i^{\mathrm{H}}\mathbf{G}_i\right) \\ &= ||\mathbf{G}_i^{\mathrm{H}}\mathbf{H}_i\mathbf{V}_{-i}||_{\mathrm{F}}^2. \end{aligned} \tag{A.1}$$

Substituting $\mathbf{G}_i^{\mathrm{H}} = (\mathbf{C}_i^{-1}\mathbf{F}_i^{\mathrm{H}}\hat{\mathbf{F}}_i\tilde{\mathbf{U}}_i)^{\mathrm{H}}$, $\mathbf{V}_j = (\frac{P}{d})^{\frac{1}{2}}\tilde{\mathbf{V}}_j$ and $\mathbf{H}_i = \mathbf{C}_i^{\mathrm{H}}\mathbf{F}_i^{\mathrm{H}}$ gives

$$\begin{aligned} L_i &= \frac{P}{d}||\tilde{\mathbf{U}}_i^{\mathrm{H}}\hat{\mathbf{F}}_i^{\mathrm{H}}\mathbf{F}_i\mathbf{C}_i^{-\mathrm{H}}\mathbf{C}_i^{\mathrm{H}}\mathbf{F}_i^{\mathrm{H}}\tilde{\mathbf{V}}_{-i}||_{\mathrm{F}}^2 \\ &= \frac{P}{d}||\tilde{\mathbf{U}}_i^{\mathrm{H}}\hat{\mathbf{F}}_i^{\mathrm{H}}\mathbf{F}_i\mathbf{F}_i^{\mathrm{H}}\tilde{\mathbf{V}}_{-i}||_{\mathrm{F}}^2. \end{aligned} \tag{A.2}$$

Using the alignment equation (3.33) and the fact that $\hat{\mathbf{F}}_i^{\mathrm{H}}\hat{\mathbf{F}}_i = \mathbf{I}_N$ yields $\tilde{\mathbf{U}}_i^{\mathrm{H}}\hat{\mathbf{F}}_i^{\mathrm{H}}\hat{\mathbf{F}}_i\hat{\mathbf{F}}_i^{\mathrm{H}}\tilde{\mathbf{V}}_{-i} = 0$, therefore (A.2) can be rewritten as

$$L_i = \frac{P}{d}||\tilde{\mathbf{U}}_i^{\mathrm{H}}\hat{\mathbf{F}}_i^{\mathrm{H}}(\mathbf{F}_i\mathbf{F}_i^{\mathrm{H}} - \hat{\mathbf{F}}_i\hat{\mathbf{F}}_i^{\mathrm{H}})\tilde{\mathbf{V}}_{-i}||_{\mathrm{F}}^2. \tag{A.3}$$

Using the facts that $||\mathbf{X}||_{\mathrm{F}} \leq \sqrt{\mathrm{rank}(\mathbf{X})}\,||\mathbf{X}||_2$, $||\mathbf{X}||_2 \leq ||\mathbf{X}||_{\mathrm{F}}$ and $||\mathbf{XY}||_2 \leq ||\mathbf{X}||_2\,||\mathbf{Y}||_2$, we have

$$\begin{aligned} L_i &= \frac{P}{d}||\tilde{\mathbf{U}}_i^{\mathrm{H}}\hat{\mathbf{F}}_i^{\mathrm{H}}(\mathbf{F}_i\mathbf{F}_i^{\mathrm{H}} - \hat{\mathbf{F}}_i\hat{\mathbf{F}}_i^{\mathrm{H}})\tilde{\mathbf{V}}_{-i}||_{\mathrm{F}}^2 \\ &\leq P||\tilde{\mathbf{U}}_i^{\mathrm{H}}\hat{\mathbf{F}}_i^{\mathrm{H}}(\mathbf{F}_i\mathbf{F}_i^{\mathrm{H}} - \hat{\mathbf{F}}_i\hat{\mathbf{F}}_i^{\mathrm{H}})\tilde{\mathbf{V}}_{-i}||_2^2 \\ &\leq P||\tilde{\mathbf{U}}_i^{\mathrm{H}}||_2^2\,||\hat{\mathbf{F}}_i^{\mathrm{H}}||_2^2\,||(\mathbf{F}_i\mathbf{F}_i^{\mathrm{H}} - \hat{\mathbf{F}}_i\hat{\mathbf{F}}_i^{\mathrm{H}})||_2^2\,||\tilde{\mathbf{V}}_{-i}||_2^2 \\ &= P||(\mathbf{F}_i\mathbf{F}_i^{\mathrm{H}} - \hat{\mathbf{F}}_i\hat{\mathbf{F}}_i^{\mathrm{H}})||_2^2 \\ &\leq P||(\mathbf{F}_i\mathbf{F}_i^{\mathrm{H}} - \hat{\mathbf{F}}_i\hat{\mathbf{F}}_i^{\mathrm{H}})||_{\mathrm{F}}^2 \\ &= 2Pd_c^2(\hat{\mathbf{F}}_i, \mathbf{F}_i). \end{aligned} \tag{A.4}$$

The second equality holds because $\tilde{\mathbf{U}}_i^{\mathrm{H}}$, $\hat{\mathbf{F}}_i^{\mathrm{H}}$ and $\tilde{\mathbf{V}}_{-i}$ are truncated unitary matrices, which implies that their spectral norm is 1.

From [114, Theorem 5], if a codebook is generated using the sphere-packing procedure, the maximum value of the quantization error in terms of the chordal distance can be upper bounded as

$$\max_{\mathbf{F}_i \in \mathcal{G}_{(K-1)M,N}} d_c(\hat{\mathbf{F}}_i, \mathbf{F}_i) \leq \frac{2}{\left(c\,2^{B_{\mathrm{G}}}\right)^{\frac{1}{N_{\mathrm{G}}}}}\left(1 + o\left(2^{-\frac{B_{\mathrm{G}}}{N_{\mathrm{G}}}}\right)\right). \tag{A.5}$$

The constant c in (3.15) is obtained from [60, Corollary 1]. Combining (A.4) and (A.5) yields (3.14).

A.2 Proof of Lemma 4

Similar to (A.1), the power of the interference leakage at receiver i can be written as

$$\bar{L}_i = \mathrm{tr}\left(\sum_{j=1,j\neq i}^{K} \tilde{\mathbf{U}}_i^{\mathrm{H}}\mathbf{H}_{ij}\mathbf{V}_j\mathbf{V}_j^{\mathrm{H}}\mathbf{H}_{ij}^{\mathrm{H}}\tilde{\mathbf{U}}_i\right) \tag{A.6}$$

$$= \frac{P}{d}\sum_{j=1,j\neq i}^{K} ||\tilde{\mathbf{U}}_i^{\mathrm{H}}\mathbf{H}_{ij}\tilde{\mathbf{V}}_j||_{\mathrm{F}}^2 \tag{A.7}$$

$$= \frac{P}{d}\sum_{j=1,j\neq i}^{K} ||\tilde{\mathbf{U}}_i^{\mathrm{H}}(\mathbf{H}_{ij} - \alpha\hat{\mathbf{H}}_{ij})\tilde{\mathbf{V}}_j||_{\mathrm{F}}^2 \tag{A.8}$$

$$\leq \frac{P}{d}\sum_{j=1,j\neq i}^{K} ||\tilde{\mathbf{U}}_i^{\mathrm{H}}||_{\mathrm{F}}^2\,||(\mathbf{H}_{ij} - \alpha\hat{\mathbf{H}}_{ij})||_{\mathrm{F}}^2\,||\tilde{\mathbf{V}}_j||_{\mathrm{F}}^2 \tag{A.9}$$

$$\leq Pd\sum_{j=1,j\neq i}^{K} ||\mathbf{H}_{ij} - \alpha\hat{\mathbf{H}}_{ij}||_{\mathrm{F}}^2 \tag{A.10}$$

$$= Pd\sum_{j=1,j\neq i}^{K} ||\mathrm{vec}(\mathbf{H}_{ij}) - \alpha\mathrm{vec}(\hat{\mathbf{H}}_{ij})||_2^2 \tag{A.11}$$

$$\leq Pd\sum_{j=1,j\neq i}^{K} ||\mathrm{vec}(\mathbf{H}_{ij})||_2^2\left|\left|\mathbf{z}_{ij} - \alpha\frac{\hat{\mathbf{z}}_{ij}}{||\mathrm{vec}(\mathbf{H}_{ij})||_2}\right|\right|_2^2 \tag{A.12}$$

for an arbitrary scalar α. In particular, choosing $\alpha = \hat{\mathbf{z}}_{ij}^{\mathrm{H}}\mathbf{z}_{ij}||\mathrm{vec}(\mathbf{H}_{ij})||_2$ yields

$$\bar{L}_i \leq Pd \sum_{j=1,j\neq i}^{K} ||\mathrm{vec}(\mathbf{H}_{ij})||_2^2 \, ||\mathbf{z}_{ij}\mathbf{z}_{ij}^{\mathrm{H}}\mathbf{z}_{ij} - \hat{\mathbf{z}}_{ij}\hat{\mathbf{z}}_{ij}^{\mathrm{H}}\mathbf{z}_{ij}||_2^2 \tag{A.13}$$

$$\leq Pd \sum_{j=1,j\neq i}^{K} ||\mathrm{vec}(\mathbf{H}_{ij})||_2^2 \, ||\mathbf{z}_{ij}\mathbf{z}_{ij}^{\mathrm{H}} - \hat{\mathbf{z}}_{ij}\hat{\mathbf{z}}_{ij}^{\mathrm{H}}||_{\mathrm{F}}^2 \, ||\mathbf{z}_{ij}||_2^2 \tag{A.14}$$

$$= 2Pd \sum_{j=1,j\neq i}^{K} ||\mathrm{vec}(\mathbf{H}_{ij})||_2^2 \, (1 - |\mathbf{z}_{ij}^{\mathrm{H}}\hat{\mathbf{z}}_{ij}|^2) \tag{A.15}$$

$$\leq 2PdB_{\max} \sum_{j=1,j\neq i}^{K} (1 - |\mathbf{z}_{ij}^{\mathrm{H}}\hat{\mathbf{z}}_{ij}|^2) \tag{A.16}$$

$$= 2PdB_{\max} D_c^2(\mathbf{Z}_i, \hat{\mathbf{Z}}_i) \tag{A.17}$$

where $B_{\max} = \max_j ||\mathrm{vec}(\mathbf{H}_{ij})||_2^2$.

From [47, theorem II.1], the distance on the composite Grassmann manifold can be bounded for any codebook obtained via sphere-packing as $\max_{\mathbf{Z}_i \in \mathcal{G}_{MN,1}^{K-1}} D_c(\mathbf{Z}_i, \hat{\mathbf{Z}}_i) \leq \frac{2}{(\bar{c}\, 2^{B_{\mathrm{INM}}})^{\frac{1}{N_{\mathrm{INM}}}}} \triangleq \bar{\Delta}$ which results in

$$\bar{L}_i \leq 2PdB_{\max}\bar{\Delta}^2 \leq \frac{8PdB_{\max}}{(\bar{c}\, 2^{B_{\mathrm{INM}}})^{\frac{2}{N_{\mathrm{INM}}}}} \tag{A.18}$$

where N_{INM} was defined in Section 3.2.3 and $\bar{c}$ is a constant. It is clear from (A.18) that quantizing $\mathbf{Z}_i$ with $B_{\mathrm{INM}} = \frac{N_{\mathrm{INM}}}{2}\log P$ bits at receiver i guarantees that $\bar{L}_i$ remains bounded regardless of the SNR.

A.3 Proof of Lemma 5

Consider the following quantity

$$R_i'' - R_i' = \log\left|\mathbf{G}_i^{\mathrm{H}}\mathbf{G}_i + \mathbf{Q}_{\mathrm{I}}^i\right| - A^i \tag{A.19}$$

$$\leq \log\left|\mathbf{G}_i^{\mathrm{H}}\mathbf{G}_i + \mathbf{Q}_{\mathrm{I}}^i\right|, \tag{A.20}$$

where $A^i = \log\left|\mathbf{G}_i^{\mathrm{H}}\mathbf{G}_i + (\mathbf{Q}_{\mathrm{S}}^i + \mathbf{Q}_{\mathrm{I}}^i)\right| - \log\left|\mathbf{G}_i^{\mathrm{H}}\mathbf{G}_i + \mathbf{Q}_{\mathrm{S}}^i\right|$ and $A^i \geq 0$ since $\mathbf{Q}_{\mathrm{I}}^i$ is positive semi-definite[1].

Since the argument of the determinant is of rank at most d,

$$R_i'' - R_i' \leq d\log\left(\lambda_{\max}\left(\mathbf{G}_i^{\mathrm{H}}\mathbf{G}_i + \mathbf{Q}_{\mathrm{I}}^i\right)\right) \tag{A.21}$$

$$\leq d\log\left(\lambda_{\max}\left(\mathbf{G}_i^{\mathrm{H}}\mathbf{G}_i\right) + \lambda_{\max}\left(\mathbf{Q}_{\mathrm{I}}^i\right)\right) \tag{A.22}$$

[1] In fact, when the number of feedback bits is scaled according to (3.16), the bound in (A.20) gets tighter as the SNR increases. This can be seen by noticing that $\lim_{P\to\infty} A^i = \lim_{P\to\infty} \log\left|\mathbf{I}_d + \mathbf{Q}_{\mathrm{I}}^i\left(\mathbf{G}_i^{\mathrm{H}}\mathbf{G}_i + \mathbf{Q}_{\mathrm{S}}^i\right)^{-1}\right| = \lim_{P\to\infty} \log\left|\mathbf{I}_d + \mathbf{Q}_{\mathrm{I}}^i{\mathbf{Q}_{\mathrm{S}}^i}^{-1}\right| = \lim_{P\to\infty} \log\left|\mathbf{I}_d + \frac{d}{P}\mathbf{Q}_{\mathrm{I}}^i{\mathbf{W}_{\mathrm{S}}^i}^{-1}\right|$, which goes to zero since $\mathbf{W}_{\mathrm{S}}^i$ is full rank almost surely and when feedback scales according to (3.16) we have $\frac{d}{P}||\mathbf{Q}_{\mathrm{I}}^i||_2 \to 0$.

$$\leq \quad d \log \left(||\mathbf{G}_i||_2^2 + \left|\left|\mathbf{G}_i^{\mathrm{H}} \mathbf{H}_i \mathbf{V}_{-i}\right|\right|_2^2 \right), \tag{A.23}$$

where the second inequality follows by the fact that $\mathbf{G}_i^{\mathrm{H}}\mathbf{G}_i$ and $\mathbf{Q}_{\mathrm{I}}^i$ are Hermitian matrices. Furthermore $||\mathbf{G}_i||_2 = ||\mathbf{C}_i^{-1}\mathbf{F}_i^{\mathrm{H}}\hat{\mathbf{F}}_i\tilde{\mathbf{U}}_i||_2 \leq ||\mathbf{C}_i^{-1}||_2 \, ||\mathbf{F}_i^{\mathrm{H}}||_2 \, ||\hat{\mathbf{F}}_i||_2 \, ||\tilde{\mathbf{U}}_i||_2 = ||\mathbf{C}_i^{-1}||_2$. From eqs. (A.1)–(A.4) we have $||\mathbf{G}_i^{\mathrm{H}}\mathbf{H}_i\mathbf{V}_{-i}||_2^2 \leq L_i \leq 2Pd_c^2(\hat{\mathbf{F}}_i, \mathbf{F}_i)$. Using these bounds,

$$R_i'' - R_i' \quad \leq \quad d \log \left(||\mathbf{C}_i^{-1}||_2^2 + 2Pd_c^2(\hat{\mathbf{F}}_i, \mathbf{F}_i) \right). \tag{A.24}$$

Combining with (A.5) yields (3.21).

A.4 Proof of Lemma 6

It suffices to prove that $\lim_{P\to\infty} \frac{\log\left|\mathbf{G}_i^{\mathrm{H}}\mathbf{G}_i + \mathbf{Q}_{\mathrm{S}}^i\right|}{\log P} = d$ for almost all channel realizations. Note however that the proof is complicated by the fact that we need to consider quantization codebooks of increasing sizes when letting $P \to \infty$; let $\mathbf{Q}_{\mathrm{S}}^i = \frac{P}{d}\mathbf{W}_{\mathrm{S}}^i$ with $\mathbf{W}_{\mathrm{S}}^i = \tilde{\mathbf{U}}_i^{\mathrm{H}}\hat{\mathbf{F}}_i^{\mathrm{H}}\mathbf{F}_i\mathbf{C}_i^{-\mathrm{H}}\mathbf{H}_{ii}\tilde{\mathbf{V}}_i\tilde{\mathbf{V}}_i^{\mathrm{H}}\mathbf{H}_{ii}^{\mathrm{H}}\mathbf{C}_i^{-1}\mathbf{F}_i^{\mathrm{H}}\hat{\mathbf{F}}_i\tilde{\mathbf{U}}_i$, where $\tilde{\mathbf{U}}_i$, $\hat{\mathbf{F}}_i$ and $\tilde{\mathbf{V}}_i$ all depend on the choice of the codebook, it is not clear whether $\mathbf{W}_{\mathrm{S}}^i$ admits a limit for asymptotically large SNR[2]. Therefore, we resort to compactness arguments to show th at there exists a series of codebooks of increasing size for which $\mathbf{W}_{\mathrm{S}}^i$ admits a limit.

Let us consider an infinite sequence of SNRs $\mathcal{P} = \{P_n\}_{n\in\mathbb{N}}$ such that $\lim_{n\to\infty} P_n = \infty$, as well as an infinite sequence of quantization codebooks $\{\mathcal{S}_n\}_{n\in\mathbb{N}}$, such that $|\mathcal{S}_n| = P_n^{N((K-1)M-N)}$, following (3.16). For each SNR value P_n, we let $\hat{\mathbf{F}}_{i,n} = \arg\min_{\mathbf{S}\in\mathcal{S}_n} \; d_c(\mathbf{S}, \mathbf{F}_i)$ and denote $(\tilde{\mathbf{V}}_{1,n}, \ldots, \tilde{\mathbf{V}}_{K,n}, \tilde{\mathbf{U}}_{1,n}, \ldots, \tilde{\mathbf{U}}_{K,n}) \in \mathcal{G}_{M,d}^K \times \mathcal{G}_{N,d}^K$ a set of matrices constituting an IA solution based on $\hat{\mathbf{F}}_{i,n}$. In other words, we solve (3.10) and (3.33) for each n, yielding an infinite series of solutions. Let us denote $\mathbf{X}_n = (\hat{\mathbf{F}}_{1,n}, \ldots, \hat{\mathbf{F}}_{K,n}, \tilde{\mathbf{V}}_{1,n}, \ldots, \tilde{\mathbf{V}}_{K,n}, \tilde{\mathbf{U}}_{1,n}, \ldots, \tilde{\mathbf{U}}_{K,n})$. $\mathcal{G}_{(K-1)M,N}^K \times \mathcal{G}_{M,d}^K \times \mathcal{G}_{N,d}^K$ is compact, as a Cartesian product of compact sets. Therefore, we can extract a convergent subseries[3] from $\{\mathbf{X}_n\}_{n\in\mathbb{N}}$. We let $g(m) \in \mathbb{N}$ denote the index of the m-th element of the convergent subseries, where g is a monotonically increasing function. We also denote

$$(\hat{\mathbf{F}}_1^\star, \ldots, \hat{\mathbf{F}}_K^\star, \tilde{\mathbf{V}}_1^\star, \ldots, \tilde{\mathbf{V}}_K^\star, \tilde{\mathbf{U}}_1^\star, \ldots, \tilde{\mathbf{U}}_K^\star) = \lim_{m\to\infty} \mathbf{X}_{g(m)}. \tag{A.25}$$

Letting $\mathbf{W}_{\mathrm{S}}^{i,n} = \tilde{\mathbf{U}}_{i,n}^{\mathrm{H}}\hat{\mathbf{F}}_{i,n}^{\mathrm{H}}\mathbf{F}_i\mathbf{C}_i^{-\mathrm{H}}\mathbf{H}_{ii}\tilde{\mathbf{V}}_{i,n}\tilde{\mathbf{V}}_{i,n}^{\mathrm{H}}\mathbf{H}_{ii}^{\mathrm{H}}\mathbf{C}_i^{-1}\mathbf{F}_i^{\mathrm{H}}\hat{\mathbf{F}}_{i,n}\tilde{\mathbf{U}}_{i,n}$, we can now write the limit $\lim_{m\to\infty} \mathbf{W}_{\mathrm{S}}^{i,g(m)} = \mathbf{W}_{\mathrm{S}}^{\star i}$, where $\mathbf{W}_{\mathrm{S}}^{\star i} = \tilde{\mathbf{U}}_i^{\star\mathrm{H}}\hat{\mathbf{F}}_i^{\star\mathrm{H}}\mathbf{F}_i\mathbf{C}_i^{-\mathrm{H}}\mathbf{H}_{ii}\tilde{\mathbf{V}}_i^\star\tilde{\mathbf{V}}_i^{\star\mathrm{H}}\mathbf{H}_{ii}^{\mathrm{H}}\mathbf{C}_i^{-1}\mathbf{F}_i^{\mathrm{H}}\hat{\mathbf{F}}_i^\star\tilde{\mathbf{U}}_i^\star$. Therefore we have

$$\lim_{m\to\infty} \frac{\log\left|\mathbf{G}_i^{\mathrm{H}}\mathbf{G}_i + \frac{P_{g(m)}}{d}\mathbf{W}_{\mathrm{S}}^{i,g(m)}\right|}{\log P_{g(m)}} = \lim_{m\to\infty} \frac{\log|\frac{P_{g(m)}}{d}\mathbf{W}_{\mathrm{S}}^{\star i}|}{\log P_{g(m)}} = \mathrm{rank}\left(\mathbf{W}_{\mathrm{S}}^{\star i}\right). \tag{A.26}$$

[2]Although it is clear that the subspace spanned by $\hat{\mathbf{F}}_i$ admits a limit on the Grassmann manifold when $B_{\mathrm{G}} \to \infty$, the definition of $\tilde{\mathbf{U}}_i$ and $\tilde{\mathbf{V}}_i$ as one (possibly among several) solution of (3.33) prevents the extension of the convergence result to those variables.

[3]In order to obtain the same convergence properties for a point on $\mathcal{G}_{a,b}$ and for the corresponding unitary matrix representation $\mathbf{F} \in \mathbb{C}^{a,b}$, it is useful to make this representation unique, e.g. by requiring that the top square $b \times b$ subblock of $\mathbf{F}$ is equal to $\mathbf{I}_b$. For the sake of notational simplicity, we omit those details.

Since $\hat{\mathbf{F}}_i^{\star}$ and $\mathbf{F}_i$ span the same subspace, $\hat{\mathbf{F}}_i^{\star \mathrm{H}}\mathbf{F}_i$ is unitary. Therefore, considering the product of matrices in $\mathbf{W}_{\mathrm{S}}^{\star i}$, we note that $\tilde{\mathbf{U}}_i^{\star \mathrm{H}}\hat{\mathbf{F}}_i^{\star \mathrm{H}}\mathbf{F}_i\mathbf{C}_i^{-\mathrm{H}}$ has full row rank d, $\tilde{\mathbf{V}}_i^{\star}$ has full column rank d, and both are independent of $\mathbf{H}_{ii}$, from which we conclude that $\mathrm{rank}\left(\mathbf{W}_{\mathrm{S}}^{\star i}\right) = d$ a.s., which proves the lemma.

A.5 Proof of Theorem 2

Let us first recall that $R_i \geq R_i'$, which holds also in expectation:

$$\mathrm{E}_{\mathcal{S}}(R_i) \geq \mathrm{E}_{\mathcal{S}}(R_i'). \tag{A.27}$$

Furthermore, from (A.24),

$$\begin{aligned} \mathrm{E}_{\mathcal{S}}(R_i') &\geq R_i'' - d\,\mathrm{E}_{\mathcal{S}}\left(\log\left(||\mathbf{C}_i^{-1}||_2^2 + 2P d_c^2(\hat{\mathbf{F}}_i, \mathbf{F}_i)\right)\right) \\ &\geq R_i'' - d\log\left(||\mathbf{C}_i^{-1}||_2^2 + 2P\mathrm{E}_{\mathcal{S}}\left(d_c^2(\hat{\mathbf{F}}_i, \mathbf{F}_i)\right)\right) \end{aligned} \tag{A.28}$$

where the second inequality follows by application of Jensen's inequality to the $\log$ function. The term $\mathrm{E}_{\mathcal{S}}(d_c^2(\hat{\mathbf{F}}_i, \mathbf{F}_i))$ represents the expected value of the distortion while using a random codebook, and can be further bounded using [114, Theorem 6], which can be summarized as follows: for asymptotically large codebook size, when using a random codebook for quantizing a matrix $\mathbf{F}$ arbitrarily distributed over a manifold, the k-th moment of the chordal distance $D^{(k)} = \mathrm{E}_{\mathcal{S},\mathbf{F}}(d_c^k(\hat{\mathbf{F}}, \mathbf{F}))$ can be bounded as

$$\frac{N_m}{(N_m + k)(c\,2^{B_{\mathrm{G}}})^{\frac{k}{N_m}}} \leq D^{(k)} \leq \frac{\Gamma(\frac{k}{N_m})}{\frac{N_m}{k}(c\,2^{B_{\mathrm{G}}})^{\frac{k}{N_m}}}, \tag{A.29}$$

where the codebooks have $2^{B_{\mathrm{G}}}$ elements and N_m is the real dimension of the corresponding manifold. Using the upper bound in (A.29) for $k = 2$ over the Grassmann manifold, combined with (A.27) and (A.28) results in (3.24).

A.6 The Perturbation Method

Let us consider a point on $\mathcal{G}_{n,p}$, represented by a $n \times p$ truncated unitary matrix $\mathbf{F}$. Here, we assume that $n \geq 2p$ (otherwise it is more efficient to consider the complementary $n - p$ dimensional subspace). Since the columns of $\mathbf{F}$ are orthonormal, they can be completed to form an orthonormal basis of the n-dimensional space. In fact, according to [115], any other point on $\mathcal{G}_{n,p}$ can be represented in the basis constituted by the columns of the unitary matrix $\mathbf{W} = [\mathbf{F}\ \mathbf{F}^{\mathrm{c}}]$ as

$$\bar{\mathbf{F}} = \mathbf{W}\begin{bmatrix} \mathbf{C} \\ \mathbf{S} \\ \mathbf{0}_{n-2p} \end{bmatrix}, \tag{A.30}$$

for some $\mathbf{F}^{\mathrm{c}}$ in the null space of $\mathbf{F}$ and

$$\mathbf{C} = \begin{bmatrix} \cos\theta_1 & \cdots & 0 \\ \vdots & \ddots & \vdots \\ 0 & \cdots & \cos\theta_p \end{bmatrix}, \ \mathbf{S} = \begin{bmatrix} \sin\theta_1 & \cdots & 0 \\ \vdots & \ddots & \vdots \\ 0 & \cdots & \sin\theta_p \end{bmatrix} \tag{A.31}$$

where $\theta_1, \ldots, \theta_p$ are real angles. Clearly, for $\theta_1 = \ldots = \theta_p = 0$, we obtain $\bar{\mathbf{F}} = \mathbf{F}$. More generally, the squared chordal distance between the two points on $\mathcal{G}_{n,p}$ represented by $\mathbf{F}$ and $\bar{\mathbf{F}}$ is

$$r = d_c^2(\bar{\mathbf{F}}, \mathbf{F}) = \sum_{i=1}^{p} \sin^2\theta_i \,. \tag{A.32}$$

Therefore, in order to generate random perturbations of a certain chordal distance $\sqrt{r}$ from $\mathbf{F}$, we propose to generate random values for the angles $\theta_1, \ldots, \theta_p$ such that $\sum_{i=1}^{p} \sin^2\theta_i = r$, and to pick a random orthonormal basis $\mathbf{F}^{\mathrm{c}}$ of the null subspace of $\mathbf{F}$. The perturbed matrix is then computed using (A.30).

The histogram (not shown) of the squared quantization error $d_c^2(\hat{\mathbf{F}}, \mathbf{F})$ obtained from an implementation of the RVQ quantizer suggests that the Gaussian distribution is a good approximation for the probability density function of r. The parameters of this distribution can be obtained from [114, Theorem 6] which provides bounds on the k-th moment of the chordal distance $D^{(k)} = \mathrm{E}_{\mathcal{S},\mathbf{F}}(d_c^k(\hat{\mathbf{F}}, \mathbf{F}))$. Since those bounds are asymptotically tight when the codebook size increases, we arbitrarily choose to use the upper bound[4] as an approximation of $D^{(k)}$, i.e.

$$\bar{r} \triangleq \frac{\Gamma(\frac{2}{N_{\mathrm{G}}})}{\frac{N_{\mathrm{G}}}{2}(c\,2^{B_{\mathrm{G}}})^{\frac{2}{N_{\mathrm{G}}}}} \approx D^{(2)} \tag{A.33}$$

is the mean and

$$\sigma_r^2 \triangleq \frac{\Gamma(\frac{4}{N_{\mathrm{G}}})}{\frac{N_{\mathrm{G}}}{4}(c\,2^{B_{\mathrm{G}}})^{\frac{4}{N_{\mathrm{G}}}}} - \bar{r}^2 \approx D^{(4)} - (D^{(2)})^2 \tag{A.34}$$

is the variance. We propose generate the values for r according to $\mathcal{N}(\bar{r}, \sigma_r^2)$ truncated to $\mathbb{R}^+$. This process is summarized in Algorithm 5.

Algorithm 5 Generating random perturbations around $\mathbf{F}$

- Draw a random realization of the squared chordal distance r from $\mathcal{N}(\bar{r}, \sigma_r^2)$
- If $r < 0$, generate a new sample
- Draw independent $s_1, \ldots, s_p$ uniformly from the interval $(0, 1)$
- Compute the angles $\theta_i = \sin^{-1}\left(\frac{s_i\sqrt{r}}{\sqrt{\sum_{i=1}^{p} s_i^2}}\right)$
- Generate a random orthonormal basis $\mathbf{F}^{\mathrm{c}}$ of the null space of $\mathbf{F}$
- Compute $\bar{\mathbf{F}}$ according to (A.30).

[4] Experiments have shown no noticeable performance difference when using the lower bound instead.

B

B.1 Proof of Theorem 5

In order to prove the theorem, the following conditions need to be verified :

C.I : $d_i \leq \min(M_i, N_i),\ i = 1, 2$ and $N_2 < d_1 + d_2 \leq N_1$

C.II : $T(d_1 + d_2) \leq (T - q)N_1 + qM_2 + min(qN_1, qM_1, (T - q)N_2)$

C.III : $Td_1 \leq (T - q)M_1$

For simplicity, we verify the conditions for every case of group G_1 separately. The proof is complete if the above three conditions hold for all cases.

- **Case A.II.2**: $\mathrm{M}_1 > \mathrm{N}_1 > \mathrm{M}_2 \geq \mathrm{N}_2$:

  In this case we have $d_1 = \frac{M'_1(N_1-N_2)}{(M'_1-N_2)}$ and $d_2 = \frac{N_2(M'_1-N_1)}{(M'_1-N_2)}$ with $M'_1 = \min(M_1, N_1+N_2)$. We set $T = (M'_1 - N_2)$ which gives $q = \frac{d_2^*}{N_2} = (M'_1 - N_1)$. The first condition is clearly satisfied. The second condition can be simplified as follows:

  $$T(d_1+d_2) \leq (T-q)N_1 + qM_2 + \min(qN_1, (T-q)N_2). \tag{B.1}$$

  If $qN_1 < (T-q)N_2$ then the condition simplifies to

  $$T(d_1+d_2) \leq TN_1 + qM_2, \tag{B.2}$$

  which holds since in group G_1 we have $d_1 + d_2 \leq N_1$. Therefore we consider the remaining case where $qN_1 \geq (T-q)N_2$. In this case, the condition simplifies to

  $$T(d_1+d_2) \leq (T-q)(N_1+N_2) + qM_2. \tag{B.3}$$

  Here we show that the resulting condition always holds: Substituting for T, d_1, d_2 and using the fact that $M'_1 \leq (N_1+N_2)$, we have

  $$T(d_1+d_2) = M'_1(N_1-N_2)+qN_2 \leq (N_1+N_2)(N_1-N_2)+qM_2 = (T-q)(N_1+N_2)+qM_2. \tag{B.4}$$

  The third condition is also satisfied since we have $d_1^* = M'_1(N_1-N_2) \leq M_1(N_1-N_2) = (T-q)M_1$.

- **Case B.I**: $N_1 \geq M_1 > N_2 > M_2$:

  In this case we have $d_1 = \frac{M_1(N_2-M_2)}{N_2}$ and $d_2 = M_2$. We choose $T = N_2$ which gives $q = M_2$. The first condition is straightforward.

  Substituting for T, d_1, d_2, q, the second condition simplifies as follows:

  $$M_1(N_2-M_2) + M_2N_2 \leq (N_2-M_2)N_1 + M_2^2 + \min(M_1M_2, N_2(N_2-M_2)). \tag{B.5}$$

  Here we show that this condition holds: It is easy to see that

  $$(M_2 + M_1 - N_1) \leq M_2 < N_2, \tag{B.6}$$

  therefore we have

  $$(M_2+M_1-N_1)(N_2-M_2) < \min(M_1M_2, N_2(N_2-M_2)). \tag{B.7}$$

  This will simplify to

  $$M_1(N_2-M_2) + M_2N_2 \leq (N_2-M_2)N_1 + M_2^2 + \min(M_1M_2, N_2(N_2-M_2)). \tag{B.8}$$

  Clearly the third condition is satisfied with equality.

- **Case B.II.1**: $M_1 > N_1 > N_2 > M_2$ and $M_2 \leq N_2\frac{M'_1-N_1}{M'_1-N_2}$ with $M'_1 = \min(M_1, N_1 + N_2 - M_2)$:

  In this case we have $d_1 = N_1 - M_2$, $d_2 = M_2$. We choose $T = N_2$ which gives $q = M_2$. The first condition is straightforward. For the second condition we get: $N_2(N_1 - M_2 + M_2) \leq (N_2 - M_2)N_1 + M_2^2 + \min(M_2N_1, (N_2 - M_2)N_2)$. If $M_2N_1 \leq (N_2 - M_2)N_2$ then the inequality is satisfied. We consider the case where $M_2N_1 > (N_2 - M_2)N_2$. Therefore with some simplification, we have to verify the following inequality:

  $N_2^2 \geq M_2(N_1 + N_2 - M_2)$.

  Proof: We have $M_2 \leq N_2\frac{M'_1-N_1}{M'_1-N_2}$ with $M'_1 = min(M_1, N_1 + N_2 - M_2)$ therefore

  $M'_1(N_2 - M_2) \geq N_2(N_1 - M_2) \Rightarrow M_2M'_1 \leq N_2(M'_1 + M_2 - N_1)$. Now if $M'_1 = N_1 + N_2 - M_2$ then the condition is satisfied. If $M'_1 = M_1$ then we have $M_1 \leq N_1 + N_2 - M_2$ which gives

  $$\begin{aligned}
  & M_1 + M_2 \leq N_1 + N_2 \\
  \Rightarrow\ & (N_2 - N_1)(M_1 + M_2) \geq (N_2 - N_1)(N_1 + N_2) \\
  \Rightarrow\ & N_2M_1 + M_2N_2 - N_2^2 \geq N_1M_1 + N_1M_2 - N_1^2 \\
  \Rightarrow\ & \frac{N_2 - M_2}{N_1 - M_2} \geq \frac{M_1 - N_1}{M_1 - N_2} \\
  \Rightarrow\ & N_2\frac{N_2 - M_2}{N_1 - M_2} \geq N_2\frac{M_1 - N_1}{M_1 - N_2} \geq M_2 \\
  \Rightarrow\ & N_2(N_2 - M_2) \geq M_2(N_1 - M_2) \\
  \Rightarrow\ & N_2^2 \geq M_2(N_1 + N_2 - M_2).
  \end{aligned}$$

  For the third condition if we have $M'_1 = M_1$ then $M_2 \leq N_2\frac{M'_1-N_1}{M'_1-N_2}$ gives $N_2(N_1 - M_2) \leq M_1(N_2 - M_2)$ which proves the condition. If we have $M'_1 = N_1 + N_2 - M_2$ then $M_2 \leq N_2\frac{M'_1-N_1}{M'_1-N_2}$ gives $N_2(N_2 - M_2) \geq M_2(N_1 - M_2)$. Therefore

  $$\begin{aligned}
  & M_1 + M_2 \geq N_1 + N_2 \\
  \Rightarrow\ & (M_1 - N_2)(N_2 - M_2) \geq (N_1 - M_2)(N_2 - M_2) \\
  \Rightarrow\ & N_2(N_2 - M_2) + (M_1 - N_2)(N_2 - M_2) \geq M_2(N_1 - M_2) + (N_1 - M_2)(N_2 - M_2) \\
  \Rightarrow\ & M_1(N_2 - M_2) \geq N_2(N_1 - M_2)
  \end{aligned}$$

  which proves the condition.

- **Case B.II.2**: $M_1 > N_1 > N_2 > M_2$ and $M_2 > N_2\frac{M_1-N_1}{M_1-N_2}$ and $M_1 + M_2 \leq N_1 + N_2$:

  In this case we have $d_1 = \frac{M_1}{N_2}(N_2 - M_2)$, $d_2 = M_2$. We choose $T = N_2$ which gives $q = M_2$. The first condition is straightforward. The second condition simplifies as follows:

  $$M_1(N_2 - M_2) + M_2N_2 \leq (N_2 - M_2)N_1 + M_2^2 + \min(N_1M_2, (N_2 - M_2)N_2) \qquad \text{(B.9)}$$

Here we have two possibilities. If $N_1M_2 < (N_2 - M_2)N_2$ then we get

$$(N_2 - M_2)N_1 + M_2^2 + \min(N_1M_2, (N_2 - M_2)N_2) = N_2N_1 - M_2N_1 + M_2^2 + N_1M_2 = M_2^2 + N_1N_2 > N_1N_2. \tag{B.10}$$

From $M_2 > N_2\frac{M_1-N_1}{M_1-N_2}$ we get $N_1N_2 > M_1(N_2 - M_2) + N_2M_2$. Combining this with (B.10) gives the desired condition.

If $N_1M_2 \geq (N_2 - M_2)N_2$ then the condition becomes:

$$M_1N_2 - M_1M_2 + M_2N_2 \leq N_2N_1 - M_2N_1 + M_2^2 + N_2^2 - M_2N_2.$$

Here we show that this condition is satisfied. We have $M_1 + M_2 \leq N_1 + N_2$ and $N_2 > M_2$ therefore we have

$$M_2(N_1 + N_2 - M_1 - M_2) < N_2(N_1 + N_2 - M_1 - M_2) \tag{B.11}$$

which gives the desired condition.

Clearly the third condition is satisfied by equality.

- **Case B.III.1**: $M_1 > N_1 > N_2 > M_2$ and $M_2 > N_2\frac{N_2-M_2}{N_1-M_2}$ and $M_1 + M_2 \geq N_1 + N_2$ and also we have $M_1 \geq N_1 + N_2 - N_2\frac{N_2-M_2}{N_1-M_2}$:

  In this we have two points on the corner of the region. First we look at the point $d_1 = \frac{(N_1+N_2-M_2)(N_2-M_2)}{N_2}$ and $d_2 = M_2$. Here we choose $T = N_2$ which gives $q = M_2$. The first condition is straightforward. From $M_2 > N_2\frac{N_2-M_2}{N_1-M_2}$ we have $N_2(N_2 - M_2) < M_2(N_1 - M_2) < M_2N_1$. Therefore the second condition simplifies to:

  $$(N_1 + N_2 - M_2)(N_2 - M_2) + N_2M_2 \leq (N_2 - M_2)N_1 + M_2^2 + N_2(N_2 - M_2) \tag{B.12}$$

  which is always satisfied by equality.

  Since we have $N_1 + N_2 - M_2 \leq M_1$ therefore the third condition is satisfied.

  The other corner point is $d_1 = N_1 - \frac{N_2^2}{N_1+N_2-M_2}$ and $d_2 = \frac{N_2^2}{N_1+N_2-M_2}$. We choose $T = N_1 + N_2 - M_2$ which gives $q = N_2$. The first condition is straightforward. The second condition becomes:

  $$N_1(N_1 + N_2 - M_2) \leq (N_1 - M_2)N_1 + N_2M_2 + (N_1 - M_2)N_2 \tag{B.13}$$

  which is satisfied by equality. To verify the third condition we have

  $$\begin{aligned} & M_1 \geq N_1 + N_2 - N_2\frac{N_2 - M_2}{N_1 - M_2} \\ \Rightarrow\ & (N_1 - M_2)M_1 \geq N_1(N_1 + N_2 - M_2) - N_2^2 \\ \Rightarrow\ & (T - q)M_1 \geq Td_1. \end{aligned}$$

- **Case B.III.2**: $M_1 > N_1 > N_2 > M_2$ and $M_2 > N_2\frac{N_2-M_2}{N_1-M_2}$ and $M_1 + M_2 \geq N_1 + N_2$ and also we have $M_1 < N_1 + N_2 - N_2\frac{N_2-M_2}{N_1-M_2}$:

  In this case also there are two points. The first point is $d_1 = \frac{M_1(N_1-N_2)}{M_1-N_2}$ and $d_2 = \frac{N_2(M_1-N_1)}{M_1-N_2}$. Therefore we choose $T = M_1 - N_2$ which gives $q = M_1 - N_1$. The first condition is straightforward.

  For the second condition we need to verify the following inequality:

  $$M_1(N_1 - N_2) + N_2(M_1 - N_1) \leq (N_1 - N_2)N_1 + (M_1 - N_1)M_2 + (N_1 - N_2)N_2. \tag{B.14}$$

  Here we show that this condition holds. Clearly we have

  $$(N_1 - N_2)(M_1 + M_2 - N_1 - N_2) \geq 0, \tag{B.15}$$

  therefore

  $$\begin{aligned} &N_2^2 - N_1^2 + M_1N_1 + M_2N_1 \geq M_2N_2 + M_1N_2 \\ &\Rightarrow \ (N_1 + N_2 - M_1)(N_1 - N_2) \geq (N_2 - M_2)(M_1 - N_1) \end{aligned}$$

  which simplifies to the desired condition.

  Clearly the third condition is satisfied by equality.

  The second point is $d_1 = \frac{M_1(N_2-M_2)}{N_1+2N_2-M_1-M_2}$ and $d_2 = \frac{N_2(N_1+N_2-M_1)}{N_1+2N_2-M_1-M_2}$. Therefore we choose $N_1+2N_2-M_1-M_2$ which gives $q = N_1 + N_2 - M_1$. The first condition is straightforward.

  The second condition simplifies to

  $$M_1(N_2 - M_2) + N_2(N_1 + N_2 - M_1) \leq (N_2 - M_2)N_1 + (N_1 + N_2 - M_1)M_2 + (N_2 - M_2)N_2$$

  which is satisfied by equality.

  Clearly the third condition is satisfied by equality.

B.2 Proof of Theorem 7

In order to prove the theorem we need to verify the conditions $\bar{\text{C}}$.I and $\bar{\text{C}}$.III for group G_2 which consists of the case A.I.3. We first prove $\bar{\text{C}}$.I :

Here we show that in the case A.I.3 we have $d_1+d_2 > N_2$ and $d_1+d_2 > N_1$. Using the fact that $M_2 > N_2$ and $M_1 > N_2$ and knowing that $M'_i = \min(M_i, N_1 + N_2)$ we have

$$\begin{aligned} &N_1(M'_1 - N_2)(M'_2 - N_2) > 0 \Rightarrow M'_1N_1M'_2 - M'_1N_1N_2 - M'_2N_1N_2 > -N_1N_2^2 \\ &\Rightarrow M'_1N_1M'_2 - M'_1N_1N_2 - M'_2N_1N_2 + M'_2M'_1N_2 > M'_2M'_1N_2 - N_1N_2^2 \\ &\Rightarrow d_1^* + d_2^* > TN_2 \Rightarrow d_1 + d_2 > N_2. \end{aligned}$$

For the second part, since we have $M_2 > N_1$ this gives

$$N_2(M'_1 - N_1)(M'_2 - N_1) > 0 \Rightarrow M'_1 N_2 M'_2 - M'_1 N_1 N_2 - M'_2 N_1 N_2 > -N_1^2 N_2$$
$$\Rightarrow M'_1 N_2 M'_2 - M'_1 N_1 N_2 - M'_2 N_1 N_2 + M'_1 N_1 M'_2 > M'_1 N_1 M'_2 - N_1^2 N_2$$
$$\Rightarrow d_1^* + d_2^* > T N_1 \Rightarrow d_1 + d_2 > N_1.$$

The proof of $\bar{\text{C}}$.III is straightforward :
$d_j^* = N_j M'_j (M'_i - N_i) \leq N_j M_j (M'_i - N_i) = (T - q_i) M_j.$

C

C.1 Calculating the Power of the Interference Terms

Since $\sqrt{1-\rho_0^2}\mathbf{E}_{ij} = \mathbf{H}_{ij} - \rho_0\hat{\mathbf{H}}_{ij}$ we have

$$I_{i,q} = \sqrt{1-\rho_0^2} \sum_{\substack{1\leq l\leq d \\ l\neq q}} \hat{\mathbf{u}}_{i,q}^{\mathrm{H}} \mathbf{E}_{ii} \hat{\mathbf{v}}_{i,l} \mathbf{x}_i(l), \tag{C.1}$$

$$I'_{i,q} = \sqrt{1-\rho_0^2} \sum_{\substack{1\leq j\leq K \\ j\neq i}} \hat{\mathbf{u}}_{i,q}^{\mathrm{H}} \mathbf{E}_{ij} \hat{\mathbf{V}}_{j} \mathbf{x}_j. \tag{C.2}$$

Since the entries of $\mathbf{E}_{ij}$ are Gaussian i.i.d. random variables, their distribution is invariant by multiplication with independent truncated unitary matrices. Therefore we use $e_{iql} \triangleq \hat{\mathbf{u}}_{i,q}^{\mathrm{H}} \mathbf{E}_{ii} \hat{\mathbf{v}}_{i,l}$ and $\mathbf{e}_{iqj} \triangleq \hat{\mathbf{u}}_{i,q}^{\mathrm{H}} \mathbf{E}_{ij} \hat{\mathbf{V}}_{j}$ in the expression of $I_{i,q}$ and $I'_{i,q}$ respectively knowing that their entries have the same distribution as those of $\mathbf{E}_{ij}$. This gives the following

$$\begin{aligned} \mathrm{E}\{|I_{i,q}|^2\} =& (1-\rho_0^2)\mathrm{E}\left\{ \sum_{\substack{1\leq l\leq d \\ l\neq q}} |e_{iql}\mathbf{x}_i(l)|^2 \right\} \\ =& (1-\rho_0^2) \sum_{\substack{1\leq l\leq d \\ l\neq q}} \mathrm{E}\{|e_{iql}|^2\}\mathrm{E}\{|\mathbf{x}_i(l)|^2\} \\ =& \Delta_{ii}(1-\rho_0^2) \sum_{\substack{1\leq l\leq d \\ l\neq q}} \bar{P}_i(l). \end{aligned} \tag{C.3}$$

Similarly for $I'_{i,q}$ we get

$$\mathrm{E}\{|I'_{i,q}|^2\} = (1-\rho_0^2) \sum_{\substack{1\leq j\leq K \\ j\neq i}} \Delta_{ij} \sum_{1\leq l\leq d} \bar{P}_i(l). \tag{C.4}$$

C.2 Calculating the Correlation Coefficient ρ

By definition of correlation we have

$$\begin{aligned}\rho &= \frac{\mathrm{E}\{\gamma_i^q\hat{\gamma}_i^q\} - \mathrm{E}\{\gamma_i^q\}\mathrm{E}\{\hat{\gamma}_i^q\}}{\sqrt{\mathrm{var}(\gamma_i^q)\mathrm{var}(\hat{\gamma}_i^q)}} \\ &= \frac{\mathrm{E}\{|G_i^q|^2|\hat{G}_i^q|^2\} - \mathrm{E}\{|G_i^q|^2\}\mathrm{E}\{|\hat{G}_i^q|^2\}}{\sqrt{\mathrm{var}(|G_i^q|^2)\mathrm{var}(|\hat{G}_i^q|^2)}}.\end{aligned} \tag{C.5}$$

To compute ρ we need to find $\mathrm{E}\{|G_i^q|^2|\hat{G}_i^q|^2\}$ which is calculated as follows

$$\mathrm{E}\{|G_i^q|^2|\hat{G}_i^q|^2\} = \mathrm{E}_{\hat{\mathbf{H}}_{ij}}\{|\hat{G}_i^q|^2\mathrm{E}_{\mathbf{H}_{ij}|\hat{\mathbf{H}}_{ij}}\{|G_i^q|^2\}\}. \tag{C.6}$$

The conditional term can be written as

$$\begin{aligned}\mathrm{E}_{\mathbf{H}_{ij}|\hat{\mathbf{H}}_{ij}}\{|G_i^q|^2\} &= \sum_{m=1}^{N_r}\sum_{n=1}^{N_t}\mathrm{E}_{\mathbf{H}_{ij}|\hat{\mathbf{H}}_{ij}}\{|\mathbf{H}_{ii}(m,n)|^2\}|\hat{\mathbf{u}}_{i,q}(m)^{\mathrm{H}}|^2|\hat{\mathbf{v}}_{i,q}(n)|^2 \\ &= \sum_{m=1}^{N_r}\sum_{n=1}^{N_t}((1-\rho_0^2)\Delta_{ii} + \rho_0^2|\hat{\mathbf{H}}_{ii}(m,n)|^2)|\hat{\mathbf{u}}_{i,q}(m)^{\mathrm{H}}|^2|\hat{\mathbf{v}}_{i,q}(n)|^2 \\ &= (1-\rho_0^2)\Delta_{ii} + \rho_0^2|\hat{G}_i^q|^2.\end{aligned} \tag{C.7}$$

For an exponential-distributed random variable Z we have $\mathrm{E}\{Z^2\} = \mathrm{E}\{Z\} + (\mathrm{E}\{Z\})^2$, therefore

$$\begin{aligned}\mathrm{E}\{|G_i^q|^2|\hat{G}_i^q|^2\} &= \mathrm{E}_{\hat{\mathbf{H}}_{ij}}\{|\hat{G}_i^q|^2(1-\rho_0^2)\Delta_{ii} + \rho_0^2|\hat{G}_i^q|^4\} \\ &= (1-\rho_0^2)\Delta_{ii}^2 + \rho_0^2(\Delta_{ii} + \Delta_{ii}^2) \\ &= \Delta_{ii}^2 + \rho_0^2\Delta_{ii}.\end{aligned} \tag{C.8}$$

Therefore (C.5) simplifies to $\rho = \rho_0^2$.

C.3 Proof of Lemma 13

Letting $S_m = \frac{A_m}{\Psi(\hat{\gamma})A'_m(1-\rho_0^2)\Gamma+1}$ and simplifying condition $(C'2)$ using (6.2) and (6.23) we have

$$\begin{aligned}\mathrm{E}\{p_e(\Psi(\hat{\gamma})\gamma, \Phi(\hat{\gamma}))|\hat{\gamma}\} \le B_0 \;&\Leftrightarrow \int_0^\infty A_m \mathrm{exp}\left\{-A'_m\gamma\Psi(\hat{\gamma})\right\} f_{\gamma|\hat{\gamma}}(\gamma|\hat{\gamma})d\gamma \le B_0 \\ &\Leftrightarrow S_m \mathrm{exp}\left\{\frac{-\rho_0^2\hat{\gamma}}{(1-\rho_0^2)\hat{\Gamma}}(1-S_m)\right\} \le B_0\end{aligned} \tag{C.9}$$

Since $S_m \le A_m$, to satisfy the BER condition it is sufficient to have

$$A_m \mathrm{exp}\left\{\frac{-\rho_0^2\hat{\gamma}}{(1-\rho_0^2)\hat{\Gamma}}(1-S_m)\right\} \le B_0 \;\Leftrightarrow\; \frac{\frac{-1}{A'_m}\ln(\frac{B_0}{A_m})}{\rho_0^2\frac{\Gamma}{\hat{\Gamma}}\hat{\gamma} + (1-\rho_0^2)\Gamma\ln(\frac{B_0}{A_m})} \le \Psi(\hat{\gamma}). \tag{C.10}$$

Since (6.26) implies (C.10), the lemma is proved.

C.4 Calculating the Gradient of Rate

Expanding $\tilde{\delta}_i^+$ in (6.51) using standard matrix inversion formulas, we obtain

$$\tilde{\delta}_i^+ = \frac{1}{N}\sum_{j=1}^{K} \mathrm{tr}\left(\frac{\mathbf{Q}_j \mathbf{Z}_{ij}(\delta_i^+)\mathbf{\Psi}_i^+}{\bar{\sigma}^2}\right)$$

where

$$\mathbf{\Psi}_i^+ = \left(\mathbf{I}_{N_j} - \mathbf{Q}_j^{\frac{1}{2}}\bar{\mathbf{H}}_{ij}^{\mathrm{H}}(\mathbf{\Delta}_i^+)^{-1}\bar{\mathbf{H}}_{ij}\mathbf{Q}_j^{\frac{1}{2}}\frac{\mathbf{Z}_{ij}(\delta_i^+)}{\bar{\sigma}^2}\right) \tag{C.11}$$

and

$$\mathbf{\Delta}_i^+ = (1+\tilde{\delta}_i^+)\mathbf{I}_{M_i} + \sum_{j=1}^{K}\bar{\mathbf{H}}_{ij}\mathbf{Q}_j^{\frac{1}{2}}\frac{\mathbf{Z}_{ij}(\delta_i^+)}{\bar{\sigma}^2}\mathbf{Q}_j^{\frac{1}{2}}\bar{\mathbf{H}}_{ij}^{\mathrm{H}}. \tag{C.12}$$

Using the fact that $\mathbf{Z}_{ij}(x)$ and $\mathbf{Q}_j^{\frac{1}{2}}$ commute, (6.54) reads

$$\bar{R}_i^+ = \log\left|\mathbf{F}_i(\delta_i^+)\right| - \sum_{j=1}^{K}\log\left|\mathbf{Z}_{ij}(\delta_i^+)\right| - N\bar{\sigma}^2\delta_i^+\tilde{\delta}_i^+ \tag{C.13}$$

in which

$$\mathbf{F}_i(x) = (1+\tilde{x})\mathbf{I}_{M_i} + \frac{1}{\bar{\sigma}^2}\sum_{j=1}^{K}\bar{\mathbf{H}}_{ij}\mathbf{Z}_{ij}(x)\mathbf{Q}_j\bar{\mathbf{H}}_{ij}^{\mathrm{H}}. \tag{C.14}$$

Defining $d_n\mathbf{X} = \frac{\partial \mathbf{X}}{\partial \mathbf{V}_n^*}d\mathbf{V}_n^*$, the differential of $\bar{R}_i^+$ w.r.t. $\mathbf{V}_n$

$$\begin{aligned} d_n\bar{R}_i^+ &= \mathrm{tr}\left((\mathbf{F}_i(\delta_i^+))^{-1}d_n\mathbf{F}_i(\delta_i^+) - (\mathbf{Z}_{in}(\delta_i^+))^{-1}d_n(\mathbf{Z}_{in}(\delta_i^+))\right) \\ &= \frac{1}{\bar{\sigma}^2}\mathrm{tr}\left(\bar{\mathbf{H}}_{in}^{\mathrm{H}}(\mathbf{F}_i(\delta_i^+))^{-1}\bar{\mathbf{H}}_{in}d_n\left(\mathbf{Z}_{in}(\delta_i^+)\mathbf{Q}_n\right)\right) - \mathrm{tr}\left((\mathbf{Z}_{in}(\delta_i^+))^{-1}d_n(\mathbf{Z}_{in}(\delta_i^+))\right) \\ &= \mathrm{tr}\left(\mathbf{\Omega}_{in}^+ d_n\mathbf{Q}_n\right) \end{aligned} \tag{C.15}$$

where

$$\mathbf{\Omega}_{in}^+ = \mathbf{Z}_{in}(\delta_i^+)\left(\frac{1}{\bar{\sigma}^2}\bar{\mathbf{H}}_{in}^{\mathrm{H}}(\mathbf{F}_i(\delta_i^+))^{-1}\bar{\mathbf{H}}_{in}\mathbf{Z}_{in}(\delta_i^+) + \delta_i^+\sigma_{in}^2\mathbf{I}_{N_n}\right). \tag{C.16}$$

and the last equality is resulted by using the facts that $d(\mathbf{XY}) = d(\mathbf{X})\mathbf{Y} + \mathbf{X}d(\mathbf{Y})$, $d(\mathbf{X}^{-1}) = -\mathbf{X}^{-1}d(\mathbf{X})\mathbf{X}^{-1}$ and $\mathrm{tr}(\mathbf{AB}) = \mathrm{tr}(\mathbf{BA})$.

Considering the normalization factors λ_j, note that the power constraint is always satisfied. In other words the optimization finds the precoding matrices $\mathbf{V}_j$ such that the normalized version of the corresponding covariance matrices $\mathbf{Q}_j = \lambda_j\mathbf{V}_j\mathbf{V}_j^{\mathrm{H}}$ will maximize the expected sum rate. It can be shown that $d_n\lambda_n = -\frac{\lambda_n^2}{P_n}\mathrm{tr}\left(\mathbf{V}_n d_n\mathbf{V}_n^{\mathrm{H}}\right)$, therefore the differential of $\mathbf{Q}_n$ can be evaluated as

$$d_n\mathbf{Q}_n = d_n\left(\lambda_n\mathbf{V}_n\mathbf{V}_n^{\mathrm{H}}\right) = -\frac{\lambda_n^2}{P_n}\mathrm{tr}\left(\mathbf{V}_n d_n\mathbf{V}_n^{\mathrm{H}}\right)\mathbf{V}_n\mathbf{V}_n^{\mathrm{H}} + \lambda_n\mathbf{V}_n d_n\mathbf{V}_n^{\mathrm{H}}. \tag{C.17}$$

Inserting (C.17) into (C.15) yields

$$\begin{aligned} d_n \bar{R}_i^+ &= -\frac{\lambda_n^2}{P_n} \mathrm{tr}\left(\mathbf{\Omega}_{in}^+ \mathbf{V}_n \mathbf{V}_n^{\mathrm{H}}\right) \mathrm{tr}\left(\mathbf{V}_n d_n \mathbf{V}_n^{\mathrm{H}}\right) + \lambda_n \mathrm{tr}\left(\mathbf{\Omega}_{in}^+ \mathbf{V}_n d_n \mathbf{V}_n^{\mathrm{H}}\right) \\ &= \lambda_n \mathrm{tr}\left(\left[\mathbf{\Omega}_{in}^+ \mathbf{V}_n - \frac{\mathrm{tr}\left(\mathbf{\Omega}_{in}^+ \mathbf{V}_n \mathbf{V}_n^{\mathrm{H}}\right)}{\mathrm{tr}\left(\mathbf{V}_n \mathbf{V}_n^{\mathrm{H}}\right)} \mathbf{V}_n \right]^{\mathrm{T}} d_n \mathbf{V}_n^* \right). \end{aligned} \tag{C.18}$$

C.5 Proof of Lemma 14

From the fact that, for $\mathbf{A}, \mathbf{B} \succeq 0$, $\frac{1}{N}\mathrm{tr}\left(\mathbf{A}(\mathbf{I}_N + \mathbf{B})^{-1}\right) \leq \|\mathbf{A}\|$, we have $g(\mathbf{Q}, \delta, \tilde{\delta}) \leq (M/N)\sigma^{-2}(1+\tilde{\delta})^{-1}$ and $\tilde{g}(\mathbf{Q}, \delta, \tilde{\delta}) \leq \sigma^{-2}\|\mathbf{Q}\tilde{\mathbf{C}}\| \triangleq U$. Define now $\hat{\delta} = \frac{U}{\tilde{\delta}} - 1$ which is one-to-one with $\tilde{\delta}$ and therefore we can equivalently discuss about the solution of the following system of equations obtained by a fixed-point algorithm similar to Algorithm 3,

$$\begin{cases} \delta &= h(\mathbf{Q}, \delta, \hat{\delta}) = g(\mathbf{Q}, \delta, \frac{U}{1+\hat{\delta}}), \\ \hat{\delta} &= \hat{h}(\mathbf{Q}, \delta, \hat{\delta}) = \frac{U}{\tilde{g}(\mathbf{Q}, \delta, \frac{U}{1+\hat{\delta}})} - 1. \end{cases} \tag{C.19}$$

To prove convergence of the fixed-point algorithm to a unique positive solution, we use a result on *standard interference functions*.

Definition 2 ([116]). *A function* $\mathbf{h}(\mathbf{x}) = (h_1(\mathbf{x}), ..., h_n(\mathbf{x}))$ *in which* $h_i : R_+^n \to R_+,\ i = 1, ..., K$ *is a standard interference function if the following assumptions hold for all* $i \in \{1, ..., n\}$*:*

I. Positivity*:* $h_i(\mathbf{x}) > 0$ *for all* $\mathbf{x} \geq 0$

II. Monotonicity*: if* $\mathbf{x}' \geq \mathbf{x}$*, then* $h_i(\mathbf{x}') \geq h_i(\mathbf{x})$

III. Scalability*: for* $\alpha > 1$, $h_i(\alpha\mathbf{x}) < \alpha h_i(\mathbf{x})$.

Also a vector $\mathbf{x}$ is said to be a feasible point if $\mathbf{h}(\mathbf{x}) < \mathbf{x}$ where the inequality is element-wise.

Theorem 9 ([116]). *If* $\mathbf{h}$ *is a standard interference function, and there exists a feasible* $\mathbf{x}$*, then the fixed-point equation* $\mathbf{h}(\mathbf{x}) = \mathbf{x}$ *has a unique solution* $\mathbf{x}^*$*, given as the limit* $\mathbf{x}^* = \lim_{t\to\infty} \mathbf{x}^t$*, where, for all* $t \geq 0$*,*

$$\mathbf{x}^{t+1} = \mathbf{h}(\mathbf{x}^t)$$

and $\mathbf{x}^0 > 0$ *is arbitrary.*

In our setting, we define $\mathbf{x} = (\delta, \hat{\delta})$ and $\mathbf{h}(\mathbf{x}) = (h(\delta, \hat{\delta}), \hat{h}(\delta, \hat{\delta}))$. Then, from Theorem 9, we only need to prove that $\mathbf{h}$ is a standard interference function that admits a feasible point. This implies the convergence of Algorithm 3 (considering the one-to-one map between $\tilde{\delta}$ and $\hat{\delta}$ at each iteration).

A feasible point can always be found since the functions h and $\hat{h}$ are bounded for every positive $(\delta, \hat{\delta})$. It is also easy to show that the positivity assumption always holds. For monotonicity, we have to show that

$\delta' \geq \delta$ and $\hat{\delta}' \geq \hat{\delta}$ results in $h(\delta', \hat{\delta}') \geq h(\delta, \hat{\delta})$ and $\hat{h}(\delta', \hat{\delta}') \geq \hat{h}(\delta, \hat{\delta})$. For $\delta' \geq \delta$, we get $\mathrm{tr}\left(\delta' \mathbf{Q}^{\frac{1}{2}} \tilde{\mathbf{C}} \mathbf{Q}^{\frac{1}{2}}\right) \geq \mathrm{tr}\left(\delta \mathbf{Q}^{\frac{1}{2}} \tilde{\mathbf{C}} \mathbf{Q}^{\frac{1}{2}}\right)$. Therefore we have

$$\mathrm{tr}\Big(\mathbf{I}_N + \delta' \mathbf{Q}^{\frac{1}{2}} \tilde{\mathbf{C}} \mathbf{Q}^{\frac{1}{2}}\Big) \geq \mathrm{tr}\Big(\mathbf{I}_N + \delta \mathbf{Q}^{\frac{1}{2}} \tilde{\mathbf{C}} \mathbf{Q}^{\frac{1}{2}}\Big). \tag{C.20}$$

Therefore using this relation

$$\mathrm{tr}(\mathbf{A}^{-1} - \mathbf{B}^{-1}) \geq 0 \;\Leftrightarrow\; \mathbf{B} \succeq \mathbf{A} \tag{C.21}$$

it is clear that

$$\Big(\mathbf{I}_N + \delta \mathbf{Q}^{\frac{1}{2}} \tilde{\mathbf{C}} \mathbf{Q}^{\frac{1}{2}}\Big)^{-1} \succeq \Big(\mathbf{I}_N + \delta' \mathbf{Q}^{\frac{1}{2}} \tilde{\mathbf{C}} \mathbf{Q}^{\frac{1}{2}}\Big)^{-1}. \tag{C.22}$$

Also from $\hat{\delta}' \geq \hat{\delta}$, we have

$$\sigma^2\Big(1 + \frac{U}{1+\hat{\delta}}\Big)\mathbf{I}_M \succeq \sigma^2\Big(1 + \frac{U}{1+\hat{\delta}'}\Big)\mathbf{I}_M. \tag{C.23}$$

Multiplying both sides of (C.22) by $\bar{\mathbf{H}}\mathbf{Q}^{\frac{1}{2}}$ and its Hermitian from left and right respectively, adding the result to (C.23), and using the equivalence in (C.21) results in $h(\delta', \hat{\delta}') \geq h(\delta, \hat{\delta})$ in which from (C.19), $h(\delta, \hat{\delta})$ is written as

$$h(\delta, \hat{\delta}) = \frac{1}{N}\mathrm{tr}\left(\sigma^2\Big(1 + \frac{U}{1+\hat{\delta}}\Big)\mathbf{I}_M + \bar{\mathbf{H}}\mathbf{Q}^{\frac{1}{2}}\mathbf{G}(\delta)\mathbf{Q}^{\frac{1}{2}}\bar{\mathbf{H}}^{\mathrm{H}}\right)^{-1}. \tag{C.24}$$

Using the same line of arguments, monotonicity of $\hat{h}$ is then proved. Here we prove the scalability of h. We need to show that for $\alpha > 1$, $h(\alpha\delta, \alpha\hat{\delta}) < \alpha h(\delta, \hat{\delta})$ (and similarly for $\hat{h}$). Since $\alpha > 1$, we have $\alpha \mathrm{tr}\Big(\mathbf{I}_N + \delta \mathbf{Q}^{\frac{1}{2}} \tilde{\mathbf{C}} \mathbf{Q}^{\frac{1}{2}}\Big) > \mathrm{tr}\Big(\mathbf{I}_N + \alpha\delta \mathbf{Q}^{\frac{1}{2}} \tilde{\mathbf{C}} \mathbf{Q}^{\frac{1}{2}}\Big)$. Therefore using (C.21) we have

$$\mathbf{G}(\alpha\delta) \succ \frac{1}{\alpha}\mathbf{G}(\delta). \tag{C.25}$$

Also we can conclude that

$$\sigma^2\Big(1 + \frac{U}{1+\alpha\hat{\delta}}\Big)\mathbf{I}_M \succ \frac{\sigma^2}{\alpha}\Big(1 + \frac{U}{1+\hat{\delta}}\Big)\mathbf{I}_M. \tag{C.26}$$

Again multiplying both sides of (C.25) by $\bar{\mathbf{H}}\mathbf{Q}^{\frac{1}{2}}$ and its Hermitian from left and right respectively, adding the result to (C.26), and using (C.21) results in $h(\alpha\delta, \alpha\hat{\delta}) < \alpha h(\delta, \hat{\delta})$.

Bibliography

[1] C. E. Shannon, "Two-way communication channels," in *Proc. 4th Berkeley Symp. on Mathematical Statistics and Probability*, vol. 1, pp. 611–644, 1961.

[2] T. S. Han and K. Kobayashi, "A new achievable rate region for the interference channel," *IEEE Trans. Inf. Theory*, vol. IT-27, 1981.

[3] R. H. Etkin, D. N. C. Tse, and H. Wang, "Gaussian interference channel capacity to within one bit," *IEEE Trans. Inf. Theory*, vol. 54, pp. 5534–5562, Dec. 2008.

[4] A. B. Carleial, "A case where interference does not reduce capacity," *IEEE Trans. Inf. Theory*, vol. IT-21, pp. 569–570, Sep. 1975.

[5] H. Sato, "The capacity of the Gaussian interference channel under strong interference," *IEEE Trans. Inf. Theory*, vol. IT-27, pp. 786–788, Nov. 1981.

[6] M. C. A. El-Gamal, "The capacity region of a class of deterministic interference channels," *IEEE Trans. Inf. Theory*, vol. 28, pp. 343–346, Mar. 1982.

[7] J. Kim, S. Moon, S. Lee, and I. Lee, "A new channel quantization strategy for MIMO interference alignment with limited feedback," *IEEE Trans. Wireless Commun.*, vol. 11, pp. 358–366, Jan. 2012.

[8] N. Jindal, "MIMO broadcast channels with finite-rate feedback," vol. 52, pp. 5045–5060, Nov. 2006.

[9] M. A. Maddah-Ali and D. Tse, "Completely stale transmitter channel state information is still very useful," *IEEE Trans. Inf. Theory*, vol. 58, pp. 4418–4431, Jul. 2012.

[10] C. S. Vaze and M. K. Varanasi, "Degrees of freedom region for the two-user MIMO broadcast channel with delayed CSIT," in *Proc. IEEE Int. Symp. Information Theory (ISIT), Russia*, Aug. 2011.

[11] C. S. Vaze and M. K. Varanasi, "The degrees of freedom region and interference alignment for the MIMO interference channel with delayed CSIT," *IEEE Journal of Selected Topics in Signal Processing*, vol. 58, pp. 4396–4417, Jul. 2012.

[12] K. Gomadam, V. R. Cadambe, and S. A. Jafar, "A distributed numerical approach to interference alignment and applications to wireless interference networks," vol. 57, pp. 3309–3322, June 2011.

[13] S. M. Alamouti, "A simple transmit diversity technique for wireless communications," *IEEE J. Selet. Areas Commun*, vol. 16, pp. 1451–1458, Oct. 1998.

[14] V. Cadambe and S. Jafar, "Interference alignment and the degrees of freedom of the K user interference channel," *IEEE Trans. Inf. Theory*, vol. 54, pp. 3425–3441, Aug. 2008.

[15] T. M. Cover and J. A. Thomas, *Elements of Information Theory*. New York: Wiley, 1991.

[16] E. Biglieri, J. Proakis, and S. Shamai, "Fading channels: Information-theoretic and communications aspects," *IEEE Trans. Inf. Theory*, vol. 44, pp. 2619–2692, Oct. 1998.

[17] W. C. Y. Lee, "Estimate of channel capacity in rayleigh fading environment," *IEEE Trans. Vehicular Technology*, vol. 39, pp. 187–189, Aug. 1990.

[18] C. G. Gunther, "Comment on estimate of channel capacity in rayleigh fading environment," *IEEE Trans. Vehicular Technology*, vol. 45, pp. 401–403, May. 1996.

[19] M.-S. Alouini and A. J. Goldsmith, "Capacity of rayleigh fading channels under different adaptive transmission and diversity-combining techniques," *IEEE Trans. Vehicular Technology*, vol. 48, pp. 1165–1181, Jul. 1999.

[20] E. Telatar, "Capacity of multi-antenna gaussian channels," *European Transactions on Telecommunications*, vol. 10, pp. 585–595, Nov. 1999.

[21] G. J. Foschini and M. J. Gans, "On limits of wireless communications in a fading environment when using multiple antennas," *Wireless Personal Communications*, vol. 6, pp. 311–335, Mar. 1998.

[22] L. Zheng and D. Tse, "Diversity and multiplexing: a fundamental tradeoff in multiple-antenna channels," *IEEE Trans. Inf. Theory*, vol. 49, pp. 1073–1096, May. 2003.

[23] V. Tarokh, N. Seshadri, and A. R. Calderbank, "Space-time codes for high data rate wireless communication: Performance criterion and code construction," *IEEE Trans. Inf. Theory*, vol. 44, pp. 744–765, Mar. 1998.

[24] H. J. V. Tarokh and A. R. Calderbank, "Space-time block codes from orthogonal designs," *IEEE Trans. Inf. Theory*, vol. 45, pp. 1456–1467, Jul. 1999.

[25] G. J. Foschini, "Layered space-time architecture for wireless communication in a fading environment when using multi-element antennas," *Bell Labs Tech. Journal*, pp. 41–59, Autumn 1996.

[26] D. Tse, P. Viswanath, and L. Zheng, "Diversity-multiplexing tradeoff in multiple-access channels," *IEEE Trans. Inf. Theory*, vol. 50, 2004.

[27] W. Yu and J. Cioffi, "Sum capacity of gaussian vector broadcast channels," *IEEE Trans. Inf. Theory*, vol. 50, 2004.

[28] P. Viswanath and D. Tse, "Sum capacity of the vector gaussian broadcast channel and uplink-downlink duality," *IEEE Trans. Inf. Theory*, 2003.

[29] S. Vishwanath, N. Jindal, and A. Goldsmith, "Duality, achievable rates, and sum-rate capacity of MIMO broadcast channels," *IEEE Trans. Inf. Theory*, 2003.

[30] S. Jafar and M. Fakhereddin, "Degrees of freedom for the MIMO interference channel," in *Proc. IEEE Int. Symp. Information Theory (ISIT)*, 2006.

[31] D. Gesbert, M. Kountouris, R. Heath, C.-B. Chae, and T. Salzer, "Shifting the MIMO paradigm," *IEEE Signal Processing Magazine*, vol. 24, pp. 36–46, Sep. 2007.

[32] H. Holma and A. Toskala, *HSDPA/HSUPA for UMTS*. Wiley, 2007.

[33] S. Sesia, I. Toufik, and M. Baker, *LTE - The UMTS Long Term Evolution*. Wiley, 2011.

[34] A. B. Carleial, "A case where interference does not reduce capacity," *(Corresp.), IEEE Trans. Inf. Theory*, vol. IT-21, 1975.

[35] H. Sato, "On degraded gaussian two-user channels," *IEEE Trans. Inf. Theory*, vol. IT-24, 1978.

[36] G. Kramer, "Outer bounds on the capacity of gaussian interference channels," *IEEE Trans. Inf. Theory*, vol. 50, 2004.

[37] M. Maddah-Ali, A. Motahari, and A. Khandani, "Signaling over MIMO multi-base systems: combination of multi-access and broadcast schemes," in *Proc. IEEE Int. Symp. Information Theory (ISIT), Seattle, WA, USA*, pp. 2104–2108, July. 2006.

[38] C. M. Yetis, T. Gou, S. A. Jafar, and A. H. Kayran, "On feasibility of interference alignment in MIMO interference networks," vol. 58, Sept. 2010.

[39] M. Razaviyayn, G. Lyubeznik, and Z.-Q. Luo, "On the degrees of freedom achievable through interference alignment in a MIMO interference channel," *IEEE Trans. Signal Processing*, vol. 60, pp. 812–821, Feb. 2012.

[40] G. Bresler, D. Cartwright, and D. Tse, "Settling the feasibility of interference alignment for the MIMO interference channel: the symmetric square case," Apr. 2011. preprint, `http://arxiv.org/abs/1104.0888`.

[41] J. Thukral and H. Bölcskei, "Interference alignment with limited feedback," in *Proc. IEEE Int. Symp. Inf. Theory (ISIT), Seoul, Korea*, Jun. 2009.

[42] R. Tresch and M. Guillaud, "Cellular interference alignment with imperfect channel knowledge," in *Proc. IEEE International Conference on Communications (ICC), Dresden, Germany*, June 2009.

[43] M. Taki, M. Rezaee, and M. Guillaud, "Adaptive modulation and coding for interference alignment with imperfect CSIT," *Submitted to IEEE Trans. Wireless Comm.*

[44] B. Nosrat-Makouei, J. Andrews, and R. Heath, "A simple SINR characterization for linear interference alignment over uncertain MIMO channels," in *Proc. IEEE Int. Symp. Inf. Theory (ISIT), Austin, TX*, June. 2010.

[45] T. Gou and S. A. Jafar, "Degrees of freedom of the K user $M \times N$ MIMO interference channel," *IEEE Trans. Information Theory*, vol. 56, pp. 6040–6057, Dec. 2010.

[46] J. Thukral and H. Bölcskei, "Interference alignment with limited feedback," in *Proc. International Symposium on Information Theory (ISIT)*, (Seoul, Korea), June 2009.

[47] R. T. Krishnamachari and M. K. Varanasi, "Interference alignment under limited feedback for MIMO interference channels," in *Proc. IEEE Int. Symp. Information Theory (ISIT), Austin, TX*, Jun. 2010.

[48] H. Sung, S. Park, K. Lee, and I.Lee, "Linear precoder designs for K-user interference channels," *IEEE Trans. on Wireless Communication*, vol. 9, pp. 291–301, Jan. 2010.

[49] S. H. Park, H. Park, Y. D. Kim, and I. Lee, "Regularized interference alignment based on weighted sum-MSE criterion for MIMO interference channels," in *Proc. IEEE Int. Conf. Commun., Cape Town, South Africa*, May 2010.

[50] I. Santamaria, O. Gonzales, R. W. Heath, Jr., and S. W. Peters, "Maximum sum-rate interference alignment algorithms for MIMO channels," in *Proc. IEEE Global Telecommunications Conference (Globecom), Miami, Florida USA*, Dec. 2010.

[51] Q. Shi, M. Razaviyayn, Z. Luo, and C. He, "An iteratively weighted MMSE approach to distributed sum-utility maximization for a MIMO interfering broadcast channel," *IEEE Trans. Signal Processing*, vol. 59, pp. 4331–4340, Sep. 2011.

[52] J. Shin and J. Moon, "Weighted-sum-rate-maximizing linear transceiver filters for the K-user MIMO interference channel," *IEEE Trans. Communications*, vol. 60, pp. 2776–2783, Oct. 2012.

[53] Z. Ho and D. Gesbert, "Balancing egoism and altruism on interference channel: The MIMO case," in *Proc. IEEE International Conference on Communications (ICC), Cape Town, South Africa*, May 2010.

[54] C. M. Yetis, T. Gou, S. A. Jafar, and A. H. Kayran, "On feasibility of interference alignment in MIMO interference networks," *IEEE Trans. Signal Processing*, vol. 58, pp. 4771–4782, Sep. 2010.

[55] D. Love and J. R. Heath, "Limited feedback unitary precoding for spatial multiplexing systems," *IEEE Trans. Inf. Theory*, vol. 51, no. 8, pp. 2967–2976, 2005.

[56] T. Inoue and J. R. Heath, "Grassmannian predictive coding for limited feedback multiuser MIMO systems," in *Proc. IEEE Int. Conf. on Acoustics, Speech and Signal Processing*, 2011.

[57] I. Kammoun and J. C. Belfiore, "A new family of Grassmann space-time codes for non-coherent MIMO systems," *IEEE Communications Letters*, vol. 7, no. 11, pp. 528–530, 2003.

[58] Z. Utkovski, P.-C. Chen, and J. Lindner, "Some geometric methods for construction of space-time codes in Grassmann manifolds," in *Proc. 46th Annual Allerton Conference on Communication, Control, and Computing*, 2008.

[59] M. Rezaee, M. Guillaud, and F. Lindqvist, "CSIT sharing over finite capacity backhaul for spatial interference alignment," in *Proc. International Symposium on Information Theory (ISIT)*, June 2013.

[60] W. Dai, Y. Liu, and B. Rider, "Quantization bounds on Grassmann manifolds and applications to MIMO communications," *IEEE Trans. Inf. Theory*, vol. 54, pp. 1108–1123, Mar. 2008.

[61] C. Suh and D. Tse, "Interference alignment for cellular networks," in *Proc. Allerton Conference on Communications, Control and Computing, Monticello, IL, USA*, Sept. 2008.

[62] J. Sun, Y. Liu, and G. Zhu, "On degrees of freedom of the cellular network," *SCIENCE CHINA Information Sciences*, vol. 53, pp. 1034–1043, 2010.

[63] C. Suh, M. Ho, and D. Tse, "Downlink interference alignment," vol. 59, pp. 2616–2626, Sept. 2011.

[64] S.-H. Park and I. Lee, "Analysis of degrees of freedom of interfering MISO broadcast channels," in *Proc. IEEE Global Telecommunications Conference (Globecom)*, Dec. 2009.

[65] M. Guillaud and D. Gesbert, "Interference alignment in partially connected interfering multiple-access and broadcast channels," in *Proc. IEEE Global Telecommunications Conference (GLOBECOM), Houston, TX*, Dec. 2011.

[66] N. Lee, D. Park, and Y.-D. Kim, "Degrees of freedom on the K-user MIMO interference channel with constant channel coefficients for downlink communications," in *Proc. IEEE Global Telecommunications Conference (Globecom)*, Dec. 2009.

[67] J. H. Conway, R. H. Hardin, and N. J. Sloane, "Packing lines, planes, etc.: Packings in grassmannian spaces.," *Experimental Mathematics*, vol. 5, no. 2, pp. 139–159, 1996.

[68] H. Moon, "Waterfilling power allocation at high SNR regimes," vol. 59, pp. 708–715, Mar. 2011.

[69] P. de Kerret and D. Gesbert, "Degrees of freedom of the network MIMO channel with distributed CSI," vol. 58, Nov. 2012.

[70] J. A. Tropp, I. Dhillon, R. W. Heath, Jr., and T. Strohmer, "Constructing packings in Grassmannian manifolds via alternating projections," *Experimental Mathematics*, vol. 17, no. 1, pp. 9–35, 2008.

[71] M. Rezaee and M. Guillaud, "Limited feedback for interference alignment in the K-user MIMO interference channel," in *Proc. IEEE Inf. Theory. Workshop (ITW), Lausanne, Switzerland*, 2012.

[72] P. de Kerret, M. Guillaud, and D. Gesbert, "Degrees of freedom of interference alignment with distributed CSI," in *Proc. IEEE International Workshop on Signal Processing Advances in Wireless Communications, Darmstadt, Germany*, Jun. 2013.

[73] C. Suh and D.Tse, "Interference alignment for cellular networks," in *Communication, Control, and Computing, 46th Annual Allerton Conference*, pp. 1037–1044, Sept. 2008.

[74] H. Maleki, S. A. Jafar, and S. Shamai, "Retrospective interference alignment over interference networks," *IEEE Journal of Selected Topics in Signal Processing*, vol. 6, pp. 228–240, Jun. 2012.

[75] A. Ghasemi, A. S. Motahari, and A. K. Khandani, "On the degrees of freedom of X channel with delayed CSIT," in *Proc. IEEE Int. Symp. Information Theory (ISIT), Russia*, Aug. 2011.

[76] M. J. Abdoli, A. Ghasemi, and A. K. Khandani, "On the degrees of freedom of the K-user SISO interference and X channels with delayed CSIT," *Available: http://arxiv.org/abs/1109.4314*, 2011.

[77] R. Tresch, M. Guillaud, and E. Riegler, "On the achievability of interference alignment in the K-user constant MIMO interference channel," in *Proc. IEEE Workshop on Statistical Signal Processing (SSP), Cardiff, U.K.*

[78] F. R. Kschischang, B. J. Frey, and H.-A. Loeliger, "Factor graphs and the sum-product algorithm," vol. 47, pp. 498–519, Feb. 2001.

[79] S. M. Aji and R. J. McEliece, "The generalized distributive law," vol. 46, pp. 325–343, Mar. 2000.

[80] J. M. Walsh and P. A. Regalia, "Connecting belief propagation with maximum likelihood detection," in *Proc. Int. Symposium on Turbo Codes and Related Topics, Munich, Germany*, 2006.

[81] J. S. Yedidia, "Message-passing algorithms for inference and optimization," *Journal of Statistical Physics*, vol. 145, pp. 860–890, Nov. 2011.

[82] I. Sohn, S. H. Lee, and J. G. Andrews, "Belief propagation for distributed downlink beamforming in cooperative MIMO cellular networks," vol. 10, pp. 4140–4149, Dec. 2011.

[83] I. M. Guerreiro, D. Hui, and C. C. Cavalcante, "A distributed approach to precoder selection using factor graphs for wireless communication networks," vol. 83, 2013.

[84] D. Schmidt, W. Utschick, and M. Honig, "Large system performance of interference alignment in single-beam MIMO networks," in *Proc. IEEE Global Telecommunications (Globecom) Conference, Miami, FL, USA*, Dec. 2010.

[85] V. Isham, "An introduction to spatial point processes and Markov random fields," *Int. Stat. Rev*, vol. 49, 1981.

[86] R. Kindermann and J. L. Snell, *Markov random fields and their applications*. Providence, Rhode Island: American mathematical society, 1980.

[87] C. J. Preston, *Gbibs states on countable sets*. Cambridge university press, 1974.

[88] F. V. Jensen, *An introduction to Bayesian networks*. New York: Springer Verlag, 1996.

[89] J. Pearl, *Probabilistic reasoning in intelligent systems*. San Francisco: Morgan Kaufmann, 1988.

[90] R. M. Tanner, "A recursive approach to low complexity codes," *IEEE Trans. Inf. Theory*, vol. IT-27, 1981.

[91] N. Wiberg, *Codes and decoding on general graphs*. PhD thesis: Linkoping university, Sweden, 1996.

[92] C. M. Yetis, S. A. Jafar, and A. H. Kayran, "Feasibility conditions for interference alignment," in *Proc. IEEE Globecom, Honolulu, HI, USA*, 2009.

[93] L. Ruan and V. Lau, "Dynamic interference mitigation for generalized partially connected quasi-static MIMO interference channel," vol. 59, pp. 3788–3798, Aug. 2011.

[94] M. Guillaud and D. Gesbert, "Interference alignment in the partially connected K-user MIMO interference channel," in *Proc. European Signal Processing Conference (EUSIPCO), Barcelona, Spain*, Aug. 2011.

[95] C. C. Moallemi and B. V. Roy, "Convergence of min-sum message-passing for convex optimization," vol. 56, pp. 2041–2050, Apr. 2010.

[96] O. El Ayach and R. W. Heath, "Interference alignment with analog channel state feedback," *IEEE Trans. Wireless Commun.*, vol. 11, pp. 626–636, Feb. 2012.

[97] B. Nosrat-Makouei, J. Andrews, and R. Heath, "MIMO interference alignment over correlated channels with imperfect CSI," *IEEE Trans. Signal Processing.*, vol. 59, pp. 2783–2794, June. 2011.

[98] H. M. B. Xie, Y. Li and A. Nosratinia, "Adaptive interference alignment with CSI uncertainty," *IEEE Trans. Comm.*, vol. 61, pp. 792–801, Feb. 2013.

[99] S. T. Chung and A. J. Goldsmith, "Degrees of freedom in adaptive modulation: a unified view," *IEEE Trans. Commun.*, vol. 49, pp. 1561–1571, Sep. 2001.

[100] K. J. Hole, H. Holm, and G. E. Oien, "Adaptive multidimensional coded modulation over flat fading channels," *IEEE J. Select. Areas Commun.*, vol. 18, 2000.

[101] A. Olfat and M. Shikh-Bahaei, "Optimum power and rate adaptation for MQAM in Rayleigh flat fading with imperfect channel estimation," *IEEE Trans. Veh. Technol.*, vol. 57, pp. 2622–2627, Jul. 2008.

[102] S. Ye, R. S. Blum, and L. J. Cimini, "Adaptive OFDM systems with imperfect channel state information," *IEEE Trans. Wireless Commun.*, vol. 5, pp. 3255–3265, Nov. 2006.

[103] Z. Song, K. Zhang, and Y. L. Guan, "Statistical adaptive modulation for QAM-OFDM systems," in *Proc. IEEE Global Telecommunications Conference (Globecom)*, Nov. 2002.

[104] H. Zhang, S. Wei, G. Ananthaswamy, and D. L. Goeckel, "Adaptive signaling based on statistical characterizations of outdated feedback in wireless communications," in *Proc. IEEE*, Dec. 2007.

[105] J. F. Paris and A. J. Goldsmith, "Adaptive modulation for MIMO multiplexing under average BER constraints and imperfect CSI," in *Proc. IEEE Int. Conf. on Communications*, Jun. 2006.

[106] E. Visotsky and U. Madhow, "Space-time transmit precoding with imperfect feedback," *IEEE Trans. Inf. Theory*, vol. 47, pp. 2632–2639, Sep. 2001.

[107] S. A. Jafar and A. Goldsmith, "Transmitter optimization and optimality of beamforming for multiple antenna systems," *IEEE Trans. Wireless Commun.*, vol. 3, pp. 1165–1175, Jul. 2004.

[108] S. Venkatesan, S. H. Simon, and R. A. Valenzuela, "Capacity of a gaussian MIMO channel with nonzero mean," in *Proc. IEEE Vehicular Technology Conference, Orlando, Florida USA*, Oct. 2003.

[109] R. Couillet and M. Debbah, *Random matrix theory methods for wireless communications*. Cambridge University Press, 2011.

[110] J. Dumont, W. Hachem, S. Lasaulce, P. Loubaton, and J. Najim, "On the capacity achieving covariance matrix for Rician MIMO channels: An asymptotic approach," *IEEE Trans. Inf. Theory*, vol. 56, pp. 1048–1069, Mar. 2010.

[111] J. S. Harsini and F. Lahouti, "QoS constrained throughput optimization for joint adaptive transmission with ARQ over block-fading channels," *IET Communications*, vol. 3, pp. 1030–1040, Jun. 2009.

[112] M. Taki, M. Rezaee, and M. Guillaud, "Adaptive modulation and coding for interference alignment with imperfect CSIT," *Submitted to Trans. Wireless Comm*, 2013.

[113] J. Nocedal and S. J. Wright, *Numerical optimization*. Springer Verlag, Berlin, New York, 2nd edition, 2006.

[114] R. T. Krishnamachari, *A Geometric Framework for Analyzing the Performance of Multiple-Antenna Systems under Finite-Rate Feedback*. PhD thesis, University of Colorado, Boulder, 2011.

[115] A. Barg and D. Y. Nogin, "Bounds on packings of spheres in the Grassmann manifold," *IEEE Trans. Inf. Theory*, vol. 48, pp. 2450–2454, Sep. 2002.

[116] R. D. Yates, "A framework for uplink power control in cellular radio systems," *IEEE Journal on Selected Areas in Communications*, vol. 13, pp. 1341–1347, Sep. 1995.